

Schlumberger

Log
Interpretation
Charts

1997

© Schlumberger 1997

Schlumberger Wireline & Testing
P.O. Box 2175
Houston, Texas 77252-2175

All rights reserved. No part of this book may be reproduced, stored in a retrieval system, or transcribed in any form or by any means, electronic or mechanical, including photocopying and recording, without prior written permission of the publisher.

SMP-7006

An asterisk (*) is used throughout this document to denote a mark of Schlumberger.

Schlumberger

Log Interpretation Charts

Gen

GR

SP

Por

CP

Sw

K

EPT

Sxo

Rxo

Rcor

Rint

Tcor

GST

RST

M

1997

Contents

Foreword		ix
1. Basic Material		
Symbols Used in Log Interpretation	Gen-3	1-1
Estimation of Formation Temperature	Gen-6	1-2
Estimation of R_{mf} and R_{mc}	Gen-7	1-3
Resistivities of Solutions	Gen-8	1-4
Resistivity of NaCl Solutions	Gen-9	1-5
2. Gamma Ray and Spontaneous Potential		
Gamma Ray Corrections for Hole Size and Mud Weight	GR-1	2-1
Gamma Ray Corrections for Barite Mud in Small Boreholes	GR-2	2-2
Gamma Ray Correction for Cased Holes	GR-3	2-3
LWD Gamma Ray Correction for Hole Size and Mud Weight	GR-4	2-4
R_{weq} Determination from E_{SSP}	SP-1	2-5
R_w versus R_{weq} and Formation Temperature	SP-2	2-6
	SP-2m	2-7
SP Correction Charts	SP-3	2-8
SP Correction Chart (Empirical)	SP-4	2-9
	SP-4m	2-10
3. Porosity		
Formation Resistivity Factor Versus Porosity	Por-1	3-1
Isolated and Fracture Porosity	Por-1a	3-2
Porosity Evaluation from Sonic	Por-3	3-3
	Por-3m	3-4
Formation Density Log Determination of Porosity	Por-5	3-5
Environmental Corrections to Formation Density Log, Litho-Density* Log and Sidewall Neutron Porosity Log	Por-15a	3-6
Environmental Corrections to FGT Density Log	Por-15b	3-7
Dual-Spacing CNL* Compensated Neutron Log Charts		3-8
Epithermal Neutron Porosity Equivalence Curves	Por-13a	3-9
Thermal Neutron Porosity Equivalence Curves	Por-13b	3-10
LWD Neutron Porosity Equivalence Curves	Por-21	3-11
	Por-25	3-12
	Por-27	3-13
Dual-Spacing CNL Compensated Neutron Log Environmental Corrections for Cased Hole		3-14
Dual-Spacing CNL Compensated Neutron Log Correction Nomograph for Cased Hole	Por-14a	3-15
Dual-Spacing CNL Compensated Neutron Log Correction Nomograph for Openhole		3-16
	Por-14c	3-17
	Por-14cm	3-18
Dual-Spacing CNL Compensated Neutron Log Standoff Correction Nomograph for Openhole	Por-14d	3-19
	Por-14dm	3-20
Dual-Spacing CNL Compensated Neutron Log NPHI-TNPH Conversion Nomograph for Openhole	Por-14e	3-21
Accelerator Porosity Sonde (APS) Corrections		3-22
Openhole APS Corrections for Mud Weight and Borehole Size	Por-23a	3-23
Openhole APS Corrections for Temperature, Pressure and Formation Salinity	Por-23b†	3-24

†New or modified chart

Dual-Spacing CNL Compensated Neutron Log Formation Σ Correction Nomograph for Openhole.....	3-25
Por-16	3-26
Dual-Spacing CNL Compensated Neutron Log Matrix Σ Correction Nomograph for Openhole	Por-17 3-27
Dual-Spacing CNL Compensated Neutron Log Fluid Σ Correction Nomograph for Openhole	Por-18 3-28
CDN* Compensated Density Neutron Log Correction Nomographs.....	3-29
CDN Compensated Density Neutron Log and ADN* Azimuthal Density Neutron Log Correction Nomograph.....	Por-19 3-30
CDN Compensated Density Neutron Log Correction Nomograph for 6.5-in. Tool.....	Por-20a 3-31
	Por-20b 3-32
	Por-20c 3-33
	Por-20d 3-34
CDN Compensated Density Neutron Log Correction Nomograph for 8-in. Tool.....	Por-24c 3-35
	Por-24d 3-36
	Por-24e 3-37
ADN Azimuthal Density Neutron Log Correction Nomographs	3-38
ADN Azimuthal Density Neutron Log Correction Nomograph for 6.75-in. Tool	Por-26a 3-39
	Por-26b 3-40
 4. Crossplots for Porosity, Lithology and Saturation	
Porosity and Lithology Determination from Formation Density Log and SNP Sidewall Neutron Porosity Log	CP-1a 4-1
	CP-1b 4-2
Porosity and Lithology Determination from Litho-Density Log and CNL Compensated Neutron Log.....	CP-1e 4-3
	CP-1f 4-4
Porosity and Lithology Determination from Formation Density Log and CDN Compensated Density Neutron Log for 6.5-in. Tool.....	CP-22 4-5
Porosity and Lithology Determination from Formation Density Log and CDN Compensated Density Neutron Log for 8-in. Tool	CP-23 4-6
Porosity and Lithology Determination from Formation Density Log and ADN Azimuthal Density Neutron Log for 6.75-in. Tool	CP-24 4-7
Porosity and Lithology Determination from Sonic Log and SNP Sidewall Neutron Porosity Log	CP-2a 4-8
	CP-2am 4-9
Porosity and Lithology Determination from Litho-Density Log and Array Porosity Sonde (APS).....	CP-1g 4-10
	CP-1h 4-11
Porosity and Lithology Determination from Sonic Log and CNL Compensated Neutron Log.....	CP-2c 4-12
	CP-2cm 4-13
Lithology Identification from Formation Density Log and Sonic Log.....	CP-7 4-14
	CP-7m 4-15
Porosity and Lithology Determination from Formation Density Log and CNL Compensated Neutron Log	CP-1c 4-16
	CP-1d 4-17
Porosity and Lithology Determination from Sonic Log and CNL Compensated Neutron Log.....	CP-2b 4-18
	CP-2bm 4-19
M-N Plot for Mineral Identification.....	CP-8 4-20
	CP-8a 4-21

Determination of Apparent Matrix Parameters from Bulk Density or Interval Transit Time and Apparent Total Porosity.....	CP-14	4-22
	CP-14m	4-23
Matrix Identification (MID) Plot.....	CP-15	4-24
	CP-15m	4-25
Porosity and Lithology Determination from Litho-Density Log.....	CP-16	4-26
	CP-17	4-27
Mineral Identification from Litho-Density Log and NGS* Natural Gamma Ray Spectrometry Log.....		4-28
	CP-18	4-29
Mineral Identification from NGS Natural Gamma Ray Spectrometry Log.....	CP-19	4-30
Determination of Apparent Matrix Volumetric Photoelectric Factor.....	CP-20	4-31
Lithology Identification Plot.....		4-32
	CP-21	4-33
Porosity Estimation in Hydrocarbon-Bearing Formations.....	CP-9	4-34
Estimation of Hydrocarbon Density.....	CP-10	4-35
Gas-Bearing Formations—Porosity from Density and Neutron Logs.....	CP-5	4-36
Gas-Bearing Formations—Porosity from Density and APS Epithermal Neutron Logs.....	CP-5a [†]	4-37
Porosity and Gas Saturation in Empty Holes.....	Sw-11	4-38
Permeability from Porosity and Water Saturation.....	K-3	4-39
	K-4	4-40
 5. Electromagnetic Propagation and Microresistivity		
EPT* Propagation Time for NaCl Solutions.....	EPTcor-1	5-1
Flushed Zone Saturation from EPT Propagation Time.....	Sxo-1	5-2
EPT Attenuation for NaCl Solutions.....	EPTcor-2	5-3
EPT-G Mudcake Correction Charts for Water-Base Mud.....	EPTcor-3a	5-4
	EPTcor-3b	5-5
	EPTcor-4a	5-6
	EPTcor-4b	5-7
Flushed Zone Saturation from EPT Attenuation.....	Sxo-2	5-8
Microlog Interpretation Chart.....	Rxo-1	5-9
Microlaterolog and Proximity Log Mudcake Correction.....	Rxo-2	5-10
MicroSFL* Mudcake Correction.....	Rxo-3	5-11
 6. Resistivity		
<i>Laterolog</i>		
Dual Laterolog (D/E) Borehole Correction.....	Rcor-2b	6-1
	Rcor-2c	6-2
ARI* Azimuthal Resistivity Imager Borehole Correction.....	Rcor-14	6-3
Dual Laterolog (D/E) Bed-Thickness Corrections.....		6-4
	Rcor-10	6-5
Invasion Correction Charts.....	Rint-1	6-6
Dual Laterolog—R _{x0} Device.....	Rint-9b	6-7

Induction

Borehole Correction for 16-in. Normal	Rcor-8	6-8
SFL* Spherically Focused Resistivity Borehole Correction	Rcor-1	6-9
Induction Log Borehole Correction	Rcor-4a	6-10
Induction Log Correction for Thin Conductive Beds	Rcor-7	6-11
Induction Log Bed-Thickness Correction	Rcor-5	6-12
	Rcor-6	6-13
Invasion Correction Charts	Rint-1a	6-14
DIL Dual Induction-SFL Spherically Focused Resistivity Log	Rint-2b	6-15
	Rint-2c	6-16
Deep Induction-SFL Spherically Focused Resistivity Log-R _{x0} Device	Rint-5	6-17
DIL Dual Induction-R _{x0} Device	Rint-10	6-18

*Phasor**

SFL Borehole Correction	Rcor-3	6-19
Phasor Induction Borehole Correction		6-20
	Rcor-4b	6-21
	Rcor-4c	6-22
Phasor Induction Bed-Thickness Correction	Rcor-9	6-23
Phasor Dual Induction-SFL Spherically Focused Resistivity Log	Rint-11a	6-24
	Rint-11b	6-25
	Rint-11c	6-26
Phasor Dual Induction in Oil-Base Mud	Rint-12	6-27
Phasor Dual Induction-R _{x0} Device	Rint-13a	6-28
	Rint-13b	6-29
	Rint-13c	6-30
Phasor Dual Induction-SFL-R _{x0} Device	Rint-15a	6-31
	Rint-15b	6-32

CDR Compensated Dual Resistivity*

CDR Compensated Dual Resistivity Borehole Correction for 6.5-in. Tool	Rcor-11a	6-33
CDR Compensated Dual Resistivity Borehole Correction for 8-in. Tool	Rcor-11b	6-34
CDR Compensated Dual Resistivity Borehole Correction for 9.5-in. Tool	Rcor-11c	6-35
CDR Bed-Thickness Correction	Rcor-12	6-36
	Rcor-13	6-37

RAB Resistivity-at-the-Bit*

RAB Resistivity-at-the-Bit Borehole Correction for 6.75-in Tool	Rcor-15	6-38
---	----------------------	------

Water Saturation

Saturation Determination	Sw-1	6-39
Saturation Determination		6-40
	Sw-2	6-41

7. Through-Pipe Evaluation

Thermal Neutron Decay Time

TDT* Thermal Decay Time Log Hydrocarbon Corrections **Tcor-1** 7-1

TDT Thermal Decay Time Log **Tcor-2a** 7-2

..... **Tcor-2b** 7-3

Saturation Determination from TDT Thermal Decay Time Logs 7-4

S_w Determination from TDT Thermal Decay Time Log **Sw-12** 7-5

Graphical Determination of Total Water Saturation (S_{wt}) from TDT Thermal Decay Time Data 7-6

Graphical Determination of Water Saturation (S_w) or Total Water Saturation (S_{wt})
from TDT Thermal Decay Time Log **Sw-17** 7-7

Graphical Determination of S_w from S_{wt} and S_{wb} **Sw-14** 7-8

Gamma Spectrometry

Saturation Determination from GST* Induced Gamma Ray Spectrometry Log **GST-1** 7-9

..... **GST-2** 7-10

..... **GST-5** 7-11

Apparent Water Salinity Determination from GST Induced Gamma Ray Spectrometry Log **GST-3** 7-12

..... **GST-4** 7-13

Reservoir Saturation

RST* Reservoir Saturation Tool Carbon/Oxygen Ratio Response 7-14

..... **RST-1** 7-15

..... **RST-2** 7-16

..... **RST-3** 7-17

Cement Bond

CBL Interpretation—Casing Data 7-18

CBL Interpretation Chart **M-1** 7-19

Appendices

Appendix A Linear Grid A-1

..... Log-Linear Grid A-2

..... Water Saturation Grid for Porosity Versus Resistivity A-3

Appendix B Logging Tool Response in Sedimentary Minerals B-5

Appendix C Conversions C-7

Appendix D Symbols D-10

Appendix E Subscripts E-12

Appendix F Abbreviations F-15

Appendix G References G-17

Foreword

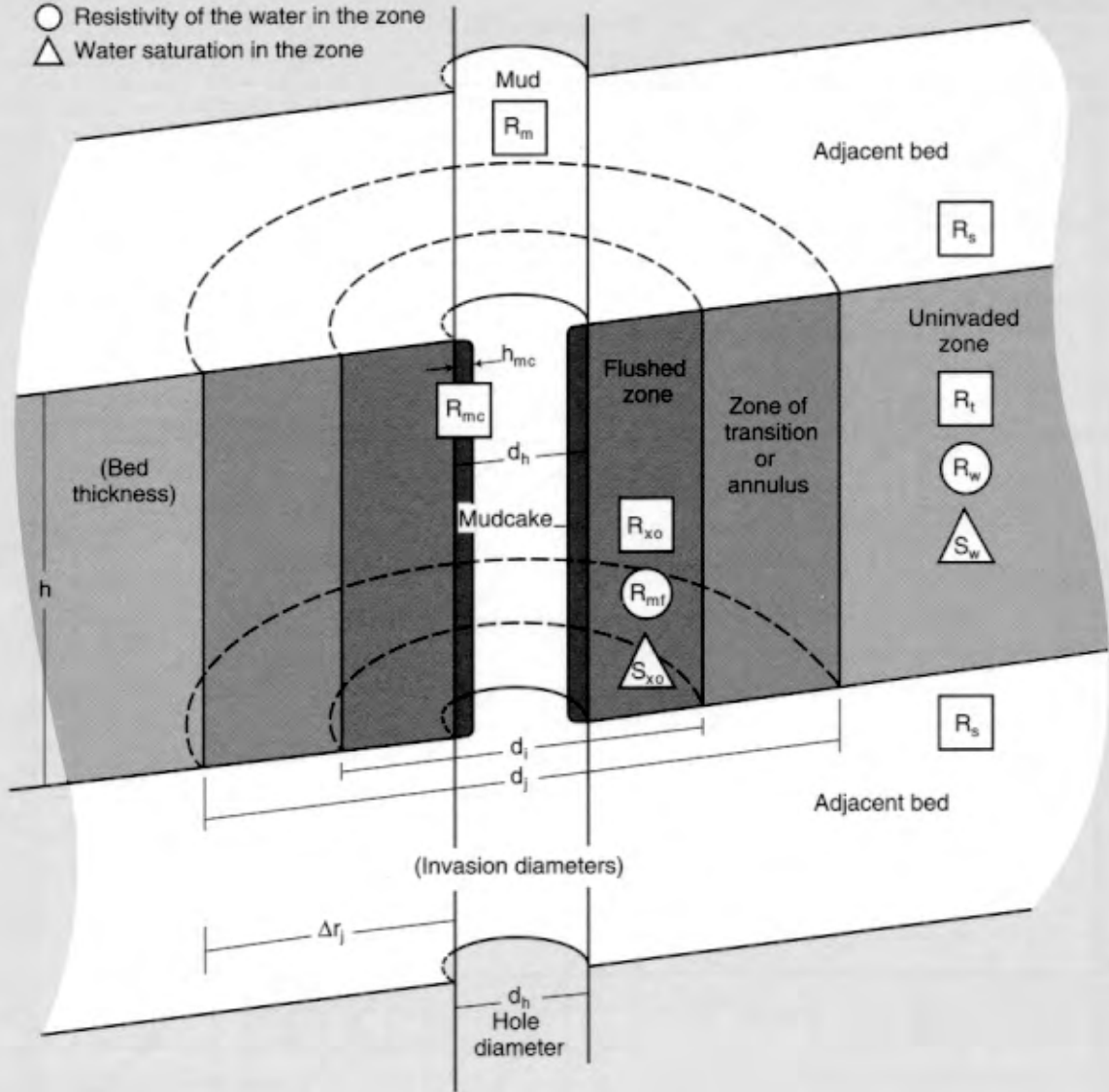
This edition of the Schlumberger Log Interpretation Charts book contains the charts, nomograms and tables necessary for quantitative interpretation of data from various Schlumberger logging tools. Several new charts are included for new services, and some of the previous charts have been replotted as a result of additional lab measurements and advanced computer modeling.

A brief description on how to use each chart or series of

charts is included. Details are available from a companion volume, *Log Interpretation Principles/Applications—1989*, which describes the principles of measurements used by our openhole logging tools, the basic principles for interpreting those measurements, and the various applications for the services. *Cased Hole Log Principles/Applications—1989* provides similar information for cased hole services.

Symbols Used in Log Interpretation

- Resistivity of the zone
- Resistivity of the water in the zone
- △ Water saturation in the zone



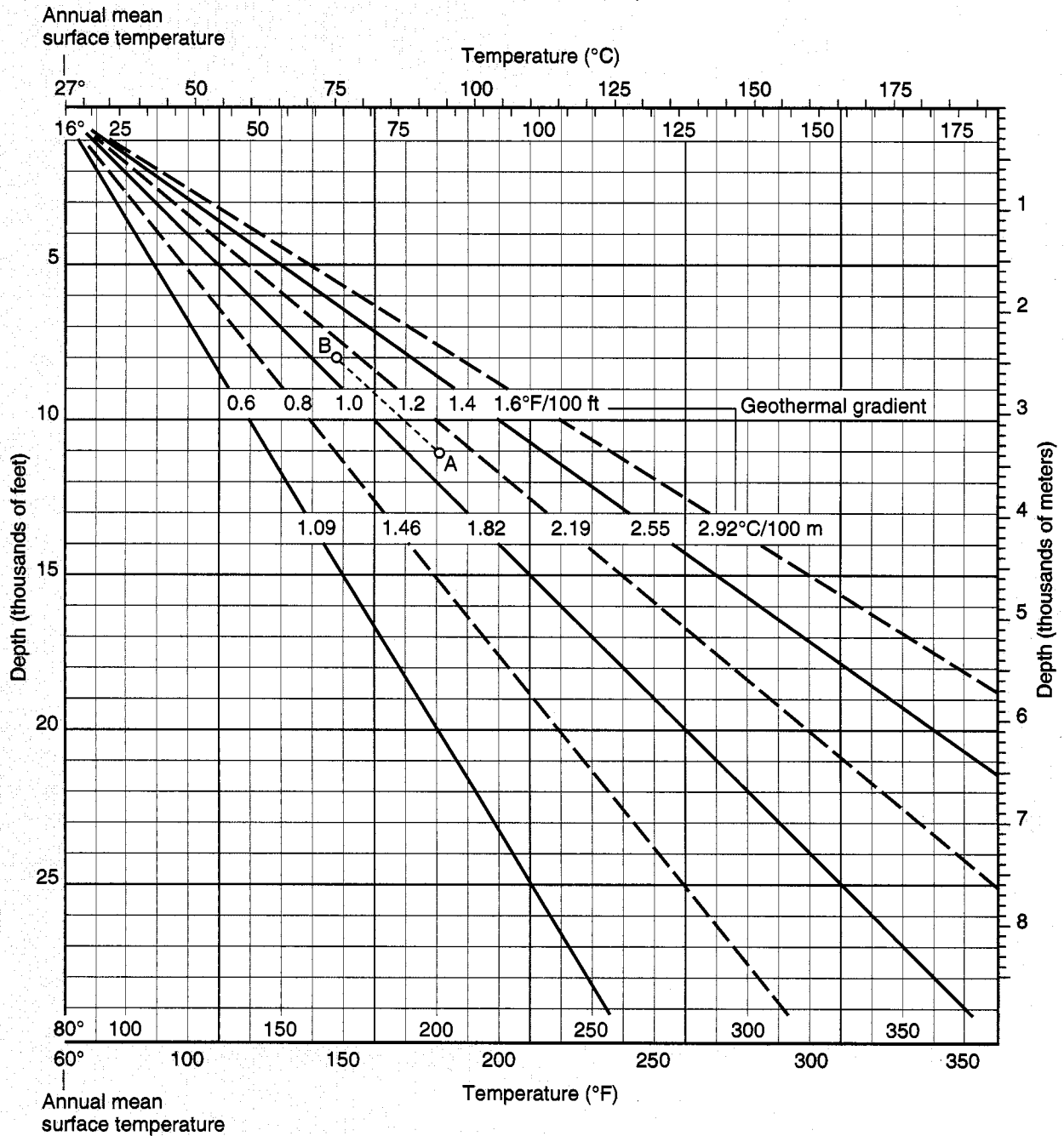
Estimation of Formation Temperature

Linear gradient assumed

Gen-6

Gen

Temperature gradient conversions: $1^{\circ}\text{F}/100\text{ ft} = 1.823^{\circ}\text{C}/100\text{ m}$
 $1^{\circ}\text{C}/100\text{ m} = 0.5486^{\circ}\text{F}/100\text{ ft}$



© Schlumberger

Example: Bottomhole temperature (BHT) at 11,000 ft = 200 $^{\circ}\text{F}$
 (Point A)
 Temperature at 8000 ft = 167 $^{\circ}\text{F}$ (Point B)

Estimation of R_{mf} and R_{mc}

Direct measurements of filtrate and mudcake samples are preferred. When not available, filtrate resistivity, R_{mf} , and mudcake resistivity, R_{mc} , may be estimated from one of the following methods.

Method 1

Lowe and Dunlap (Reference 36)

For freshwater muds with mud resistivity, R_m , in the range from 0.1 to 2.0 ohm-m at 75°F [24°C], and *measured* values of R_m and mud density, ρ_m , in pounds per gallon:

$$\log \left(\frac{R_{mf}}{R_m} \right) = 0.396 - 0.0475 \rho_m$$

Method 2

Overton and Lipson (Reference 1)

For drilling muds with mud resistivity, R_m , in the range from 0.1 to 10.0 ohm-m at 75°F [24°C], where K_m is given as a function of mud weight in the table below:

$$R_{mf} = K_m (R_m)^{1.07}$$

$$R_{mc} = 0.69 (R_{mf}) \left(\frac{R_m}{R_{mf}} \right)^{2.65}$$

Example: $R_m = 3.5$ ohm-m at 75°F [24°C]

Mud weight = 12 lbm/gal [1440 kg/m³]

Therefore, $K_m = 0.584$

$R_{mf} = (0.584)(3.5)^{1.07} = 2.23$ ohm-m at 75°F

$R_{mc} = 0.69(2.23)(3.5/2.23)^{2.65} = 5.07$ ohm-m at 75°F

The calculated value of R_{mf} is more reliable than that of R_{mc} .

Mud Weight		K_m
lbm/gal	kg/m ³	
10	1200	0.847
11	1320	0.708
12	1440	0.584
13	1560	0.488
14	1680	0.412
16	1920	0.380
18	2160	0.350

Method 3

A statistical approximation, for predominantly NaCl muds, is $R_{mc} = 1.5 R_m$, and $R_{mf} = 0.75 R_m$.

Resistivities of Solutions

Gen-8

Gen

Actual resistivity measurements are always preferred, but if necessary, the chart on the opposite page may be used to estimate the resistivity of a water sample at a given temperature when the salinity (NaCl concentration) is known, or to estimate the salinity when resistivity and temperature are known. It may also be used to convert resistivity from one temperature to another temperature.

Example: Resistivity of a water sample is 0.3 ohm-m at 25°C; what is the resistivity at 85°C?

Enter the chart with 25°C and 0.3 ohm-m. Their intersection indicates a salinity of approximately 20,000 ppm. Moving along this constant salinity line yields a water sample resistivity of 0.13 ohm-m at 85°C.

The resistivity of a water sample can be estimated from its chemical analysis. An equivalent NaCl concentration determined by use of the chart below is entered into Chart Gen-9 to estimate the resistivity of the sample.

The chart is entered in abscissa with the total solids concentration of the sample in ppm (mg/kg) to find weighting multipliers for the various ions present. The concentration of each

ion is multiplied by its weighting multiplier, and the products for all ions are summed to obtain equivalent NaCl concentration. Concentrations are expressed in ppm or mg/kg, both by weight. These units are numerically equal.

For more information see Reference 2.

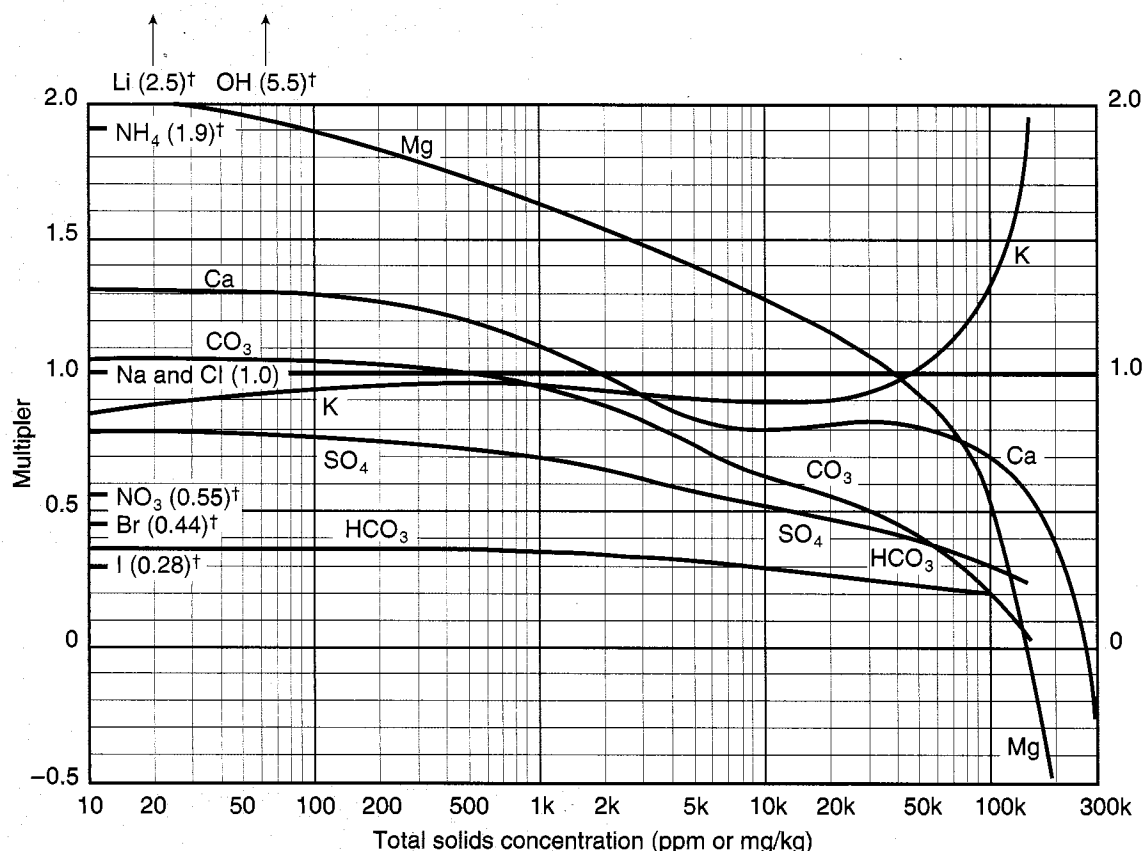
Example: A formation-water sample analysis shows 460 ppm Ca, 1400 ppm SO₄ and 19,000 ppm Na plus Cl.

Total solids concentration is $460 + 1400 + 19,000 = 20,860$ ppm.

Entering the chart below with this total solids concentration, we find 0.81 as the Ca multiplier and 0.45 as the SO₄ multiplier. Multiplying the concentration by the corresponding multipliers, the equivalent NaCl concentration is found as approximately

$460 \times 0.81 + 1400 \times 0.45 + 19,000 \times 1 \approx 20,000$ ppm.

Entering the NaCl resistivity-salinity nomograph (Gen-9) with 20,000 ppm and 75°F (24°C), the resistivity is found to be 0.3 at 75°F.



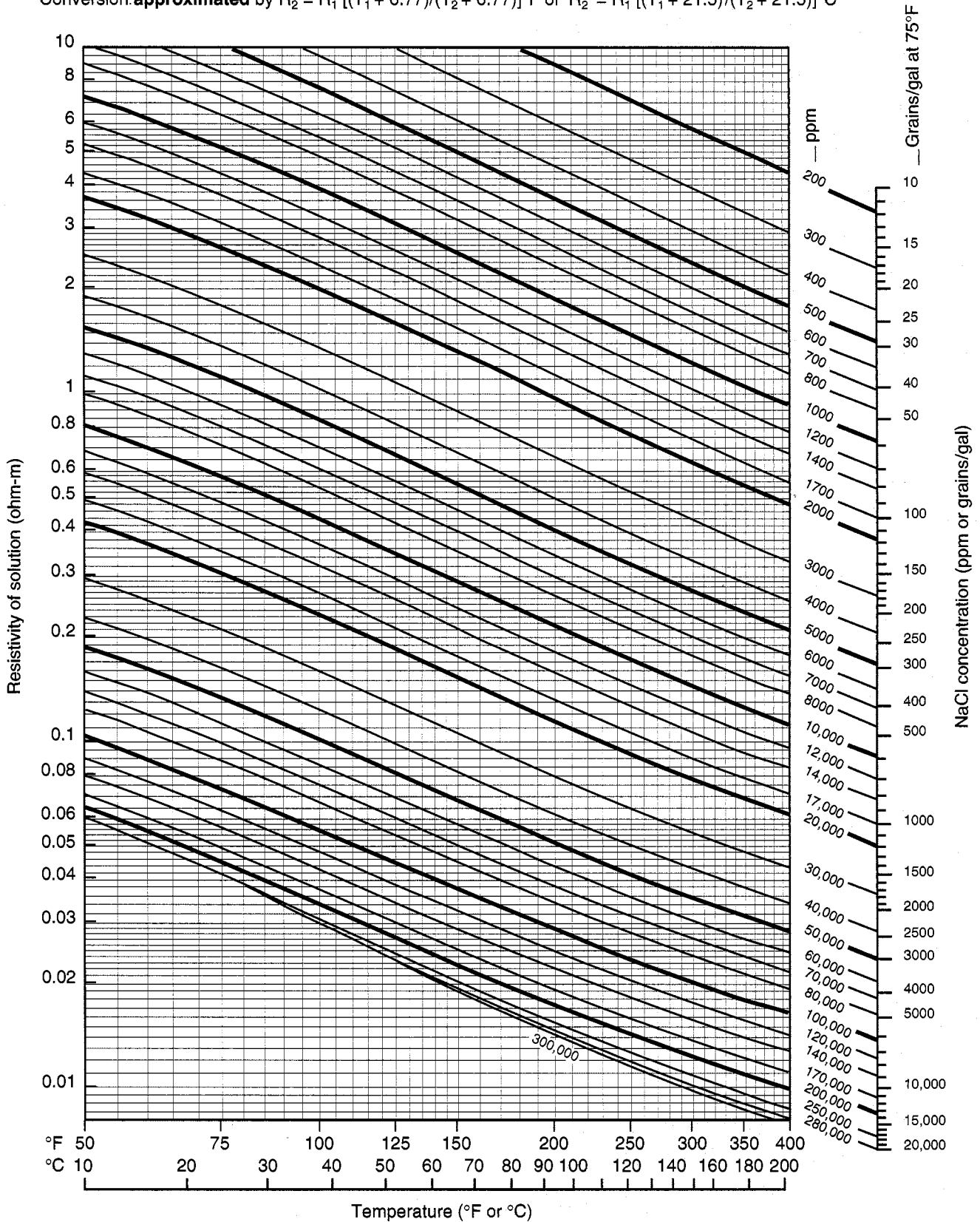
† Multipliers that do not vary appreciably for low concentrations (less than about 10,000 ppm) are shown at the left margin of the chart

Resistivity of NaCl Solutions

Gen-9

Gen

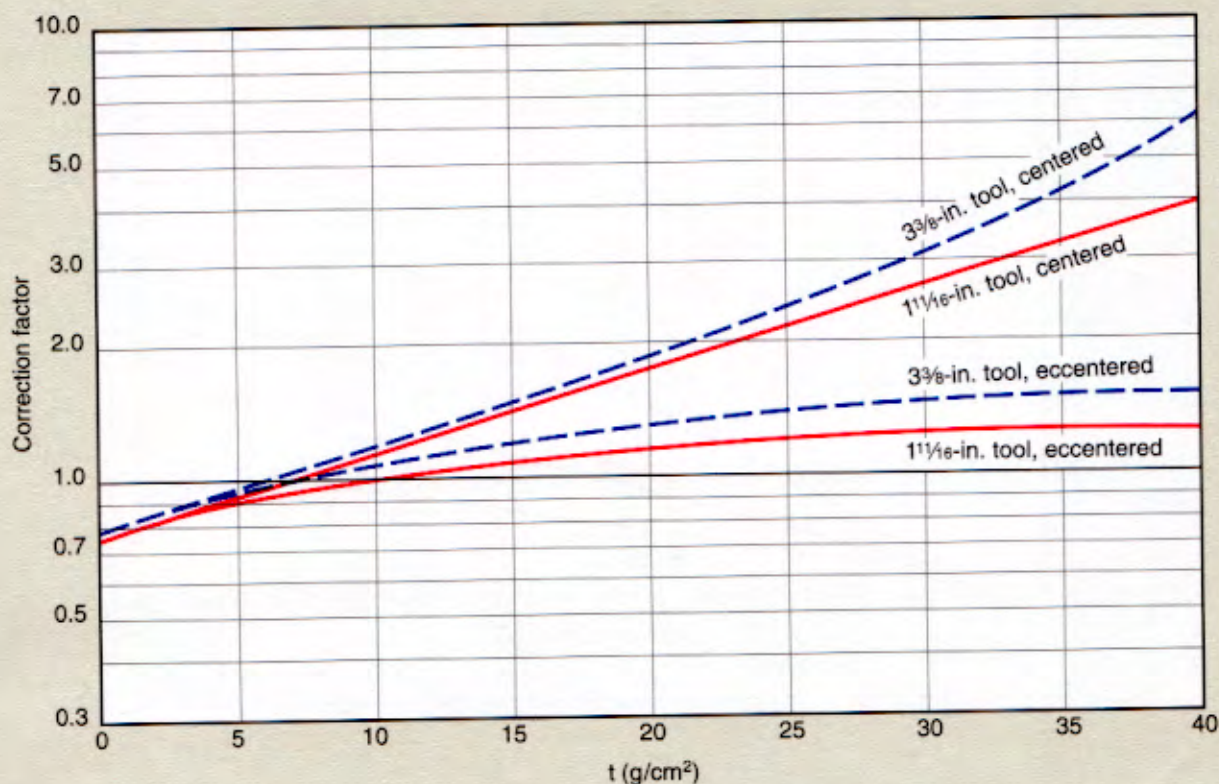
Conversion approximated by $R_2 = R_1 [(T_1 + 6.77)/(T_2 + 6.77)]^{\circ F}$ or $R_2 = R_1 [(T_1 + 21.5)/(T_2 + 21.5)]^{\circ C}$



Gamma Ray Corrections for Hole Size and Mud Weight

For 3 $\frac{3}{8}$ -in. and 1 $\frac{1}{16}$ -in. SGT wireline gamma ray tools

GR-1



© Schlumberger

Log interpretation Charts GR-1 and GR-2, replacing Chart Por-7, are based on laboratory work and Monte Carlo calculations to provide improved corrections for 3 $\frac{3}{8}$ - and 1 $\frac{1}{16}$ -in. SGT gamma ray tools. The corrections normalize the response of both tools to eccentric positions in an 8-in. borehole with 10-lbm mud. Chart GR-2 provides a correction for barite mud in small boreholes.

Although these charts are more difficult to use than the ones they replaced, the results are more exact since they are normalized to current tools, no interpolation is required, and the ranges are extended.

The input parameter, t, in g/cm², is calculated as follows:

$$t = \frac{W_{\text{mud}}}{8.345} \left(\frac{2.54(d_{\text{hole}})}{2} - \frac{2.54(d_{\text{sonde}})}{2} \right)$$

The correction for standoff is

$$CF' = CF'_m + (CF'_o - CF'_m) \left(\frac{S - S_m}{S_m} \right)^2$$

CF'_m is the correction factor for centered tools, while CF'_o is the correction factor for eccentric tools. Both are corrected for barite if it is present in the borehole. S is the actual standoff, and S_m is the standoff with the tool centered.

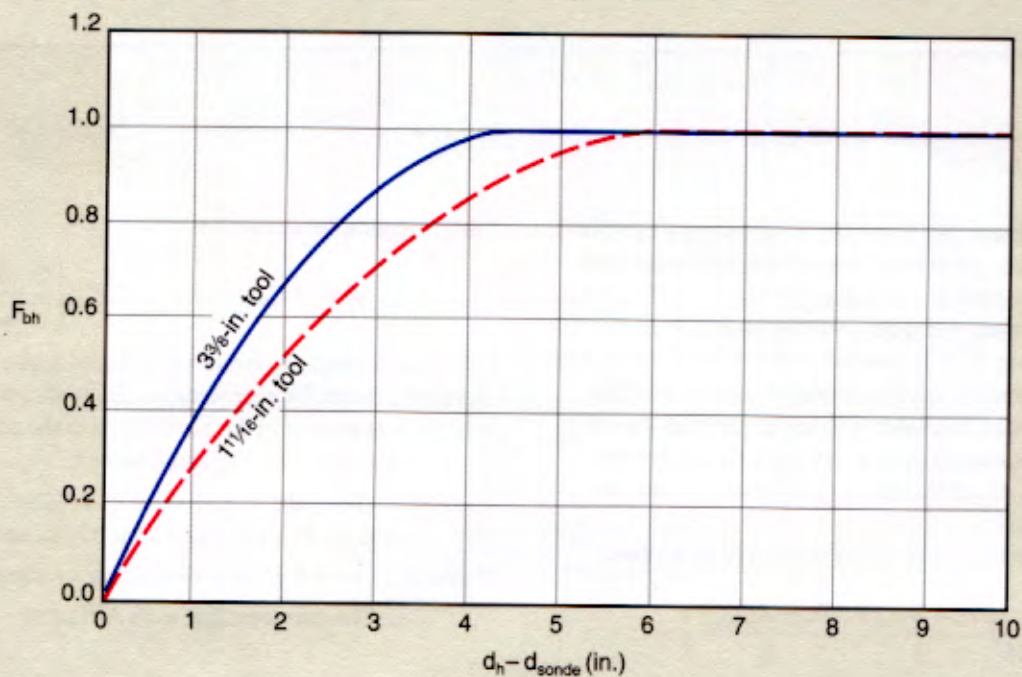
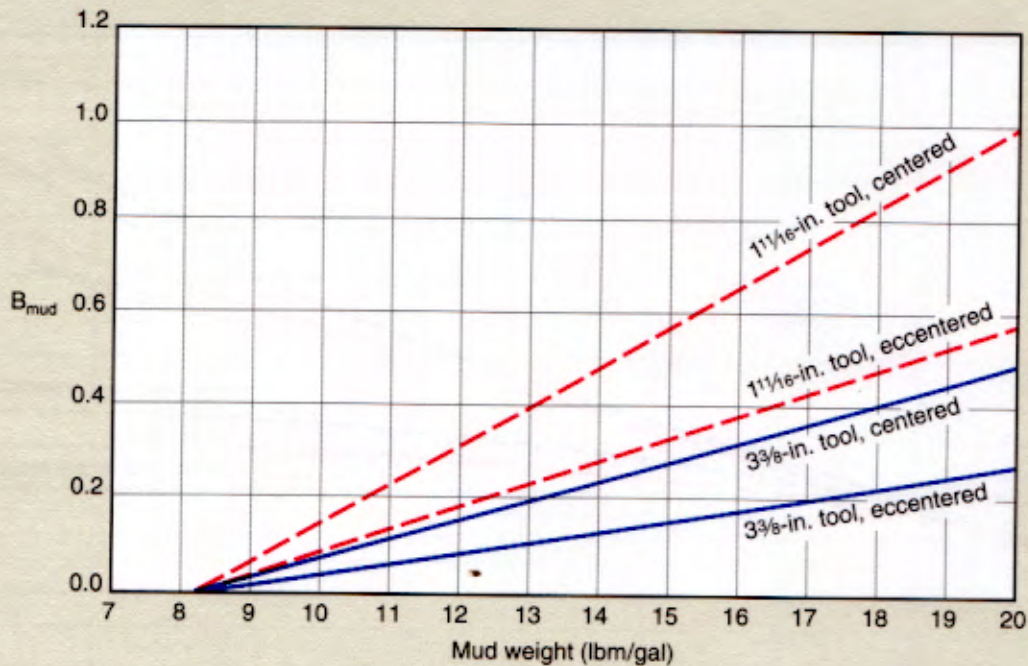
Example: GR reads 36 API units, d_h is 12 in., and mud weight is 12 lbm/gal. The tool is 3 $\frac{3}{8}$ in. and centered.

Therefore, $t = 15.8$ g/cm², resulting in a correction factor of 1.6.

The corrected GR = 58 API units.

Gamma Ray Corrections for Barite Mud in Small Boreholes

GR-2



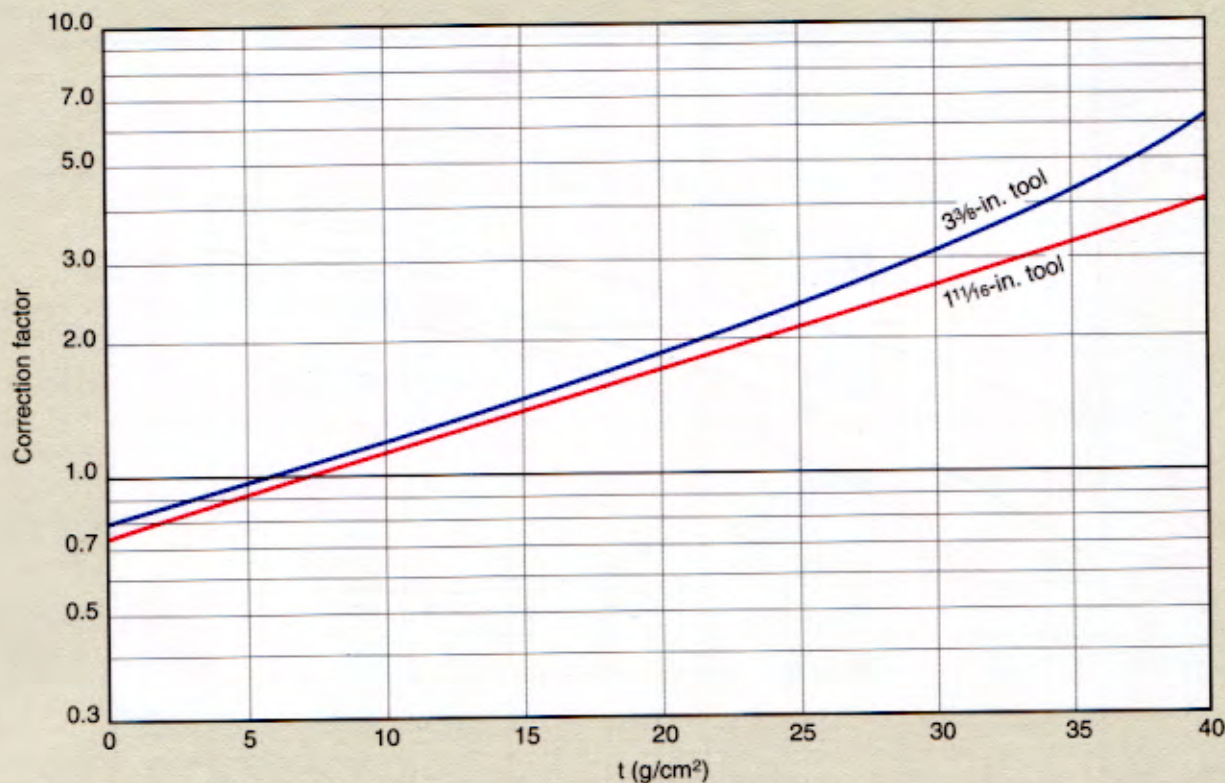
© Schlumberger

These charts correct for the barite mud effect in hole sizes smaller and larger than the 8-in. standard. In these cases, the correction factor from Chart GR-1 is multiplied by the borehole correction factor $1 + B_{\text{mud}} \times F_{\text{bh}}$.

Example: With the same conditions shown in the example on Chart GR-1 except for a 6-in. hole, $t = 4.8 \text{ g/cm}^2$, resulting in a correction factor of 0.95. Using Chart GR-2, $B_{\text{mud}} = 0.15$ and $F_{\text{bh}} = 0.81$ for a borehole correction of 1.12 and a revised correction factor of 1.06. The corrected GR = 38 API units.

Gamma Ray Correction for Cased Holes

GR-3



© Schlumberger

Log interpretation Chart GR-3 is based on laboratory work and Monte Carlo calculations to provide gamma ray corrections in cased holes. This chart is based on the openhole model in Chart GR-1. In this case, t , in g/cm^2 , is calculated as the sum of density-thickness products for the casing, cement sheath and borehole fluid. The density of J-55 casing is $7.96 \text{ g}/\text{cm}^3$, and the density of cement is typically $2.0 \text{ g}/\text{cm}^3$.

$$t = \frac{2.54}{2} \left(\frac{W_m}{8.345} (\text{ID}_{\text{csg}} - d_{\text{sonde}}) + \rho_{\text{csg}} (\text{OD}_{\text{csg}} - \text{ID}_{\text{csg}}) + \rho_{\text{cement}} (d_h - \text{OD}_{\text{csg}}) \right)$$

The chart correction factor provides a corrected gamma ray to the standard reference condition of an eccentric $3\frac{3}{8}$ -in. tool in an 8-in. borehole with 10-lbm mud.

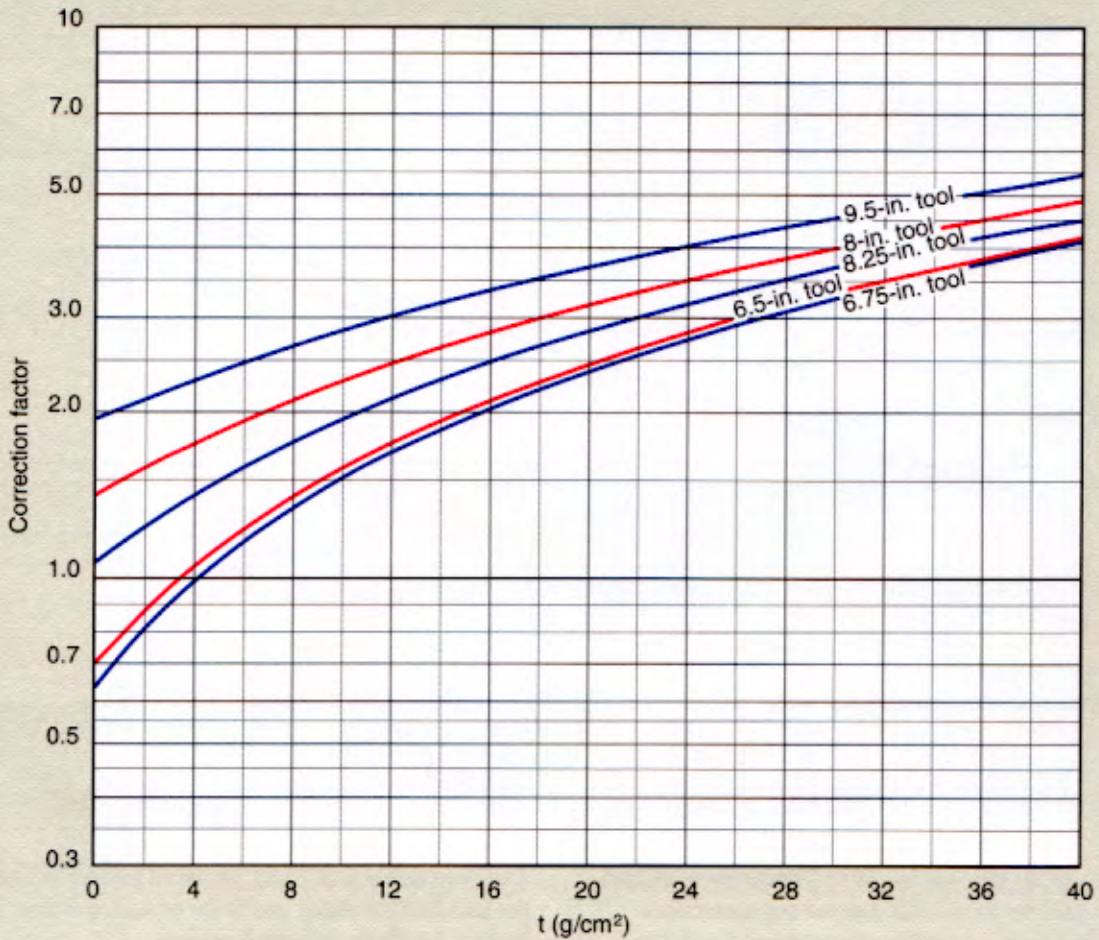
Example: GR reads 19 API units; d_h is 12 in.; casing is 9 $\frac{3}{8}$ in., 43.50 lbm/ft; GR tool is $3\frac{3}{8}$ in.; $W_m = 8.345 \text{ lbm}/\text{gal}$; and $t = 21.7 \text{ g}/\text{cm}^2$ for a correction factor of 2.1. The corrected GR = 40 API units.

GR

LWD Gamma Ray Correction for Hole Size and Mud Weight

For gamma ray with CDR* Compensated Dual Resistivity tools

GR-4



*Mark of Schlumberger
© Schlumberger

Chart GR-4 can be used to normalize gamma ray readings of the 9.5-, 8.25-, 8-, 6.75- and 6.5-in. CDR tools to the 6.5-in. tool in 10-lbm/gal mud.

The corrections illustrated by this chart are routinely applied

to LWD data before delivery; therefore, be careful not to duplicate the correction. The input parameter, t , in g/cm^2 , is calculated from

$$t = \frac{W_m}{8.345} (d_{hole} - 3.5 - ST)$$

where ST varies with tool size as follows:

Tool size (in.)	ST
6.5	2.125
6.75	2.031
8.0	3.156
8.25	2.656
9.5	3.937

R_{weq} Determination from E_{SSP}

Clean formations

This chart and nomograph calculate the equivalent formation water resistivity, R_{weq} , from the static spontaneous potential, E_{SSP} , measurement in clean formations.

Enter the nomograph with E_{SSP} in mV, turning through the reservoir temperature in °F or °C to define the R_{mfeq}/R_{weq} ratio. From this value, pass through the R_{mfeq} value to define R_{weq} .

For predominantly NaCl muds, determine R_{mfeq} as follows:

- If R_{mf} at 75°F (24°C) is greater than 0.1 ohm-m, correct R_{mf} to formation temperature using Chart Gen-9, and use $R_{mfeq} = 0.85 R_{mf}$.
- If R_{mf} at 75°F (24°C) is less than 0.1 ohm-m, use Chart SP-2 to derive a value of R_{mfeq} at formation temperature.

Example: $SSP = 100$ mV at 250°F

$R_{mf} = 0.70$ ohm-m at 100°F
or 0.33 ohm-m at 250°F

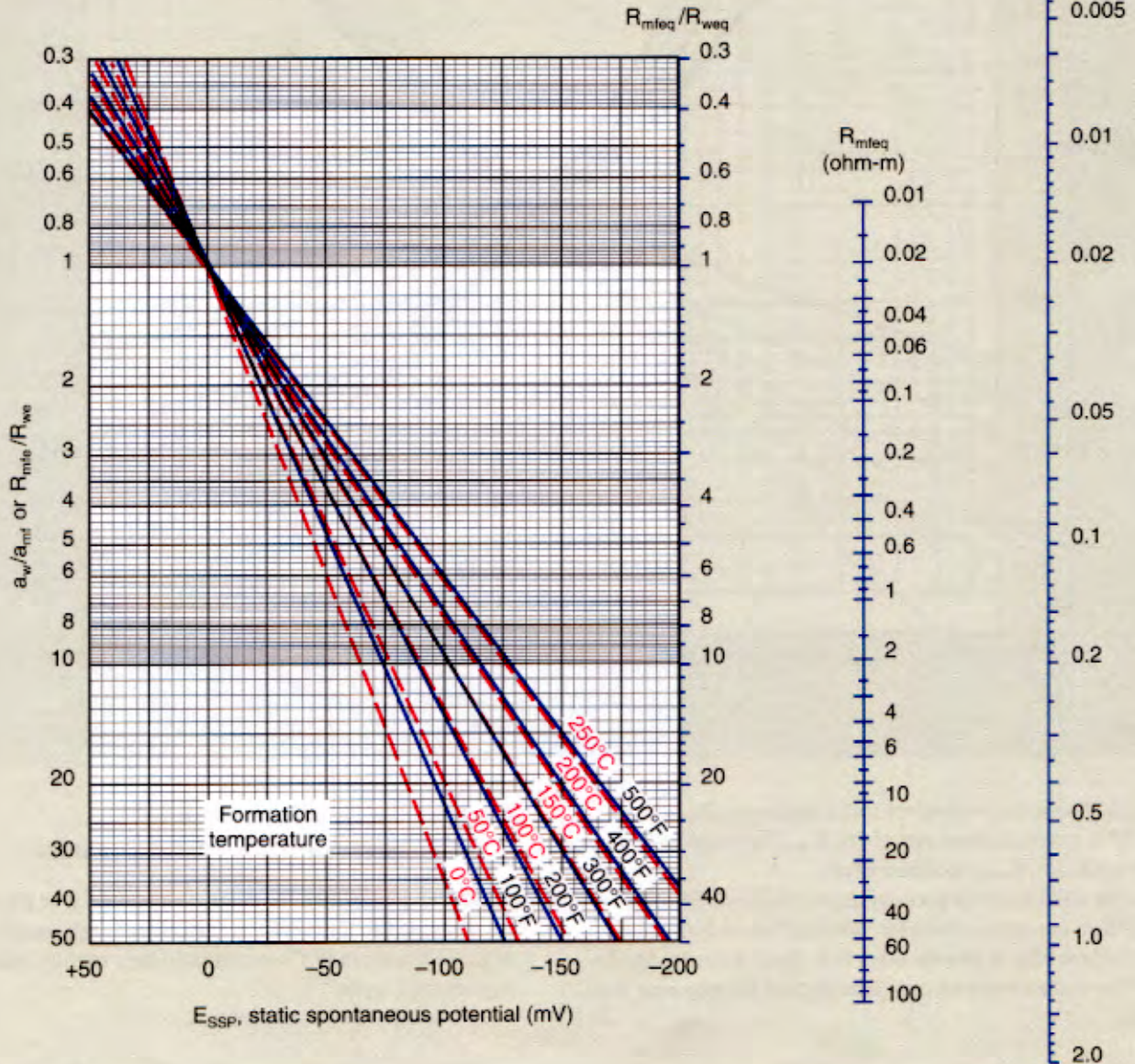
Therefore, $R_{mfeq} = 0.85 \times 0.33$
 $= 0.28$ ohm-m at 250°F

$R_{weq} = 0.025$ ohm-m at 250°F

$E_{SSP} = -K_c \log(R_{mfeq}/R_{weq})$

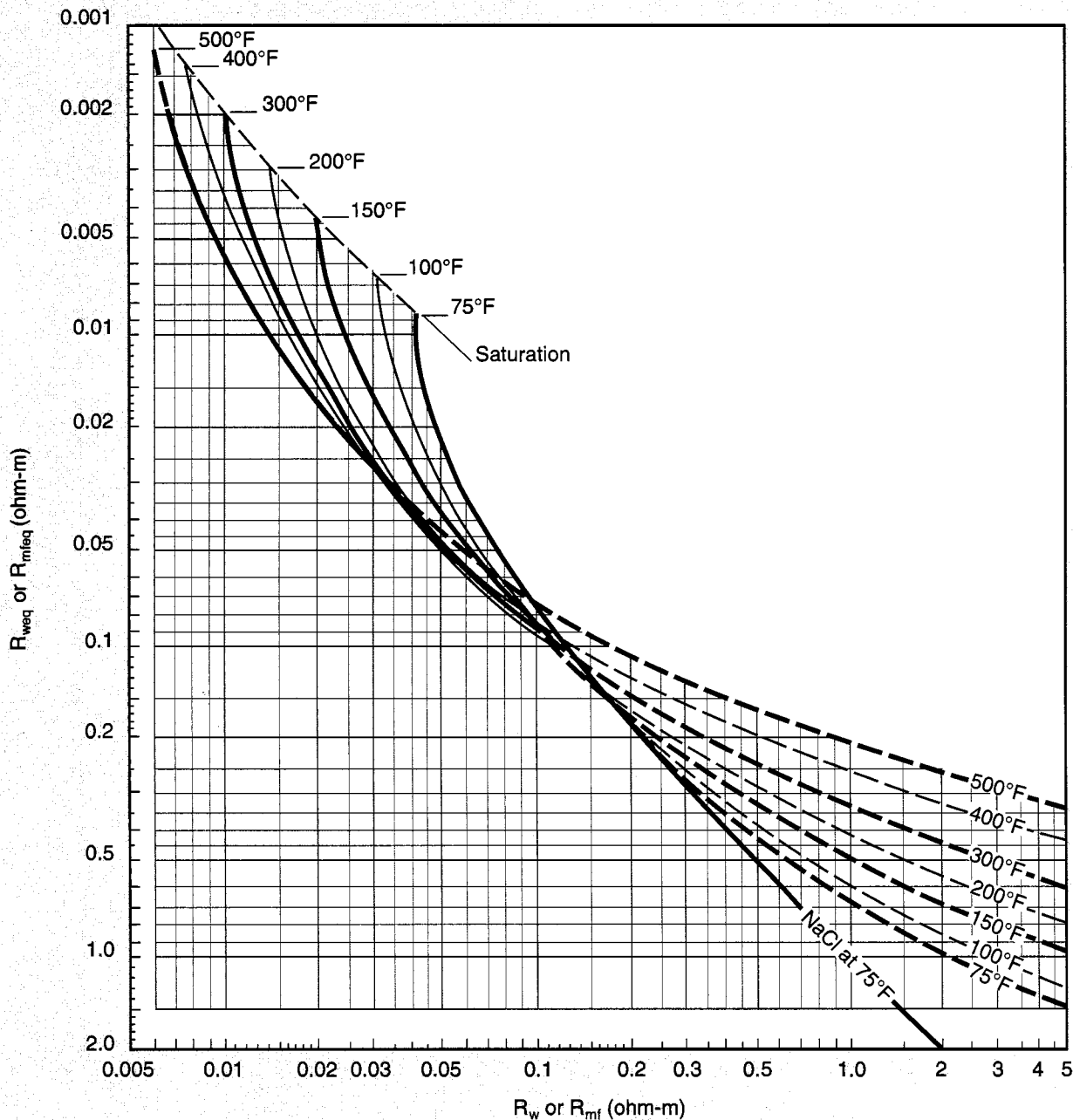
$K_C = 61 + 0.133 T_F$

$K_C = 65 + 0.24 T_C$



R_w versus R_{weq} and Formation Temperature

SP-2
(English)



© Schlumberger

These charts convert equivalent water resistivity, R_{weq} , from Chart SP-1 to actual water resistivity, R_w . They may also be used to convert R_{mf} to R_{mfeq} in saline muds.

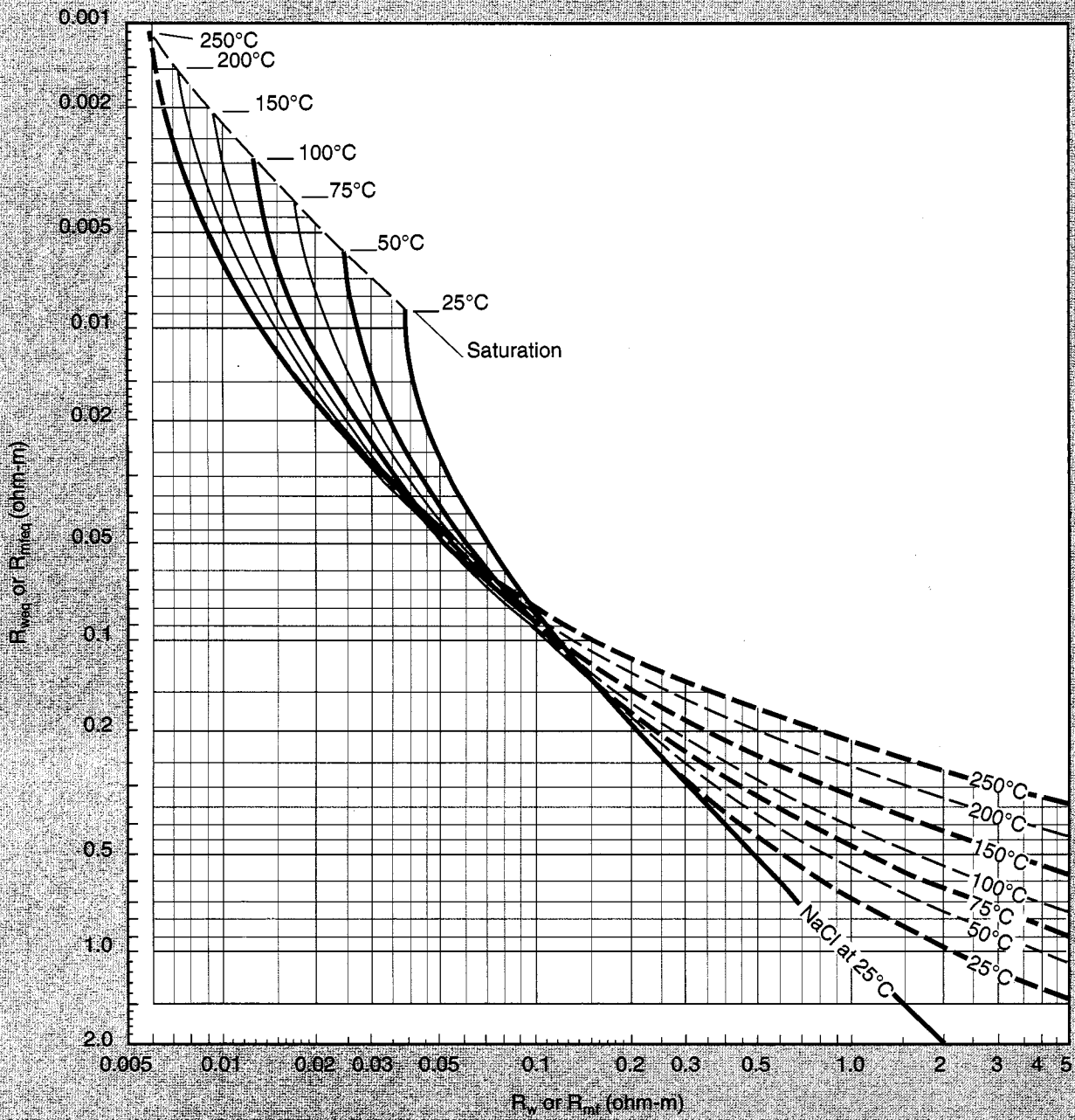
Use the solid lines for predominantly NaCl waters. The dashed lines are approximate for "average" fresh formation waters (where effects of salts other than NaCl become significant). The dashed portions may also be used for gyp-base mud filtrates.

Example: $R_{weq} = 0.025$ ohm-m at 120°C
From chart, $R_w = 0.031$ ohm-m at 120°C

Special procedures for muds containing Ca or Mg in solution are discussed in Reference 3. Lime-base muds usually have a negligible amount of Ca in solution; they may be treated as regular mud types.

R_w versus R_{weq} and Formation Temperature

SP-2m
(Metric)



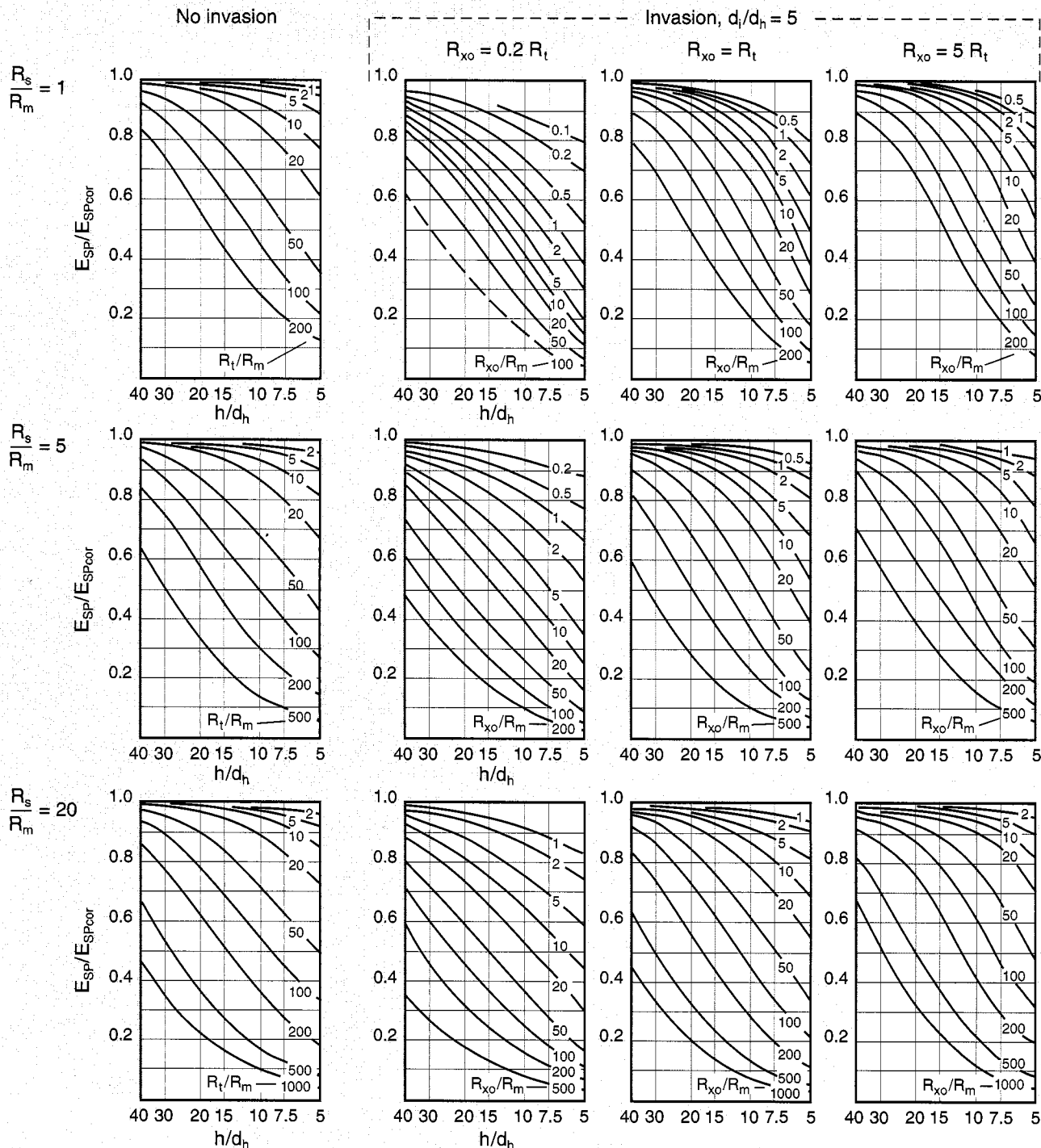
SP

SP Correction Charts

For representative cases

SP-3

SP

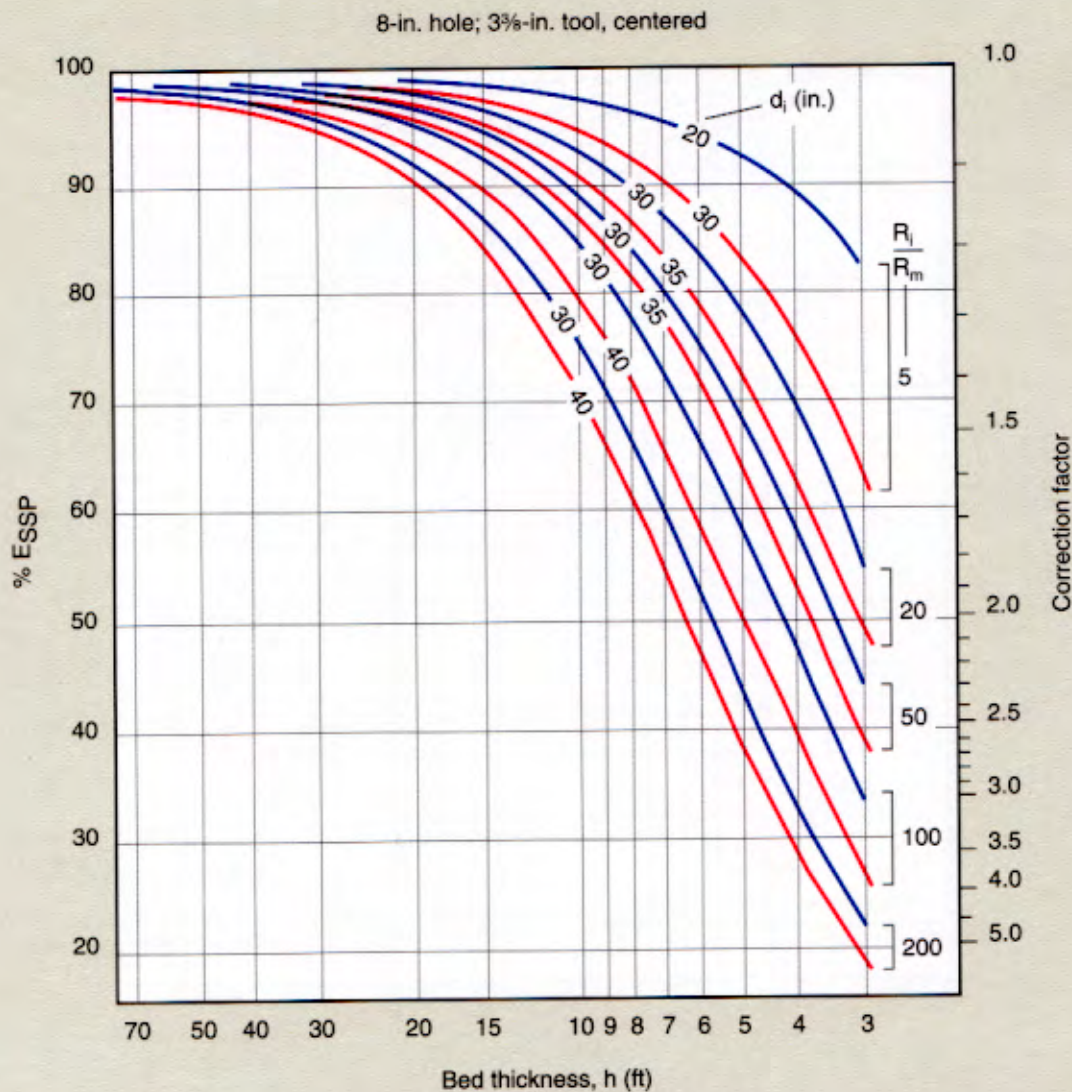


© Schlumberger

1. Select row of charts for most appropriate value of R_s/R_m .
2. Select chart for No Invasion or for Invasion of $d_i/d_h = 5$, whichever is appropriate.
3. Enter abscissa with value of h/d_h (ratio of bed thickness to hole diameter).
4. Go vertically up to curve for appropriate R_t/R_m (for no invasion) or R_{xo}/R_m (for invaded cases), interpolating between curves if necessary.
5. Read E_{SP}/E_{SPcor} in ordinate scale. Calculate $E_{SPcor} = E_{SP}/(E_{SP}/E_{SPcor})$. (E_{SP} is SP from log.)

For more detail on SP corrections, see References 4 and 33.

SP Correction Chart (Empirical)

SP-4
(English)

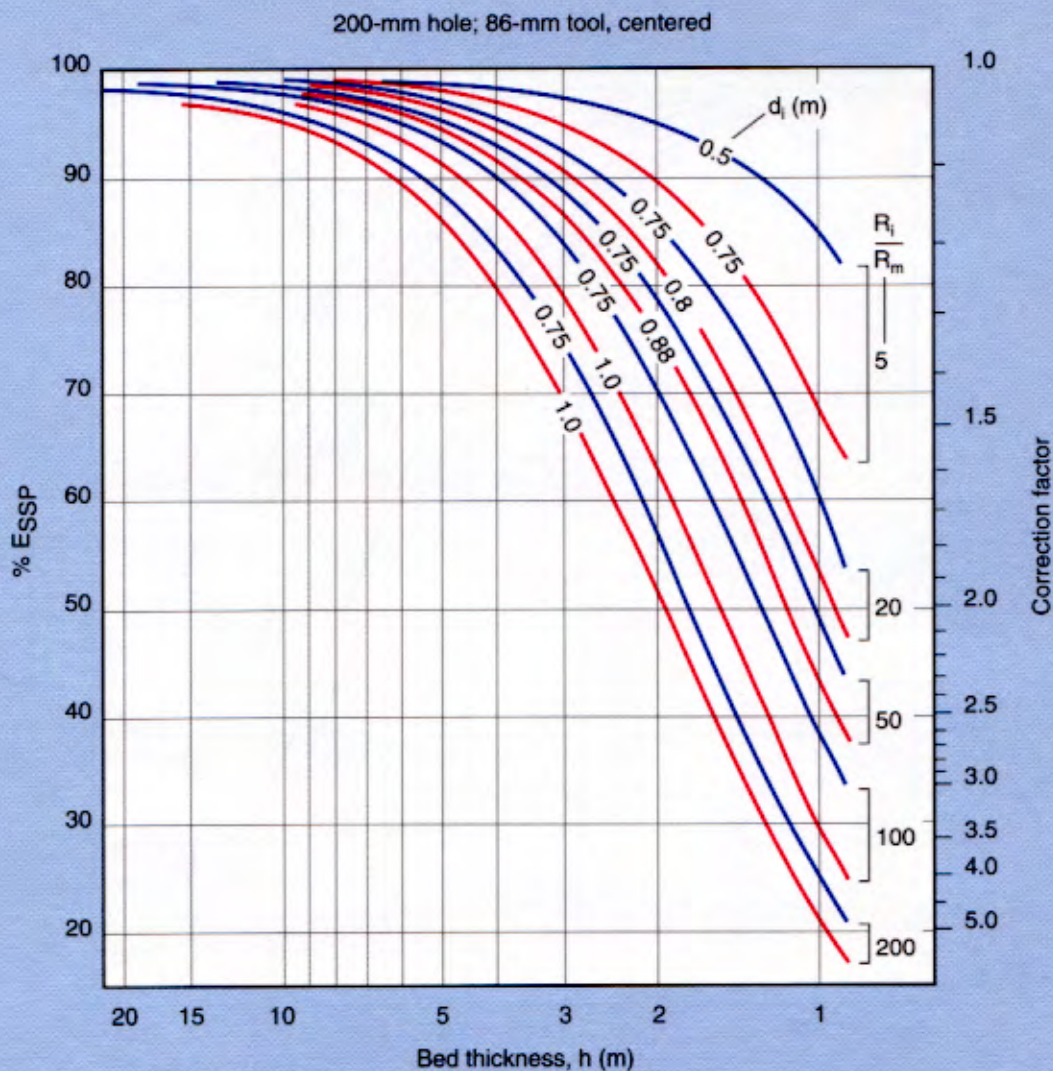
© Schlumberger

This chart provides an empirical correction to the SP for the effects of invasion and bed thickness obtained by averaging a series of thin-bed corrections in Reference 37. This chart considers only h , bed thickness, as variable, and R_i/R_m and d_i as parameters of fixed value. Hole diameter is set at 8 in.

Enter the chart with bed thickness, h ; go to the appropriate invasion diameter, d_i , and invaded zone resistivity/mud resistivity ratio, R_i/R_m . The recorded SP measurement is then corrected by the resulting correction factor.

Continued on next page

SP Correction Chart (Empirical)

SP-4m
(Metric)

© Schlumberger

Example: SP = -80 mV in a 3-m bed
 $R_m = 0.5$ ohm-m, and R_i (invaded zone resistivity) =
 10 ohm-m (both at formation temperature)
 Invasion diameter = 0.80 m

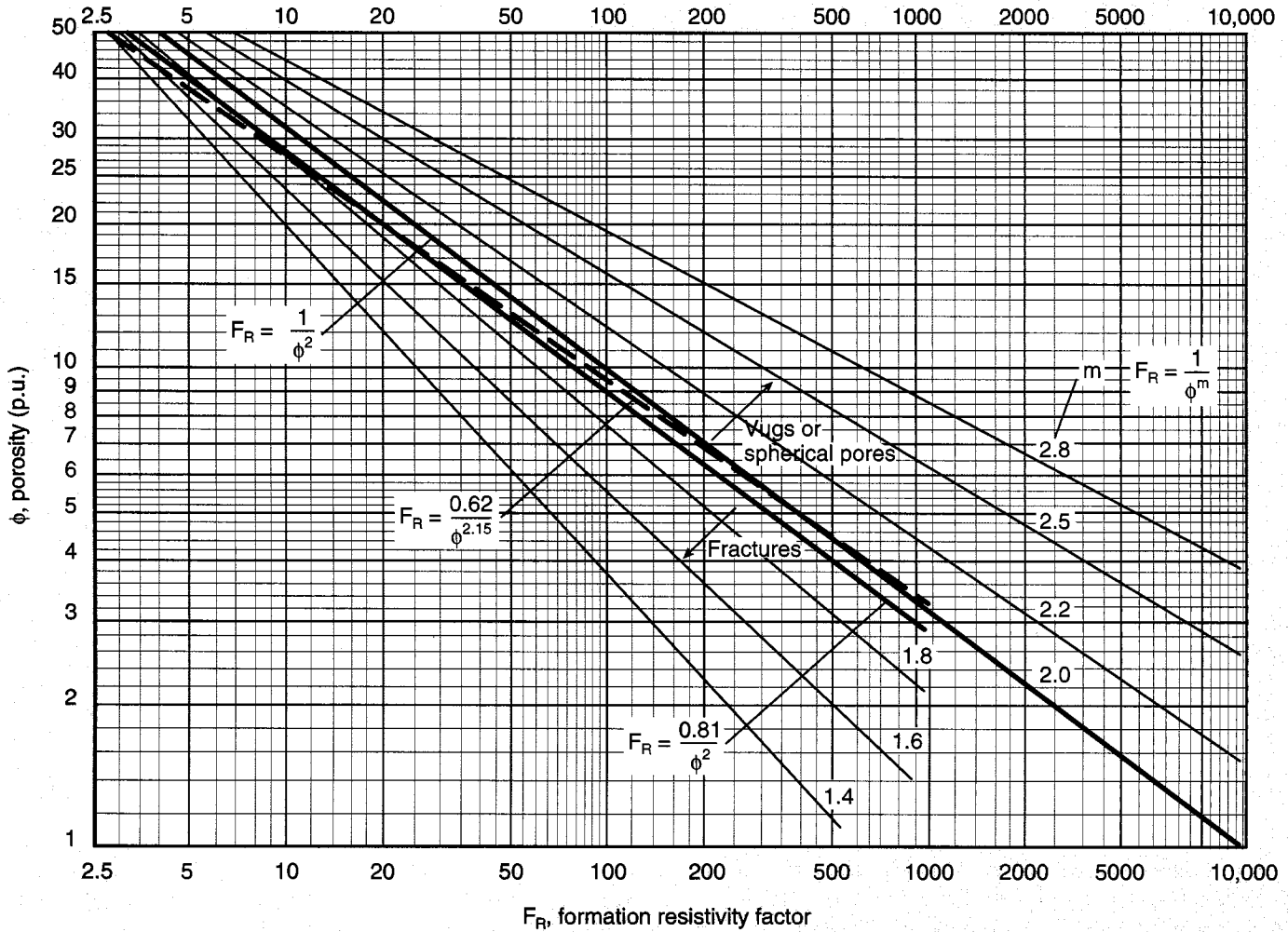
Therefore, $R_i/R_m = 10/0.5 = 20$

SP correction factor = 1.1

Corrected SP, $E_{SSP} = -80 (1.1) = -88$ mV

Formation Resistivity Factor Versus Porosity

Por-1



© Schlumberger

This chart gives a variety of formation resistivity factor-to-porosity conversions. The proper choice is best determined by laboratory measurement or experience in the area. In the absence of this knowledge, recommended relationships are the following:

For soft formations (Humble formula):

$$F_R = \frac{0.62}{\phi^{2.15}}, \text{ or } F_R = \frac{0.81}{\phi^2}$$

For hard formations:

$$F_R = \frac{1}{\phi^m}$$

with appropriate cementation factor, m.

Example: $\phi = 6\%$ in a carbonate in which a cementation factor, m, of 2 is appropriate

Therefore, from chart,

$$F_R = 280$$

Por

Isolated and Fracture Porosity

Por-1a

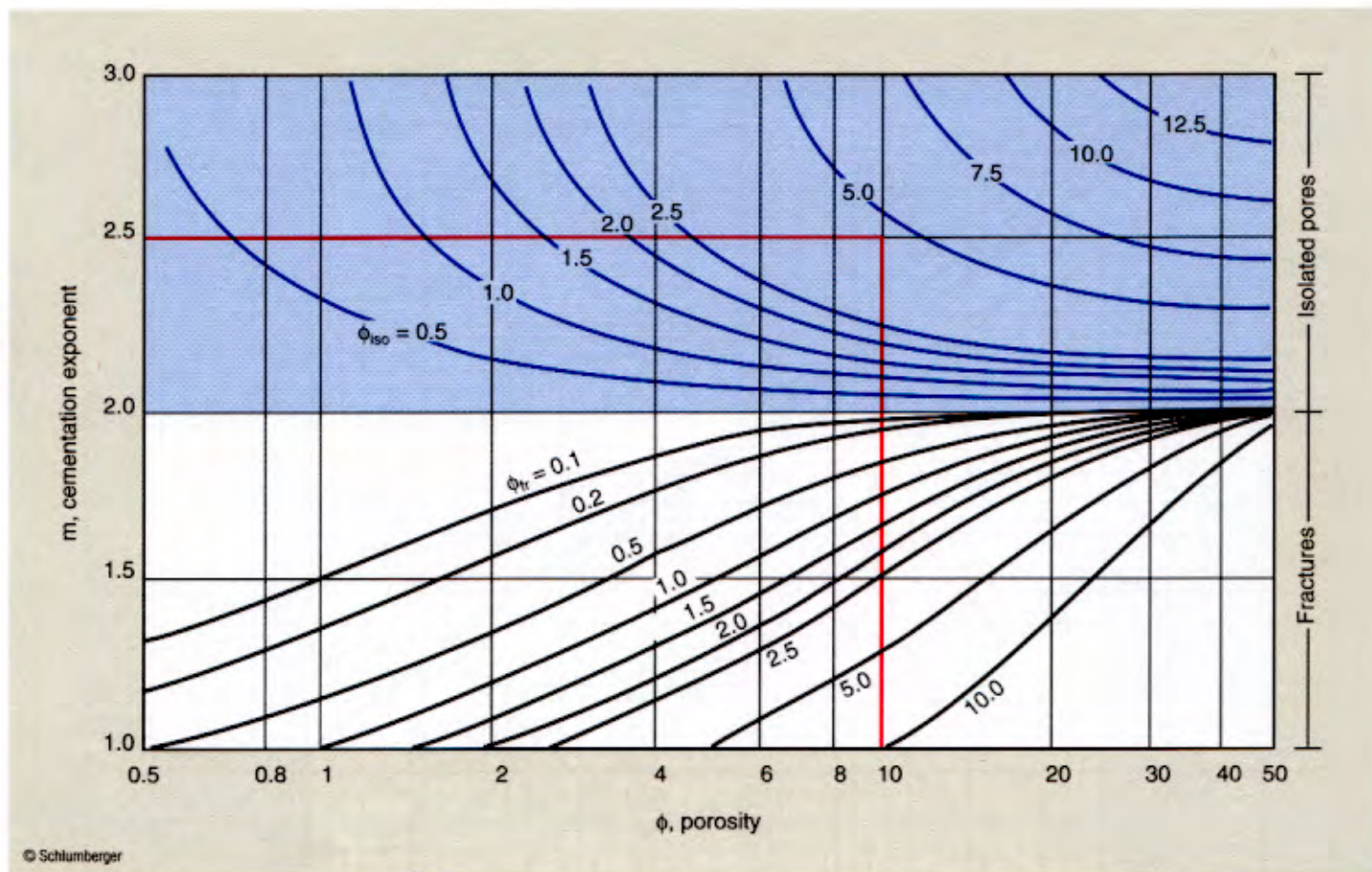


Chart Por-1a is based on a simplified model that assumes there is no contribution to formation conductivity from vugs and moldic porosity, and that the cementation exponent, m , of fractures is 1.0.

When the pores of a porous formation have an aspect ratio close to 1 (e.g., vugs or moldic porosity), the cementation exponent, m , of the formation will usually be greater than 2, while fractured formations generally have a cementation exponent less than 2.

If a value of m is available (from the interpretation of a log suite including a microresistivity measurement, such as a MicroSFL* log, and a dielectric measurement, such as an EPT* log, for example), Chart Por-1a can be used to estimate how much of the measured porosity is isolated porosity. In fractured

formations, the apparent m obtained from a microresistivity measurement assumes total flushing and provides an upper limit for the amount of fracture porosity in the rock.

Entering the chart with the porosity, ϕ , and cementation exponent, m , gives an estimate of either ϕ_{iso} , the amount of isolated porosity, or ϕ_{fr} , the porosity resulting from fractures.

Example: $\phi = 10$ p.u.

$$m = 2.5$$

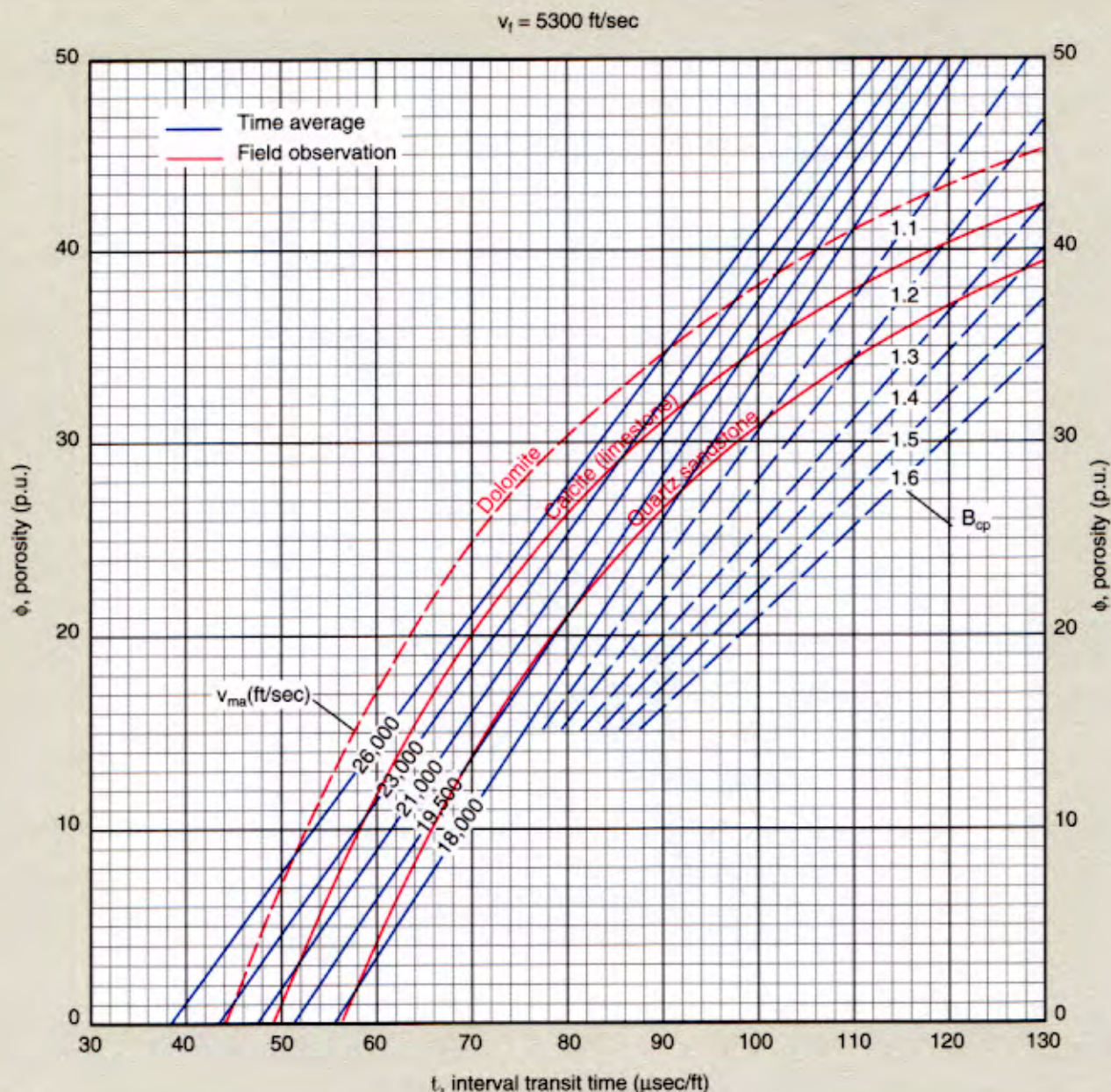
Therefore, $\phi_{iso} = 4.5$ p.u.

and intergranular porosity = $10 - 4.5 = 5.5$ p.u.

See Reference 39 for more information about the use of this chart, and Reference 40 for a discussion of spherical pores.

*Mark of Schlumberger

Porosity Evaluation from Sonic

Por-3
(English)

© Schlumberger

These two charts (Por-3) convert sonic log interval transit time, t , into porosity, ϕ . Two sets of curves are shown. The blue set employs a weighted-average transform. The red set is based on empirical observation (see Reference 20). For both, the saturating fluid is assumed to be water with a velocity of 5300 ft/sec (1615 m/sec).

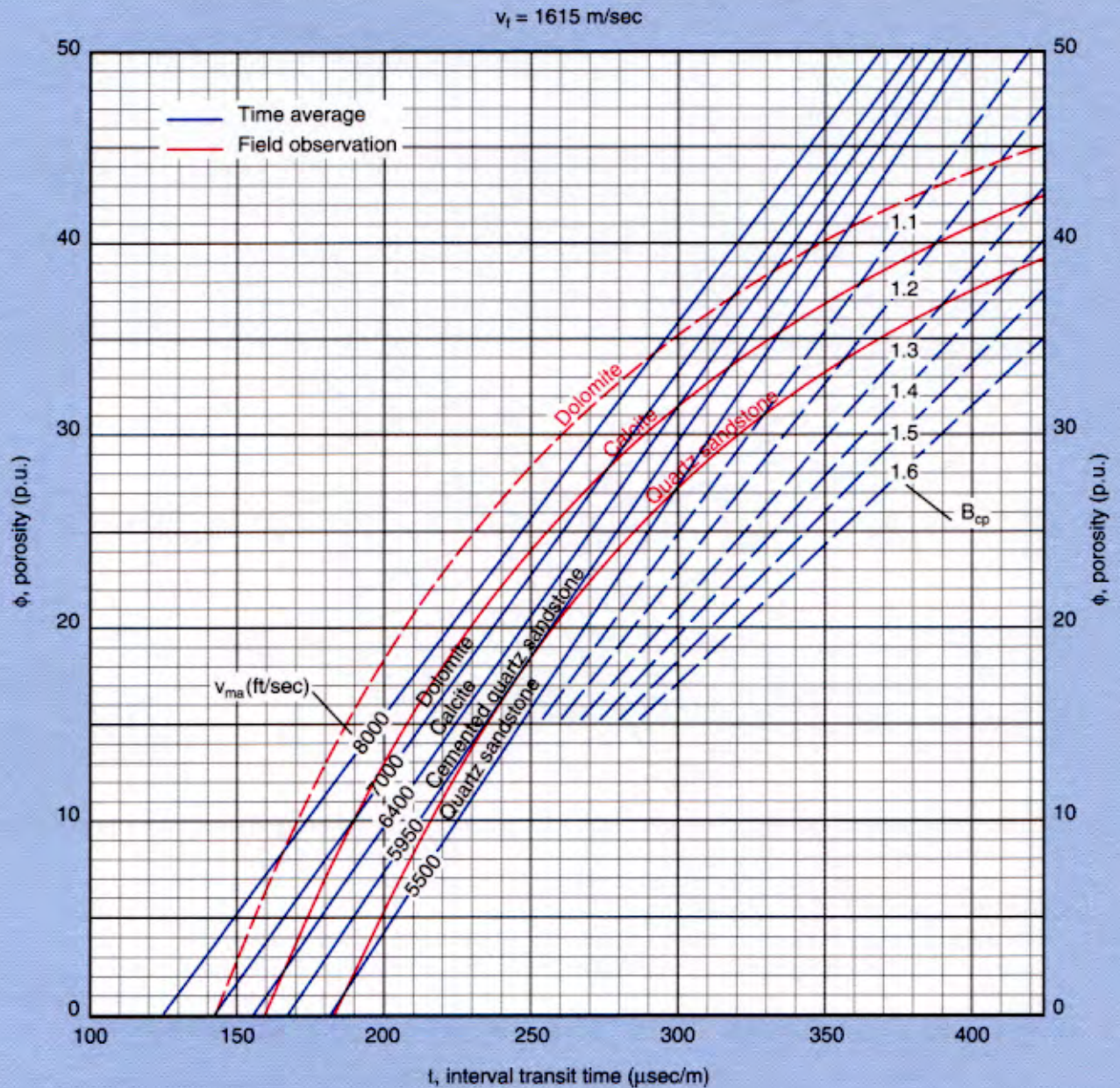
To use, enter the chart with the interval transit time from the sonic log. Go to the appropriate matrix velocity or lithology curve and read the porosity on the ordinate.

For rock mixtures such as limy sandstones or cherty dolomites, intermediate matrix lines may be required. When using the weighted-average transform in unconsolidated sand, a lack-of-compaction correction, B_{cp} , must be made. To accomplish this, enter the chart with the interval transit time; go to the appropriate compaction correction line, and read the porosity on the ordinate. If the compaction correction is unknown, it can be determined by working backward from a nearby clean water sand whose porosity is known.

Continued on next page

Porosity Evaluation from Sonic

Por-3m
(Metric)

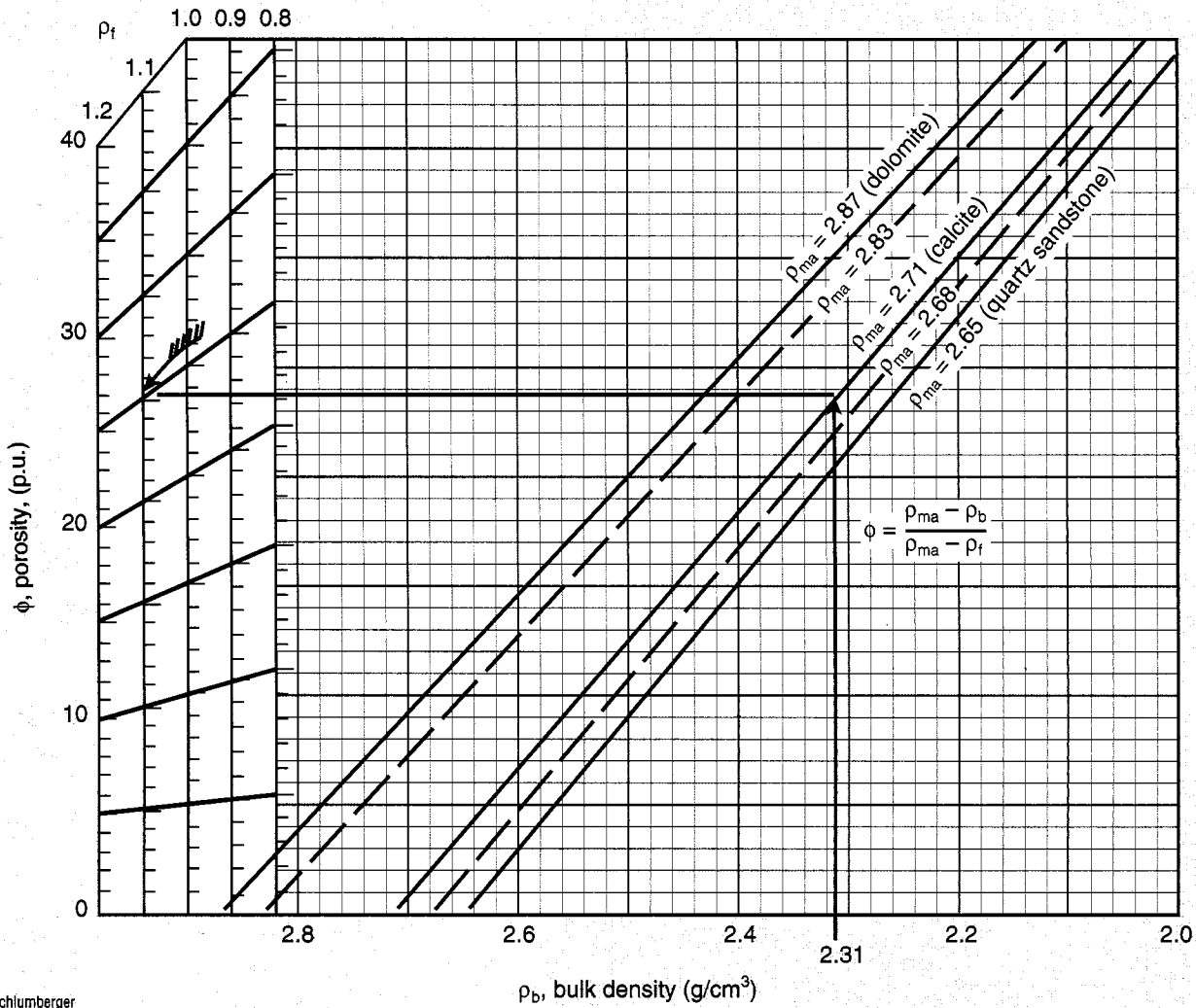


Example: $t = 76 \mu\text{sec/ft}$ [249 $\mu\text{sec/m}$]
 $v_{ma} = 19,500 \text{ ft/sec}$ [5950 m/sec]—sandstone
 Therefore, $\phi = 18\%$
 (by either weighted average or empirical transform)
 For more information see References 18, 19 and 20.

Lithology	v_{ma} (ft/sec)	t_{ma} ($\mu\text{sec/ft}$)	v_{ma} (m/sec)	t_{ma} ($\mu\text{sec/m}$)
Sandstones	18,000–19,500	55.5–51.3	5486–5944	182–168
Limestones	21,000–23,000	47.6–43.5	6400–7010	156–143
Dolomites	23,000–26,000	43.5–38.5	7010–7925	143–126

Formation Density Log Determination of Porosity

Por-5



Por

*Mark of Schlumberger
© Schlumberger

Bulk density, ρ_b, as recorded with the FDC* Compensated Formation Density or Litho-Density* logs, is converted to porosity with this chart. To use, enter bulk density, corrected for borehole size, in abscissa; go to the appropriate reservoir rock type and read porosity on the appropriate fluid density, ρ_f, scale in ordinate. (ρ_f is the density of the fluid saturating the rock immediately surrounding the borehole—usually mud filtrate.)

Example: ρ_b = 2.31 g/cm³ in limestone lithology
 ρ_{ma} = 2.71 (calcite)
 ρ_f = 1.1 (salt mud)
 Therefore, φ_D = 25 p.u.

Environmental Corrections to Formation Density Log, Litho-Density* Log and Sidewall Neutron Porosity Log

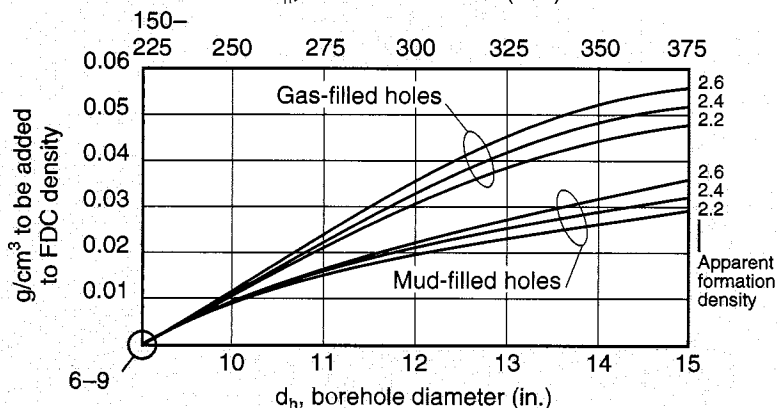
Por-15a

Under some circumstances, the FDC* Compensated Formation Density log and Litho-Density log must be corrected for borehole size, and the SNP sidewall neutron log must be corrected for mudcake thickness. These charts provide those corrections.

For the FDC log, enter the chart with borehole diameter, d_h . Go to the apparent formation density, ρ_b (FDC log density reading), and read, in ordinate, the correction to be added to the FDC log density reading.

FDC Borehole Correction

d_h , borehole diameter (mm)



Example: $d_h = 12$ in.

$\rho_b = 2.20$ g/cm³ (mud-filled borehole)

Therefore, correction = 0.02 g/cm³

$\rho_{bcor} = 2.20 + 0.02 = 2.22$ g/cm³

For the LDT log, enter the chart abscissa with the product of the borehole diameter, d_h , less 8 in. [200 mm] and the LDT density reading, ρ_b , less mud density, ρ_m . Read, in ordinate, the correction to be added to the Litho-Density bulk density reading.

Example: $d_h = 325$ mm

$\rho_b = 2.45$ g/cm³

$\rho_m = 1.05$ g/cm³

giving $(d_h - 200)(\rho_b - \rho_m) =$

$(325 - 200)(2.45 - 1.05) = 175$

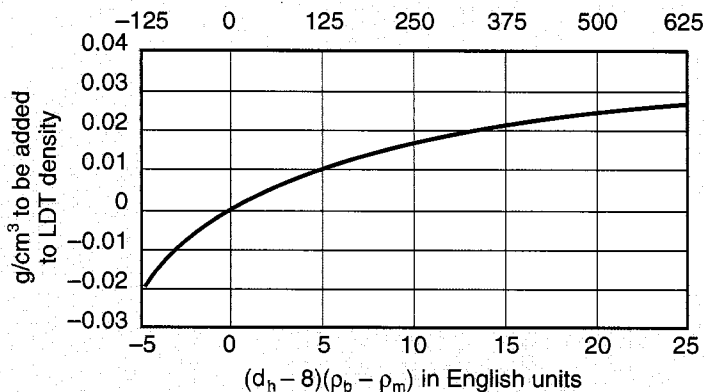
Therefore, correction = 0.014 g/cm³

$\rho_{bcor} = 2.45 + 0.014 = 2.464$ g/cm³

Note: If the borehole diameter from the FDC or LDT caliper is less than bit size, use the bit size in the above charts.

Litho-Density Borehole Correction

$(d_h - 200)(\rho_b - \rho_m)$ in metric units



For the SNP log, enter the bottom of the chart with the SNP apparent porosity, ϕ_{SNP} ; go vertically to the bit size minus caliper reading value; then, follow the diagonal curves to the top edge of the chart to obtain the corrected SNP apparent porosity.

Example: $\phi_{SNP} = 13$ p.u.

Caliper = $7\frac{5}{8}$ in.

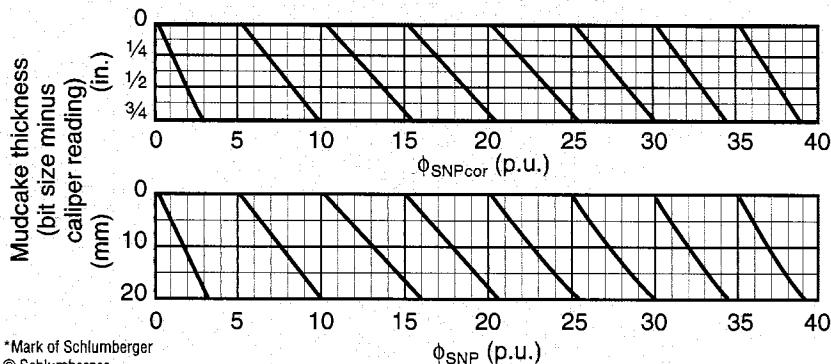
Bit size = $7\frac{7}{8}$ in.

giving Bit size - caliper = $7\frac{7}{8} - 7\frac{5}{8} = \frac{1}{4}$ in.

Therefore, $\phi_{SNPcor} = 11.3$ p.u.

Note: The full borehole diameter reduction shown on the SNP caliper is used as mudcake thickness, since the SNP backup shoe usually cuts through the mudcake.

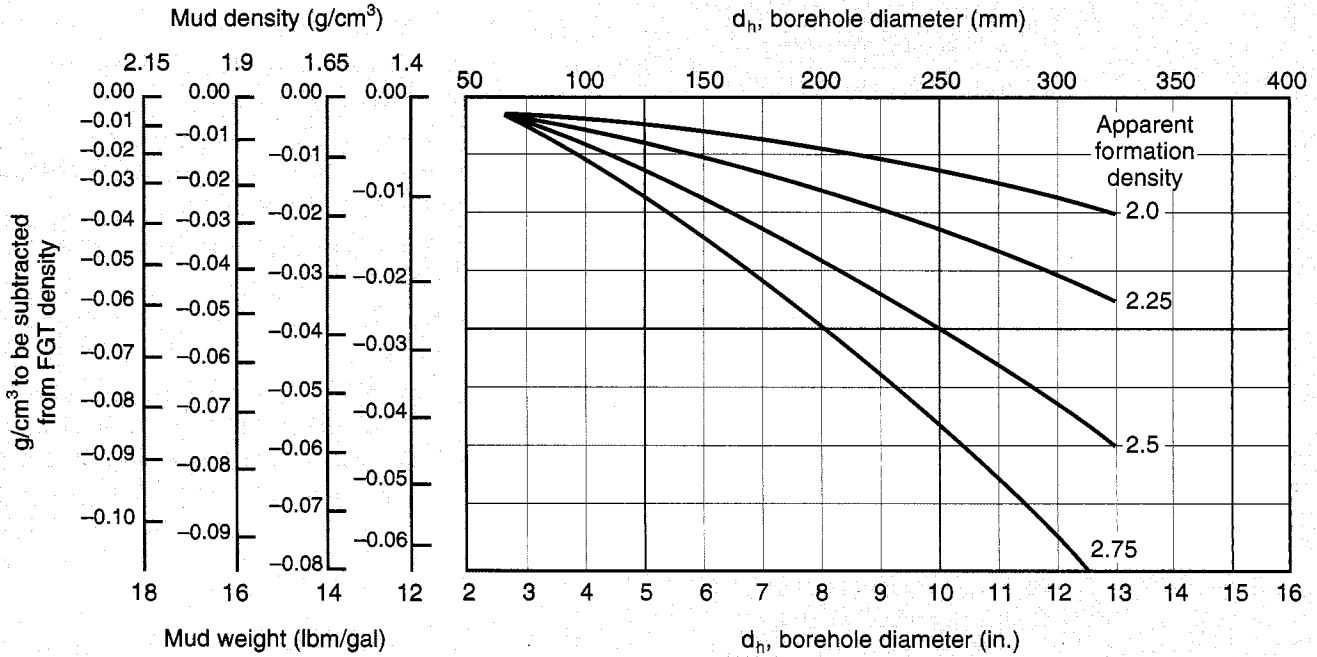
SNP Mudcake Correction



*Mark of Schlumberger
© Schlumberger

Environmental Corrections to FGT Density Log

FGT borehole correction



*Mark of Schlumberger
© Schlumberger

Borehole corrections of the slimhole 2³/₄-in. FGT formation density log can be made automatically by the logging unit. To determine if corrections have been made, refer to the log. "ALLO" (for allowed) following the constant "MWCO" indicates the FGT log was recorded with borehole correction. "DISA" (for disallowed) indicates that no borehole corrections were made.

In case the FGT log was recorded without automatic borehole correction, this chart provides the correction. Enter the chart abscissa with borehole diameter. Go to the apparent formation

density and read in ordinate, as a function of mud weight, the correction to be subtracted from the FGT log bulk density reading.

Example: $\rho_b = 2.53 \text{ g/cm}^3$

$d_h = 260 \text{ mm}$

Mud density = 1.65 g/cm^3

Therefore, correction = -0.040 g/cm^3

$\rho_{bcor} = 2.53 - 0.040 = 2.49 \text{ g/cm}^3$

Por

Dual-Spacing CNL* Compensated Neutron Log Charts

This section contains interpretation charts to cover the latest developments in CNL Compensated Neutron Log porosity transforms, environmental corrections, and porosity and lithology determination.

CSU software (versions CP-30 and later) and MAXIS* software compute three thermal porosities: NPFI, TNPH and NPOR.

NPFI is our "classic NPFI," computed from instantaneous near and far count rates, using "Mod-8" ratio-to-porosity transform with a caliper correction.

TNPH is computed from deadtime-corrected, depth- and resolution-matched count rates, using an improved ratio-to-porosity transform and performing a complete set of environmental corrections in real time. These corrections may be turned on or off by the field engineer at the wellsite. For more information see Reference 32.

NPOR is computed from the near-detector count rate and TNPH to give an enhanced resolution porosity. The accuracy of NPOR is equivalent to the accuracy of TNPH if the environmental effects on the near detector change less rapidly than the formation porosity. For more information on enhanced resolution processing, see Reference 35.

Cased hole CNL logs are recorded on NPFI, computed from instantaneous near and far count rates, with a cased hole ratio-to-porosity transform. Chart Por-14a should be used for environmental corrections.

Using the neutron correction charts

For logs labeled NPFI:

1. Enter Chart Por-14e with NPFI and caliper reading to convert to uncorrected neutron porosity.
2. Enter Charts Por-14c and -14d to obtain corrections for each environmental effect. Corrections are summed with the uncorrected porosity to give a corrected value.
3. Enter corrected porosity in Chart Por-13b for conversion to sandstone or dolomite.
4. Use Crossplots CP-1e, -1f, -2c and -2cm for porosity and lithology determination.

For logs labeled TNPH or NPOR, the CSU/MAXIS software has applied environmental corrections as indicated on the log heading. Refer to Charts Por-14c and -14d to gain an appreciation for the relative importance of each correction prior to using crossplot charts. If the CSU/MAXIS software has applied all corrections, TNPH or NPOR can be used directly with the crossplot charts. In this case, follow these steps:

1. Enter TNPH or NPOR in Chart Por-13b for conversion to sandstone or dolomite.
2. Use Crossplots CP-1e, -1f, -2c and -2cm to determine porosity and lithology.

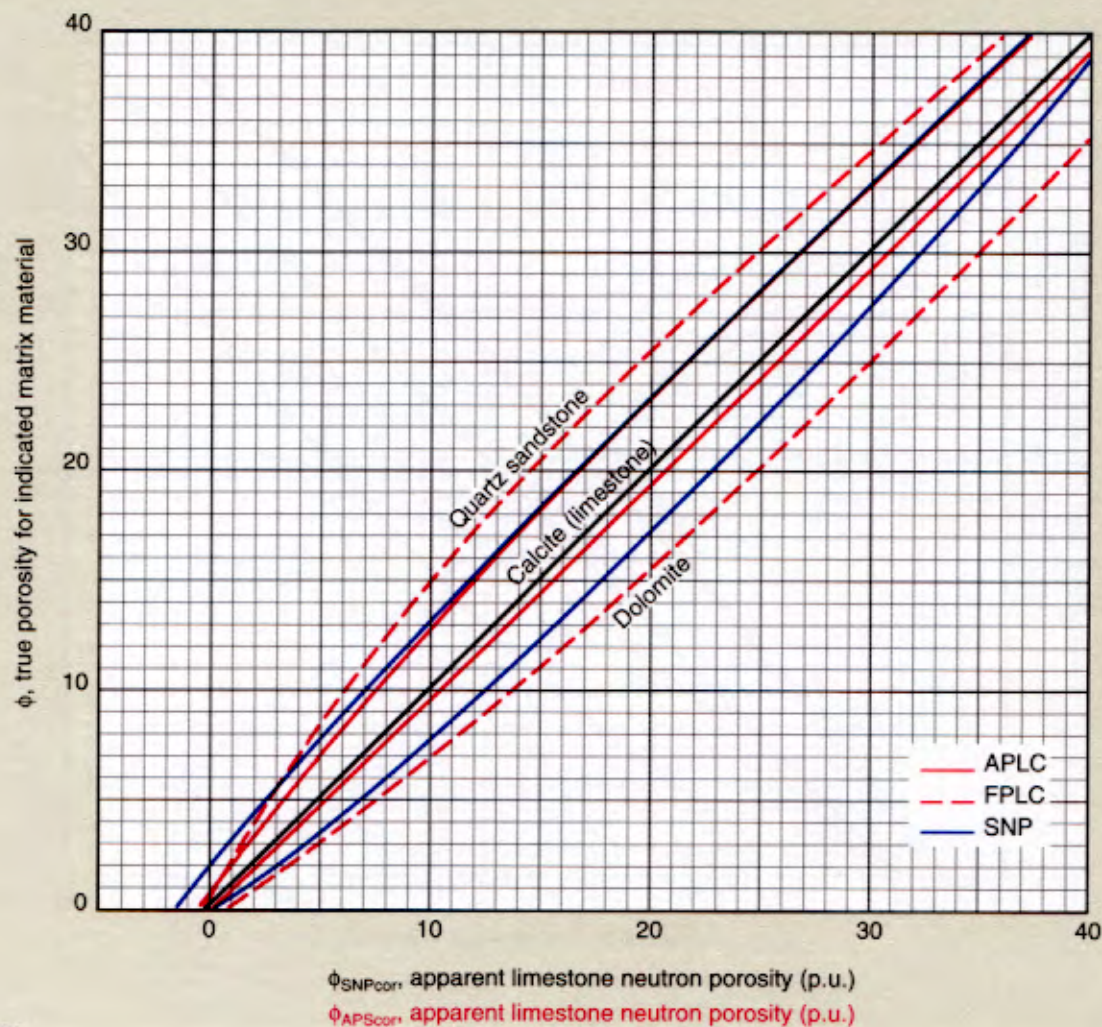
*Mark of Schlumberger

Epithermal Neutron Porosity Equivalence Curves

Sidewall Neutron Porosity (SNP) log;

Accelerator Porosity Sonde (APS) Near-to-Array (APLC) and Near-to-Far (FPLC) logs

Por-13a



When the APS or SNP log is recorded in limestone porosity units, this chart is used to find porosity in sandstones or dolomites. First, correct the SNP log for mudcake thickness (Chart Por-15a).

This chart can also be used to find apparent limestone porosity (needed for entering the various CP crossplot charts) if the APS or SNP recording is in sandstone or dolomite porosity units.

Example: Sandstone bed

$\phi_{\text{SNP}} = 13$ p.u. (apparent limestone porosity)

Bit size = $7\frac{7}{8}$ in.

SNP caliper = $7\frac{1}{2}$ in.

giving $h_{\text{mc}} = \frac{1}{4}$ in.

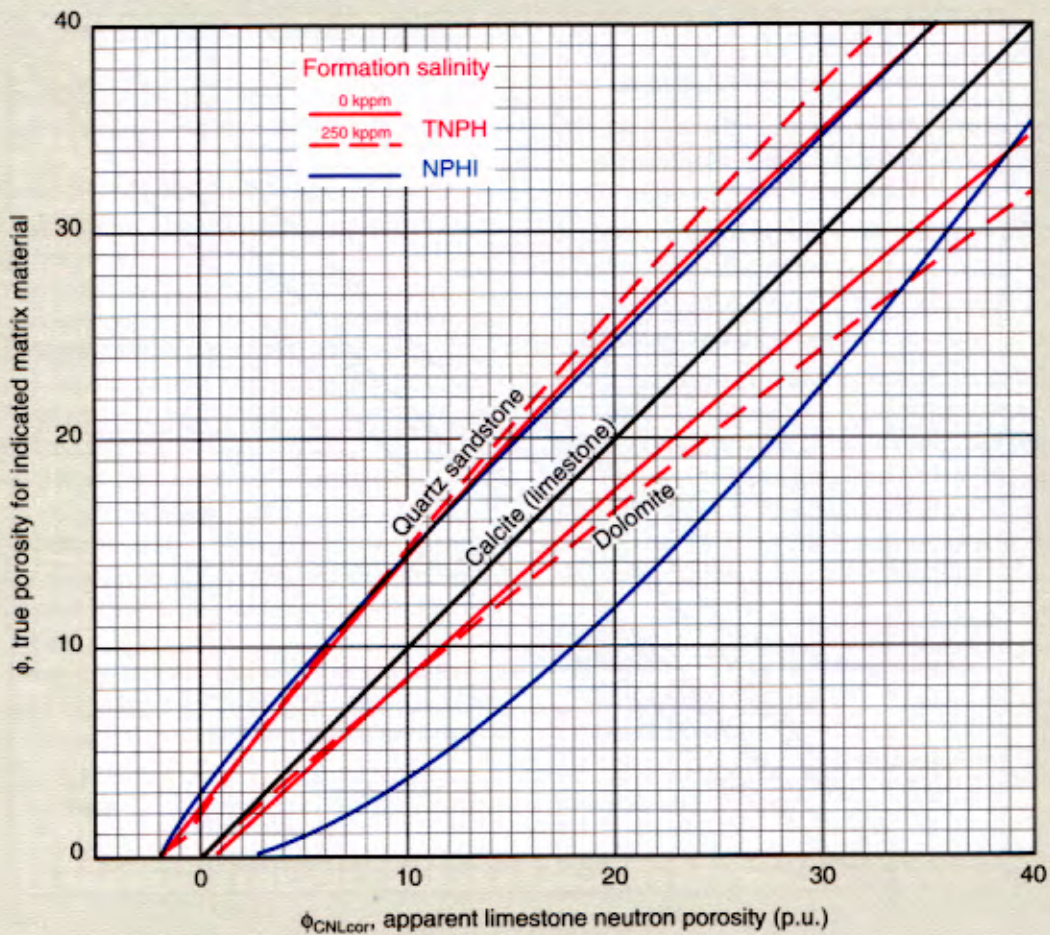
$\phi_{\text{SNP}} = 11.3$ p.u. (corrected for mudcake)

and $\phi_{\text{SNP}}(\text{sandstone}) = 14.5$ p.u.

Thermal Neutron Porosity Equivalence Curves

CNL * Compensated Neutron Log; TNPH and NPHI porosity logs

Por-13b



*Mark of Schlumberger
© Schlumberger

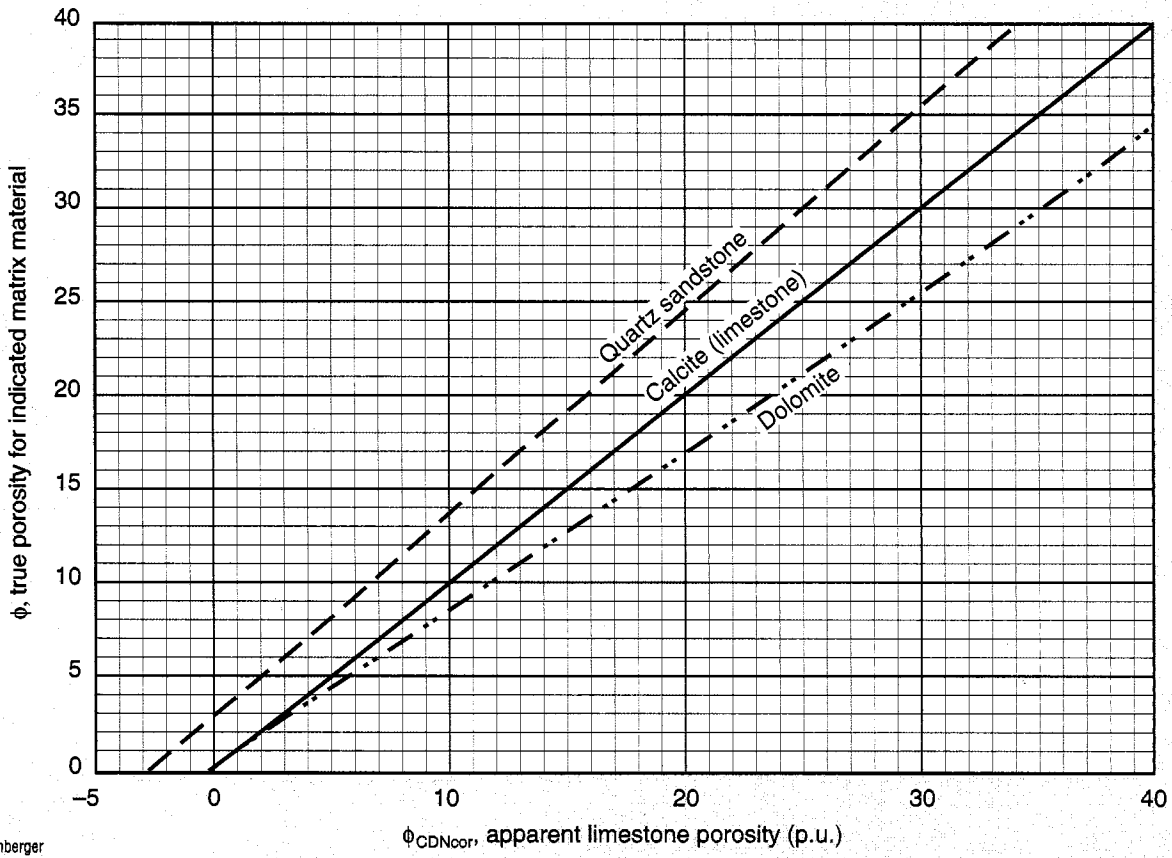
Chart Por-13b can be used in the same way as Chart Por-13a, on the previous page, to convert CNL porosity logs (TNPH or NPHI) from one lithology to another. If a log is recorded in limestone porosity units in a pure quartz sandstone formation, the true porosity can be derived.

Example: Quartz sandstone formation
 TNPH = 18 p.u. (apparent limestone porosity)
 Formation salinity = 250 kppm
 giving True porosity in sandstone = 24 p.u.

LWD Neutron Porosity Equivalence Curves

6.5-in. CDN* Compensated Density Neutron tool

Por-21



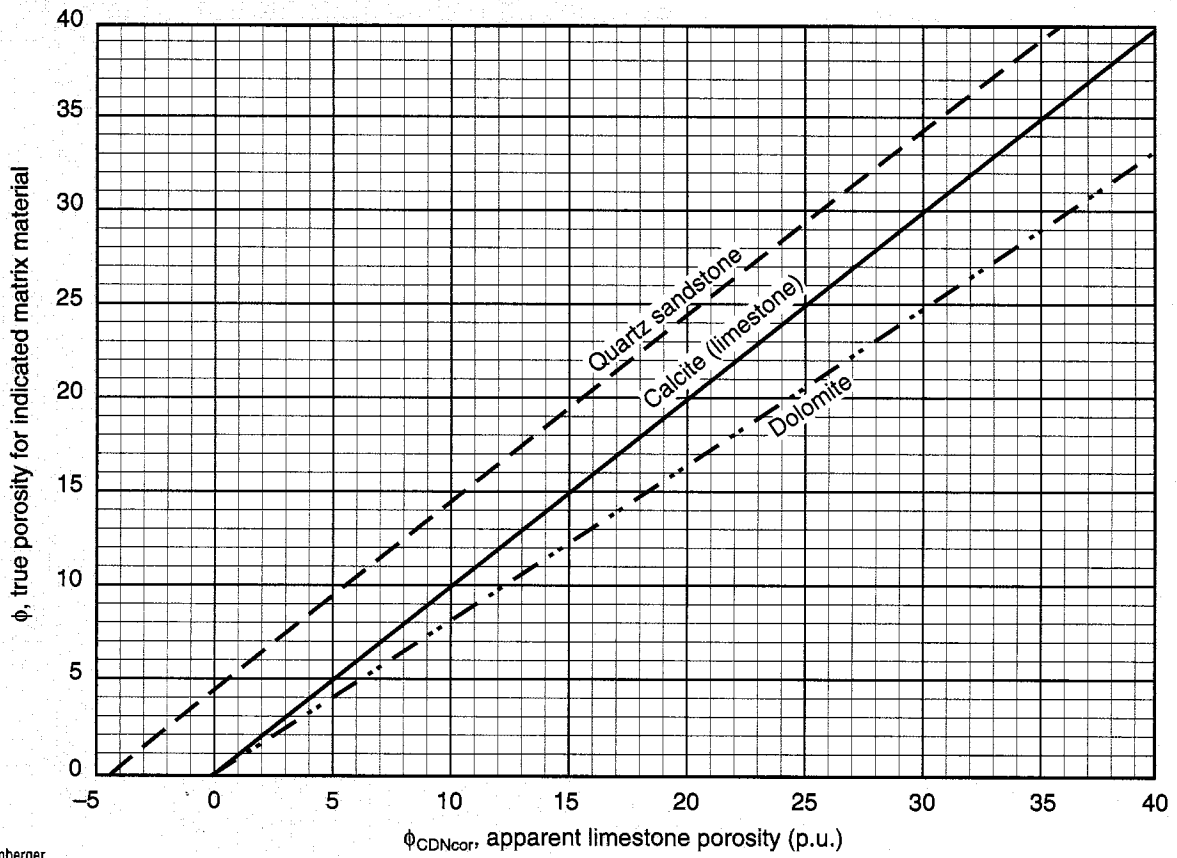
*Mark of Schlumberger
© Schlumberger

Por

LWD Neutron Porosity Equivalence Curves

8-in. CDN* Compensated Density Neutron tool

Por-25

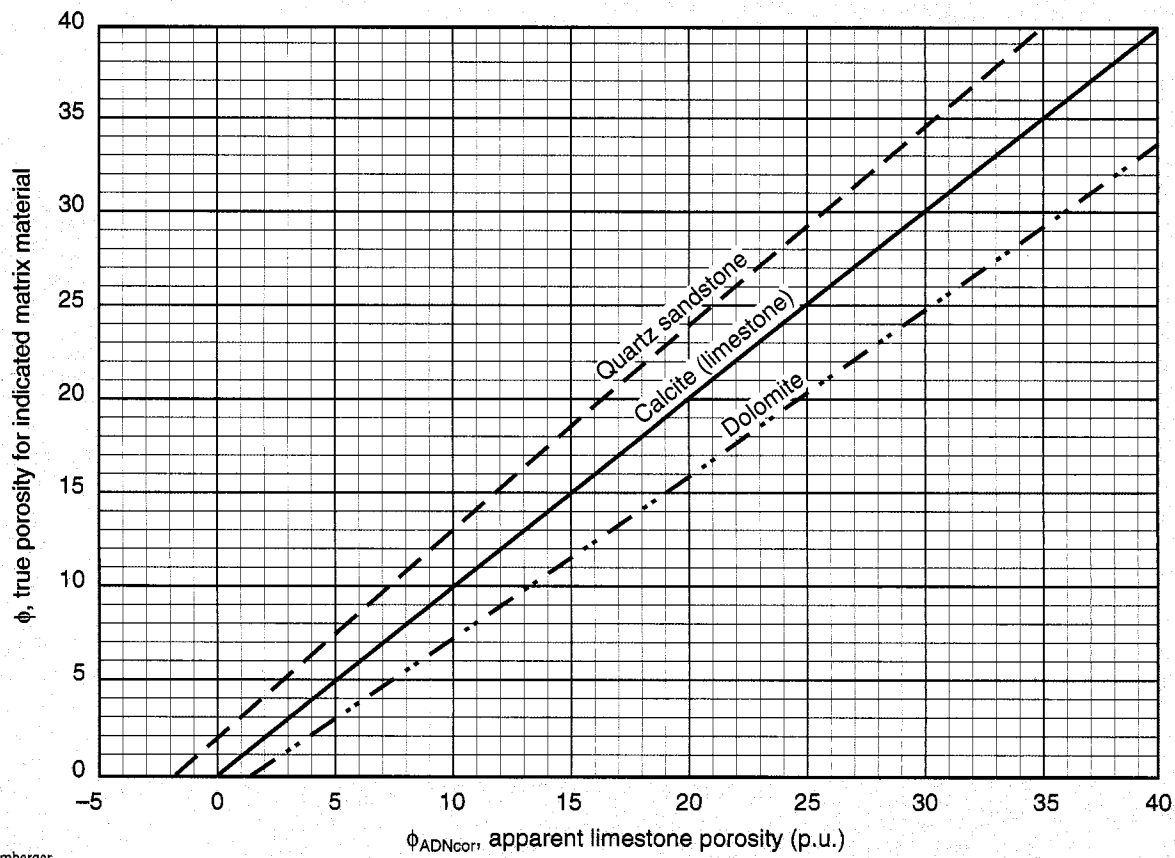


*Mark of Schlumberger
© Schlumberger

LWD Neutron Porosity Equivalence Curves

6.75-in. ADN* Azimuthal Density Neutron tool

Por-27



*Mark of Schlumberger
© Schlumberger

Por

Dual-Spacing CNL* Compensated Neutron Log Environmental Corrections for Cased Hole

The nomographs of Charts Por-14 provide environmental corrections for the CNL Compensated Neutron Log when run in cased hole or openhole. Before using the nomographs, CNL log values must be corrected for matrix effect (Chart Por-13b).

Cased hole (Chart Por-14a)

For cased hole logs, enter the appropriate Chart Por-14a with the matrix-corrected CNL reading; draw a vertical line through the chart blocks. Find the corrections, relative to the reference lines (dashed lines indicated with asterisks), for each block. Then, go to Chart Por-14c, and starting with the borehole salinity block, continue through the remaining blocks. Algebraically sum all the corrections to obtain the correction to the CNL reading.

Example: $\phi_{\text{CNL}} = 27$ p.u. (matrix corrected)

Borehole size = 10 in.

Casing thickness = 0.255 in.

Cement thickness = 1.4 in.

giving $\Sigma\Delta\phi = -1.0 + 0.3 + 0.5 + \dots$

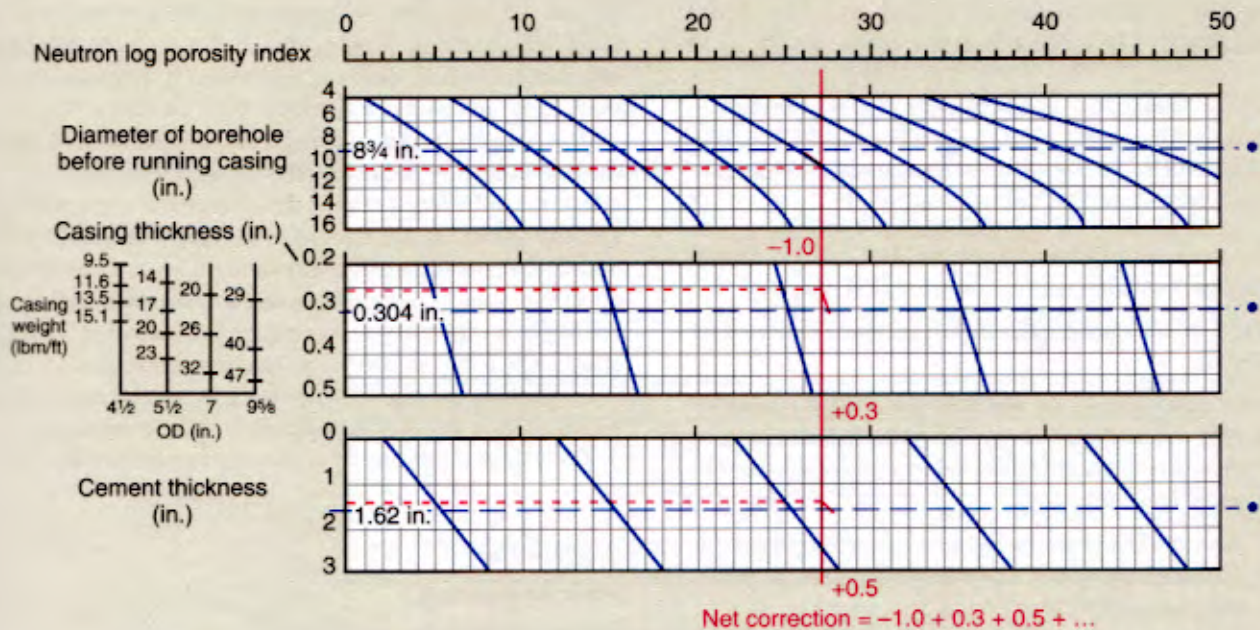
This provides casing, cement and borehole corrections for the cased hole CNL log. Continue to Chart Por-14c for salinity, borehole fluid, pressure and temperature corrections.

*Mark of Schlumberger

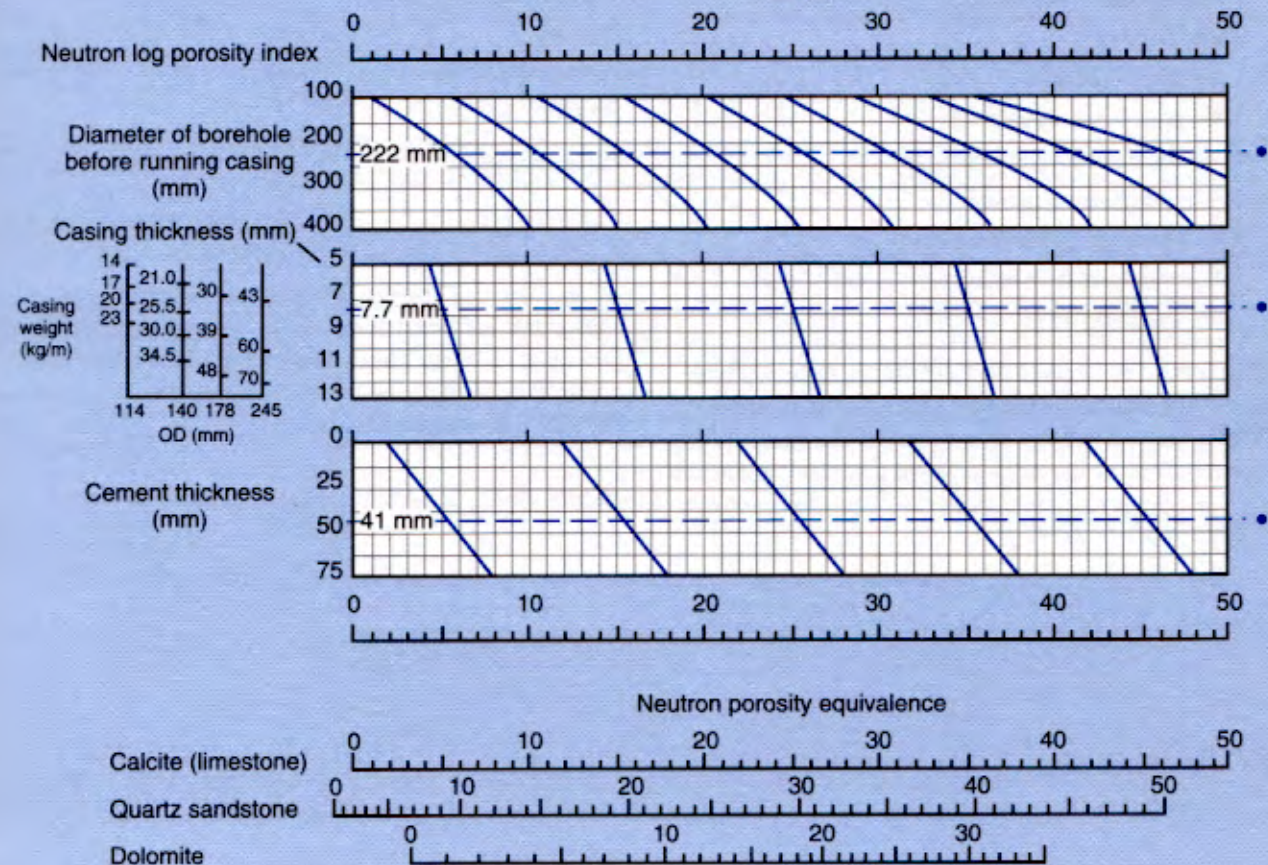
Dual-Spacing CNL* Compensated Neutron Log Correction Nomograph for Cased Hole

Por-14a

English



Metric



*Mark of Schlumberger
© Schlumberger

• Reference lines indicated by bullets

Dual-Spacing CNL* Compensated Neutron Log Correction Nomograph for Openhole

The CNL tool is normally run with only a caliper correction applied. Refer to the CNL log heading to determine whether the log was run with or without automatic caliper correction. To use Charts Por-14c and -14d, this borehole correction must be removed.

The way the "automatic" borehole correction is "backed out" depends on whether the NPHI or TNPH and NPOR curves are used. With NPHI, the correction is backed out with Chart Por-14e. For TNPH or NPOR, follow these steps:

1. Enter the top block of Chart Por-14c or -14d, labeled "actual borehole size," with the matrix-corrected CNL porosity.
2. Go to the 8-in. standard condition borehole size indicated by the bullet (•).
3. Follow the trend lines to the borehole size used to correct the log—usually the caliper reading. This value is the uncorrected TNPH value, which should be used to determine the rest of the environmental corrections.

Example: Assume TNPH on the log was 32 p.u. (apparent limestone units) in a 12-in. borehole. This gives an uncorrected TNPH of 34 p.u.

The rest of the example assumes the following:

- Uncorrected neutron porosity = 34 p.u. (apparent limestone units)
- 12-in. borehole
- ¼-in. thick mudcake
- 100-kppm borehole salinity
- 11-lbm/gal mud weight (natural mud)
- 150°F borehole temperature
- 5-kpsi pressure (water-base mud)
- 100-kppm formation salinity
- ½-in. standoff

Enter Charts Por-14c, -14cm, -14d and -14dm at the top with the uncorrected log reading in apparent limestone units, and project a line downward through all the correction nomographs. For each correction, enter the environmental parameter at the left

of the nomograph and project a line to the right. Then, follow the trend lines from the intersection of the uncorrected porosity reading and the environmental parameter to the intersection of the trend line and the standard condition (for example, for the borehole size correction, the trend line would be followed downward from 12 in. and 34 p.u. to intersect the 8-in. line at 32 p.u.).

The porosity reading where the trend line intersects the standard conditions is the corrected porosity considering only that effect; the difference between the corrected and uncorrected porosity values, or $\Delta\phi$, represents the magnitude of the correction for each environmental effect. Since several environmental effects are usually made, a net correction to the uncorrected log reading is computed by summing the individual $\Delta\phi$'s for all effects. Once the net correction has been determined, it is added to the uncorrected log value to obtain the environmentally corrected neutron porosity in apparent limestone units.

For the conditions listed above, the corrections are

	$\Delta\phi$
Borehole size	-2¾ p.u.
Mudcake thickness	≈0
Borehole salinity	+1
Mud weight	+1½
Borehole temperature	+4
Pressure	-1
Formation salinity	-3
Standoff	-2
Net correction	-2¼
Corrected porosity	34 p.u. - 2¼ p.u. = 31¾ p.u. (apparent limestone units)

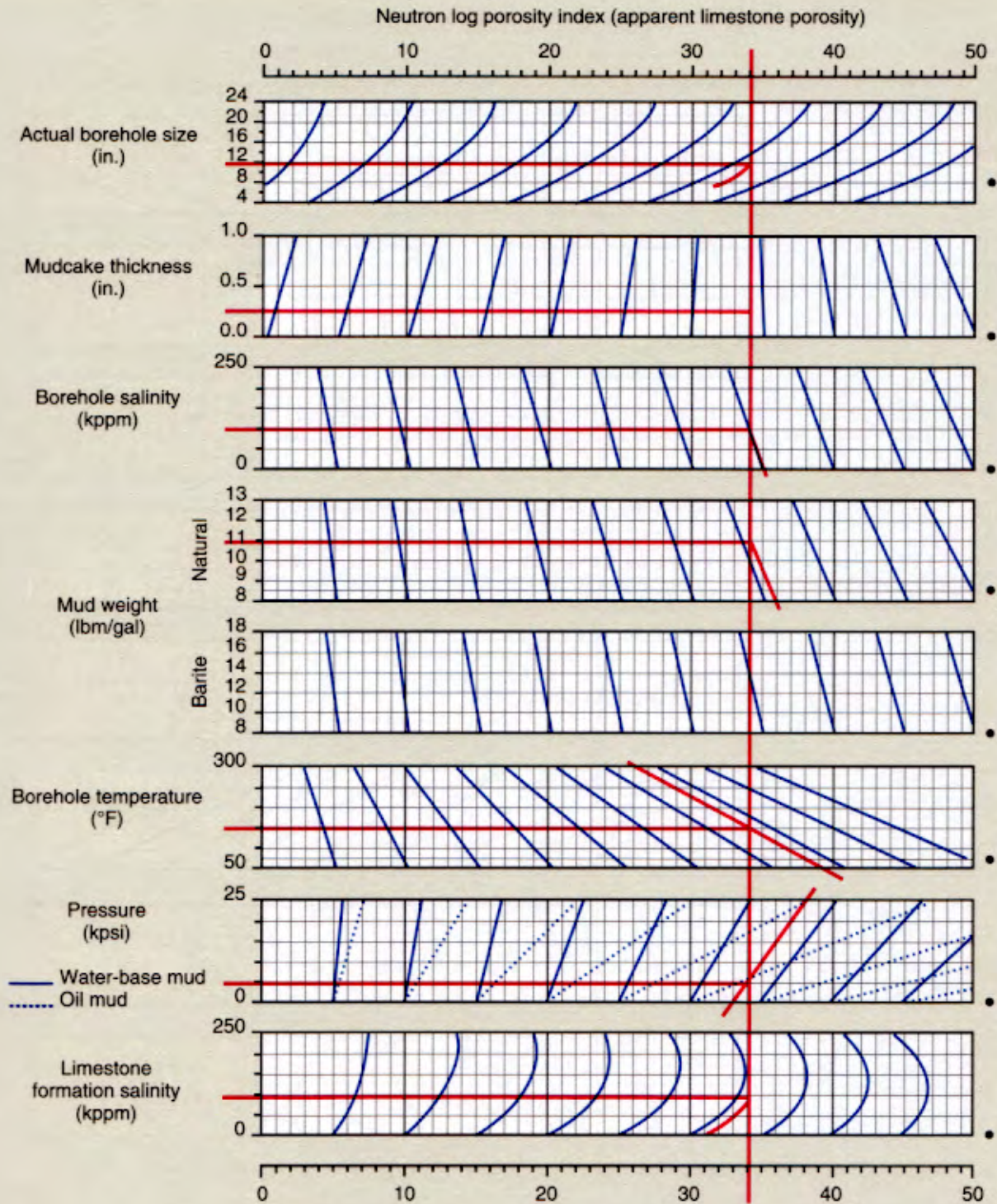
The "oil mud" curves in the pressure correction panel are appropriate for liquid components whose compressibility is four times that of water. The correction for other cases can be obtained by multiplying the WBM correction by the ratio of the OBM/WBM compressibilities.

*Mark of Schlumberger

Dual-Spacing CNL* Compensated Neutron Log Correction Nomograph for Openhole

For CNL curves without environmental corrections

Por-14c
(English)



*Mark of Schlumberger
© Schlumberger

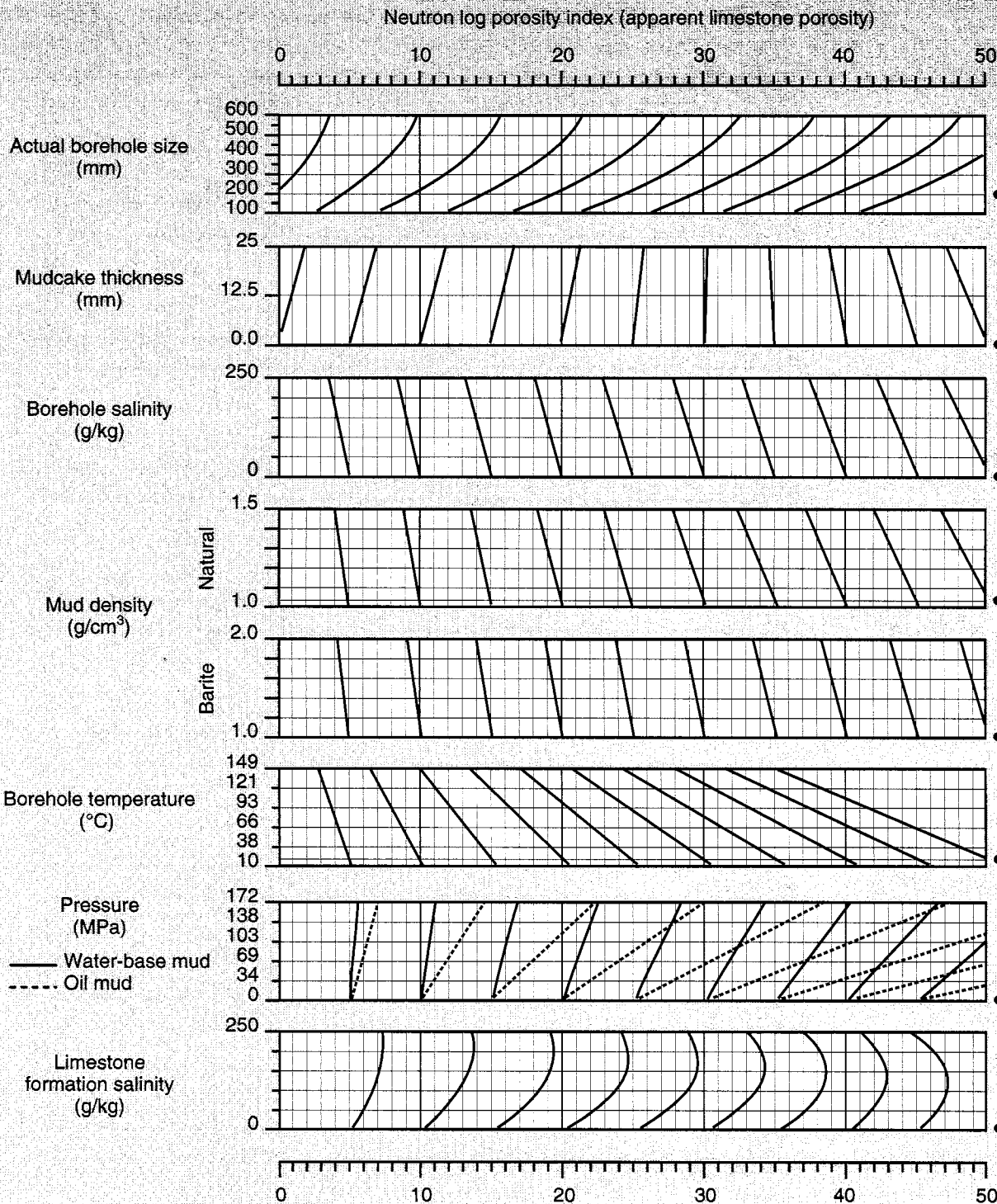
• Standard conditions

Por

Dual-Spacing CNL* Compensated Neutron Log Correction Nomograph for Openhole

For CNL curves without environmental corrections

Por-14cm
(Metric)

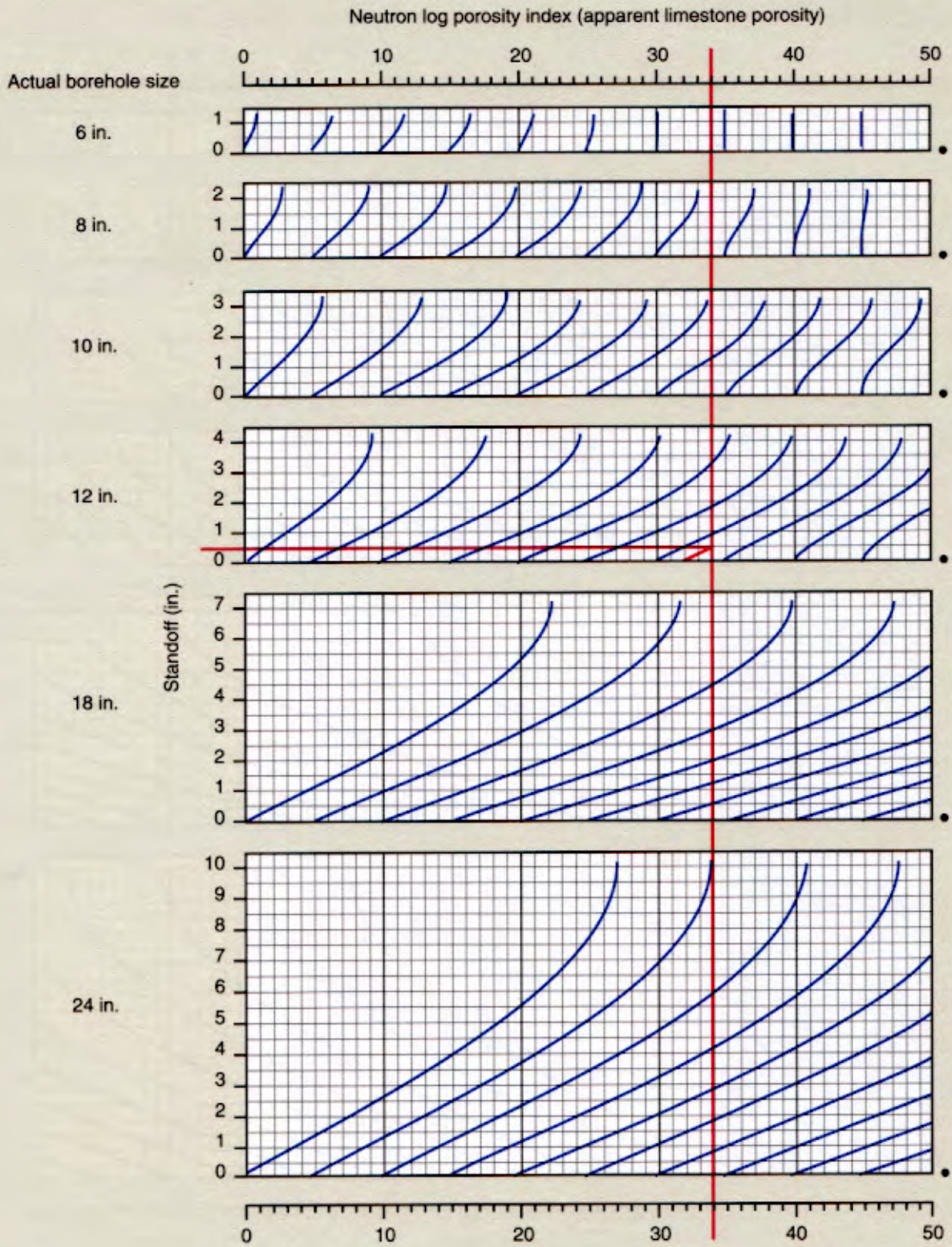


*Mark of Schlumberger
© Schlumberger

Dual-Spacing CNL* Compensated Neutron Log Standoff Correction Nomograph for Openhole

For CNL curves without environmental corrections

Por-14d
(English)



• Standard conditions

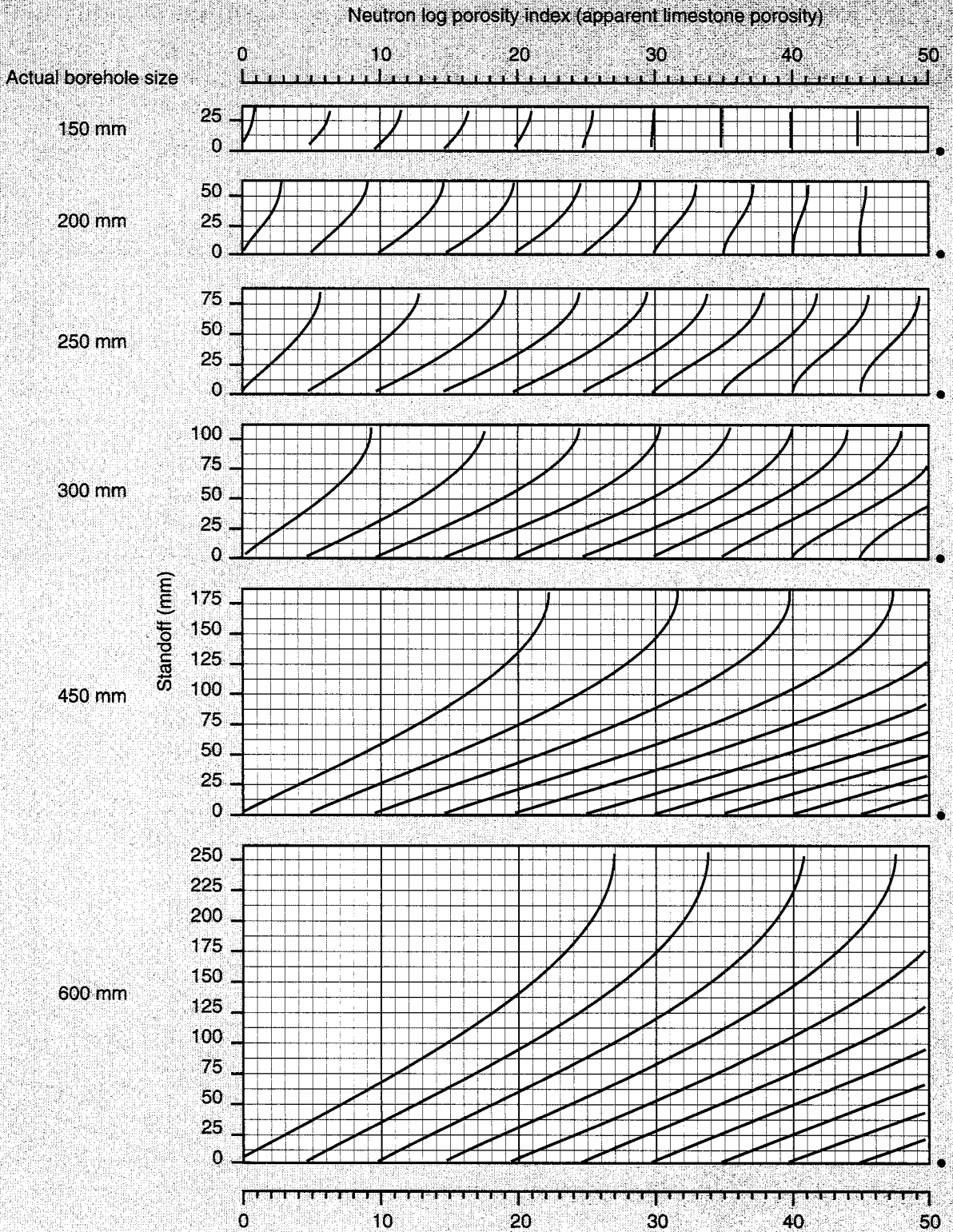
*Mark of Schlumberger
© Schlumberger

Por

Dual-Spacing CNL* Compensated Neutron Log Standoff Correction Nomograph for Openhole

For CNL curves without environmental corrections

Por-14dm
(Metric)

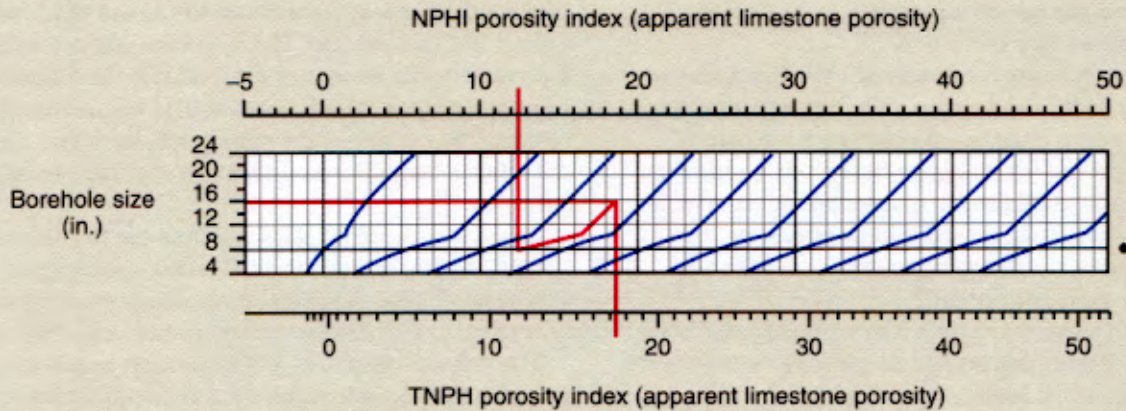


• Standard conditions

*Mark of Schlumberger
© Schlumberger

Dual-Spacing CNL* Compensated Neutron Log NPHI-TNPH Conversion Nomograph for Openhole

Por-14e



*Mark of Schlumberger
© Schlumberger

• Standard conditions

Por

Example: NPHI = 12.5 p.u.
Caliper = 16 in.

Enter the chart from the top at 12.5 p.u.; drop down to 7⁷/₈-in. hole size, labeled with a bullet (•) for standard conditions. Follow the trend lines upward to 16 in. From that point drop straight down to the TNPH scale and read the uncorrected TNPH = 17.25 p.u.

If NPHI is recorded in units other than limestone units, it must be converted using Chart Por-13 before it can be used in this chart. The NPHI scale is for use with logs recorded after January 1976.

Accelerator Porosity Sonde (APS) Corrections

Openhole APLU and FPLU logs

Epithermal neutron detection with borehole-shielded detectors considerably reduces the environmental effects on the APS response and simplifies their correction.

The near-to-array porosity measurement (APLU in apparent limestone porosity units) and the near-to-far porosity measurement (FPLU in apparent limestone porosity units) require different mud weight and borehole size corrections, so there are individual sets of correction nomographs for each measurement. Formation temperature, pressure and salinity effects are, however, the same on each measurement, so there is only one set of nomographs for these corrections.

Chart Por-23a includes corrections for mud weight and borehole size for near-to-array and near-to-far porosity measurements in both English and metric units.

The borehole size correction is slightly mudweight dependent, even with natural muds, so there are two sets of splines—solid lines for light muds (8.345 lbm/gal) and dashed lines for heavy muds (16 lbm/gal). Intermediate mud weights can be interpolated.

The nomograph for formation temperature, pressure and formation salinity correction of both APLU and FPLU curves appears in Chart Por-23b. The formation salinity correction is dependent on the amount of salt (NaCl) in the formation. This is a function of both the salinity of fluid in the formation and its volume. The last part of the nomograph, therefore, applies to the correction a multiplier proportional to the true porosity of the formation.

Standoff between the APS detectors and the formation is computed from measurements acquired while logging. This real-time standoff measurement allows realistic standoff corrections to be made to the porosity measurements for the first time.

The standoff correction is automatically applied during acquisition but is difficult to represent accurately on two-dimensional charts. No standoff correction charts are currently available, so the automatic correction should be used.

Continued on next page

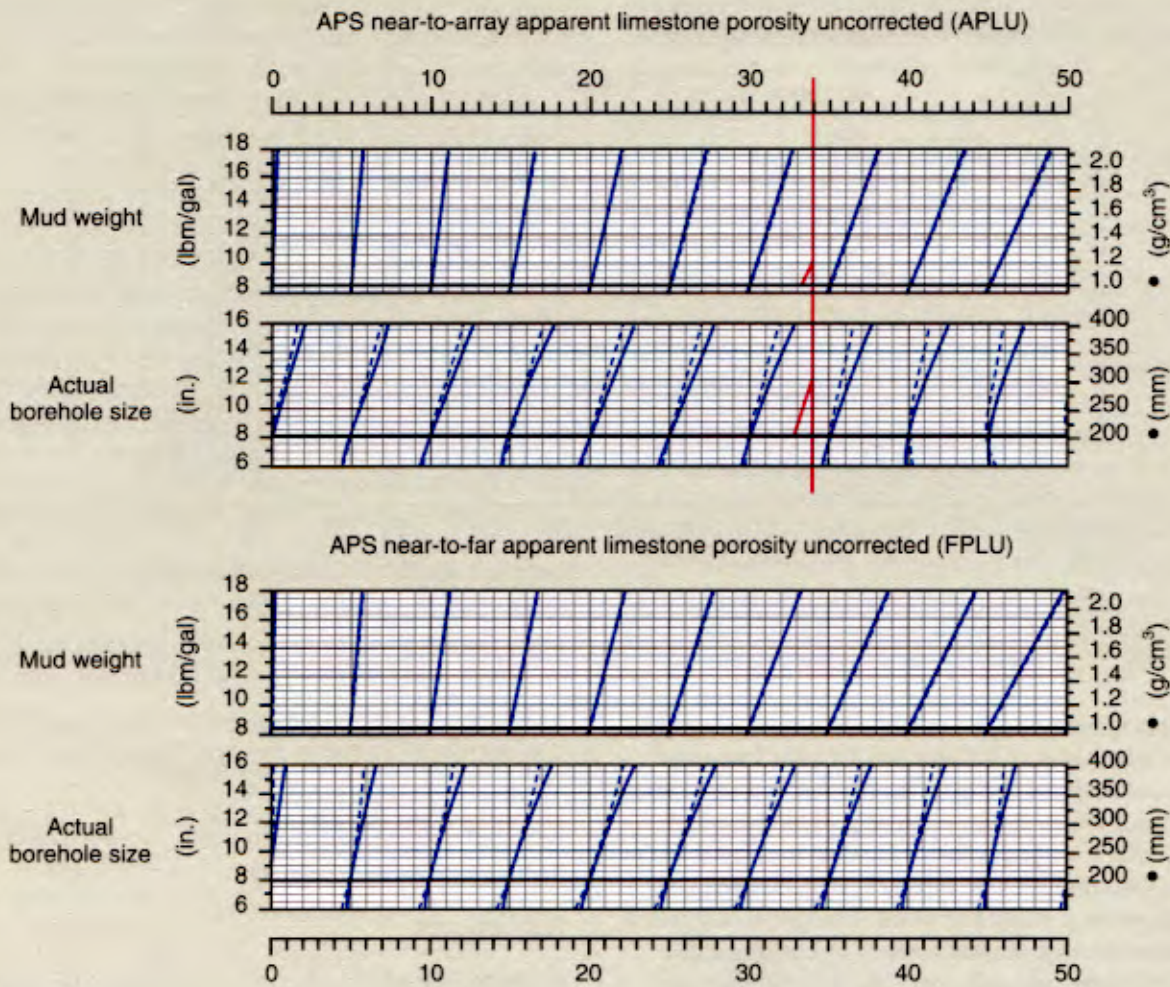
Por

Openhole APS Corrections for Mud Weight and Borehole Size

For APLU and FPLU curves without environmental correction

Por-23a

Por



© Schlumberger

Charts Por-23a and -23b are used to apply environmental corrections to APLU and FPLU measurements.

Enter at the top of each nomograph on Chart Por-23a with the relevant uncorrected log reading in apparent limestone units and project a line down through the nomographs. For each correction to be applied, enter the environmental parameter at the left of the nomograph if using English units or at the right if using metric units. Draw a horizontal line to meet the uncorrected log reading, then follow the direction of the trend lines downward to meet the standard condition (for example, 8 in. for the borehole size

correction). At this point, you will have moved to the left (minus) or the right (plus) by a distance readable on the porosity scale. Make a note of this correction, $\Delta\phi$, to be applied to the uncorrected log reading for that environmental effect.

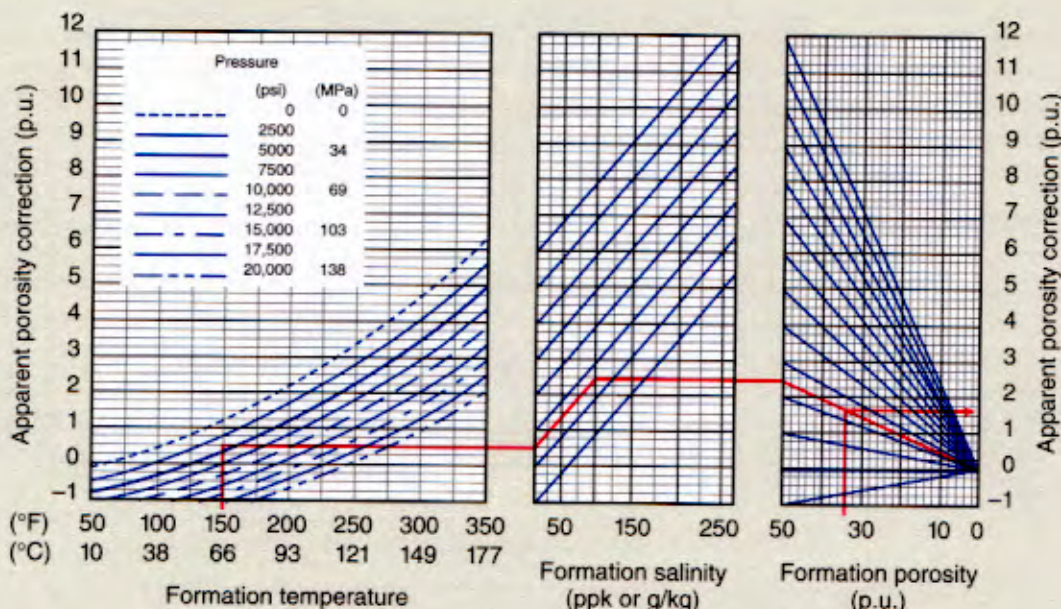
Since several small corrections are usually made for different environmental effects, including mud weight and borehole size using Chart Por-23a, and formation temperature, pressure and formation salinity using Chart Por 23b, the small corrections, $\Delta\phi$, for each relevant environmental effect are added together.

Continued on next page

Openhole APS Corrections for Temperature, Pressure and Formation Salinity

For APLU and FPLU curves without environmental corrections

Por-23b



© Schlumberger

For pressure, temperature and salinity corrections, enter the bottom of the left-hand part of Chart Por-23b with formation temperature, and project a line up to the relevant pressure curve. Draw a horizontal line to the left-hand edge of the formation salinity part of the nomograph, then follow the trend lines to the correct formation salinity. Draw another horizontal line to the left-hand edge of the porosity part of the nomograph, and follow the trend lines to the approximate porosity. A horizontal line from here to the right-hand scale gives the apparent porosity correction, $\Delta\phi$, to be applied for temperature, pressure and salinity effects. If the correction, $\Delta\phi$, given by Chart Por-23b is large and the first estimate of porosity is incorrect, it may be necessary to reiterate this correction with an improved porosity estimate.

Example: Assume an uncorrected APLU = 34 p.u. (apparent limestone porosity)
 Borehole size = 12 in.
 Mud weight = 11 lbm/gal
 Borehole temperature = 150°F
 Pressure = 5 kpsi
 Formation salinity = 100 kppm

$\Delta\phi$

Then, using Chart Por-23a,

Mud weight correction (none)	-0.7
Borehole size (interpolate mud weight)	-1
and using Chart Por-23b,	
Temperature/pressure/salinity	+1 [†]
Net correction	-0.7
Corrected porosity	34 p.u. - 0.7 p.u. = 33.3 p.u. (apparent limestone units)

The overall correction is small. If this is a limestone formation, the first estimate of porosity used in Chart Por-23b is good and no reiteration is required.

[†] The apparent porosity correction is a true hydrogen index correction. Recent detailed saltwater measurements indicate that the red correction is slightly smaller than this. It is therefore recommended the apparent correction be multiplied 0.70 for APLU values and by 0.78 for FPLU curves.

Dual-Spacing CNL* Compensated Neutron Log Formation Σ Correction Nomograph for Openhole

When measured formation Σ data are available, Chart Por-16 may be used for correcting thermal neutron porosity from the CNL log for the effect of total formation capture cross section. At the bottom of the chart, an additional nomograph is provided to correct the resulting porosity for salt displacement in cases where elevation of formation Σ is due to salinity. This chart can be used instead of the salinity correction on Chart Por-14c or Por-14cm. Do not use both charts.

In each of the lithology panels, the nominal situation for freshwater pore fluid is drawn to correspond to the values of Σ_{ma} of the formations used to calibrate the porosity response. For reference, the sloping dashed line indicates the value of Σ for the formations filled with salt-saturated water.

To use Chart Por-16, enter the apparent porosity and measured Σ into the appropriate lithology box. Follow the equiporosity trend lines down to the nominal Σ line, and read the corrected porosity there. If at least some of the Σ reading is caused by salt water, a correction for salt displacement is made as follows:

1. Enter the top of the formation salinity box at 0 ppm with the corrected porosity from the previous step.
2. Follow the equiporosity trend lines down to the known water salinity value, and read the final corrected porosity there.

If other environmental corrections are required, the amount of correction for formation Σ and formation salinity should be

calculated by taking the difference between the final corrected and apparent porosity values. This difference can then be summed with corrections for other environmental effects to determine the total correction for all effects.

Example:

Given:	Apparent neutron porosity	37.9 p.u. (sandstone)
	Formation Σ from log	32.7 c.u.
	Formation water salinity	160.0 kppm

Results:	Porosity corrected for Σ	32.9 p.u. (sandstone)
	Final corrected porosity	35.0 p.u. (sandstone)

The total formation Σ and salinity effect in this example is 2.9 p.u.

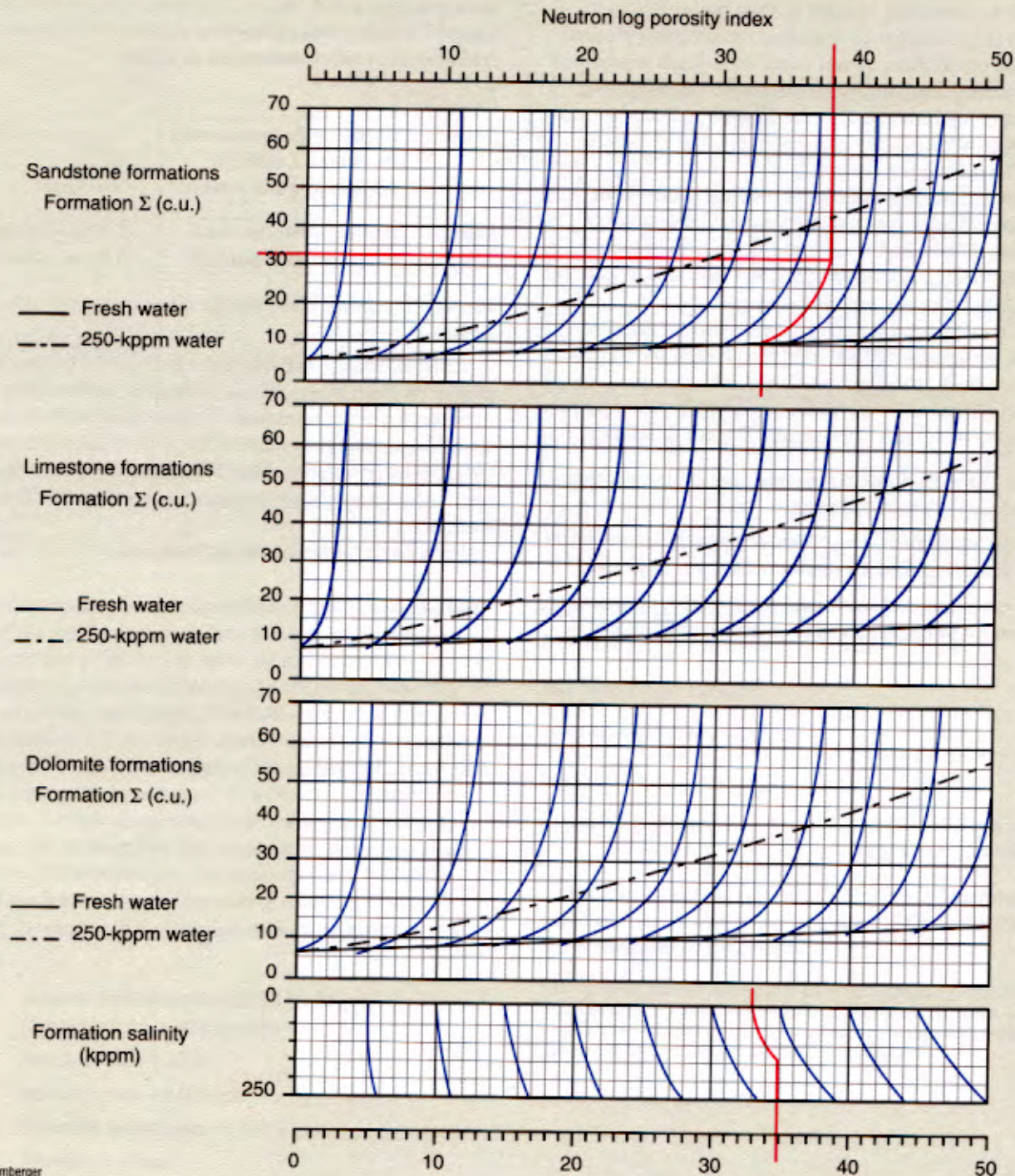
As an alternate approach, with Chart Por-17 it is possible to correct the neutron porosity for the matrix capture cross section in freshwater-filled formations if matrix Σ is known from auxiliary measurements. Chart Por-18 provides corrections for CNL thermal neutron porosity for Σ of the formation fluid and, optionally, for hydrogen displacement in saltwater-filled formations.

For more information see Reference 38.

*Mark of Schlumberger

Dual-Spacing CNL* Compensated Neutron Log Formation Σ Correction Nomograph for Openhole

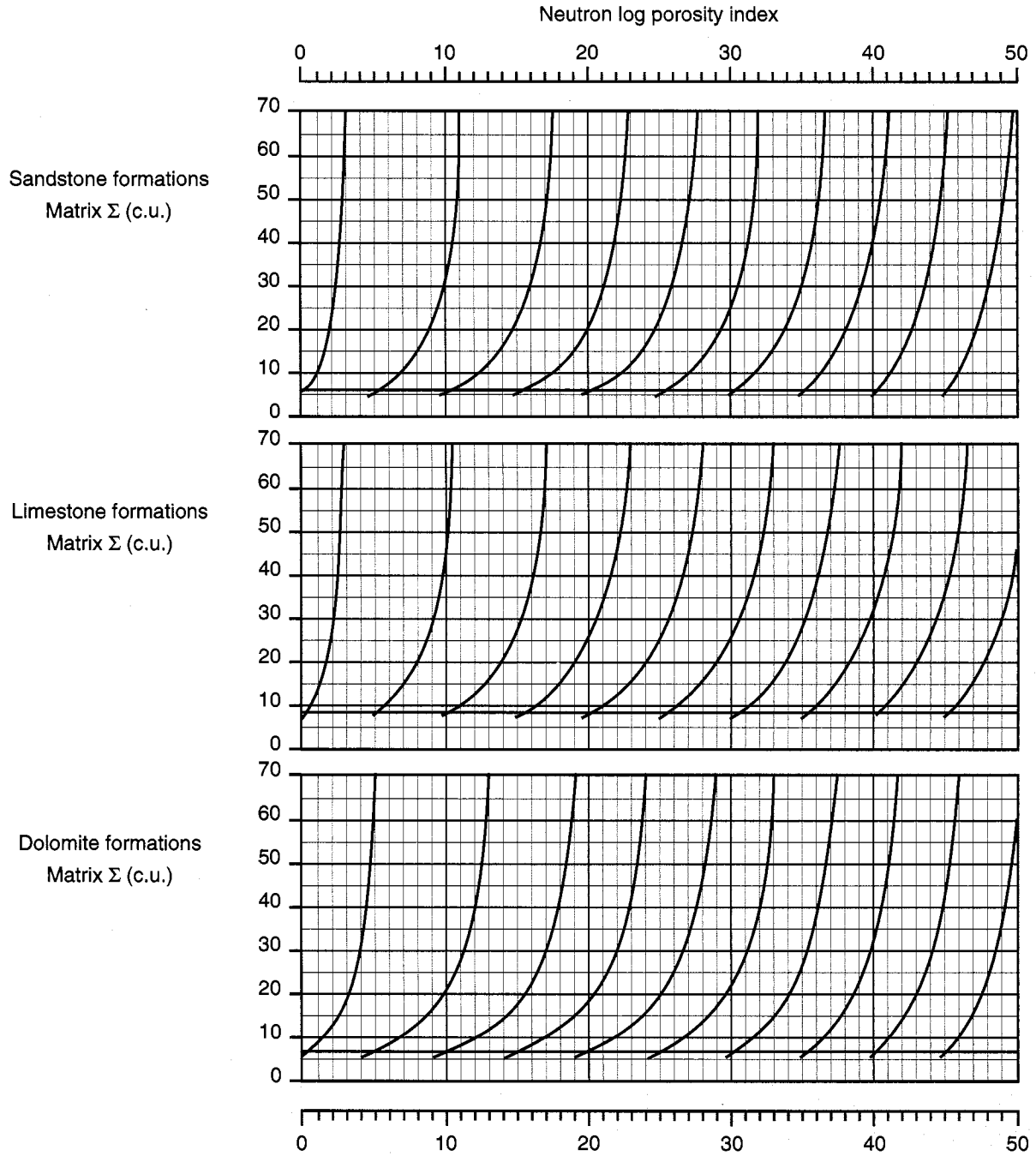
Por



*Mark of Schlumberger
© Schlumberger

Dual-Spacing CNL* Compensated Neutron Log Matrix Σ Correction Nomograph for Openhole

Por-17

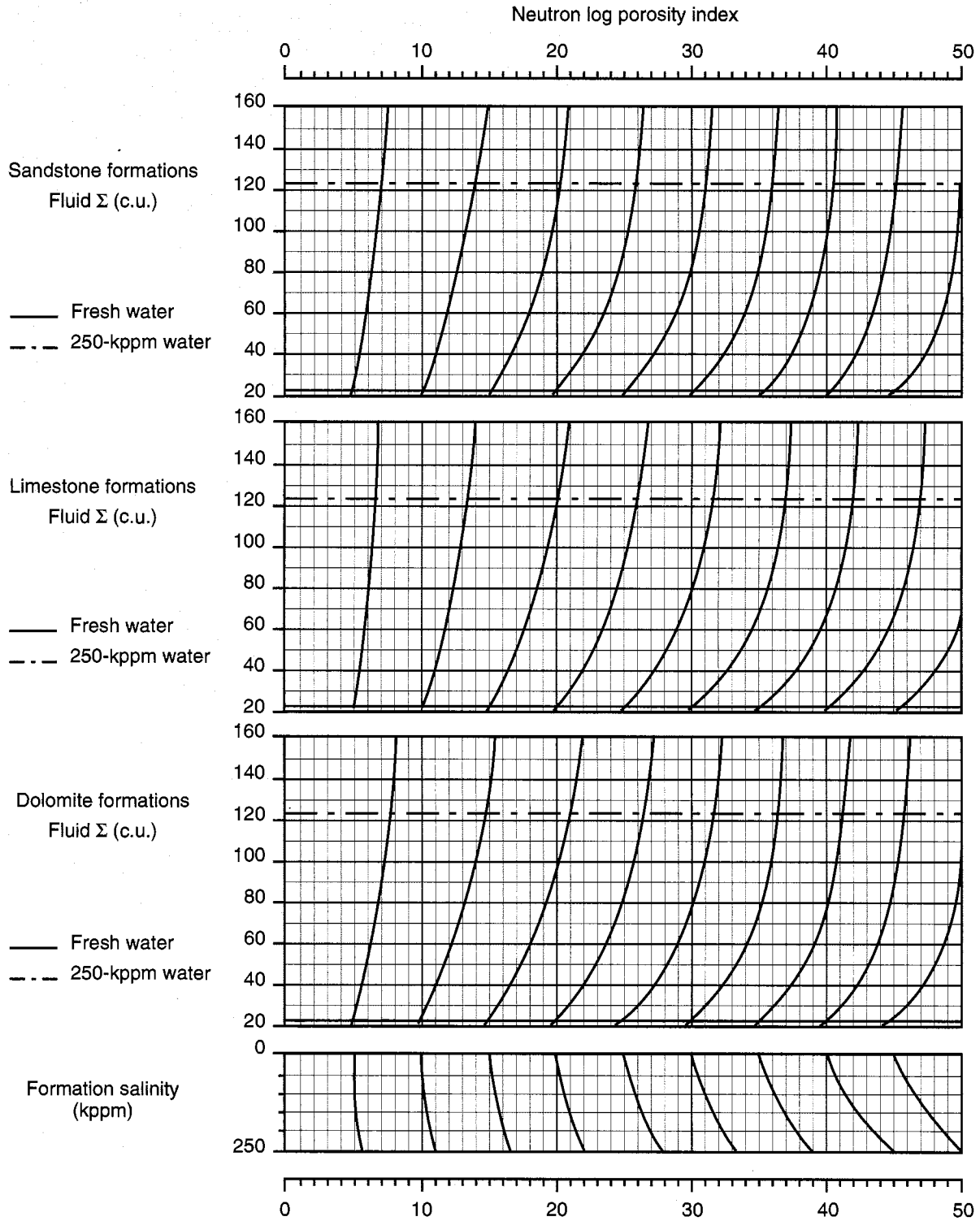


Por

*Mark of Schlumberger
© Schlumberger

Dual-Spacing CNL* Compensated Neutron Log Fluid Σ Correction Nomograph for Openhole

Por-18



*Mark of Schlumberger
© Schlumberger

CDN* Compensated Density Neutron Log Correction Nomographs

This section contains log interpretation charts for the logging-while-drilling CDN neutron porosity measurement. Correction Nomographs Por-19 through Por-21 provide an environmentally corrected neutron porosity referenced to the appropriate lithology matrix. The neutron-density crossplot, Chart CP-22, provides insight into the formation lithology and permits the determination of porosity. The following example illustrates the procedure for using the charts.

Assume the following:

Uncorrected neutron log porosity	40 p.u. (apparent limestone units)
Tool size	6.5 in.
Borehole size	10 in.
Mud weight	14 lbm/gal (barite mud)
Mud salinity	100 kppm
Mud temperature	150°F
Mud pressure	5 kpsi
Formation salinity	100 kppm

First, determine the temperature and pressure-corrected hydrogen index of the mud (H_m). Enter the left of the bottom chart of Nomograph Por-19 at the 14-lbm/gal mud weight. Project a line to the right until it intersects the line for barite mud (point A). From this point, draw a line straight up until it intersects the bottom of the middle chart (point B). Follow the trend lines up to the mud temperature of 150°F (point C), then go straight up to the bottom of the top chart (point D). Follow the trend lines up to the line for 5-kpsi mud pressure (point E) and then straight up to the top of the chart to read the value of 0.78—the corrected hydrogen index of the mud.

Second, determine the environmental corrections with the appropriate Por-20 or -24 chart. Since the hydrogen index of the mud, mud salinity and formation salinity effects is strongly dependent on the hole size, correction nomographs are provided

for 8-, 10-, 12-, 14- and 16-in. borehole sizes and for 6.5- and 8-in. tools.

Because the borehole size in the example is 10 in. and the tool size is 6.5 in., Chart Por-20b is selected for the corrections. Enter the top of the chart with the uncorrected CDN neutron porosity of 40 p.u. and drop a straight line down to the 10-in. borehole size (point B). Follow the sloping trend lines down to the standard conditions of an 8-in. borehole (point C), and then drop straight down to the borehole temperature value of 150°F (point D). Again follow the trend lines to the temperature at standard conditions, 75°F (point E). From this point drop vertically to the H_m value of 0.78, as determined from Chart Por-19. From here (point F), follow the trend lines to the standard conditions of $H_m = 1.0$ (point G). Then, drop straight down to the borehole salinity value of 100 kppm (point H). Follow the trend lines to the standard conditions of 0 kppm (point I). Drop straight down to the 100-kppm value for formation salinity (point J), and follow the trend lines down to 0 kppm, the standard condition value (point K). There, read the environmentally corrected apparent limestone porosity of 34 p.u. for this example.

Chart Por-24d shows another example for the larger 8-in. tool in a 14-in. borehole.

The porosity equivalence curves in Chart Por-21 are used to find the porosity of sandstones or dolomites. Enter the chart in abscissa with the environmentally corrected apparent limestone porosity as determined from Chart Por-20, go up to the appropriate matrix line, and read true porosity on the ordinate.

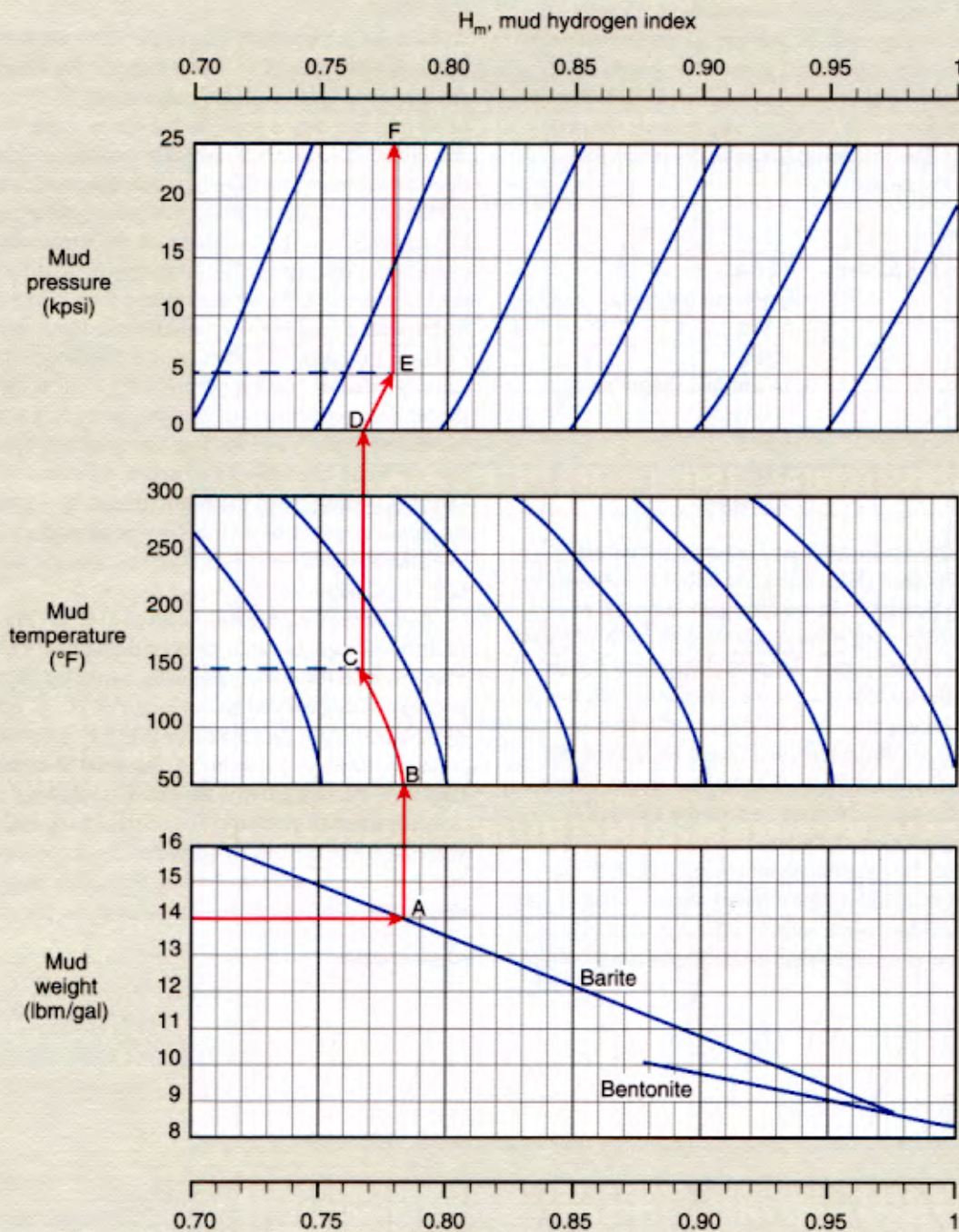
If the lithology is unknown, the neutron-density crossplot, Chart CP-22, can provide insight into lithology and permit the determination of porosity. To use this chart, enter the abscissa with the environmentally corrected apparent limestone porosity and the ordinate with the bulk density. The point of intersection defines the lithology (mineralogy) and the porosity.

*Mark of Schlumberger

CDN* Compensated Density Neutron Log and ADN* Azimuthal Density Neutron Log Correction Nomograph

Por-19

Mud hydrogen index determination

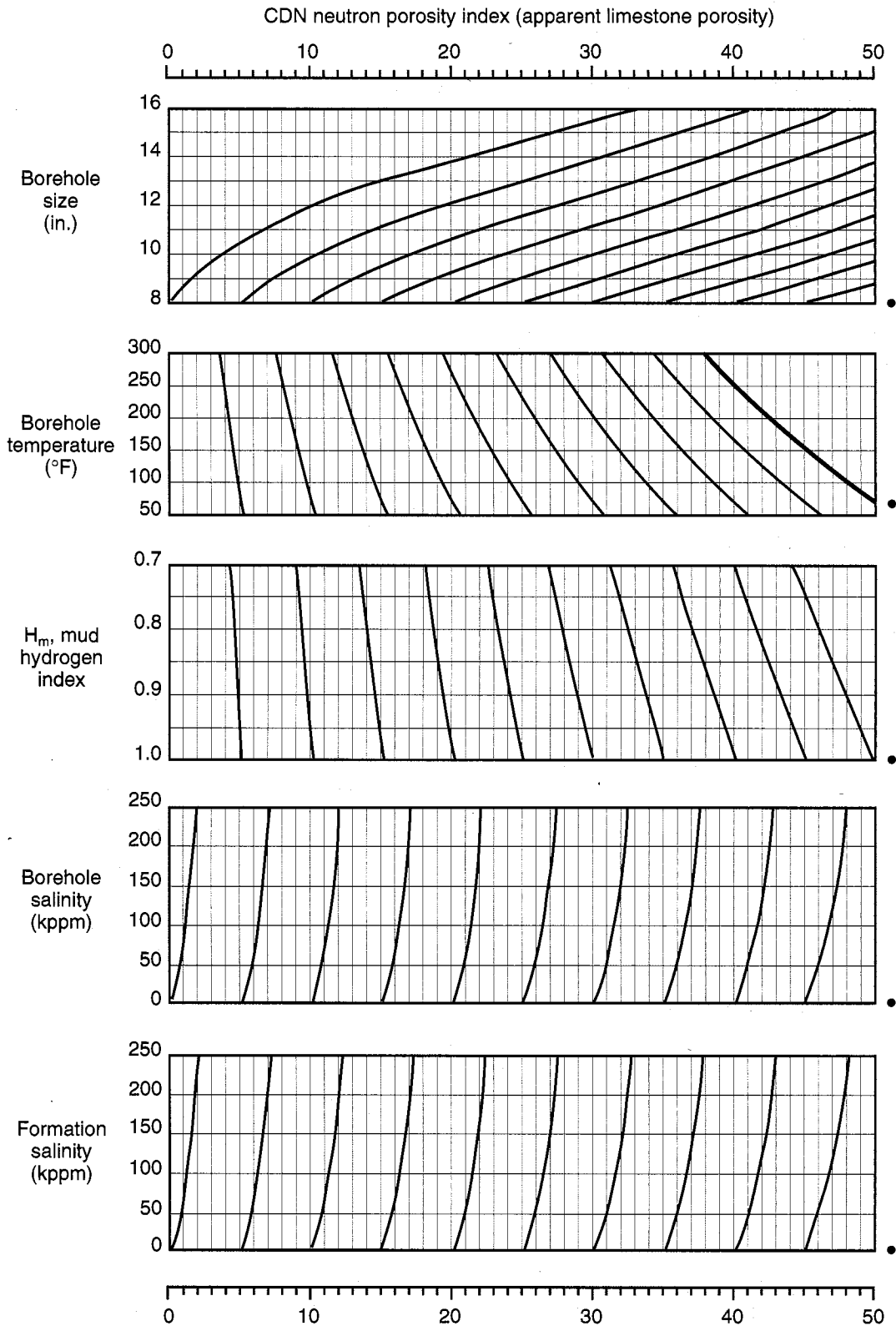


Por

*Mark of Schlumberger
© Schlumberger

CDN* Compensated Density Neutron Log Correction Nomograph for 6.5-in. Tool

8-in. borehole



Por

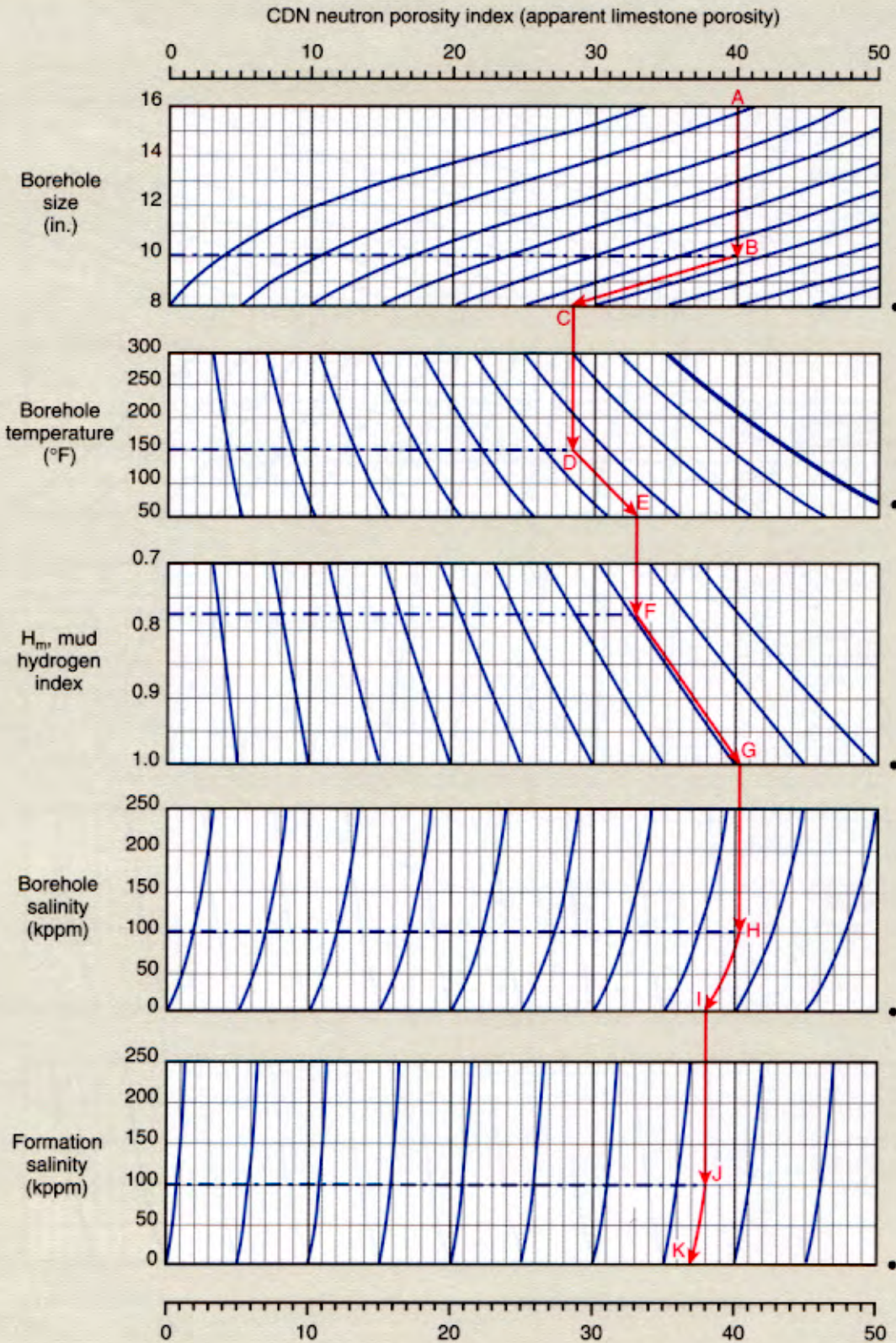
*Mark of Schlumberger
© Schlumberger

• Standard conditions

CDN* Compensated Density Neutron Log Correction Nomograph for 6.5-in. Tool

10-in. borehole

Por-20b



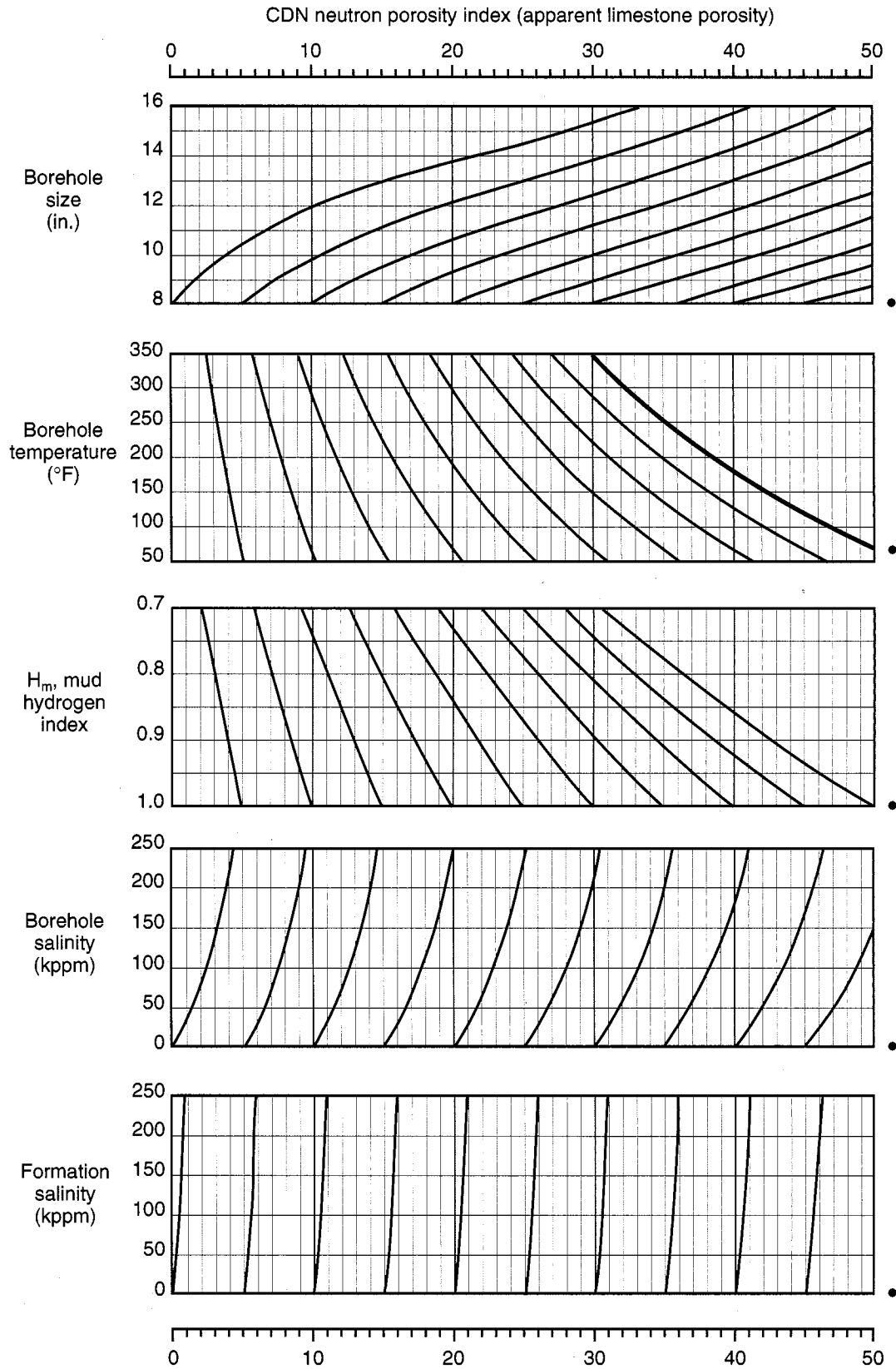
*Mark of Schlumberger
© Schlumberger

• Standard conditions

CDN* Compensated Density Neutron Log Correction Nomograph for 6.5-in. Tool

Por-20c

12-in. borehole



Por

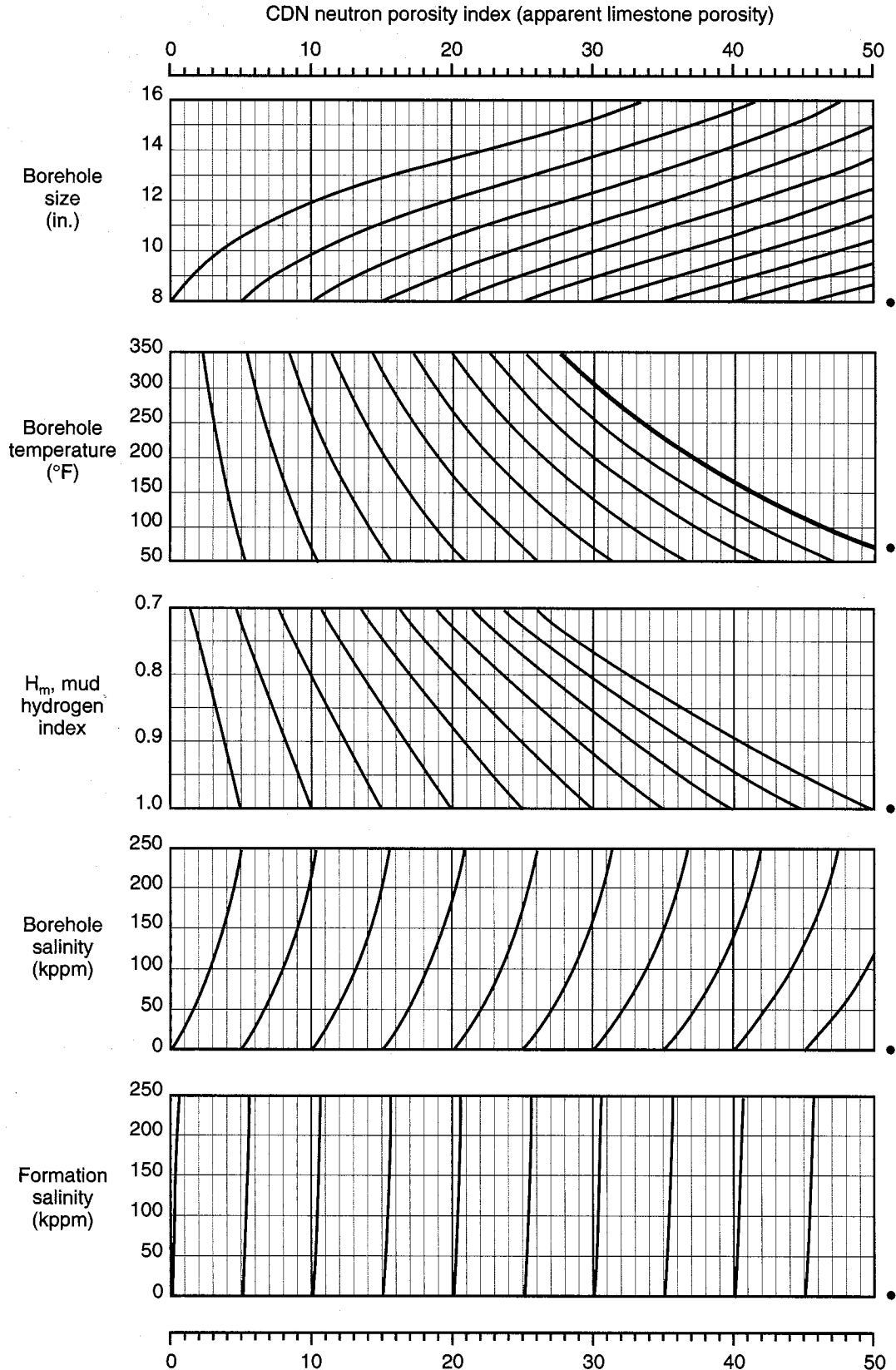
*Mark of Schlumberger
© Schlumberger

• Standard conditions

CDN* Compensated Density Neutron Log Correction Nomograph for 6.5-in. Tool 14-in. borehole

Por-20d

Por



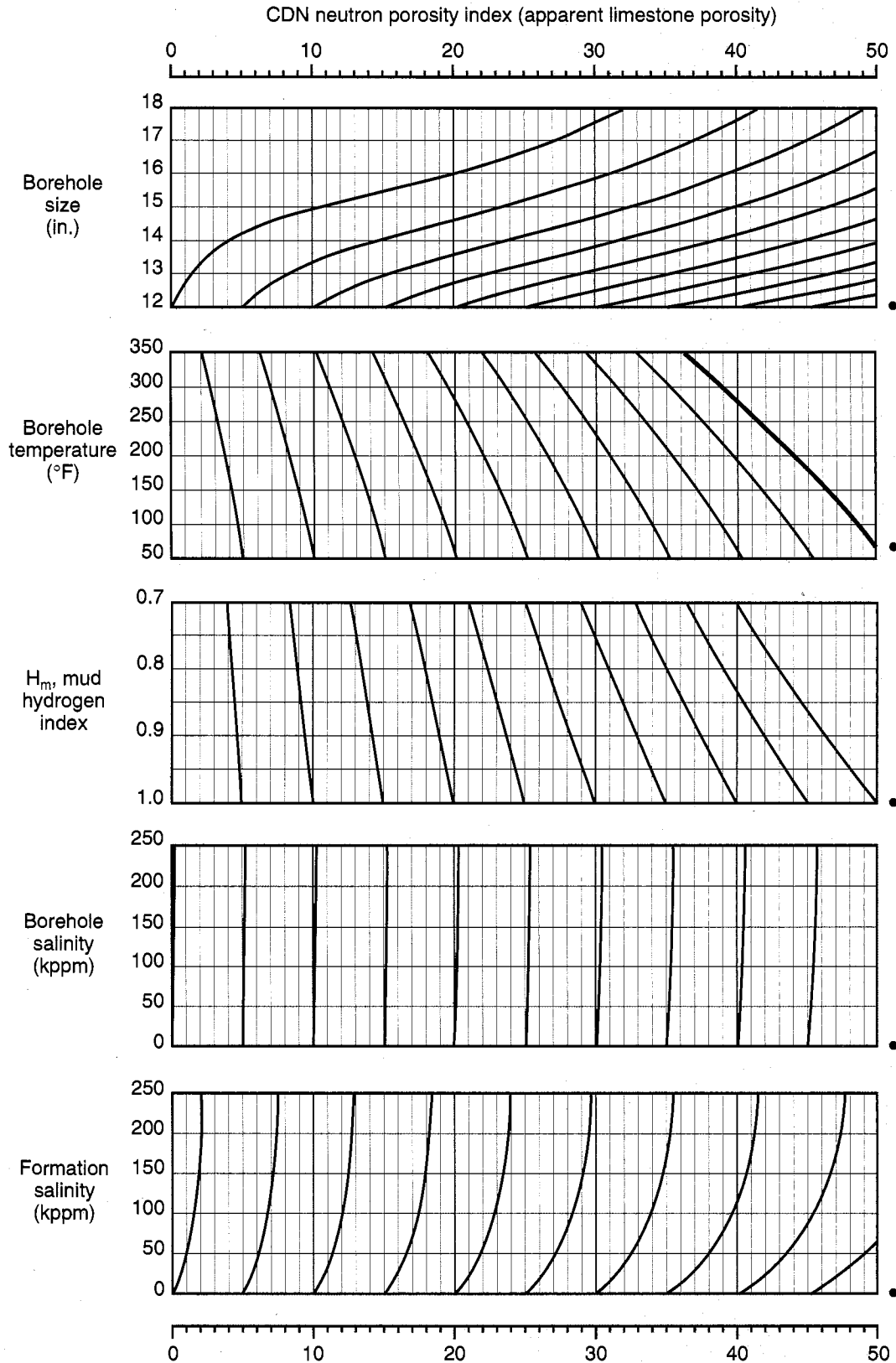
*Mark of Schlumberger
© Schlumberger

• Standard conditions

CDN* Compensated Density Neutron Log Correction Nomograph for 8-in. Tool

Por-24c

12-in. borehole



Por

*Mark of Schlumberger
© Schlumberger

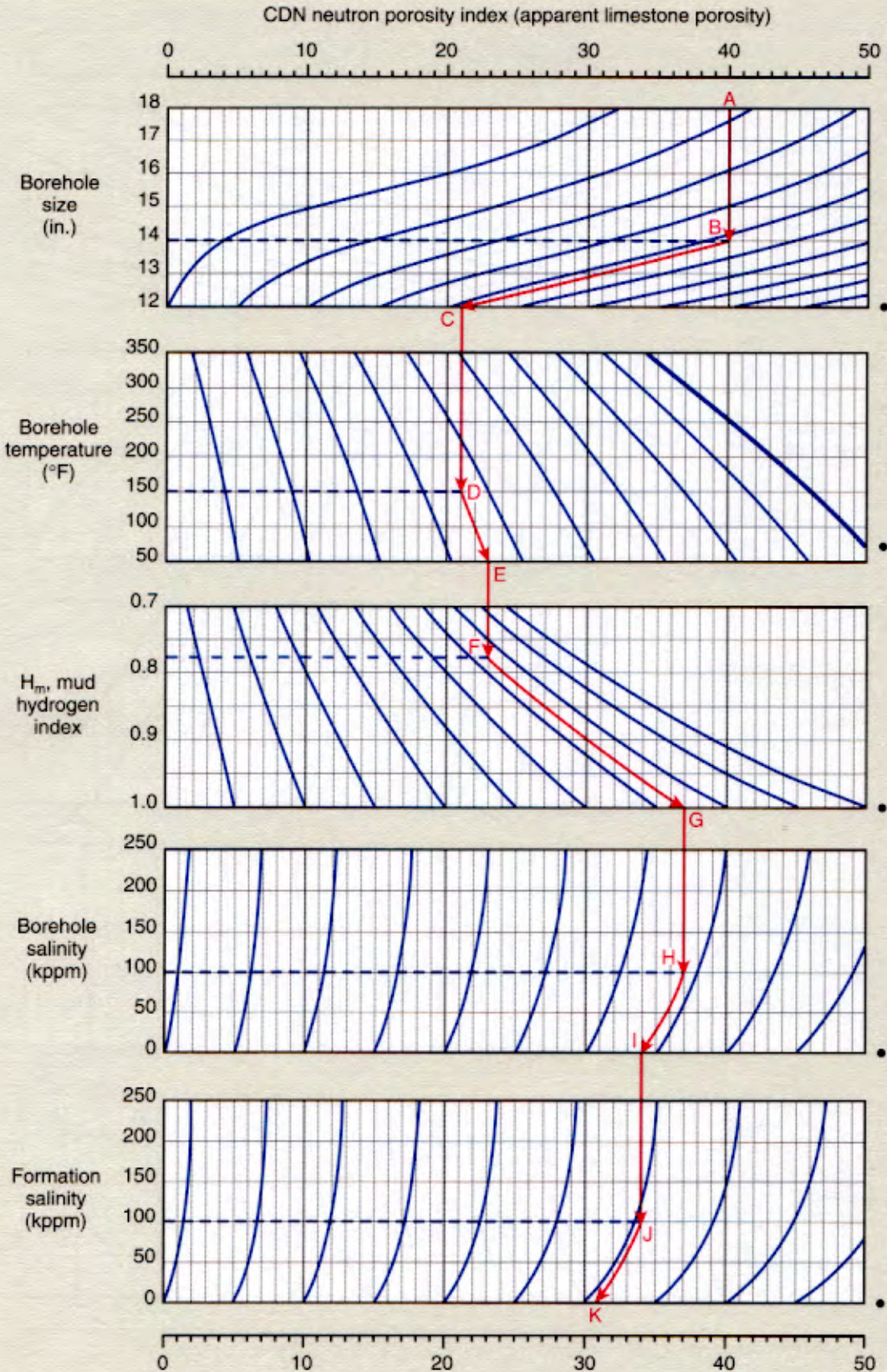
• Standard conditions

CDN* Compensated Density Neutron Log Correction Nomograph for 8-in. Tool

Por-24d

14-in. borehole

Por



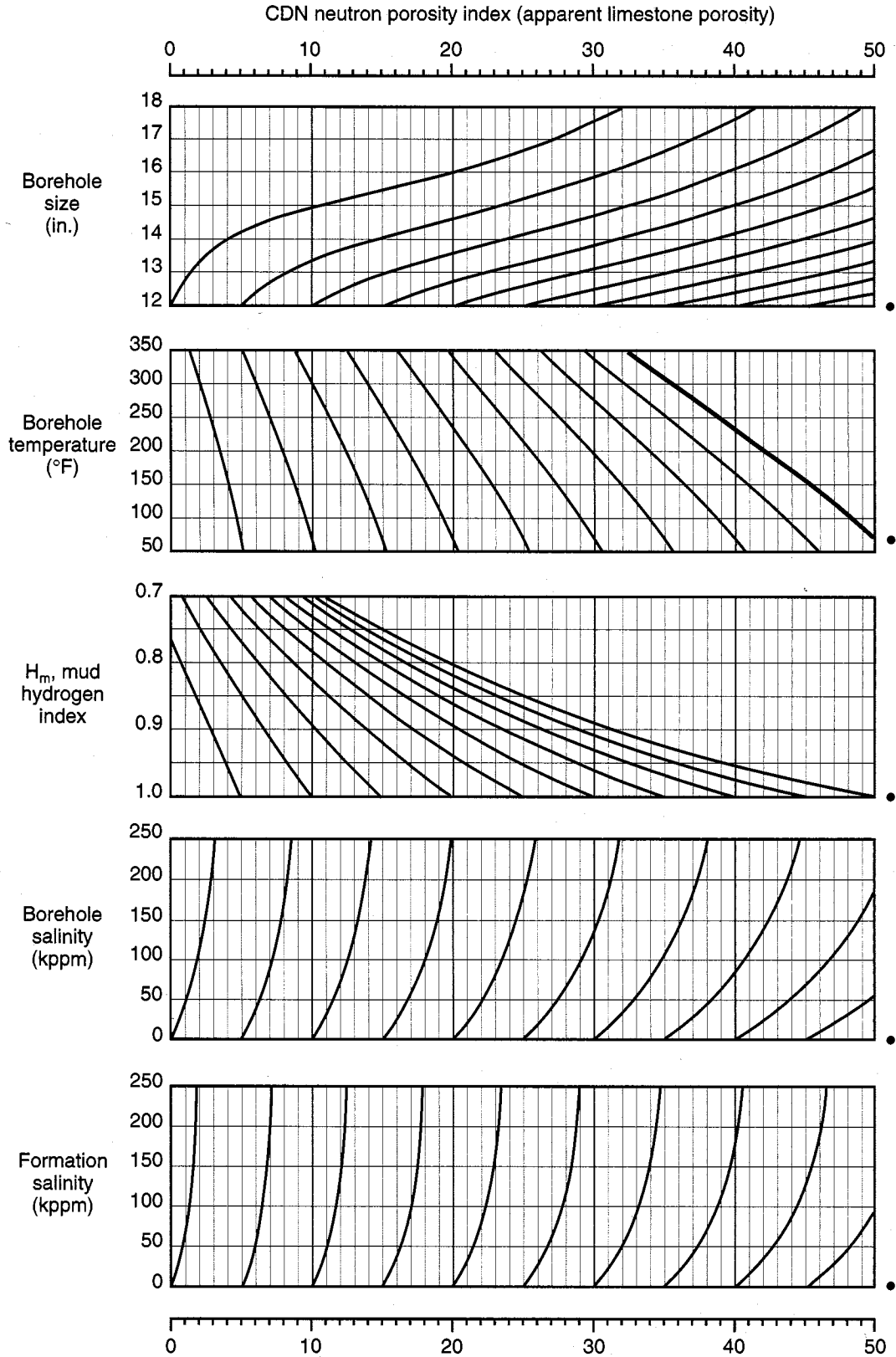
*Mark of Schlumberger
© Schlumberger

• Standard conditions

CDN* Compensated Density Neutron Log Correction Nomograph for 8-in. Tool

Por-24e

16-in. borehole



Por

ADN* Azimuthal Density Neutron Log Correction Nomographs

This section contains log interpretation charts for the logging-while-drilling ADN azimuthal neutron porosity measurement. It is assumed that the tool is stabilized in the borehole. Correction Nomographs Por-19, Por-26a and Por-26b provide an environmentally corrected neutron porosity referenced to the appropriate lithology matrix. The neutron-density crossplot, Chart CP-24, provides insight into the formation lithology and permits the determination of porosity. The following example illustrates the procedure for using the charts.

Por

Assume the following:

Uncorrected neutron log porosity	40 p.u. (apparent limestone units)
Borehole size	10 in.
Mud weight	14 lbm/gal (barite mud)
Mud salinity	100 kppm
Mud temperature	150°F
Mud pressure	5 kpsi
Formation salinity	100 kppm

First, determine the temperature and pressure-corrected hydrogen index of the mud (H_m). Enter the left of the bottom chart of Nomograph Por-19 at the 14-lbm/gal mud weight. Project a line to the right until it intersects the line for barite mud (point A). From this point, draw a line straight up until it intersects the bottom of the middle chart (point B). Follow the trend lines up to the mud temperature of 150°F (point C), then go straight up to the bottom of the top chart (point D). Follow the trend lines up to the line for 5-kpsi mud pressure (point E) and then straight up to the top of the chart to read the value of 0.78—the corrected hydrogen index of the mud.

Second, determine the environmental corrections with the appropriate Por-26 chart. Since the hydrogen index of the mud,

mud salinity and formation salinity effects is strongly dependent on the hole size, correction nomographs are provided for 8- and 10-in. borehole sizes.

Since the borehole size in the example is 10 in. and the tool size is 6.5 in., Chart Por-26b is selected for the corrections. Enter the top of the chart with the uncorrected CDN neutron porosity of 40 p.u. and drop a line straight down to the 10-in. borehole size (point B). Follow the sloping trend lines down to the standard conditions (8-in. borehole), and then drop straight down to the H_m value of 0.78, as determined from Chart Por-19. From here (point D), follow the trend lines to the standard conditions of $H_m = 1.0$ (point E). Then, drop straight down to the mud salinity value of 100 kppm (point F). Follow the trend lines to the standard conditions of 0 kppm. Drop straight down to the 100-kppm value for formation salinity (point H) and follow the trend lines down to 0 kppm—the standard condition value (point I). There, read the environmentally corrected apparent limestone porosity of 31 p.u. for this example.

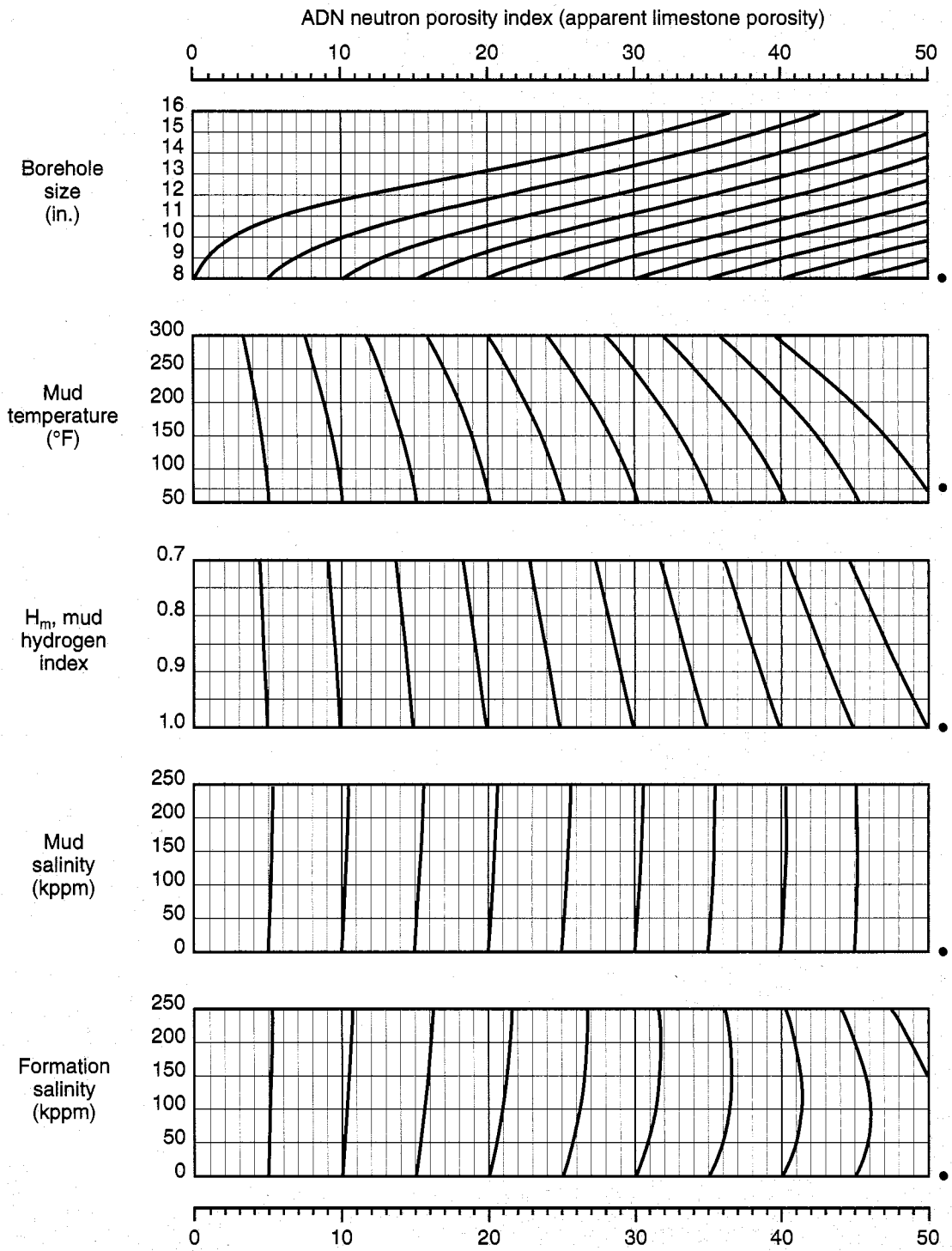
The porosity equivalence curves in Chart Por-27 are used to find the porosity of sandstones or dolomites. Enter the chart in abscissa with the environmentally corrected apparent limestone porosity as determined from Chart Por-26b, go up to the appropriate matrix line, and read true porosity on the ordinate.

If the lithology is unknown, the neutron-density crossplot, Chart CP-24, can provide insight into lithology and permit the determination of porosity. To use this chart, enter the abscissa with the environmentally corrected apparent limestone porosity and the ordinate with the bulk density. The point of intersection defines the lithology (mineralogy) and the porosity.

*Mark of Schlumberger

ADN* Azimuthal Density Neutron Log Correction Nomograph for 6.75-in. Tool 8-in. borehole

Por-26a



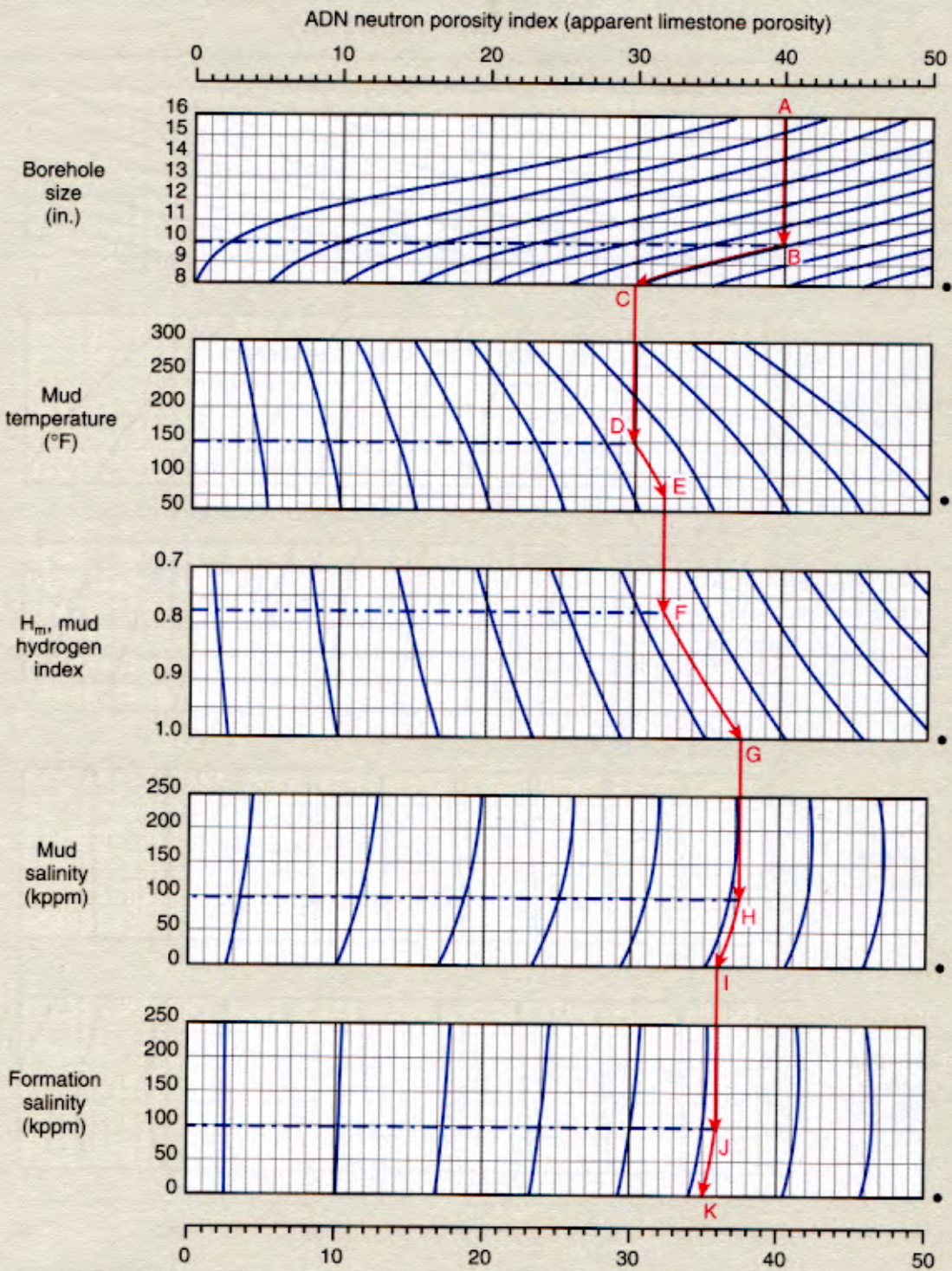
Por

*Mark of Schlumberger
© Schlumberger

• Standard conditions

ADN* Azimuthal Density Neutron Log Correction Nomograph for 6.75-in. Tool 10-in. borehole

Por-26b

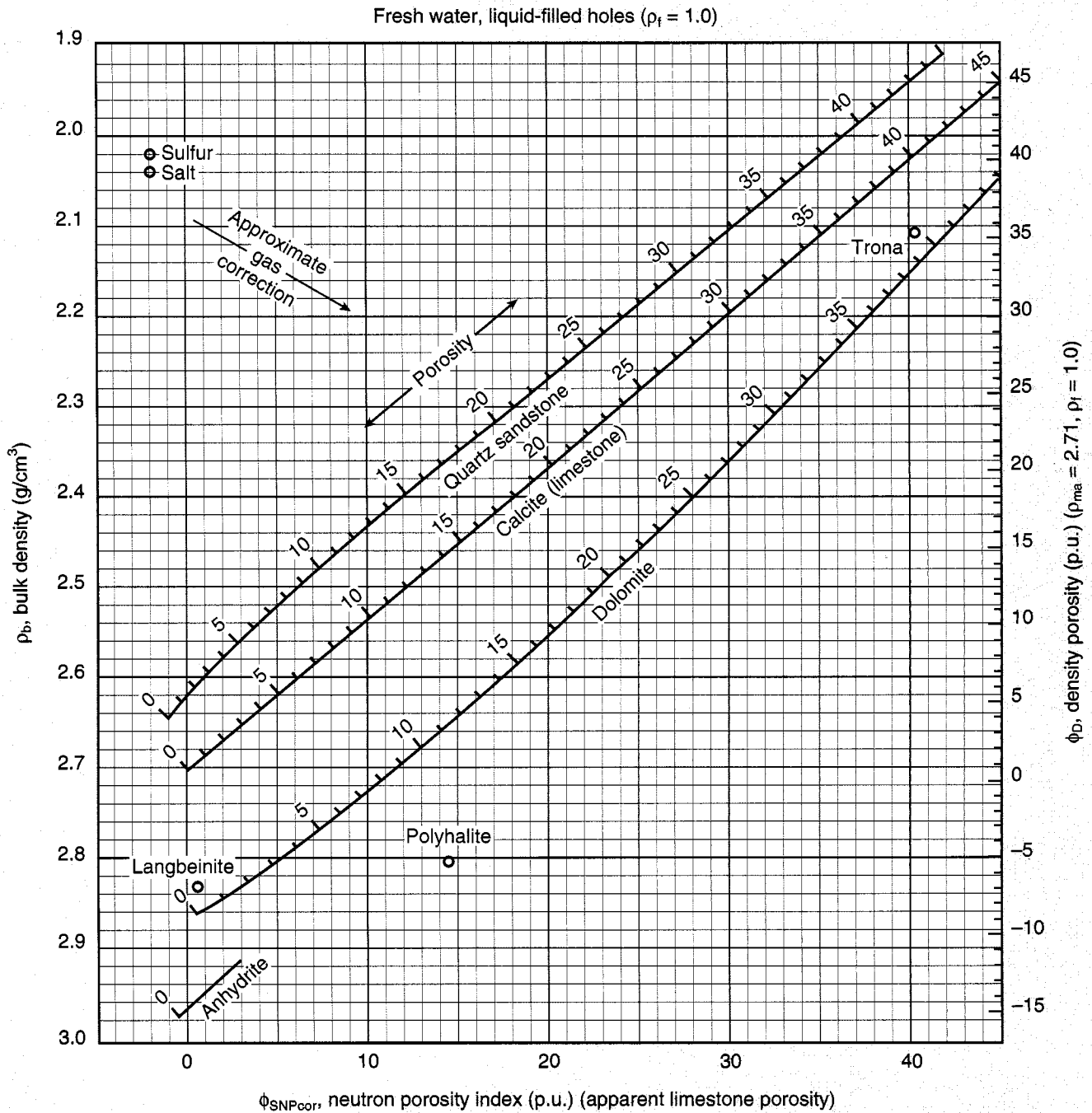


*Mark of Schlumberger
© Schlumberger

• Standard conditions

Porosity and Lithology Determination from Formation Density Log and SNP Sidewall Neutron Porosity Log

CP-1a



CP

© Schlumberger

The neutron-density-sonic crossplot charts (Charts CP-1, CP-2 and CP-7) provide insight into lithology and permit the determination of porosity. Chart selection depends on the anticipated mineralogy. Neutron-density can be used to differentiate between the common reservoir rocks [quartz sandstone, calcite (limestone) and dolomite] and shale and some evaporites.

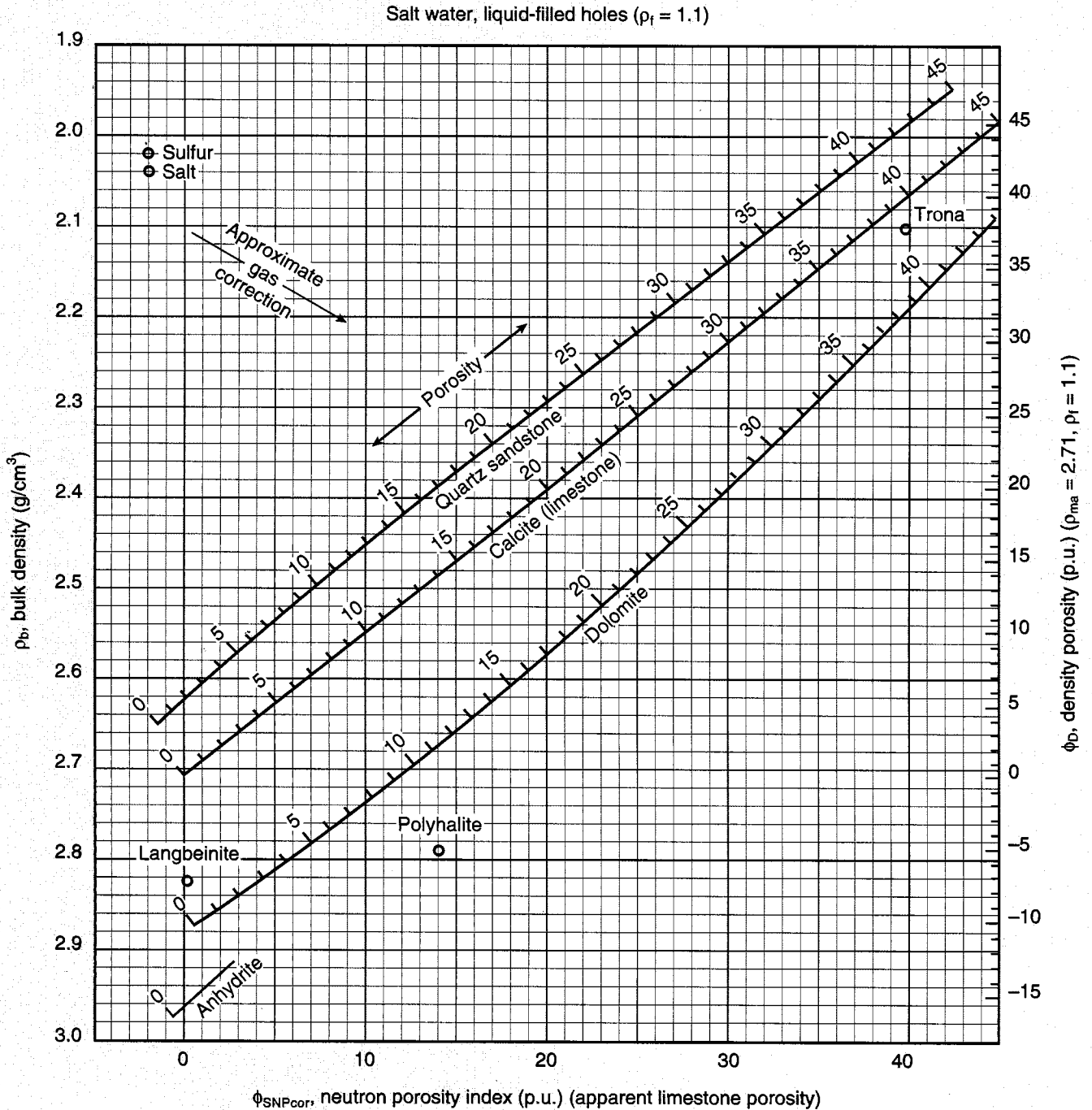
Sonic-neutron can be used to differentiate between the common reservoir rocks when clay content is negligible. Sonic-density can be used to differentiate between a single known reservoir rock and shale and to identify evaporate minerals.

Continued on next page

Porosity and Lithology Determination from Formation Density Log and SNP Sidewall Neutron Porosity Log

CP-1b

CP

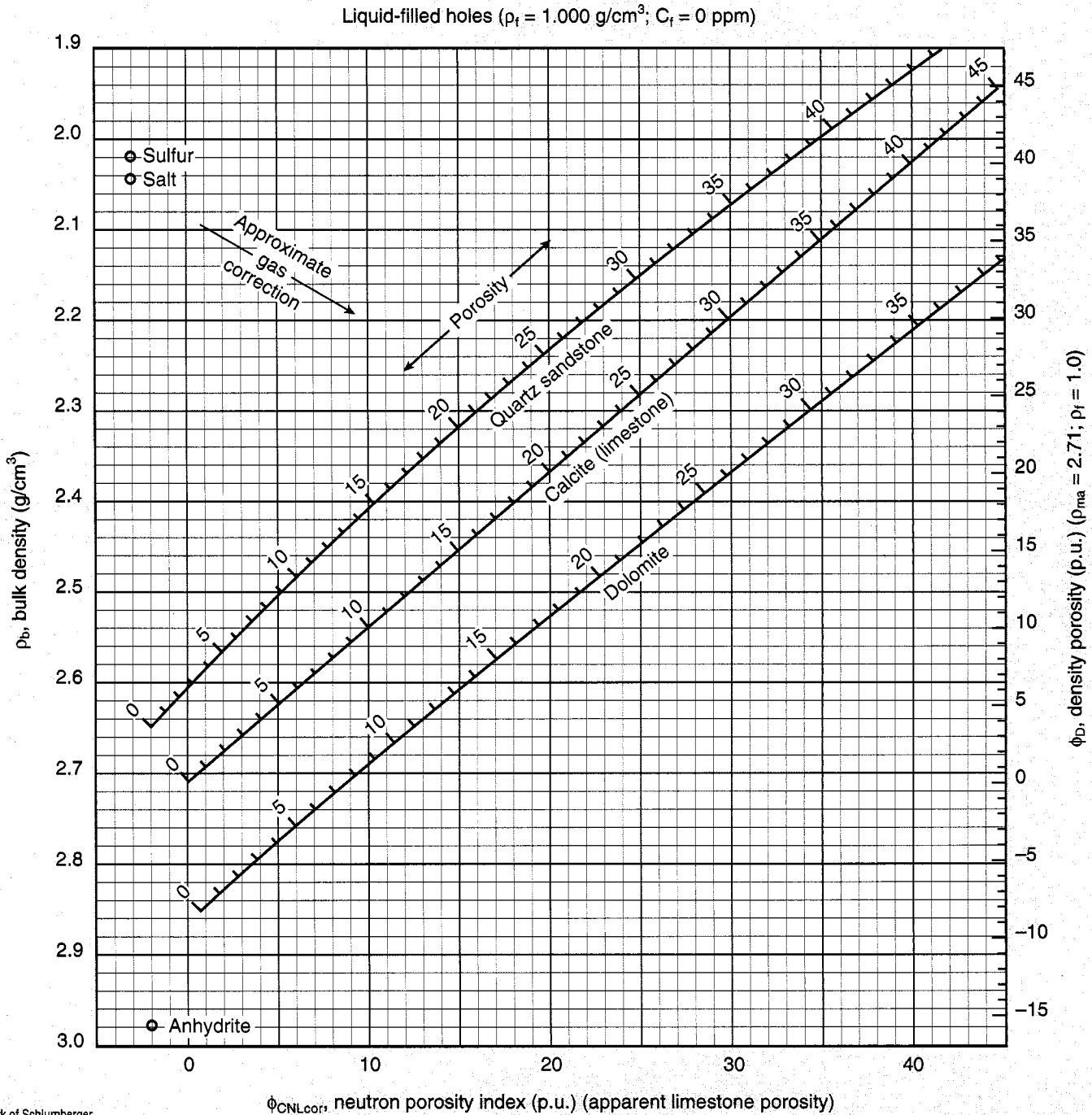


To use any of these charts, enter the abscissa and ordinate with the required neutron, density or sonic value. The point of intersection defines the lithology (mineralogy) and the porosity, ϕ .

Note that all neutron input is in apparent limestone porosity, that charts for fresh water ($\rho_f = 1.0 \text{ g/cm}^3$) and saline water ($\rho_f = 1.1 \text{ g/cm}^3$) invasion exist, and that the sonic charts contain curves assuming weighted average response (blue) and empirical observation response (red).

Porosity and Lithology Determination from Litho-Density* Log and CNL* Compensated Neutron Log

For CNL curves after 1986 labeled TNPH



CP

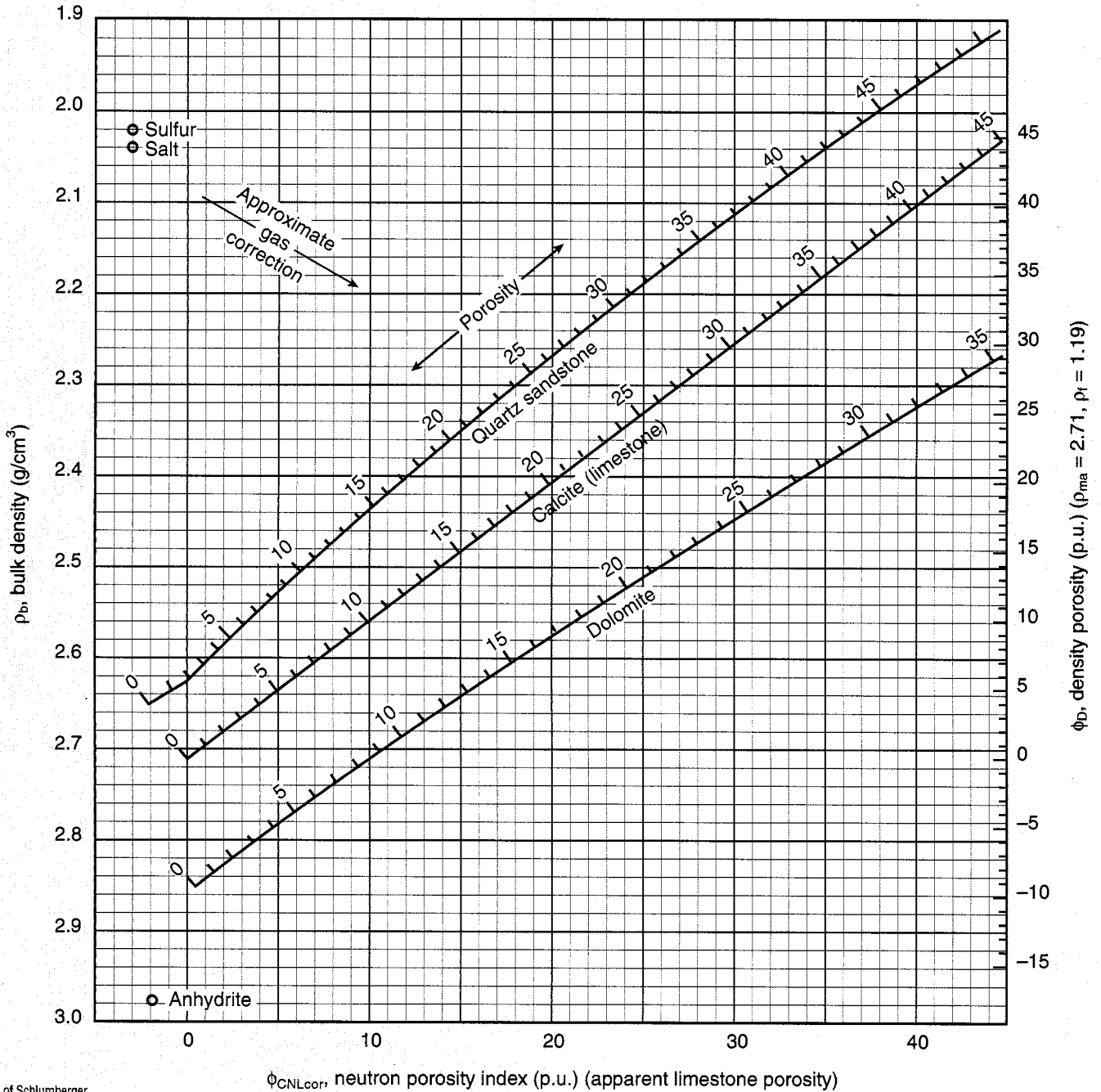
*Mark of Schlumberger
© Schlumberger

Porosity and Lithology Determination from Litho-Density* Log and CNL* Compensated Neutron Log

For CNL curves after 1986 labeled TNPH

CP-1f

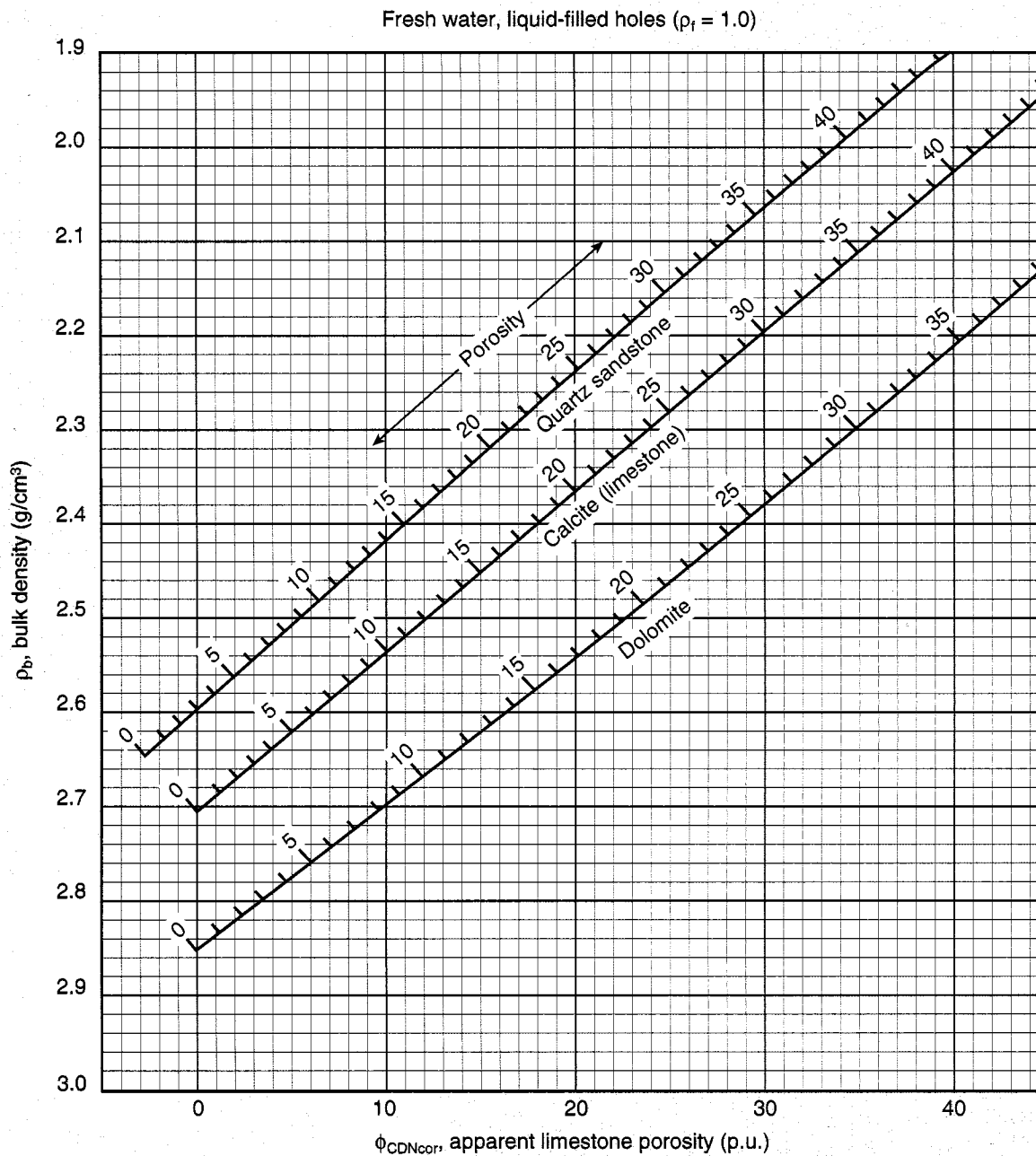
Liquid-filled holes ($\rho_f = 1.190 \text{ g/cm}^3$; $C_f = 250 \text{ kppm}$)



*Mark of Schlumberger
© Schlumberger

Porosity and Lithology Determination from Formation Density Log and CDN* Compensated Density Neutron Log for 6.5-in. Tool

GP-22



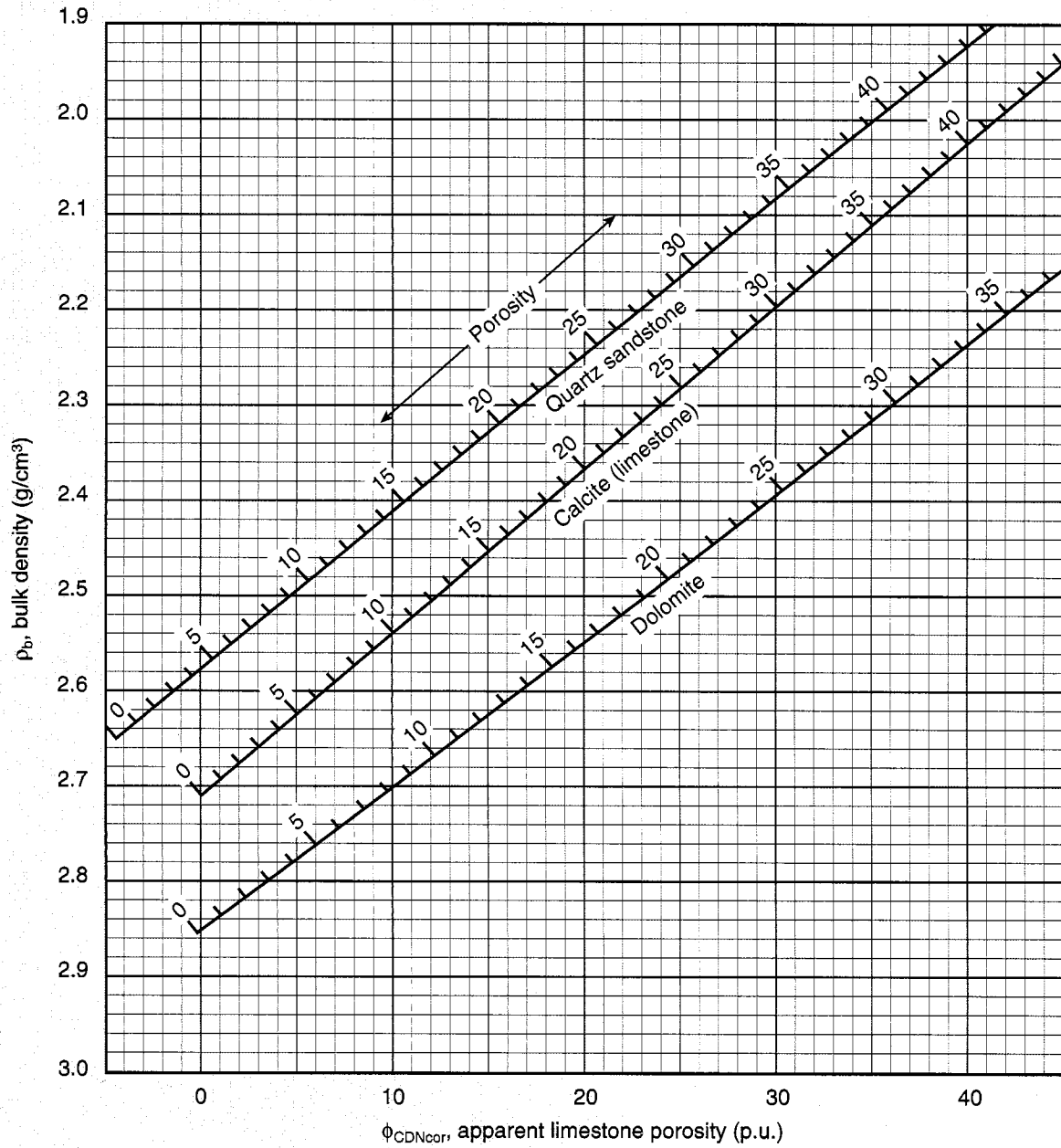
CP

*Mark of Schlumberger
© Schlumberger

Porosity and Lithology Determination from Formation Density Log and CDN* Compensated Density Neutron Log for 8-in. Tool

CP-23

Fresh water, liquid-filled holes ($\rho_f = 1.0$)

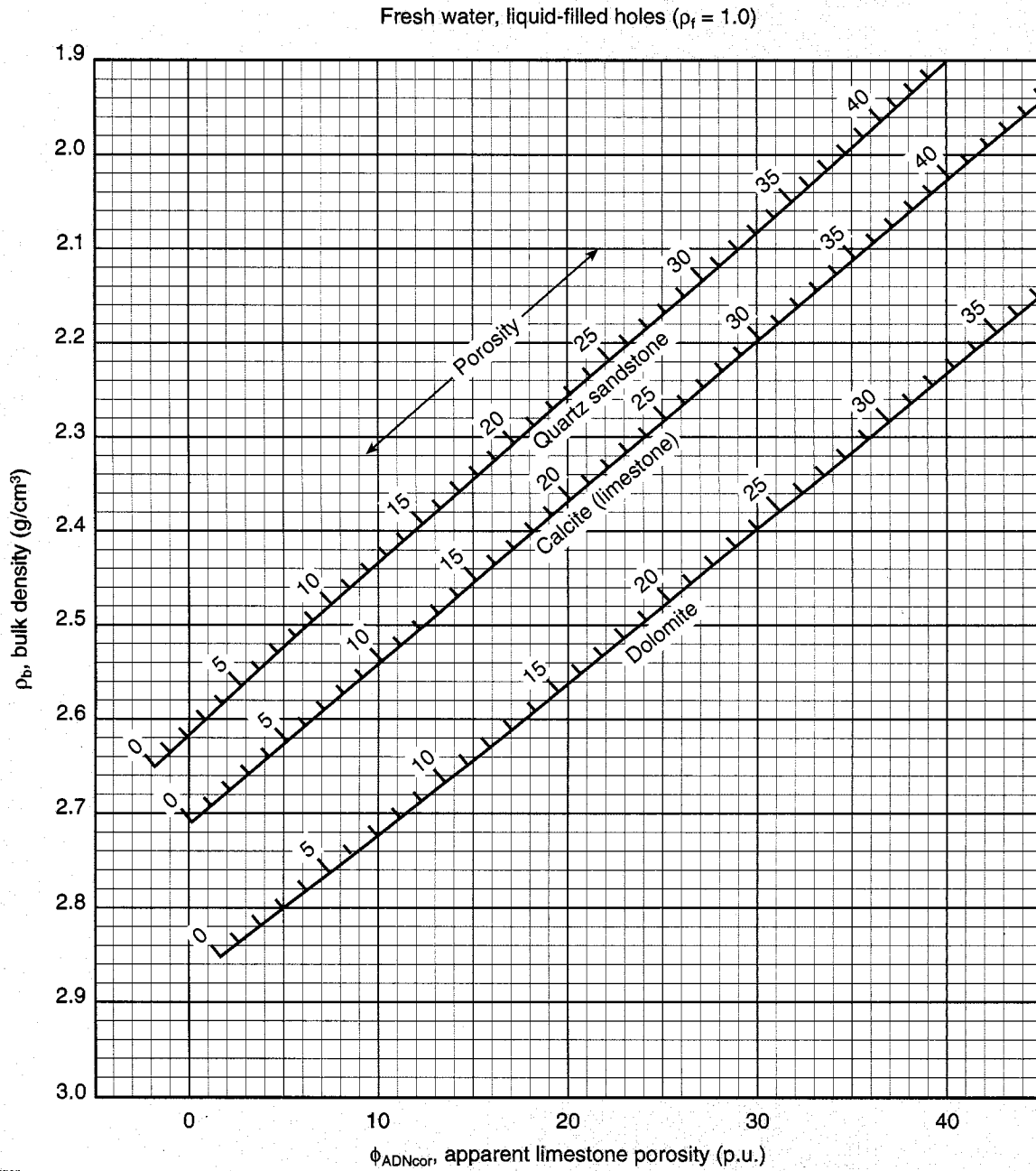


*Mark of Schlumberger
© Schlumberger

CP

Porosity and Lithology Determination from Formation Density Log and ADN* Azimuthal Density Neutron Log for 6.75-in. Tool

CP-24

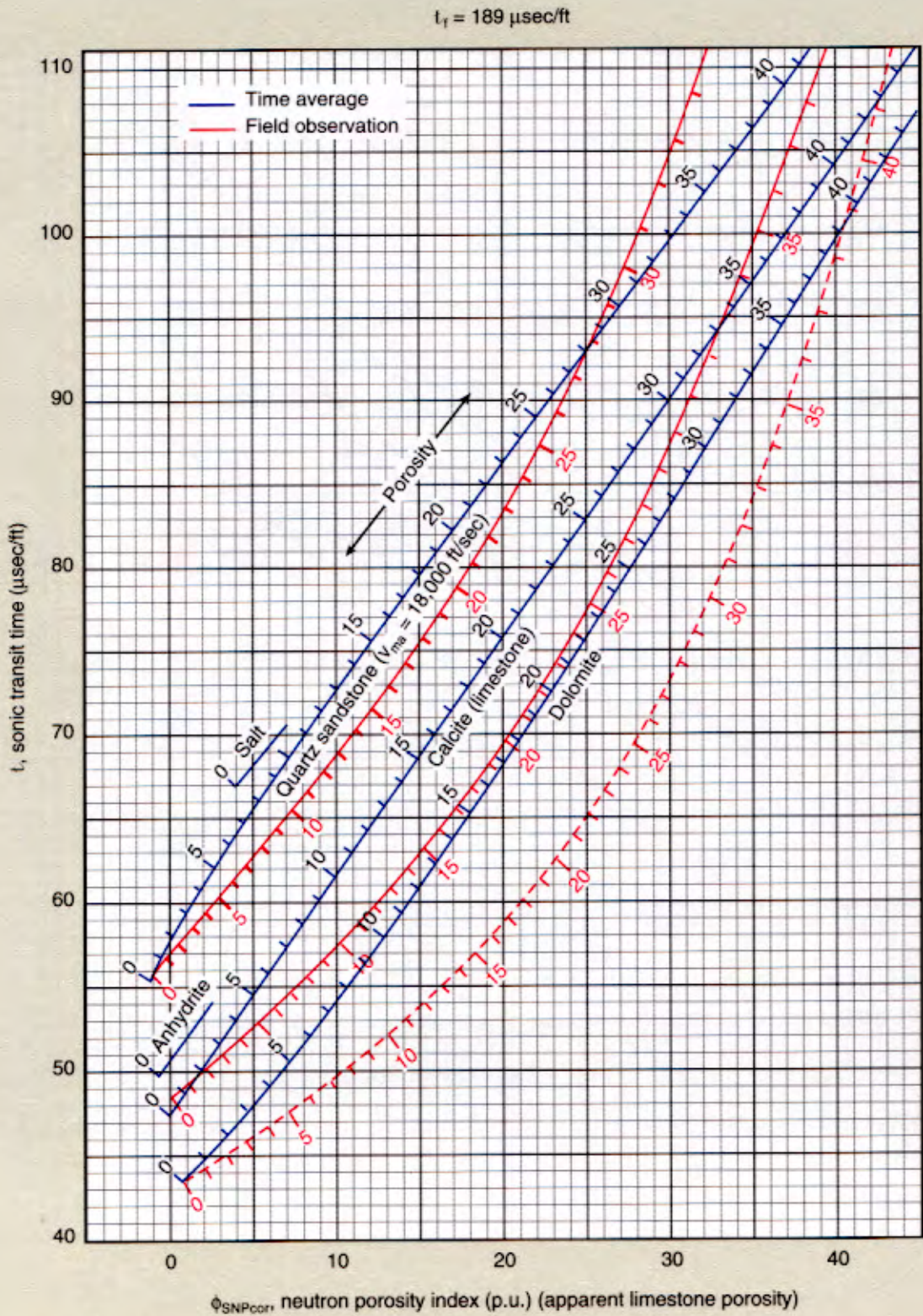


CP

*Mark of Schlumberger
© Schlumberger

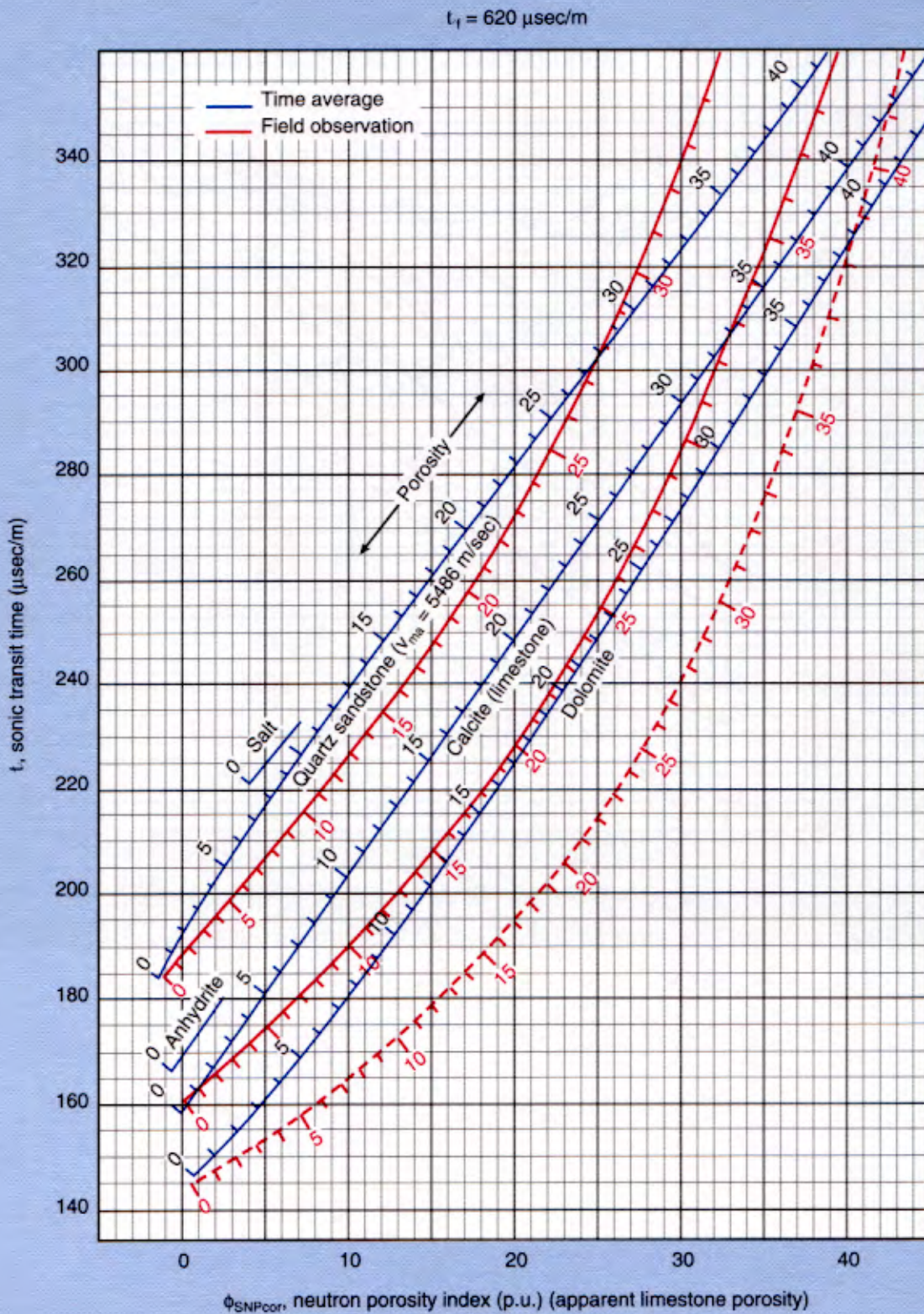
Porosity and Lithology Determination from Sonic Log and SNP Sidewall Neutron Porosity Log

CP-2a
(English)



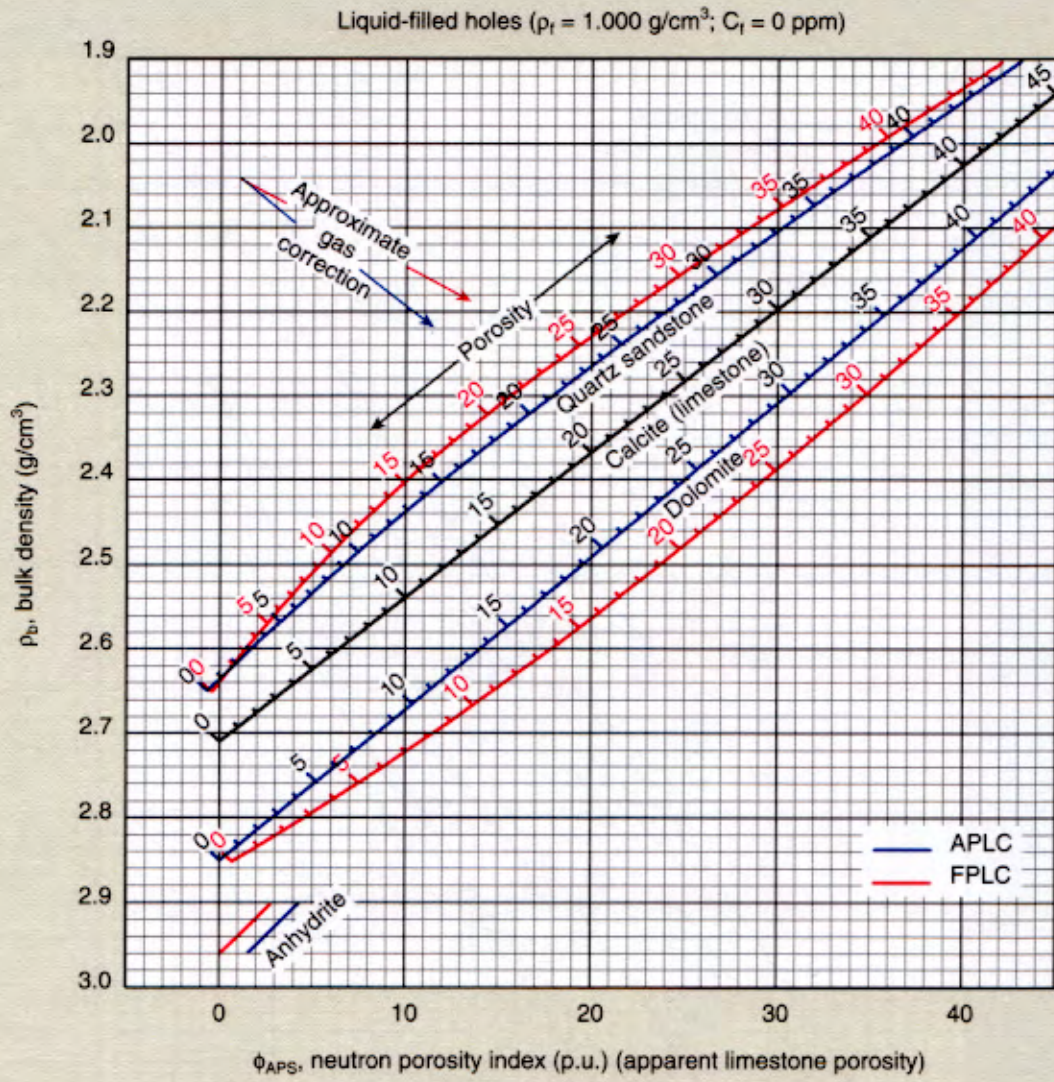
Porosity and Lithology Determination from Sonic Log and SNP Sidewall Neutron Porosity Log

CP-2am
(Metric)



Porosity and Lithology Determination from Litho-Density* Log and Array Porosity Sonde (APS)

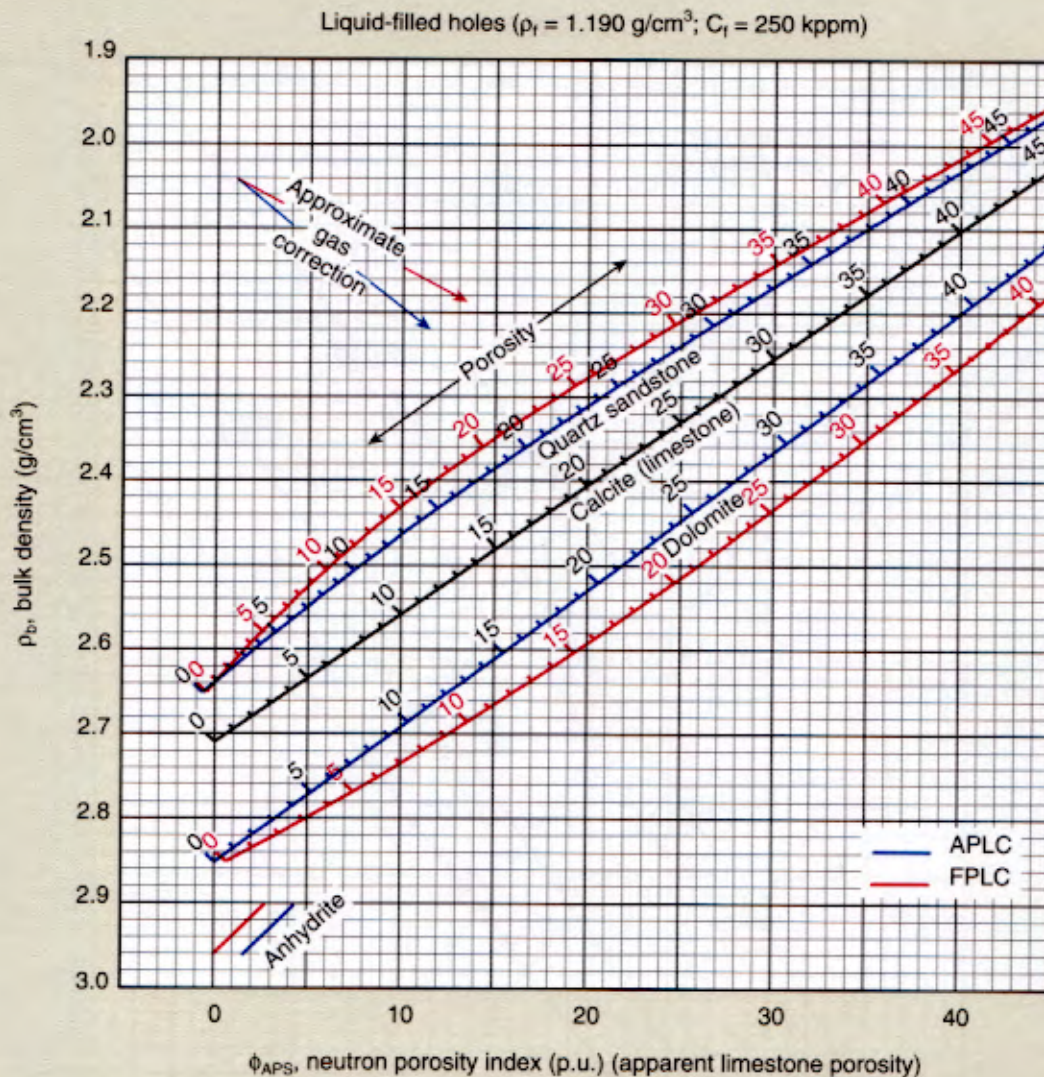
CP-1g



*Mark of Schlumberger
© Schlumberger

Porosity and Lithology Determination from Litho-Density* Log and Array Porosity Sonde (APS)

CP-1h



*Mark of Schlumberger
 © Schlumberger

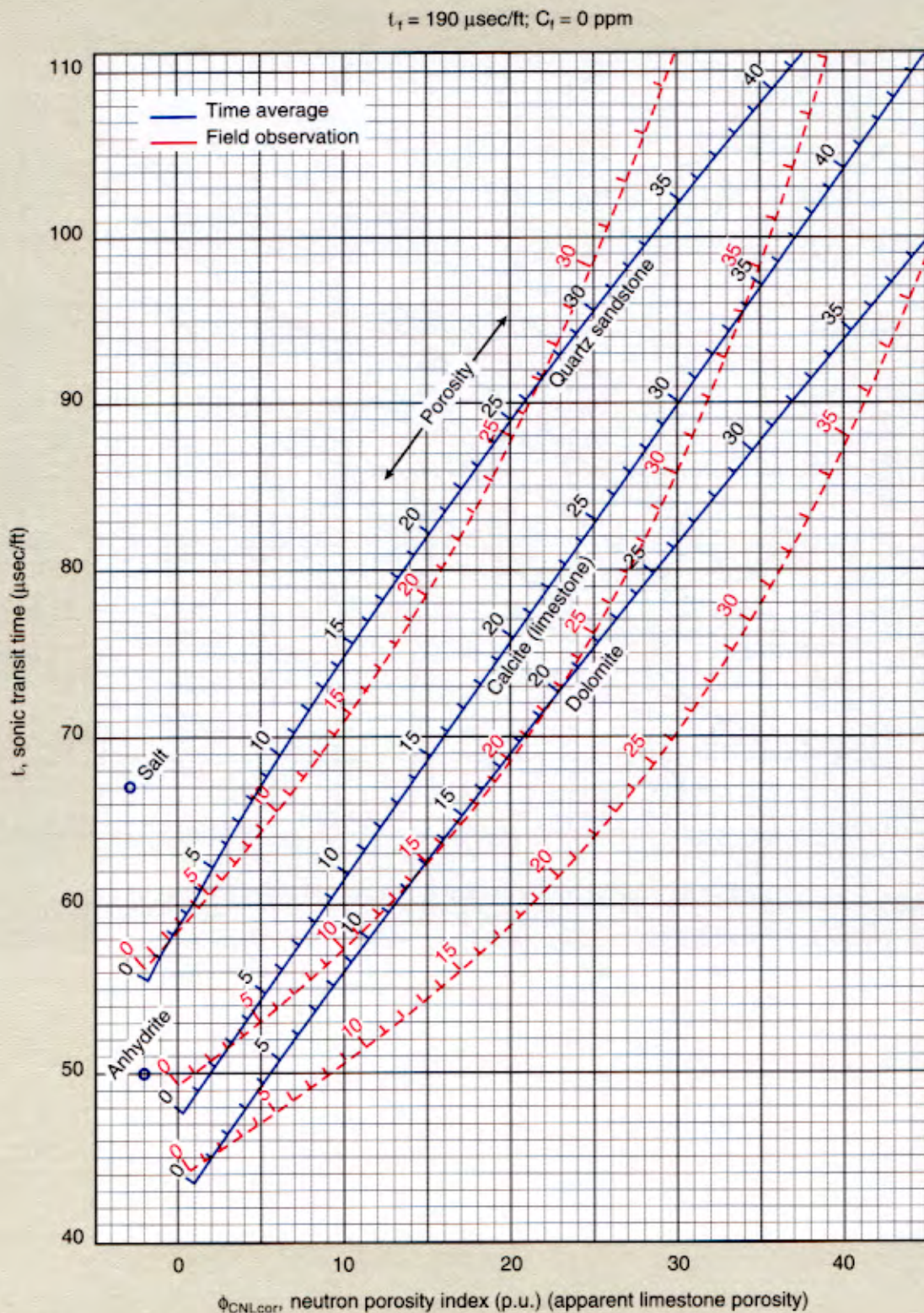
CP

Porosity and Lithology Determination from Sonic Log and CNL* Compensated Neutron Log

For CNL logs after 1986 labeled TNPH

CP-2c
(English)

CP

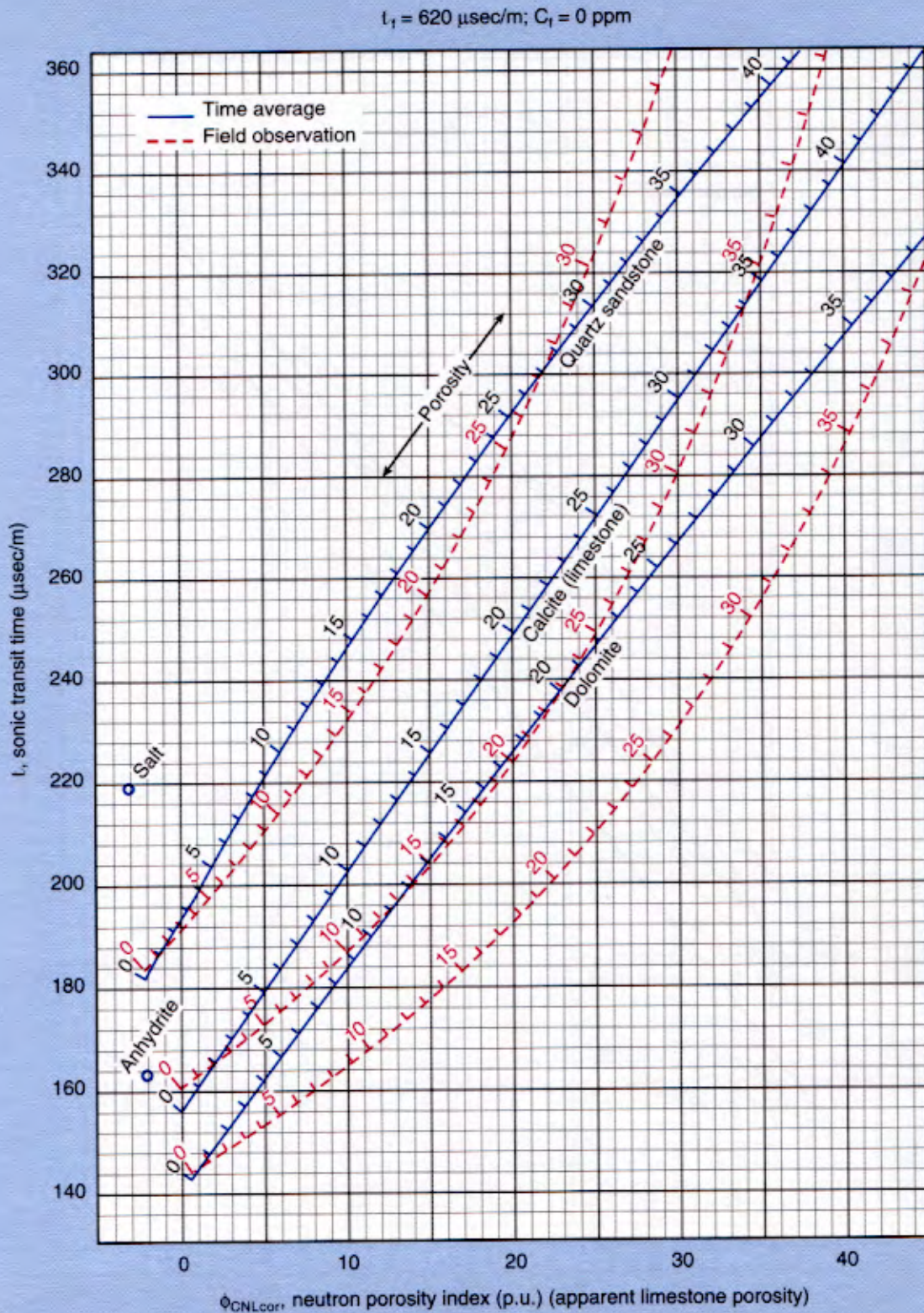


*Mark of Schlumberger
© Schlumberger

Porosity and Lithology Determination from Sonic Log and CNL* Compensated Neutron Log

For CNL logs after 1986 labeled TNPH

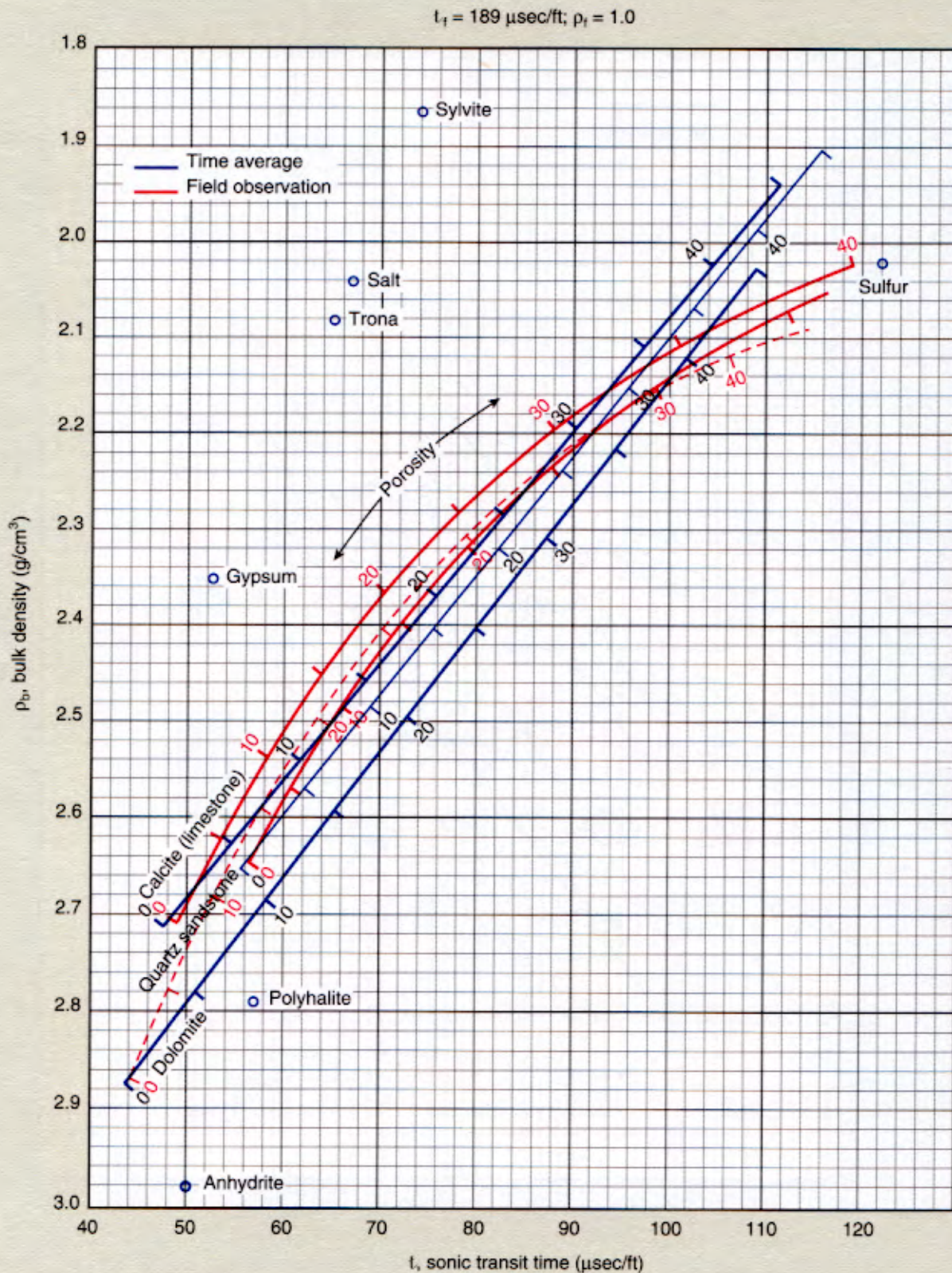
CP-2cm
(Metric)



CP

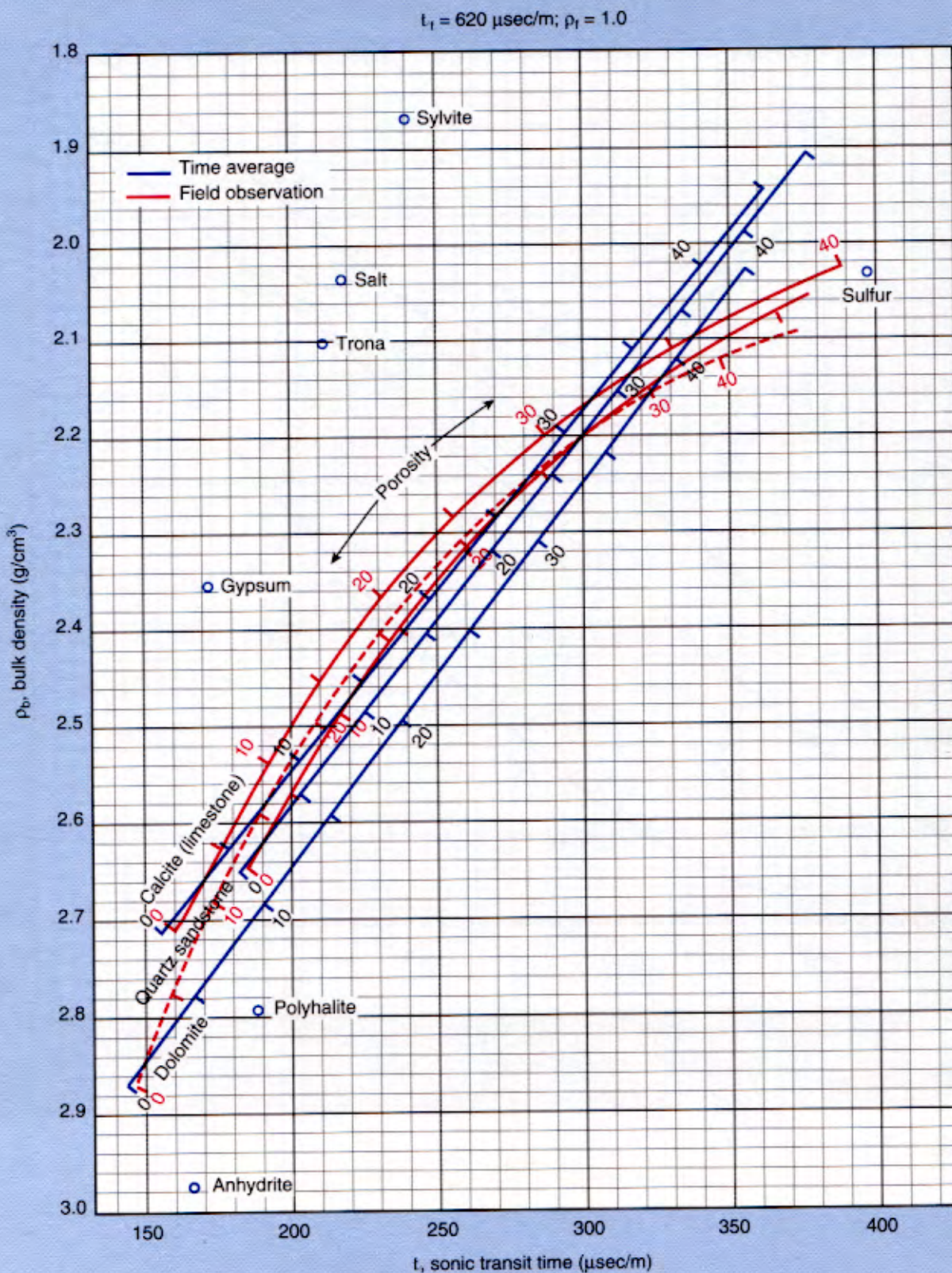
Lithology Identification from Formation Density Log and Sonic Log

CP-7
(English)



Lithology Identification from Formation Density Log and Sonic Log

CP-7m
(Metric)

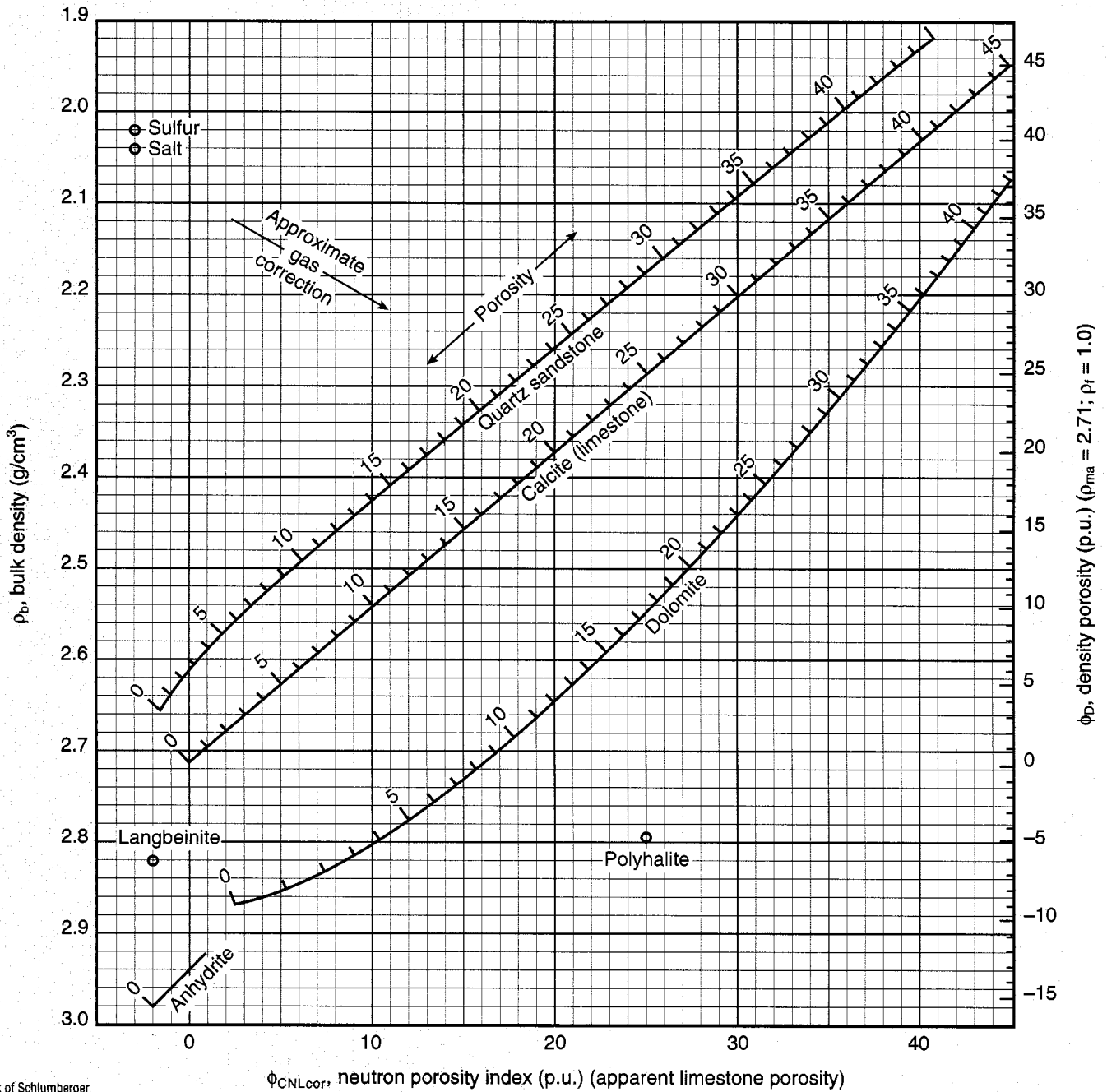


CP

Porosity and Lithology Determination from Formation Density Log and CNL* Compensated Neutron Log

For CNL logs before 1986, or labeled NPHI

Fresh water, liquid-filled holes ($\rho_f = 1.0$)



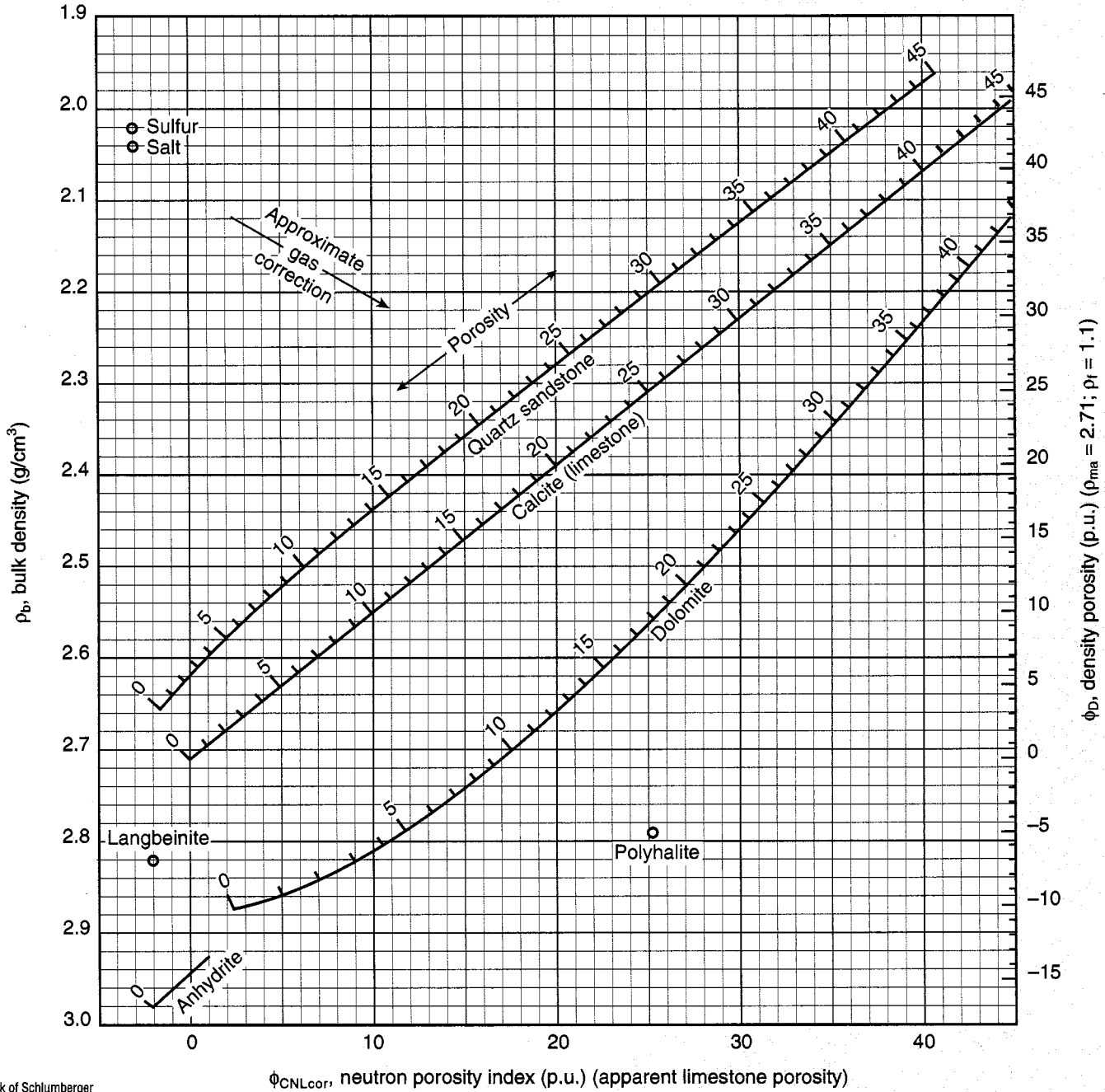
*Mark of Schlumberger
© Schlumberger

Porosity and Lithology Determination from Formation Density Log and CNL* Compensated Neutron Log

For CNL logs before 1986, or labeled NPHI

CP-1d

Salt water, liquid-filled holes ($\rho_f = 1.1$)

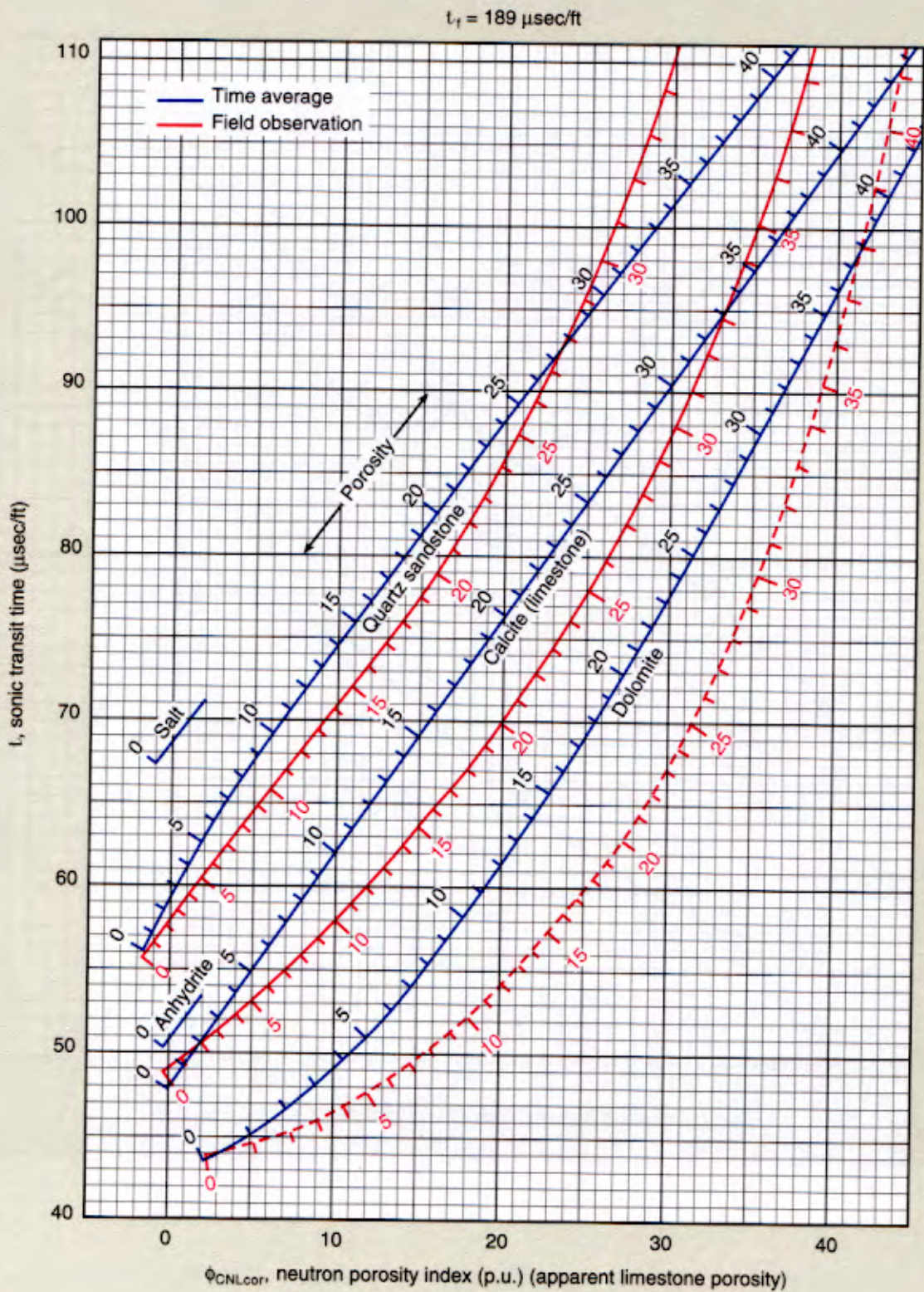


*Mark of Schlumberger
© Schlumberger

Porosity and Lithology Determination from Sonic Log and CNL* Compensated Neutron Log

For CNL logs before 1986, or labeled NPHI

CP-2b
(English)

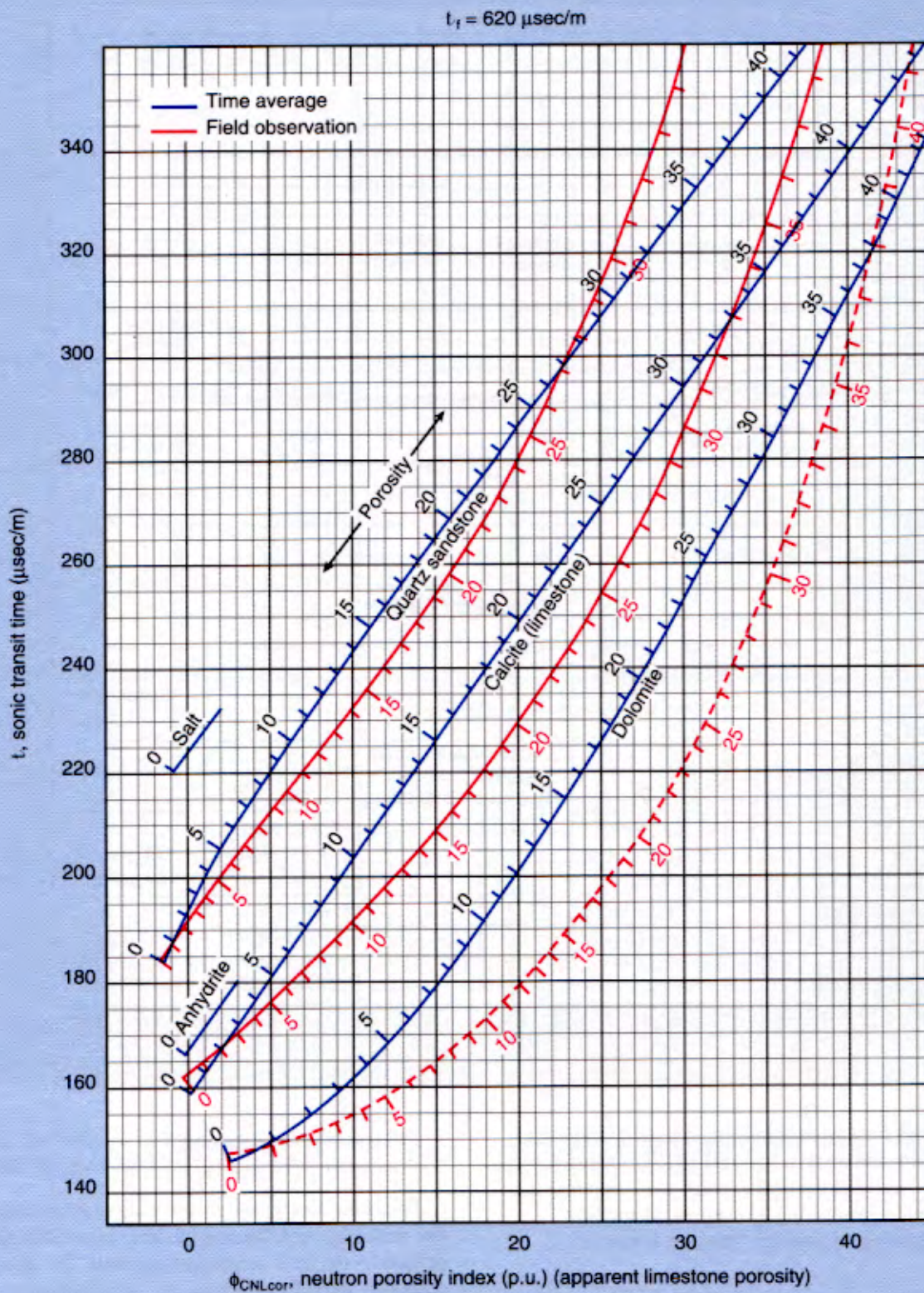


*Mark of Schlumberger
© Schlumberger

Porosity and Lithology Determination from Sonic Log and CNL* Compensated Neutron Log

CP-2bm
(Metric)

For CNL logs before 1986, or labeled NPHI

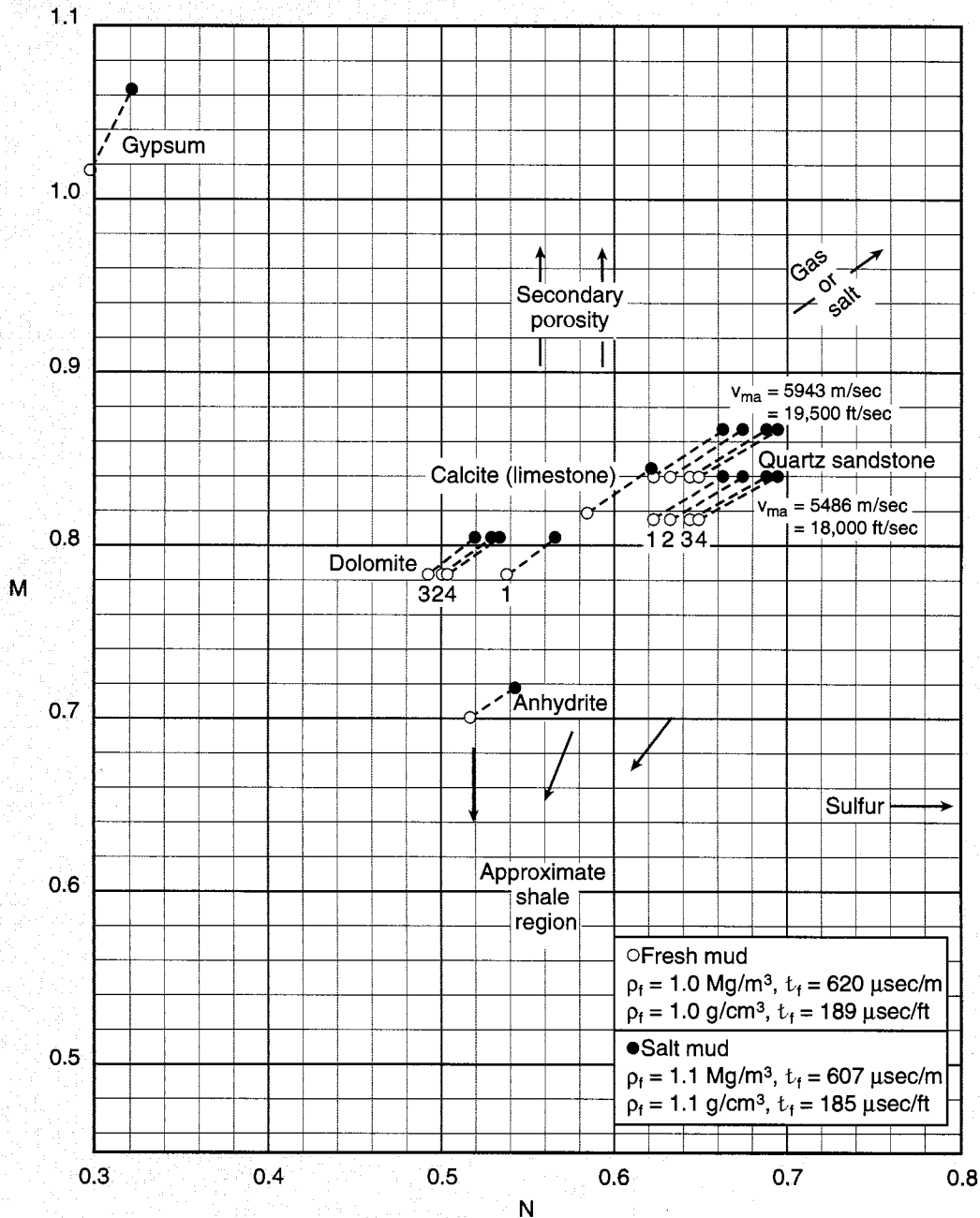


*Mark of Schlumberger
© Schlumberger

CP

M-N Plot for Mineral Identification

For CNL* curves that have been environmentally corrected



This crossplot may be used to help identify mineral mixtures from sonic, density and neutron logs. (The CNL neutron log is used in the above chart; the time average sonic response is assumed.) Except in gas-bearing formations, M and N are practically independent of porosity. They are defined as:

$$M = \frac{t_f - t}{\rho_b - \rho_f} \times 0.01 \text{ (English)}$$

$$M = \frac{t_f - t}{\rho_b - \rho_f} \times 0.003 \text{ (metric)}$$

$$N = \frac{(\phi_N)_f - \phi_N}{\rho_b - \rho_f} \text{ (English or metric)}$$

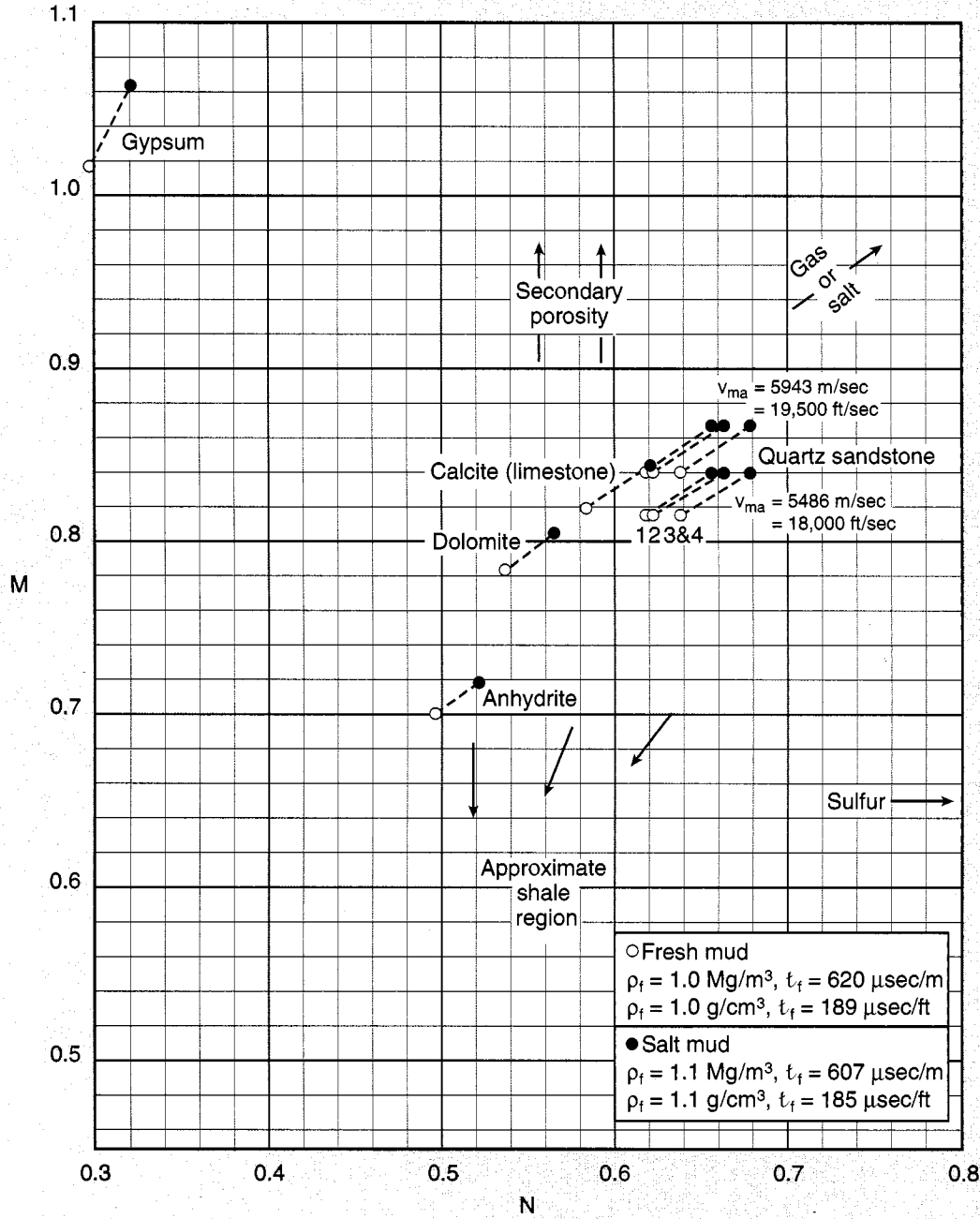
Points for binary mixtures plot along a line connecting the two mineral points. Ternary mixtures plot within the triangle defined by the three constituent minerals. The effect of gas, shaliness, secondary porosity, etc., is to shift data points in the directions shown by the arrows.

The dolomite and sandstone lines on Chart CP-8 are divided by porosity range as follows: 1) $\phi = 0$ (tight formation); 2) $\phi = 0$ to 12 p.u.; 3) $\phi = 12$ to 27 p.u.; and 4) $\phi = 27$ to 40 p.u.

M-N Plot for Mineral Identification

For APS curves that have been environmentally corrected

CP-8a



CP

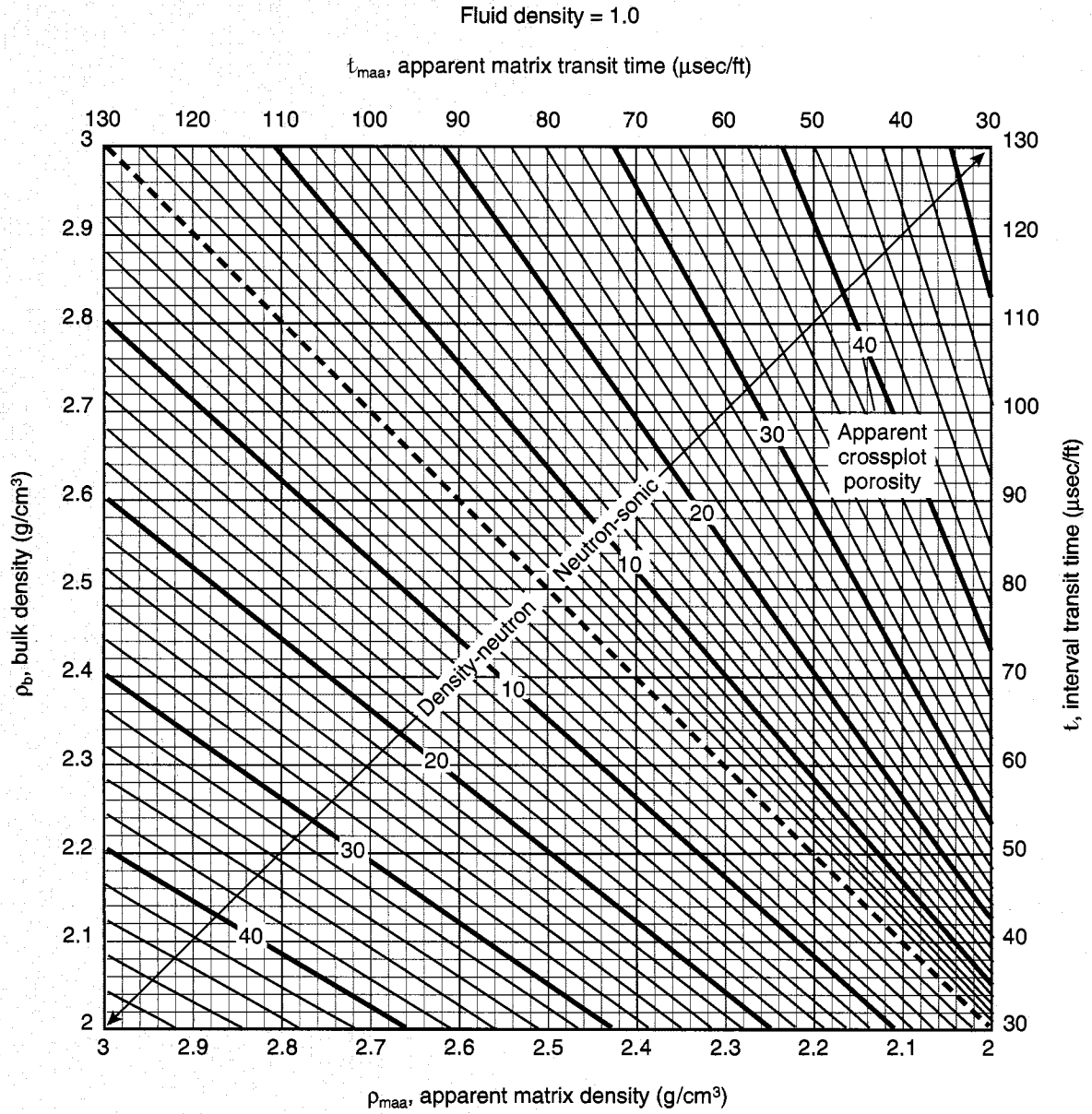
*Mark of Schlumberger
© Schlumberger

On Chart CP-8a, the APS apparent limestone porosity (APLC) replaces the CNL* apparent limestone porosity (NPHI) used on Chart CP-8.

Since there is negligible dolomite spread, a single dolomite point is plotted for each mud.

Determination of Apparent Matrix Parameters from Bulk Density or Interval Transit Time and Apparent Total Porosity

CP-14
(English)



© Schlumberger

The MID plot permits the identification of rock mineralogy or lithology through a comparison of neutron, density and sonic measurements.

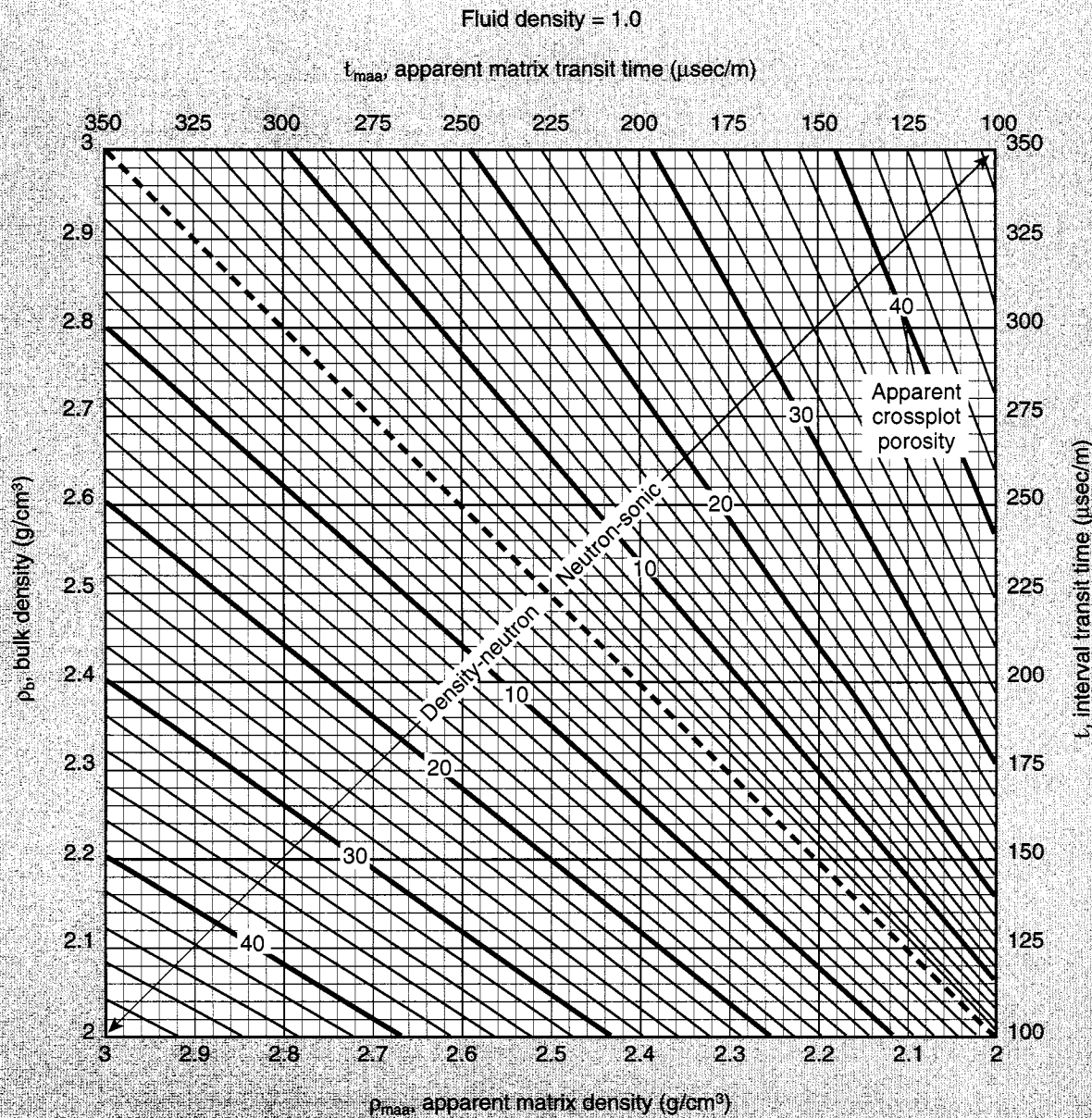
To use the MID plot, three steps are required. First, an apparent crossplot porosity must be determined using the appropriate

neutron-density and empirical (red curves) neutron-sonic crossplot (Charts CP-1 through CP-7). For any data plotting above the sandstone curve on these charts, the apparent crossplot porosity is defined by a vertical projection to the sandstone curve.

Continued on next page

Determination of Apparent Matrix Parameters from Bulk Density or Interval Transit Time and Apparent Total Porosity

CP-14m
(Metric)



© Schlumberger

CP

Next, enter the appropriate CP-14 chart with the interval transit time. Go to the apparent crossplot porosity previously found on the appropriate neutron-sonic crossplot chart. This defines an apparent matrix interval transit time, t_{maa} . Similarly, enter the same chart with the bulk density, ρ_b . Go to the apparent crossplot porosity previously found on the appropriate density-neutron crossplot chart. This defines an apparent matrix grain density, ρ_{maa} .

Finally, the crossplot of the apparent matrix interval transit

time and apparent grain density on the MID plot (Chart CP-15) identifies the rock mineralogy by its proximity to the labeled points on the plot.

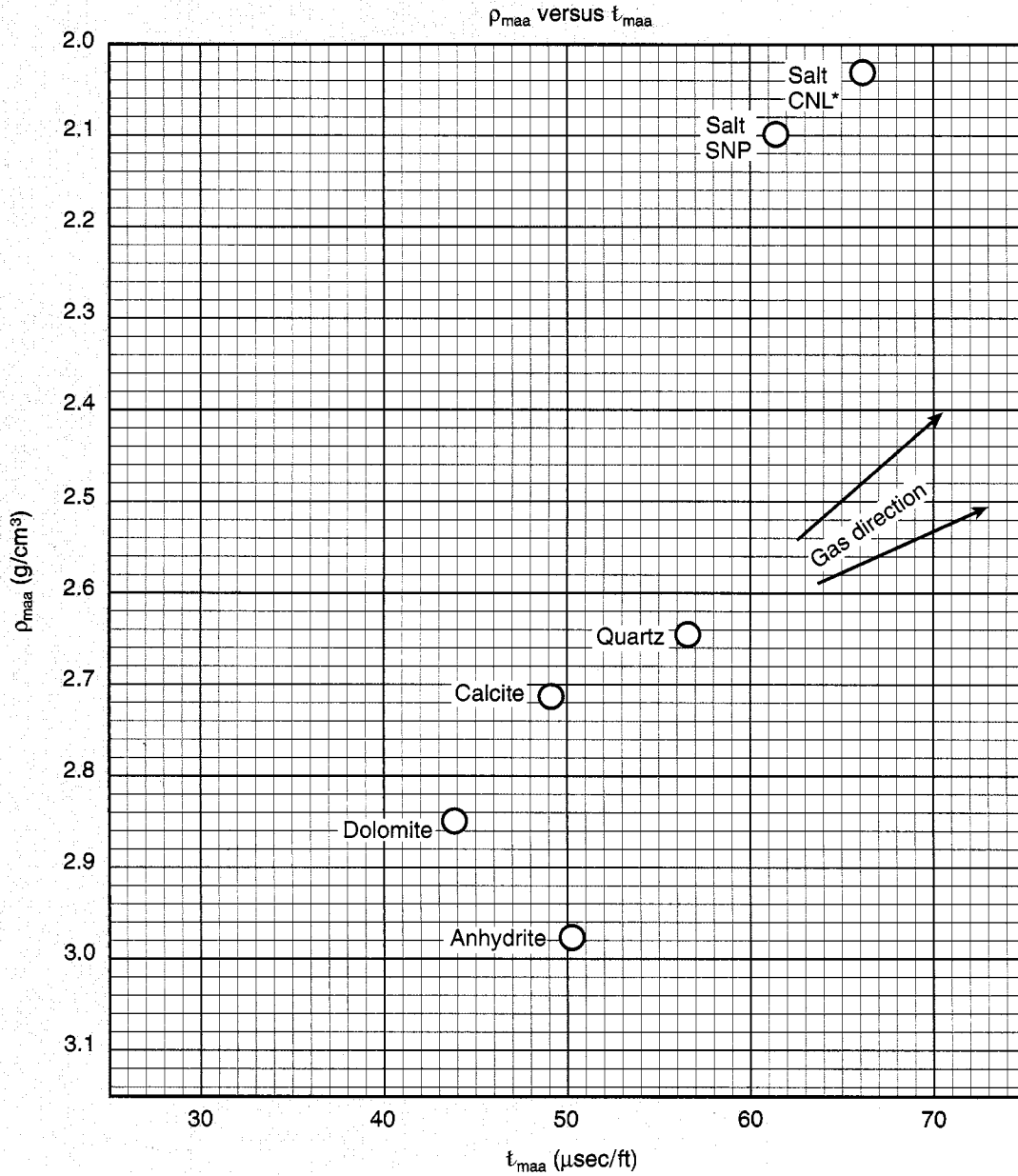
The presence of secondary porosity in the form of vugs or fractures produces displacements parallel to the t_{maa} axis. The presence of gas displaces points as shown on the MID plot. Identification of shaliness is best done by plotting some shale points to establish the shale trend lines.

Continued on next page

Matrix Identification (MID) Plot

CP-15
(English)

CP



© Schlumberger

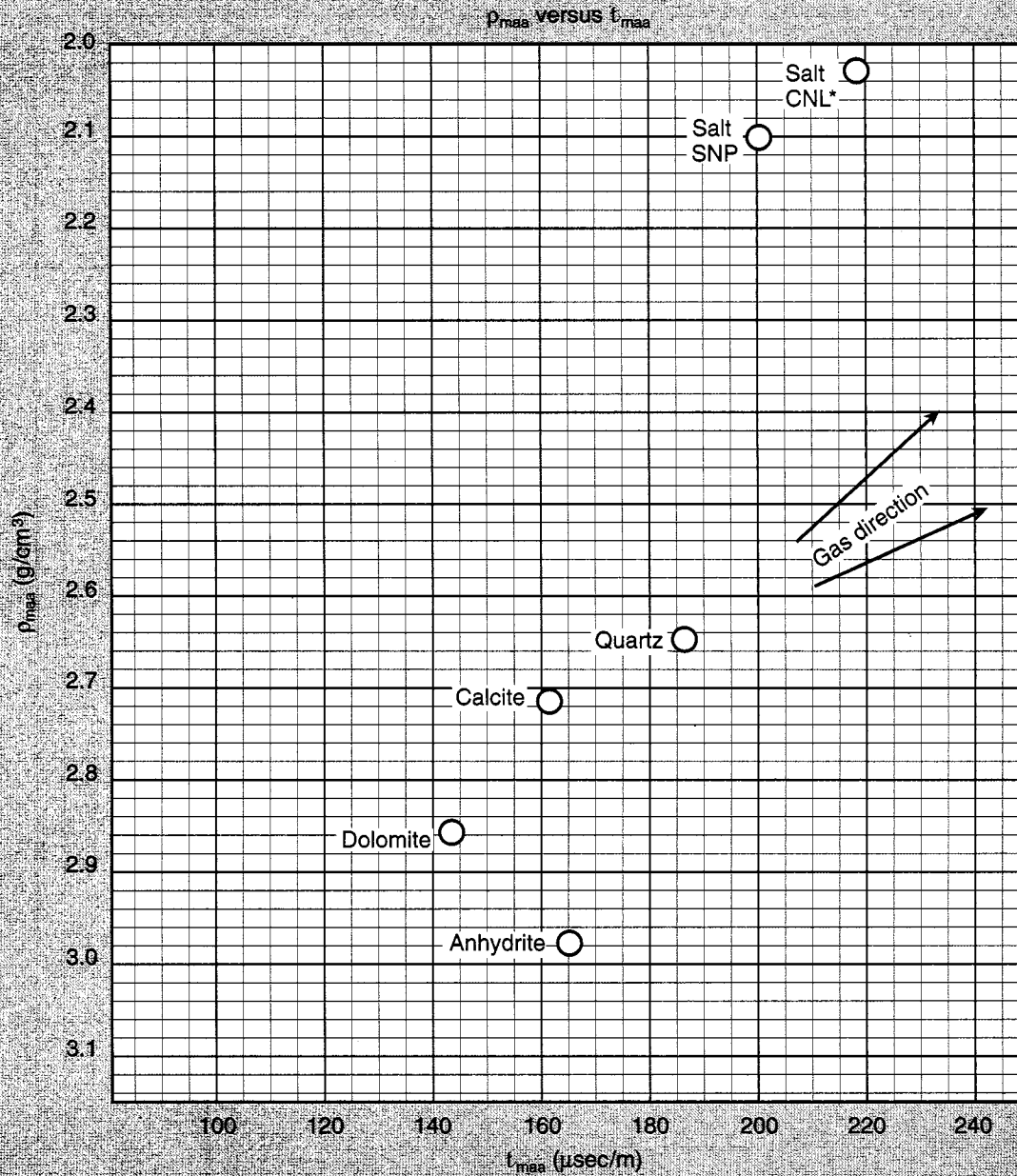
Examples:	Level 1	Level 2	giving	$\phi_{aND} = -1$	$\phi_{aND} = 21$
	$t = 67 \mu\text{sec/ft}$	$t = 63 \mu\text{sec/ft}$		$\phi_{aNS} = -1$	$\phi_{aNS} = 21$
	$\rho_b = 2.04 \text{ g/cm}^3$	$\rho_b = 2.46 \text{ g/cm}^3$	and	$t_{maa} = 66 \mu\text{sec/ft}$	$t_{maa} = 43.5 \mu\text{sec/ft}$
	$\phi_{CNL} = -3$	$\phi_{CNL} = 24 \text{ p.u.}$		$\rho_{maa} = 2.03 \text{ g/cm}^3$	$\rho_{maa} = 2.85 \text{ g/cm}^3$
	$\rho_f = 1.0 \text{ g/cm}^3$				

From the MID plot, Level 1 is identified as salt and Level 2 as dolomite.

Continued on next page

Matrix Identification (MID) Plot

CP-15m
(Metric)



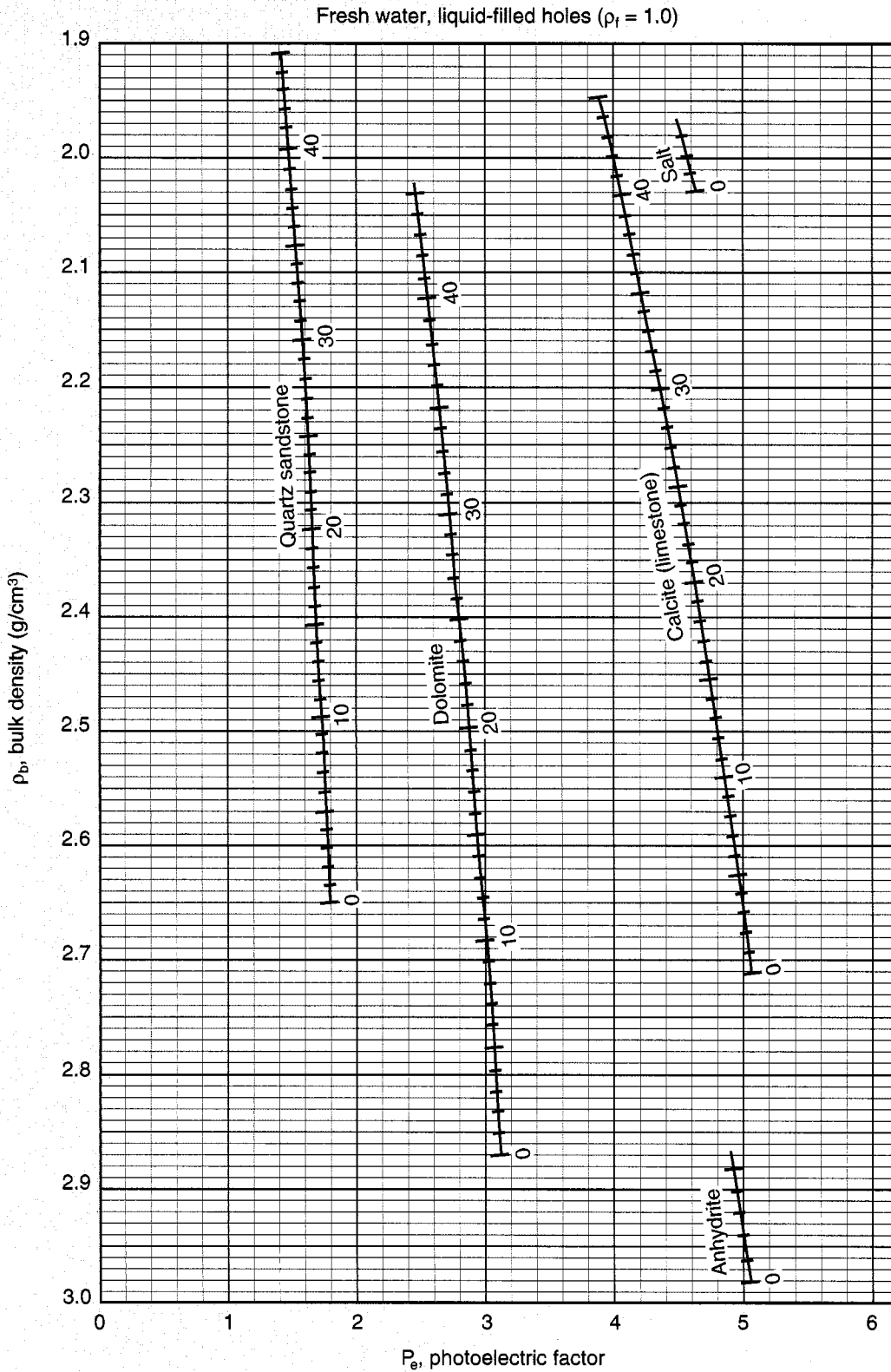
CP

For fluid density, ρ_f (other than 1.0 g/cm^3), correct (multiply) the apparent total porosity by the multiplier in the table before entry into the density portion of the chart.

For more information see Reference 8.

ρ_f	Multiplier
1.0	1.00
1.05	0.98
1.1	0.95
1.15	0.93

Porosity and Lithology Determination from Litho-Density* Log

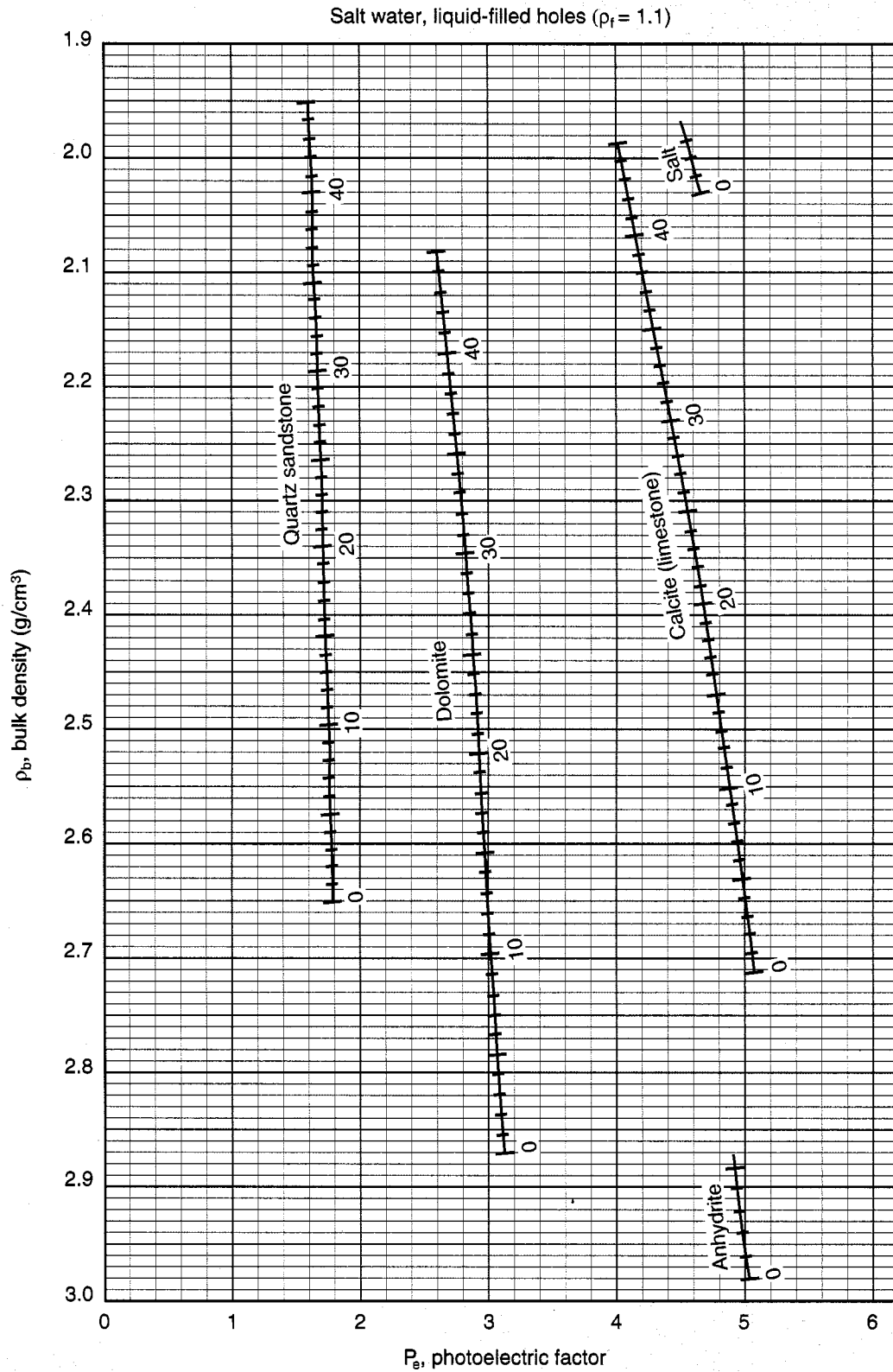


*Mark of Schlumberger
© Schlumberger

For more information see Reference 27.

CP

Porosity and Lithology Determination from Litho-Density* Log



CP

*Mark of Schlumberger
© Schlumberger

Mineral Identification from Litho-Density* Log and NGS* Natural Gamma Ray Spectrometry Log

Chart CP-18 provides clay mineralogy information using NGS Natural Gamma Ray Spectrometry and Litho-Density measurements. Because the porosity and the composition of many clay minerals may vary, the minerals plot on these crossplots not as unique points but as general areas.

After environmental correction, the appropriate parameters are plotted to provide qualitative information about the mineralogy.

Example: $Th_{NGS_{cor}} = 10.6$ ppm

$U_{NGS_{cor}} = 4.5$ ppm

$K_{NGS_{cor}} = 3.9\%$

$P_e = 3.2$

giving $Th/K = 10.6/3.9 = 2.7$

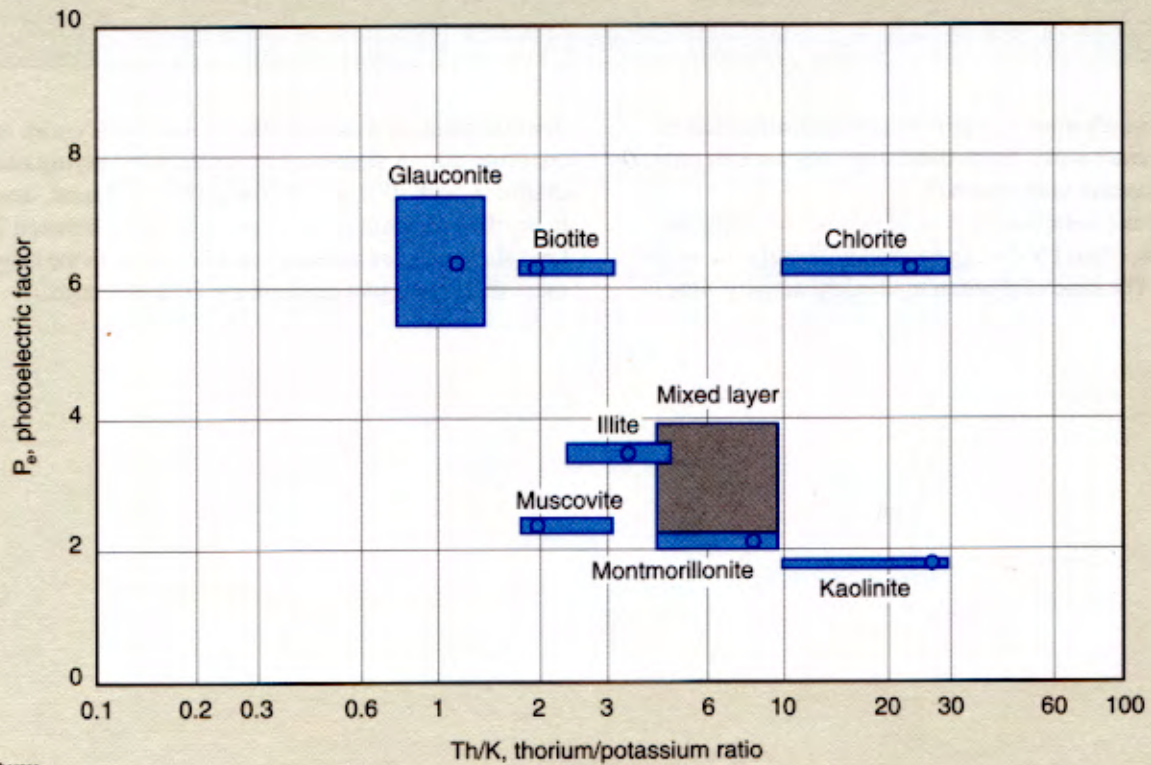
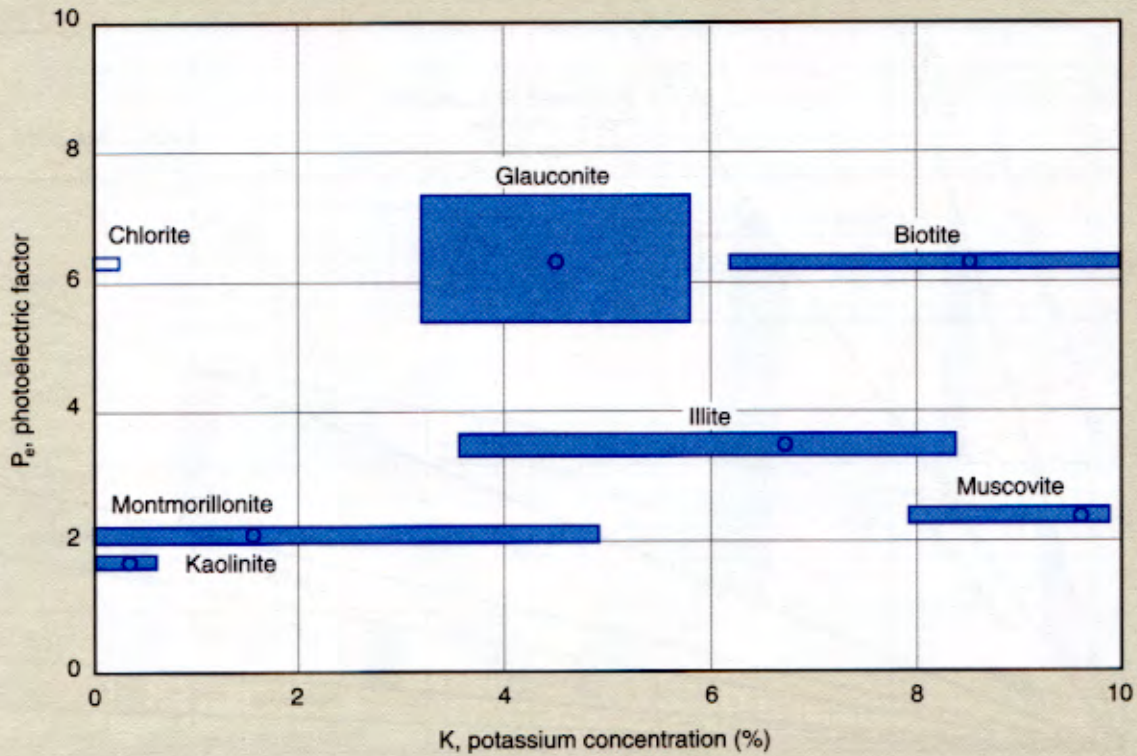
Plotting these parameters on Chart CP-18 suggests that the clay mineral is illite.

*Mark of Schlumberger

Mineral Identification from Litho-Density* Log and NGS* Natural Gamma Ray Spectrometry Log

CP-18

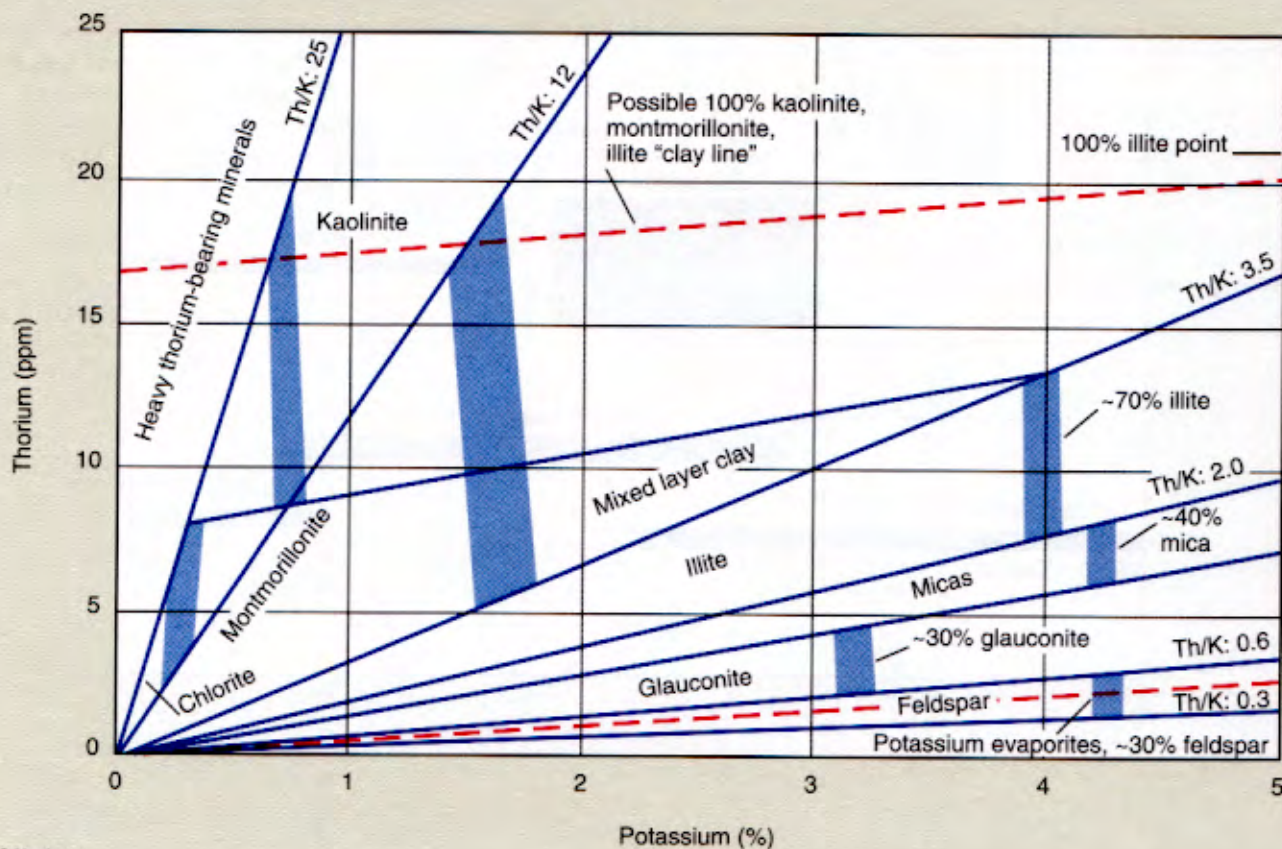
CP



*Mark of Schlumberger
© Schlumberger

Mineral Identification from NGS* Natural Gamma Ray Spectrometry Log

CP-19



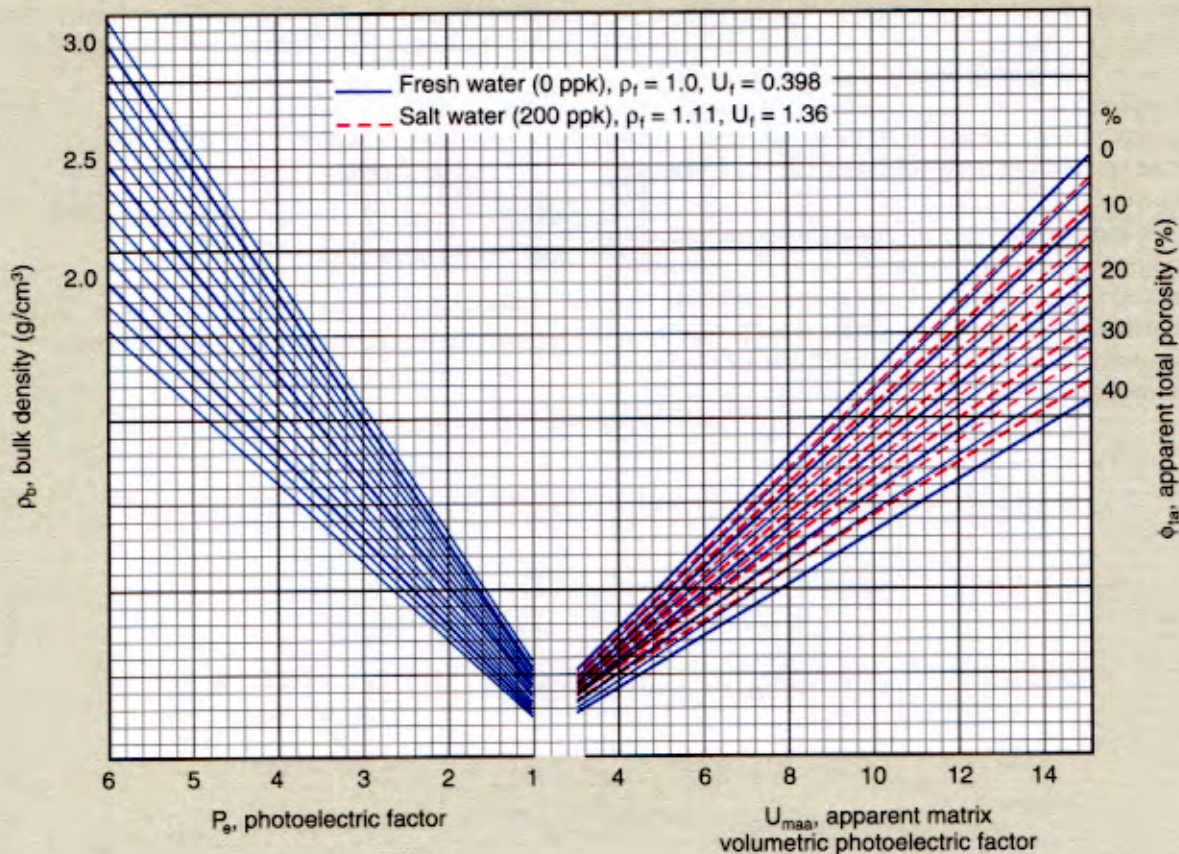
Radioactive minerals often occur in relatively small concentrations in sedimentary rocks. Even shales typically contain only 30 to 70% radioactive clay minerals.

Unless there is a complex mixture of radioactive minerals in the formation, Chart CP-19 can be used to identify the more common ones. The ratio of thorium to uranium activity—the

thorium/potassium ratio, Th/K—does not vary with mineral concentration. A sandstone reservoir with varying amounts of shaliness, with illite as the principal clay mineral, usually plots in the illite segment of the chart, with Th/K between 2.0 and 2.5. Less shaly parts of the reservoir plot closer to the origin, and more shaly parts plot closer to the 70% illite area.

Determination of Apparent Matrix Volumetric Photoelectric Factor

CP-20



Lithology Identification Plot

Plot CP-21 identifies rock mineralogy through a comparison of apparent matrix grain density and apparent volumetric photoelectric factor.

To use, apparent matrix grain density, ρ_{maa} , and apparent volumetric photoelectric factor, U_{maa} , are entered in ordinate and abscissa, respectively, on Plot CP-21. Rock mineralogy is identified by the proximity of the plotted data point to the labeled points on the plot.

To determine apparent matrix grain density, an apparent total porosity must first be determined (using, for example, a neutron-density crossplot). Then, Chart CP-14 may be used with bulk density, ρ_b , to define the apparent matrix grain density, ρ_{maa} .

To find the apparent matrix volumetric photoelectric factor, U_{maa} , enter Nomograph CP-20 with the photoelectric factor, P_e ;

go vertically to the bulk density, ρ_b ; then, go horizontally across to the total porosity, ϕ_t ; and finally, go vertically downward to define the matrix volumetric photoelectric factor, U_{maa} .

Example: $P_e = 3.65$

$$\rho_b = 2.52 \text{ g/cm}^3 \quad (\rho_f = 1.0 \text{ g/cm}^3)$$

$$\phi_{ta} = 16\%$$

giving $\rho_{maa} = 2.81 \text{ g/cm}^3$ (from Chart CP-14)

and $U_{maa} = 10.9$

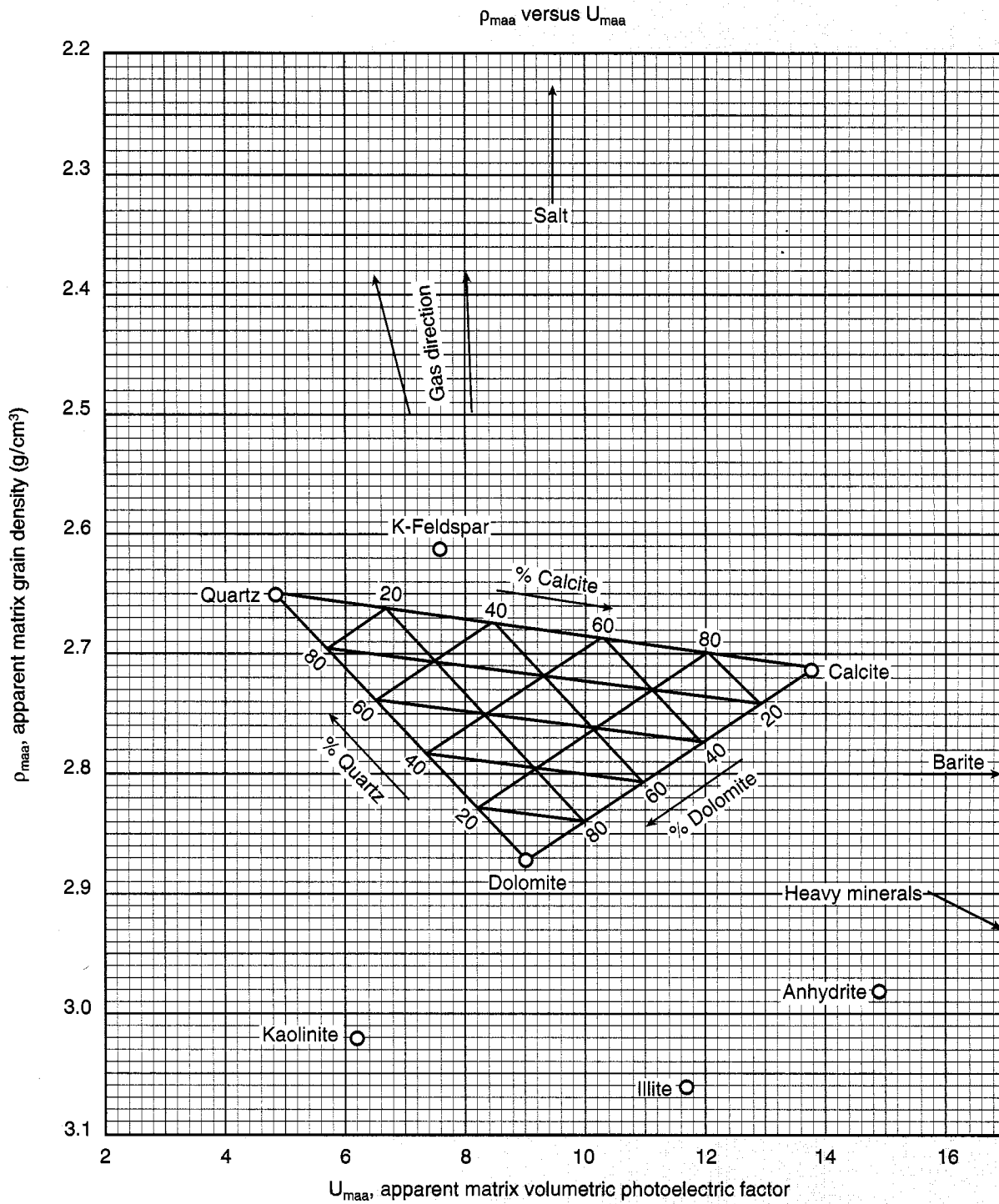
Plotting these values indicates the level to be a mixture of approximately 60% dolomite and 40% limestone.

For more information see Reference 27.

Lithology Identification Plot

CP-21

CP

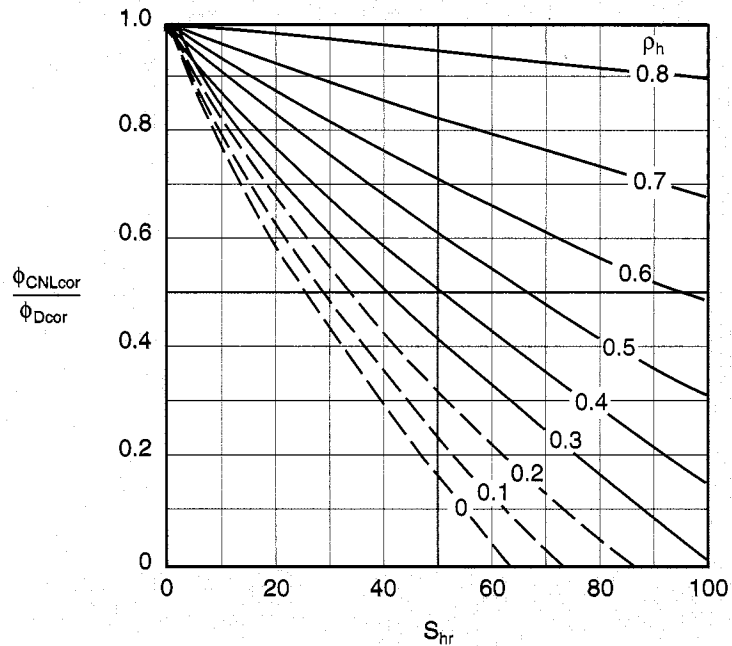
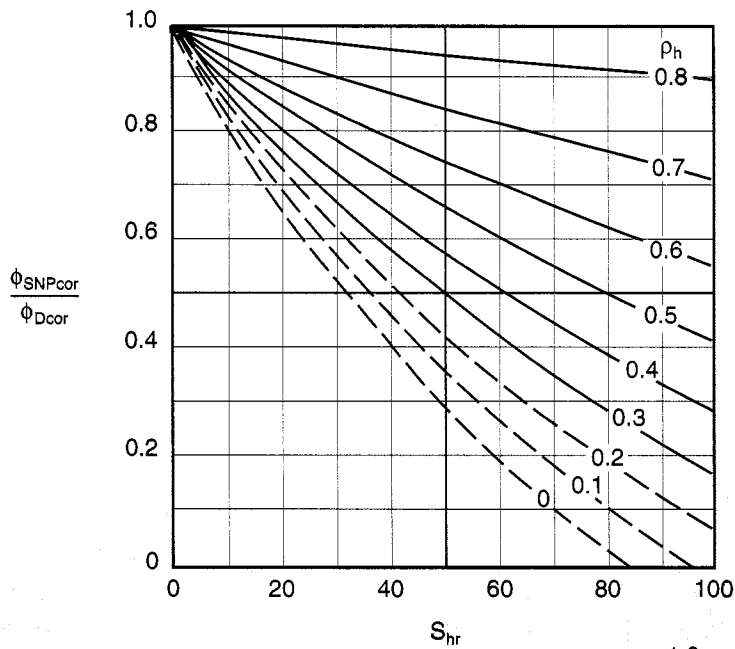


Estimation of Hydrocarbon Density

From neutron and density logs

CP-10

CP



*Mark of Schlumberger
© Schlumberger

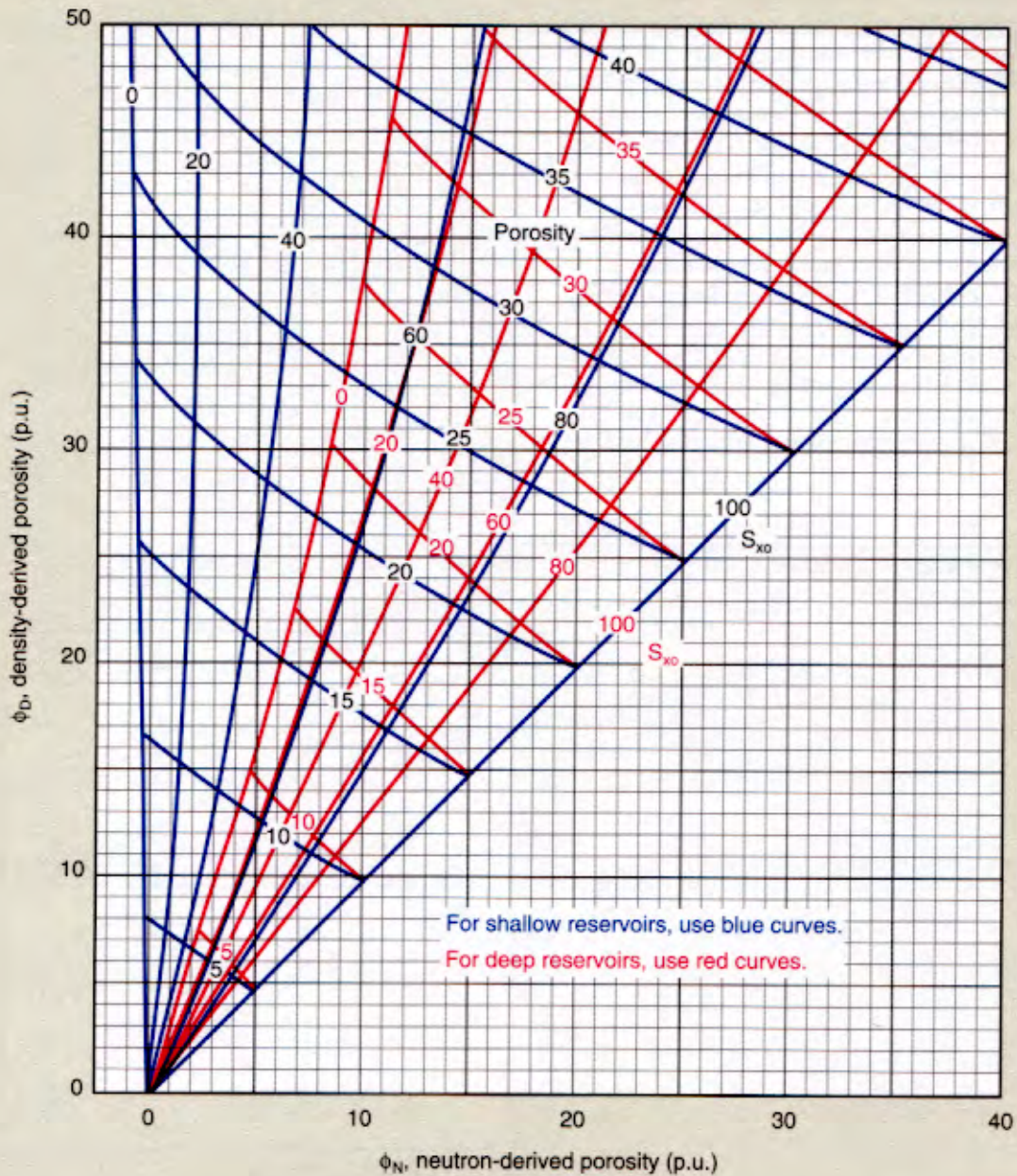
These charts estimate the density of the saturating hydrocarbon from a comparison of neutron and density measurements, and the hydrocarbon saturation in the portion of the rock investigated by the neutron and density logs (invaded or flushed zone). The neutron log (either CNL* or SNP log) and the density log must be corrected for environmental effect and lithology before entry into the charts.

To use, enter the appropriate chart with the ratio of neutron porosity to density porosity, and the hydrocarbon saturation. The intersection defines the hydrocarbon density in g/cm³.

Example: $\phi_{CNL_{cor}} = 15$ p.u.
 $\phi_{D_{cor}} = 25$ p.u.
 and $S_{hr} = 30\%$
 Therefore, $\rho_h = 0.28$ g/cm³

Charts CP-9 and CP-10 have not been updated for CNL logs run after 1986 or labeled TNPH; approximations may therefore be greater with more recent logs. For approximate results with APLC porosity (from IPL* logs), use Charts CP-9 and CP-10 for SNP logs.

Gas-Bearing Formations— Porosity from Density and Neutron Logs



Based on reservoir depth and conditions, enter the appropriate chart with matrix-corrected porosity values. Average water saturation in the flushed zone, S_{xo} , and porosity are derived. This chart assumes fresh water and gas of composition $C_{1.1}H_{4.2}$, and it includes correction of the neutron log for "excavation effect."

For more information see Reference 6.

The conditions represented by the curves are listed in the table below.

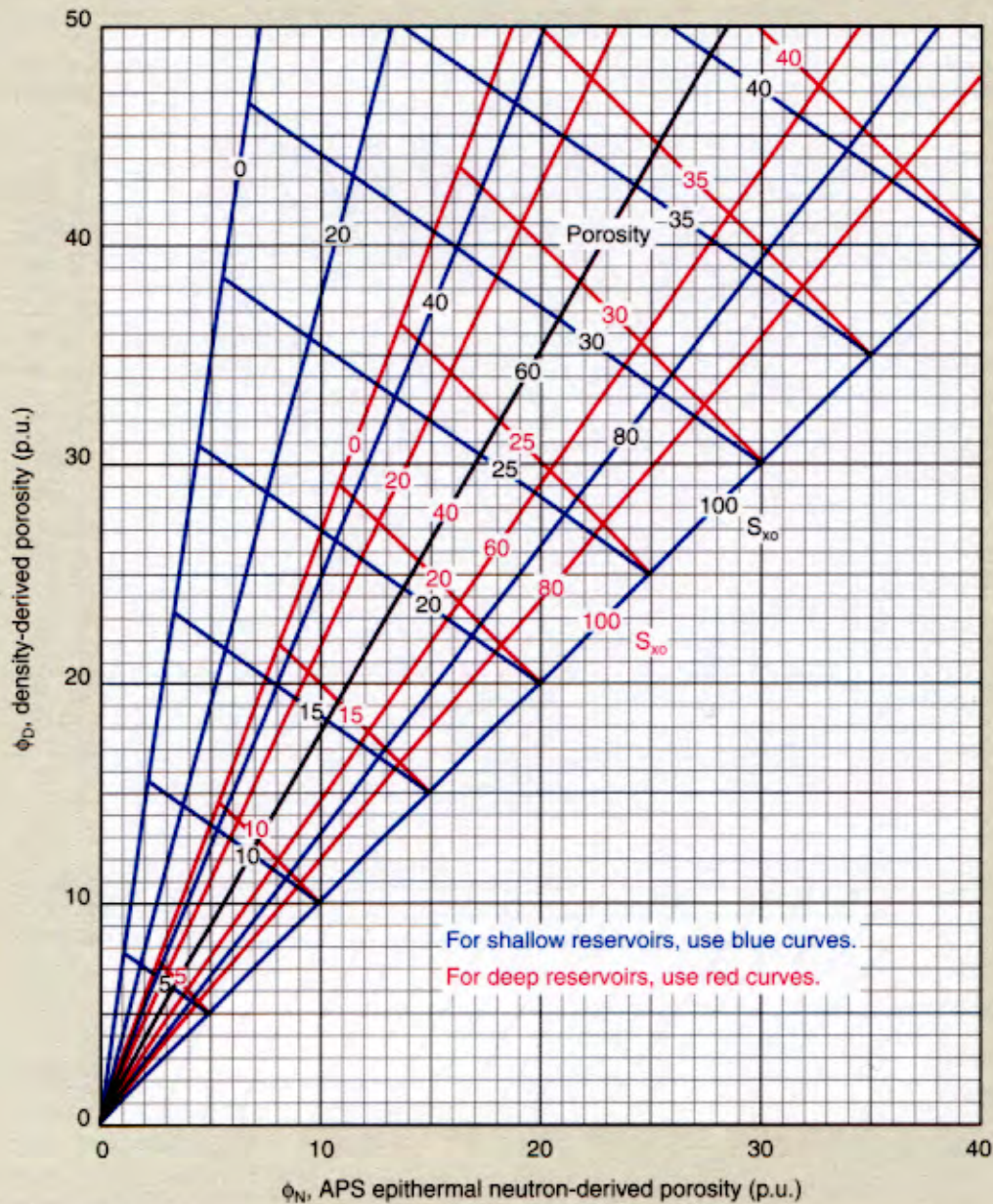
Example: ϕ_D reads 25%, and ϕ_N reads 10% in a low-pressure, shallow (4000-ft) reservoir.

Therefore, $\phi = 20\%$, and $S_{xo} = 62\%$.

Depth	Pressure	Temperature	P_w	I_{Hw}	P_g	I_{Hg}
Shallow reservoirs (blue)	~2000 psi [~14,000 kPa]	~120°F [~50°C]	1.00	1.00	0	0
Deep reservoirs (red)	~7000 psi [~48,000 kPa]	~240°F [~120°C]	1.00	1.00	0.25	0.54

Gas-Bearing Formations— Porosity from Density and APS Epithermal Neutron Logs

CP-5a



© Schlumberger

Based on reservoir depth and conditions, enter the chart with sandstone-corrected porosity values. Average water saturation in the flushed zone, S_{xo} , and porosity are derived. This chart assumes fresh water and gas of composition CH_4 .

The conditions represented by the curves are listed in the table below.

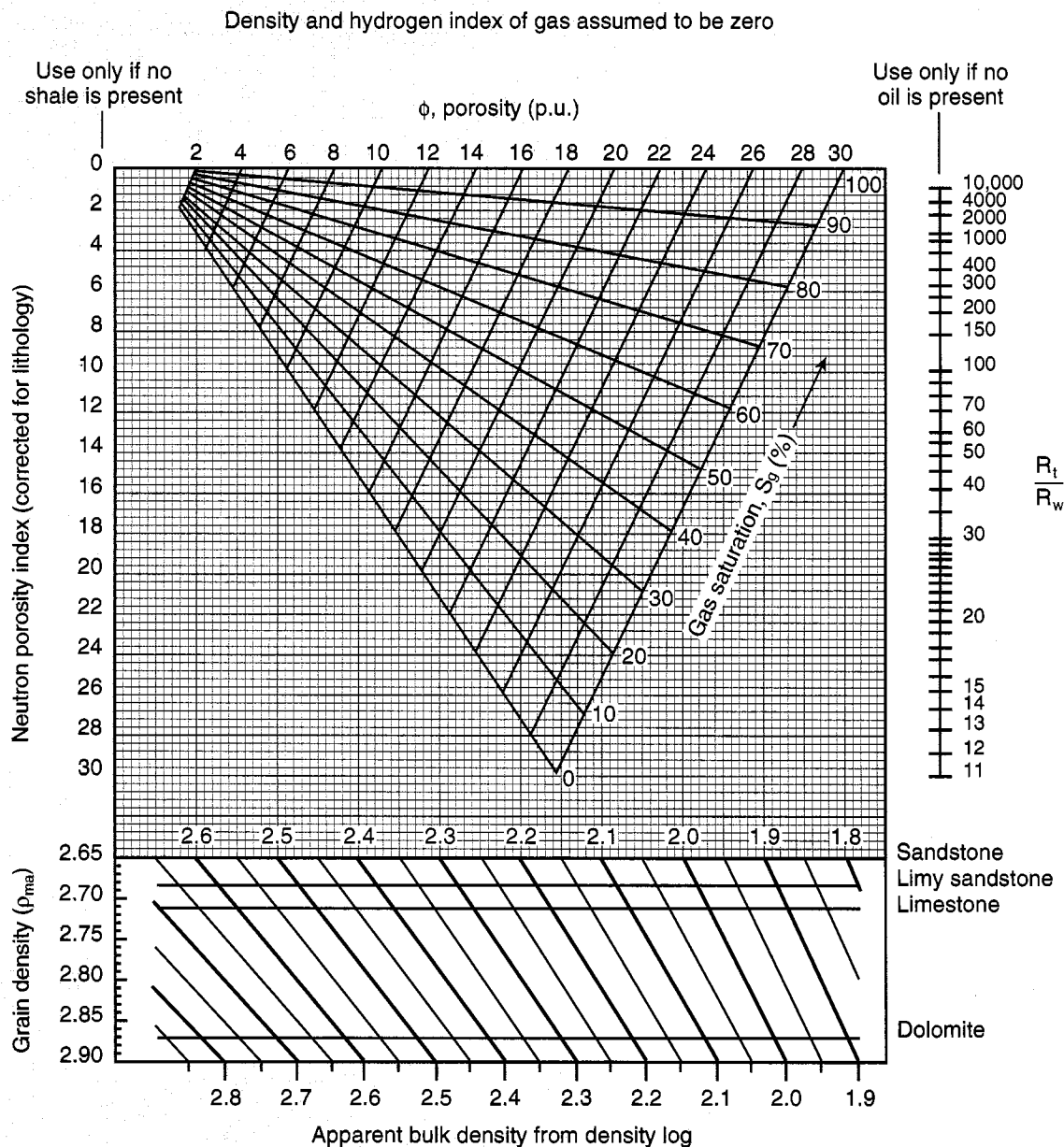
Example: ϕ_D reads 24%, and ϕ_N reads 14% in a low-pressure, shallow (4000-ft) reservoir.

Therefore, $\phi = 20\%$, and $S_{xo} = 62\%$.

Depth	Pressure	Temperature	ρ_w	I_{Hw}	ρ_g	I_{Hg}
Shallow reservoirs (blue)	~2000 psi [~14,000 kPa]	~120°F [~50°C]	1.00	1.00	0.10	0.23
Deep reservoirs (red)	~7000 psi [~48,000 kPa]	~240°F [~120°C]	1.00	1.00	0.25	0.54

Porosity and Gas Saturation in Empty Holes

SW-11



© Schlumberger

Porosity, ϕ , and gas saturation, S_g , can be determined from this chart using either the combination of density-neutron measurements or density-resistivity measurements. To use, enter the chart vertically from the intersection of the apparent bulk density and appropriate grain density values. The intersection of this line with either the neutron porosity (corrected for lithology) or the R_t/R_w ratio (true resistivity/connate water resistivity) defines actual porosity and gas saturation.

With all three measurements (density, neutron and resistivity), oil saturation can be determined as well. To do so, enter the chart with apparent bulk density and neutron porosity (as described above) to define porosity and gas saturation. Moving along the defined porosity to its intersection with the R_t/R_w ratio gives the

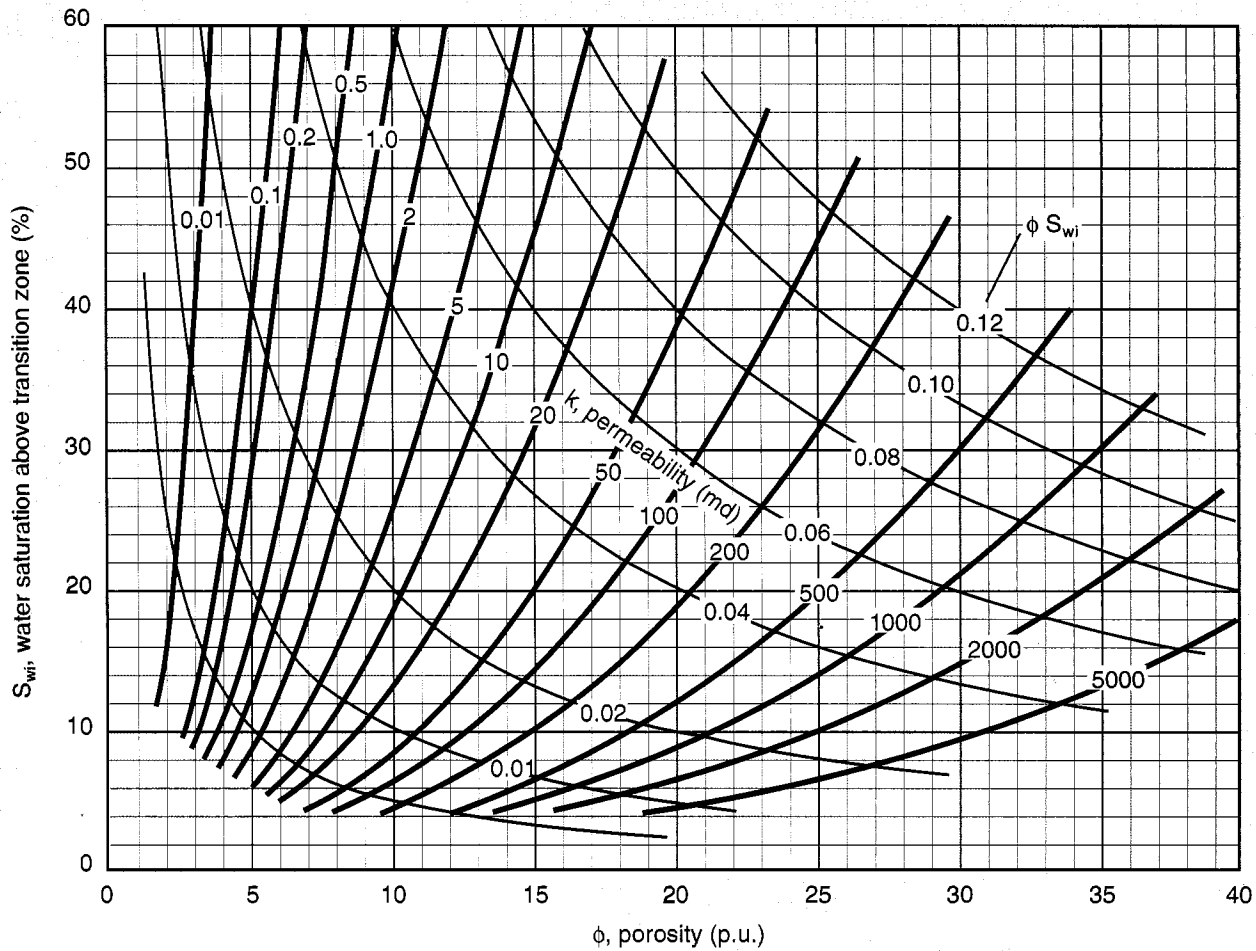
total hydrocarbon saturation. For more information see Reference 14.

Example: In a limy sandstone ($\rho_{ma} = 2.68$)
 $\rho_b = 2.44 \text{ g/cm}^3$
 $\phi_N = 9 \text{ p.u.}$
 $R_t = 74$
 $R_w = 0.1$

Therefore, $R_t/R_w = 740$
 and $\phi = 12 \text{ p.u.}$
 $S_g = 25\%$
 $S_h = 70\%$ (total hydrocarbon saturation)
 $S_o = 70 - 25 = 45\%$
 $S_w = 100 - 70 = 30\%$

Permeability from Porosity and Water Saturation

K-3



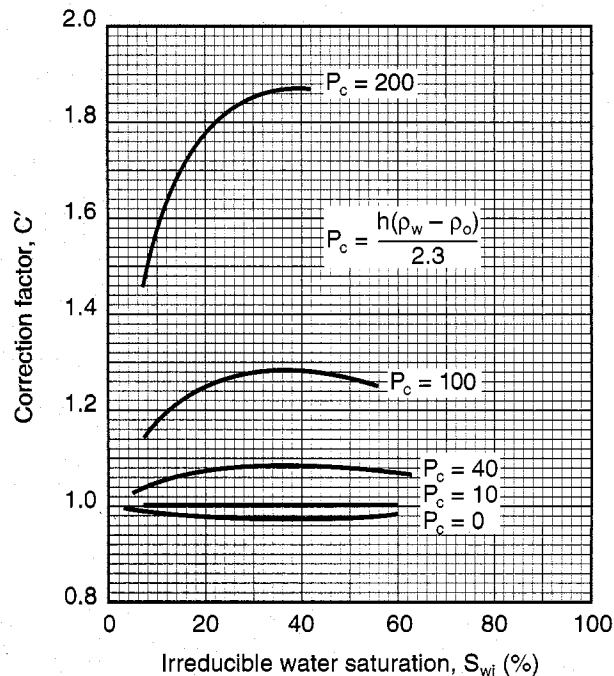
© Schlumberger

Charts K-3 and K-4 provide an estimate of permeability for sands, shaly sands or other hydrocarbon-saturated intergranular rocks at irreducible water saturation, S_{wi} . Both charts are based on empirical observations and are similar in form to a general expression proposed by Wyllie and Rose (1950): $k^{1/2} = (c\phi/S_{wi}) + C'$.

Chart K-3 presents the results of one study; the relationship observed was $k^{1/2} = 100 \phi^{2.25}/S_{wi}$. Chart K-4 presents the results of another study; the relationship observed was $k^{1/2} = 70 \phi_e^2[(1 - S_{wi})/S_{wi}]$. Both charts are valid only for zones at irreducible water saturation.

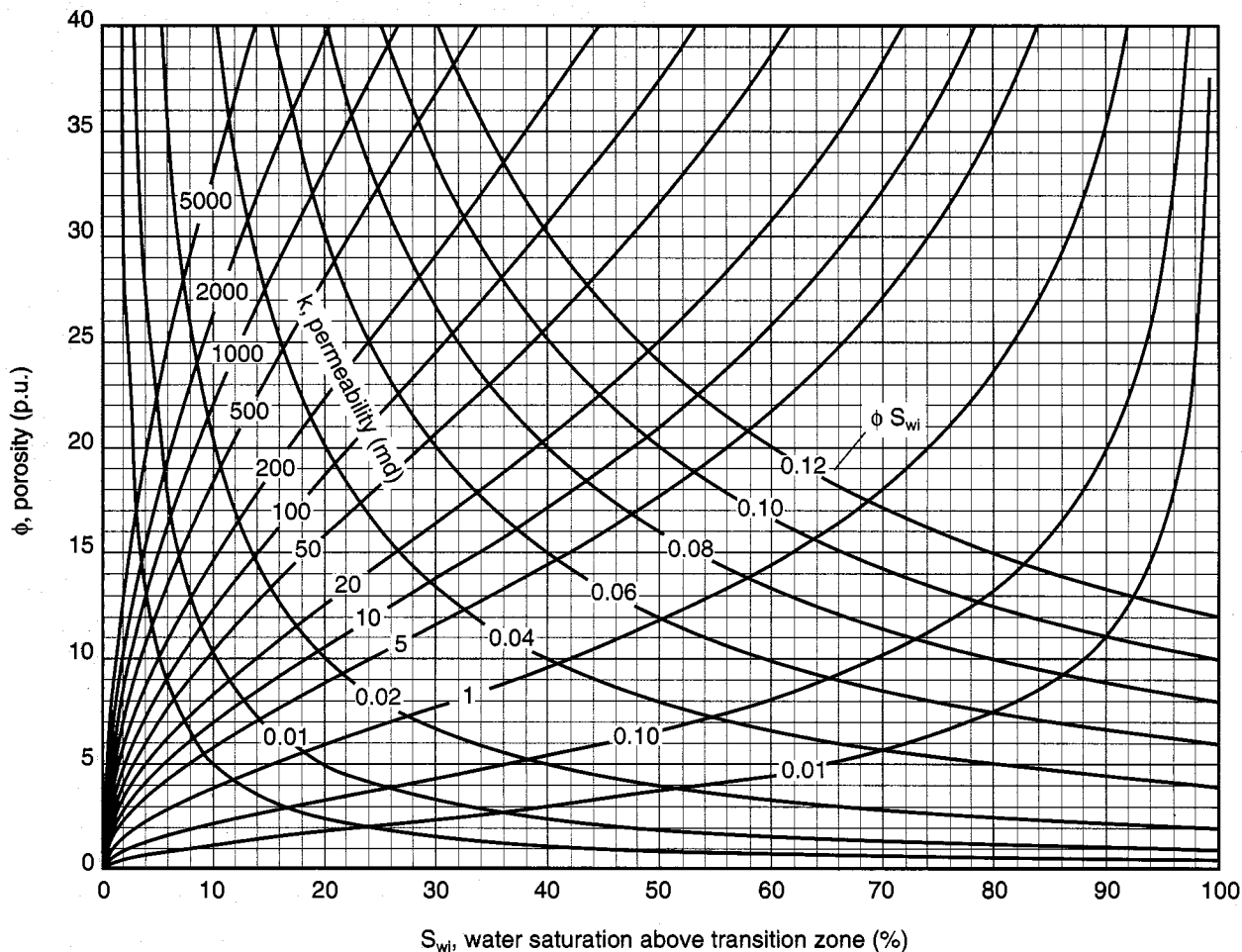
To use, porosity, ϕ , and irreducible water saturation, S_{wi} , are entered. Their intersection defines the intrinsic (absolute) rock

Continued on next page



Permeability from Porosity and Water Saturation

K-4



© Schlumberger

permeability. A medium-gravity oil is assumed. If the saturating hydrocarbon is other than a medium-gravity oil, a correction factor based upon fluid densities, ρ_w and ρ_h , and elevation above the free water level, h , should be applied to the irreducible water saturation prior to entry into Chart K-3 or K-4. The inset figure provides this correction factor.

Example: $\phi = 23\%$
 $S_{wi} = 30\%$
 Gas saturation ($\rho_h = 0.3 \text{ g/cm}^3$, $\rho_w = 1.1 \text{ g/cm}^3$)
 h (elevation above water) $\approx 120 \text{ ft}$

$$\text{Therefore, } P_c = \frac{h(\rho_w - \rho_h)}{2.3} = \frac{120(1.1 - 0.3)}{2.3} = 42$$

C' correction factor = 1.08

Corrected S'_{wi} for chart entry = 1.08 (30) = 32.4%

giving $k \approx 130 \text{ md}$ (Chart K-3)

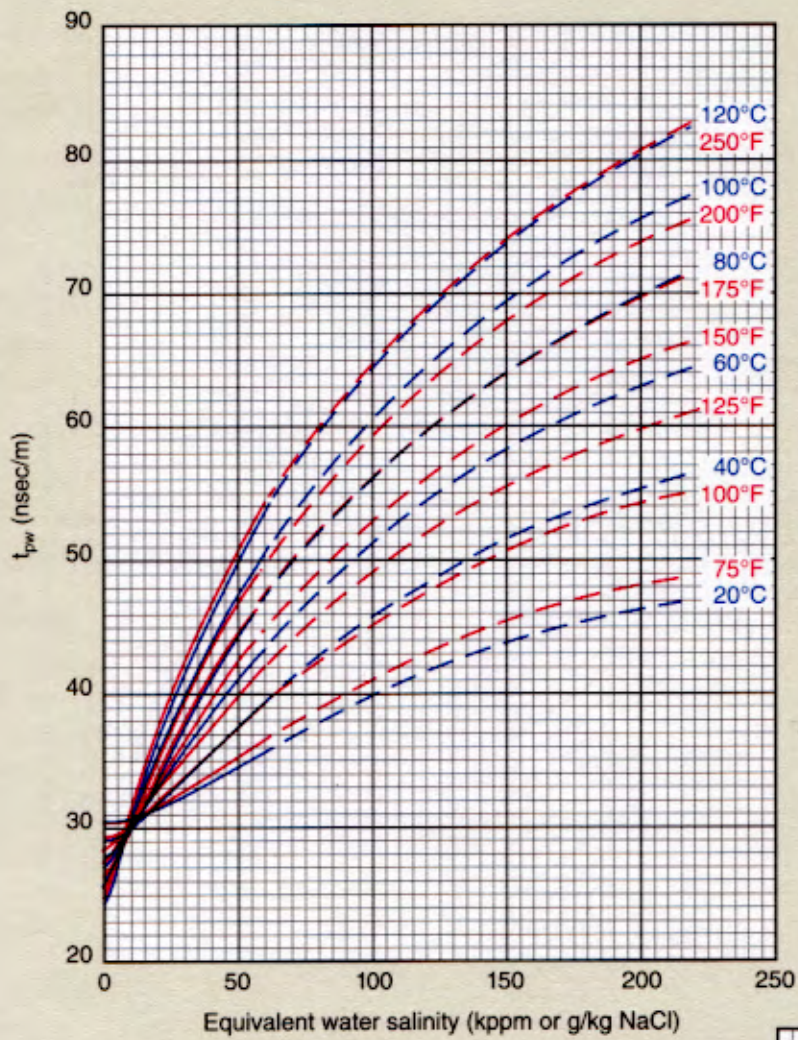
or $k \approx 65 \text{ md}$ (Chart K-4)

These charts can also be used to recognize zones at irreducible water saturation. Over intervals at irreducible water saturation, the product of porosity and water saturation is generally a constant; thus, data points from levels at irreducible water saturation should plot in a fairly coherent pattern on or parallel to one of the $\phi \cdot S_w$ lines.

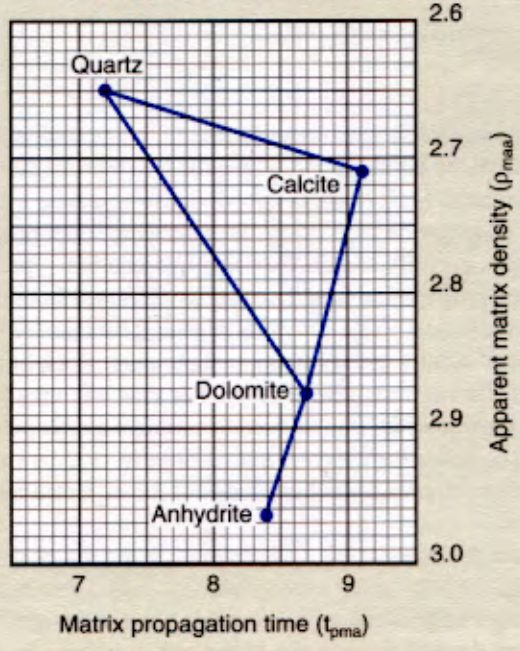
For more information see References 16, 17, 21 and 22.

EPT* Propagation Time for NaCl Solutions

EPTcor-1



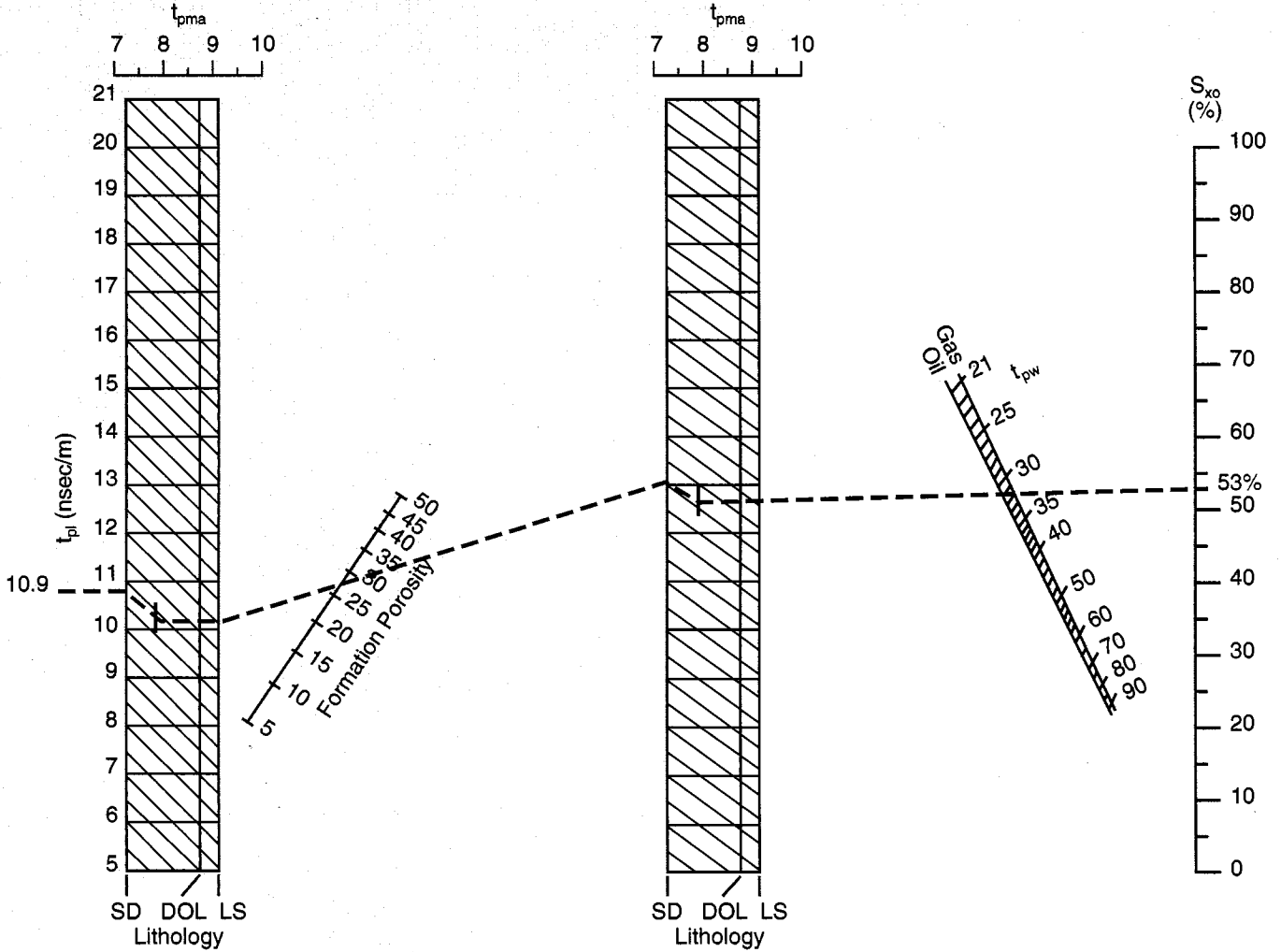
EPT Matrix Propagation Travel Time



*Mark of Schlumberger
© Schlumberger

Flushed Zone Saturation from EPT* Propagation Time

Sxo-1



Sxo

*Mark of Schlumberger
© Schlumberger

This nomograph defines water saturation in the rock immediately adjacent to the borehole, S_{xo} , using the EPT* propagation time measurement, t_{pi} . It requires knowledge of reservoir lithology or matrix propagation time (t_{pma}), the saturating water propagation time (t_{pw}), porosity and the expected hydrocarbon type.

Water propagation time, t_{pw} , can be estimated from the appropriate chart on the previous page as a function of equivalent water salinity and formation temperature. Rock lithology must be known from other sources. For rock mixtures the chart on the previous page can be used to estimate matrix propagation time, t_{pma} , when the apparent matrix density, ρ_{maa} , is known. The estimation requires some knowledge of the expected mineral mixture.

To use the nomograph, t_{pi} is entered on the left grid; follow the diagonal lines to the appropriate t_{pma} value, then horizontal to the right edge of the grid. From this point, a straight line is extended through the porosity to the center grid; again follow

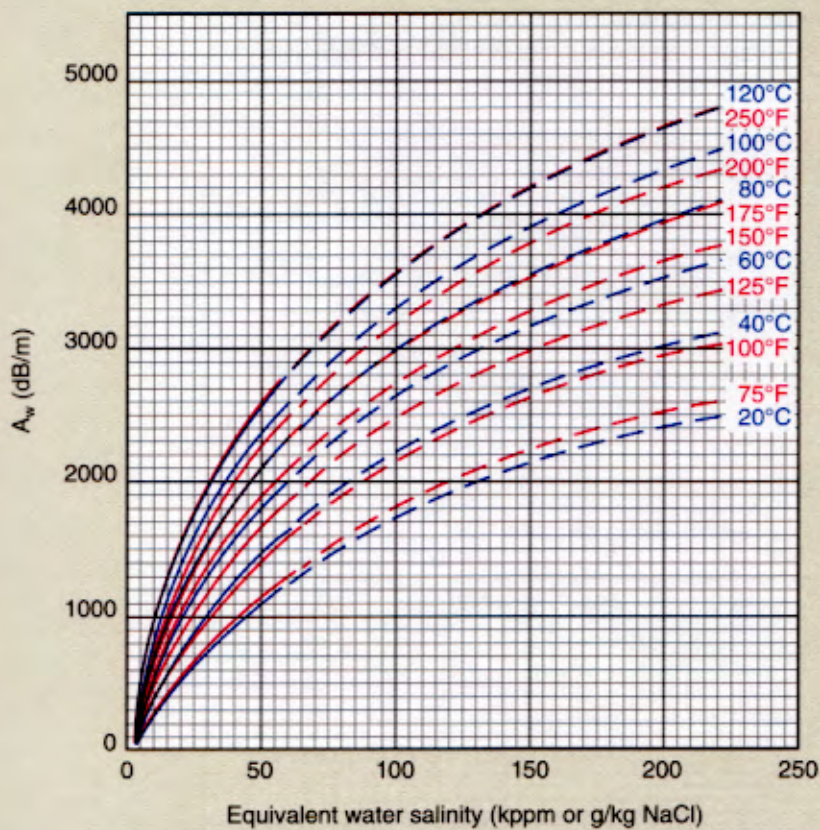
the diagonal lines to the appropriate t_{pma} value, then horizontal to the right edge of the grid. From this point, extend a straight line through the intersection of t_{pw} and hydrocarbon type point to the S_{xo} axis.

For more information see Reference 25.

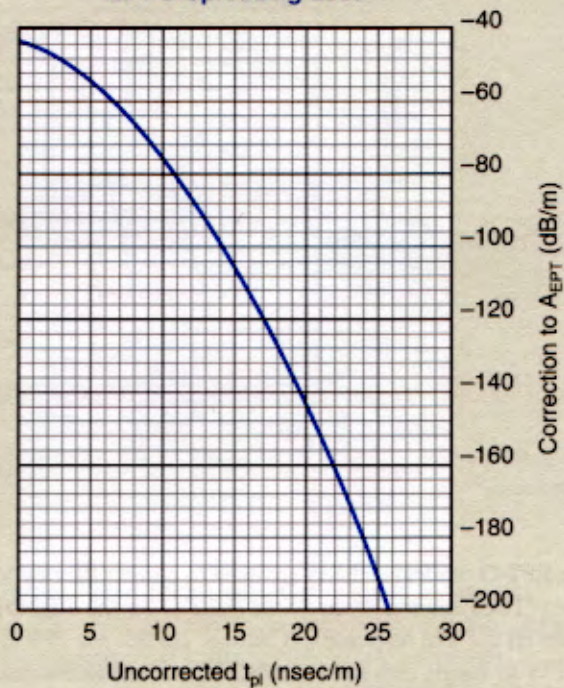
Example: $t_{pi} = 10.9$ nsec/m
 $\phi = 28\%$
 Limy sandstone with $\rho_{maa} = 2.67$ g/cm³
 Water salinity ≈ 20 kppm
 BHT = 150°F
 Gas saturation expected
 giving $t_{pma} = 7.8$ nsec/m (sand-lime mixture)
 $t_{pw} = 32$ nsec/m
 and $S_{xo} = 53\%$

EPT* Attenuation for NaCl Solutions

EPTcor-2



EPT-D Spreading Loss

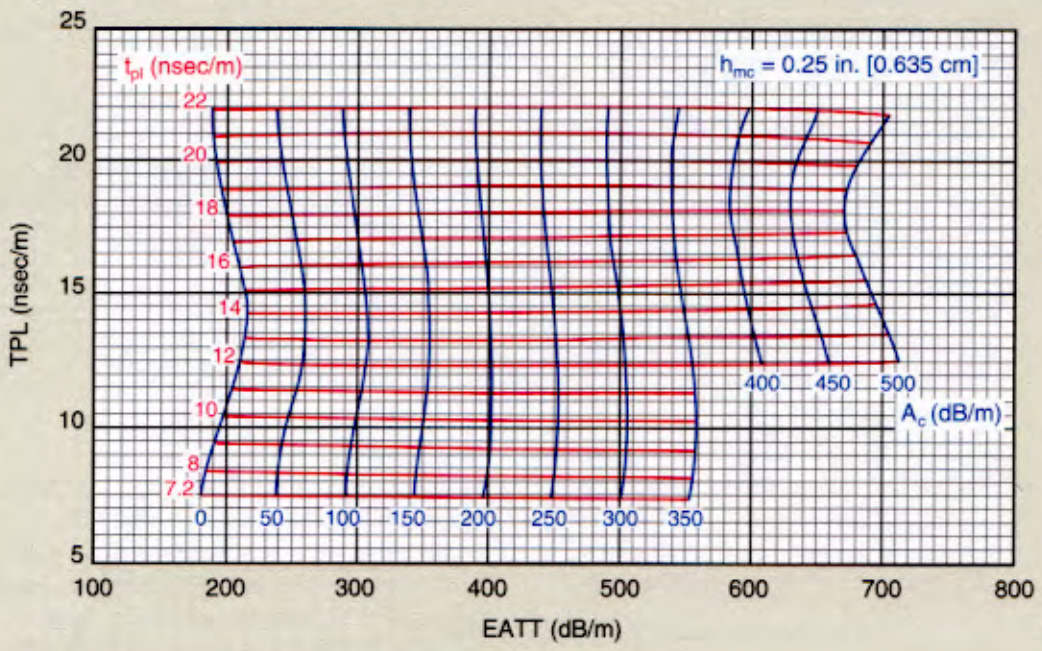
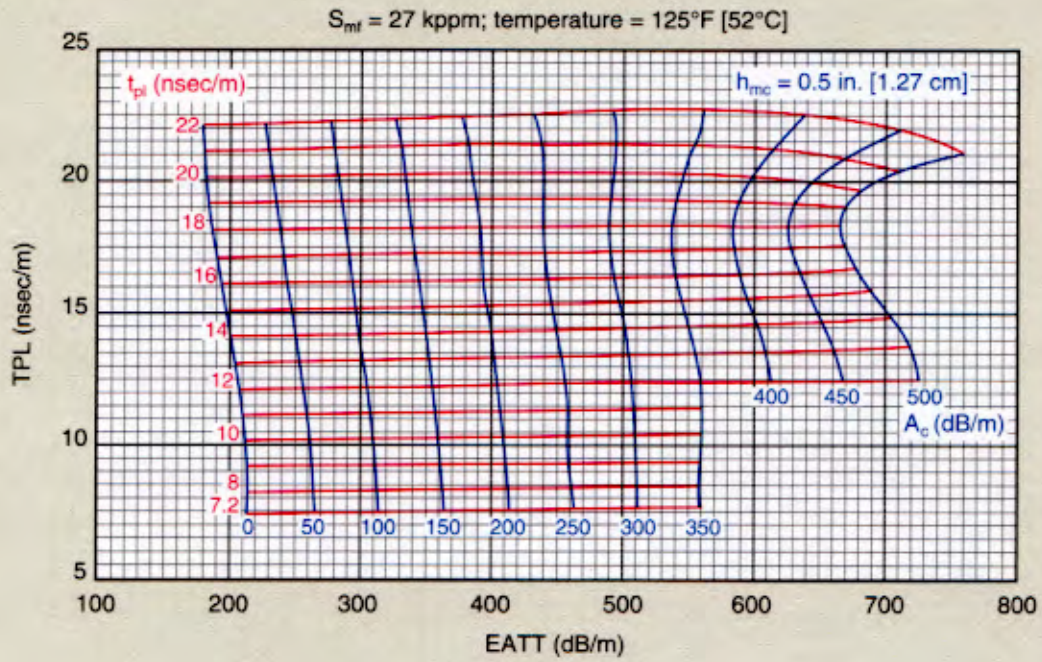


*Mark of Schlumberger
© Schlumberger

EPT-G Mudcake Correction Charts for Water-Base Mud

EMD-L (endfire array)

EPTcor-3a



© Schlumberger

The EPT-G mudcake charts are used to correct the raw log travel times (TPL) and log attenuations (EATT) for the effects of mudcakes on the tool responses. (Caution: Do not use TPPW and EAPW as inputs into these charts.) The charts also correct the log attenuations for spreading losses so that no further corrections are required. The chart outputs are the true formation travel

times (t_{pi}) and attenuations (A_c), which are used to evaluate the flushed zone. For example, these latter quantities are the inputs to petrophysical models such as the Complex Refractive Index Method (CRIM).

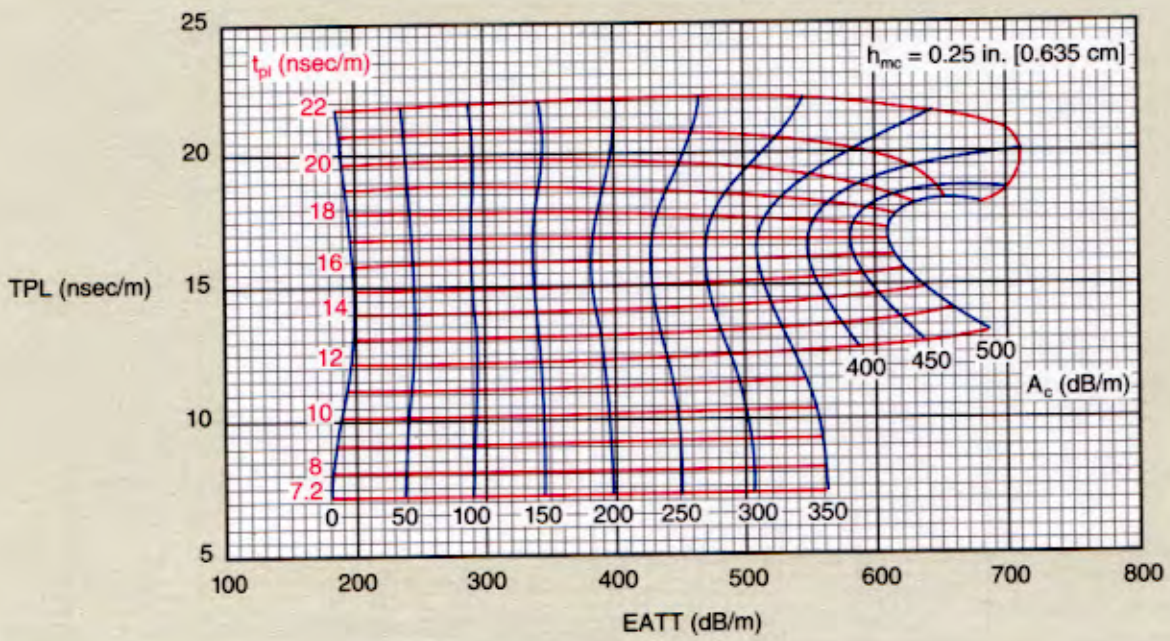
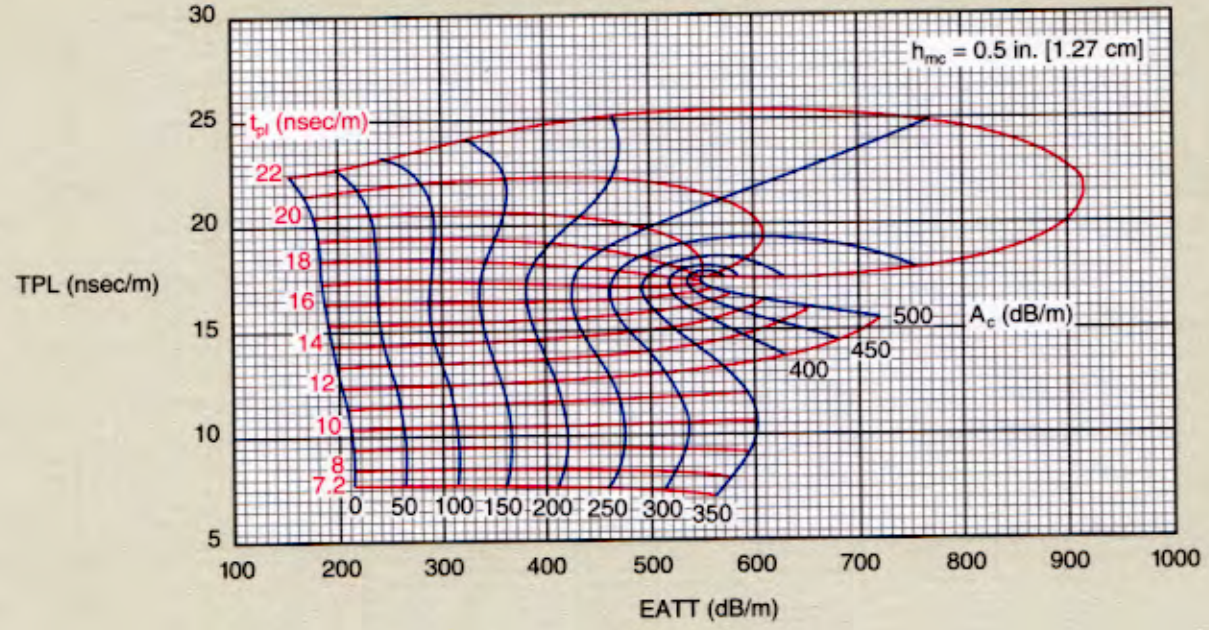
Continued on next page

EPT-G Mudcake Correction Charts for Water-Base Mud

EMD-L (endfire array)

EPTcor-3b

$S_{mf} = 10$ kppm; temperature = 125°F [51.67°C]



© Schlumberger

The true travel times, t_{pl} , can also be used in nomograms such as Sxo-1 to determine flushed-zone water saturations, S_{xo} . The charts displayed here are for water-base muds and are applicable, as indicated, for the EMD-L and BMD-S arrays. The charts are valid for the indicated mudcake thicknesses (h_{mc}), borehole

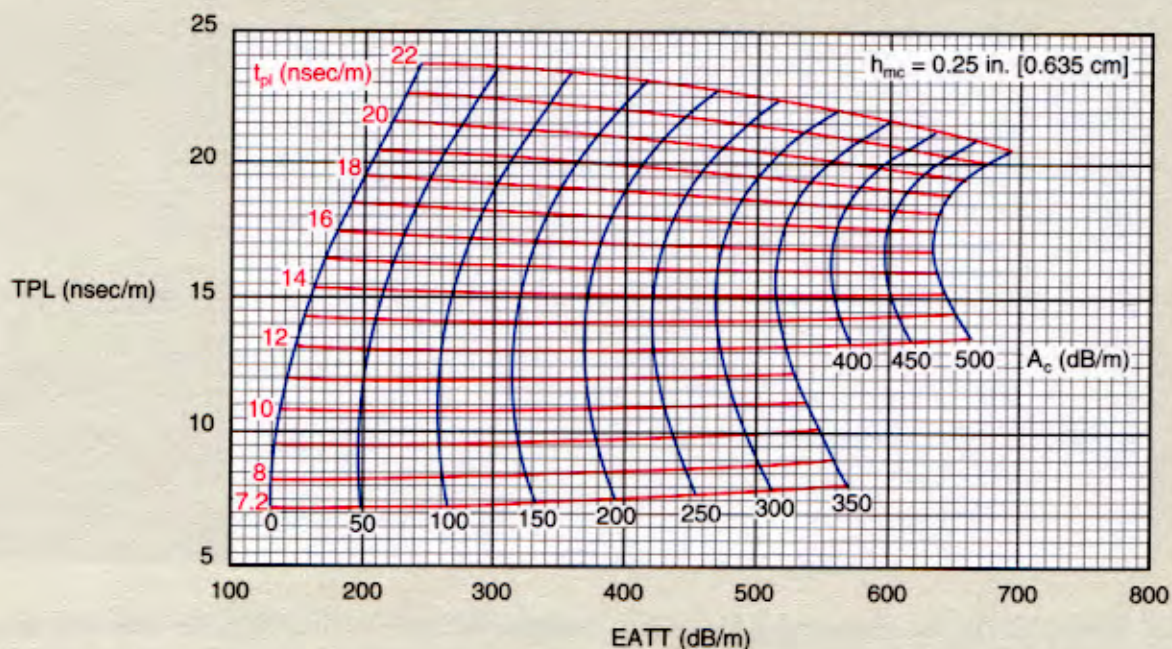
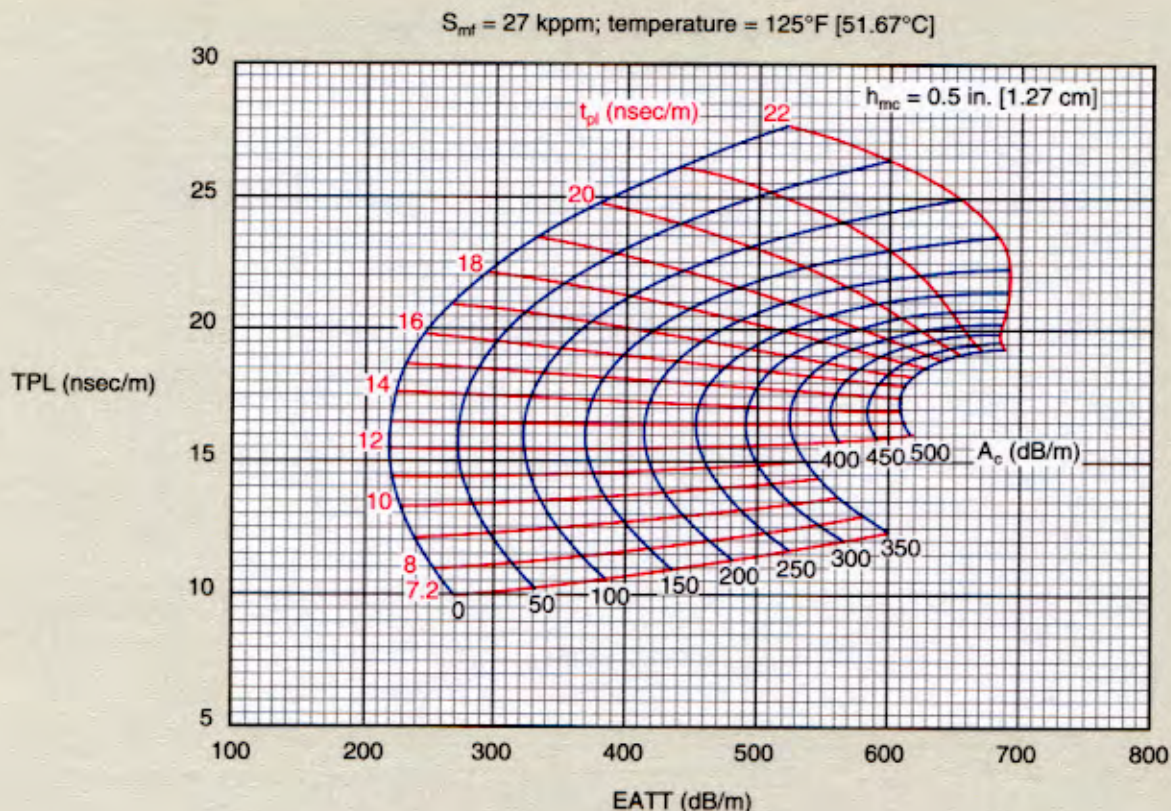
temperatures and mud-filtrate salinities in kppm by weight NaCl (S_{mf}). The mudcake effects depend on h_{mc} and the contrast between the mudcake and formation dielectric properties.

Continued on next page

EPT-G Mudcake Correction Charts for Water-Base Mud

BMD-S (broadside array)

EPTcor-4a



© Schlumberger

In general, low-conductivity muds produce the largest effects so that increases in temperature, mudcake porosity and salinity generally reduce the mudcake effects. The charts displayed here assume a mudcake porosity of 40 p.u. (For more information see

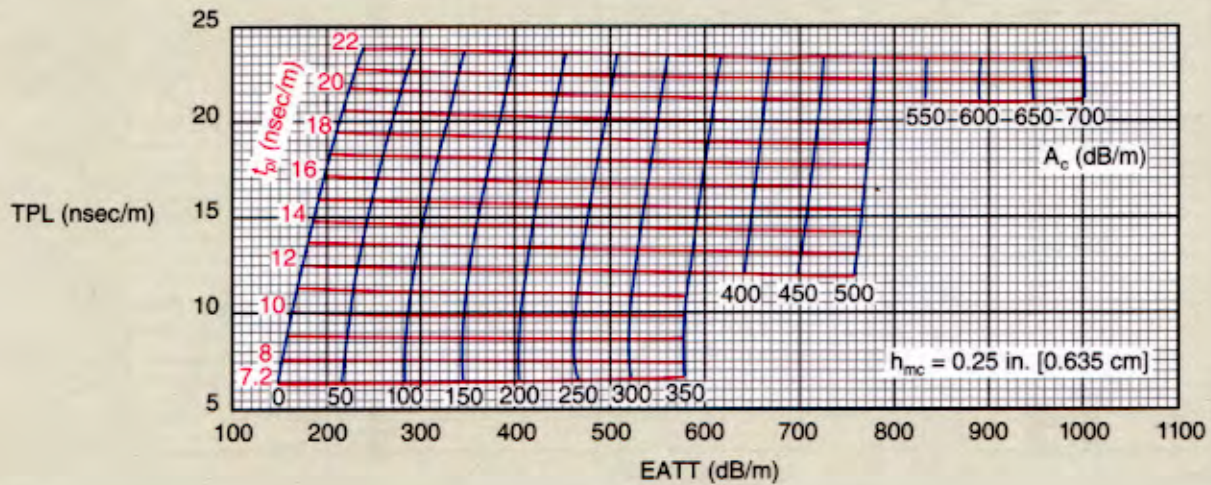
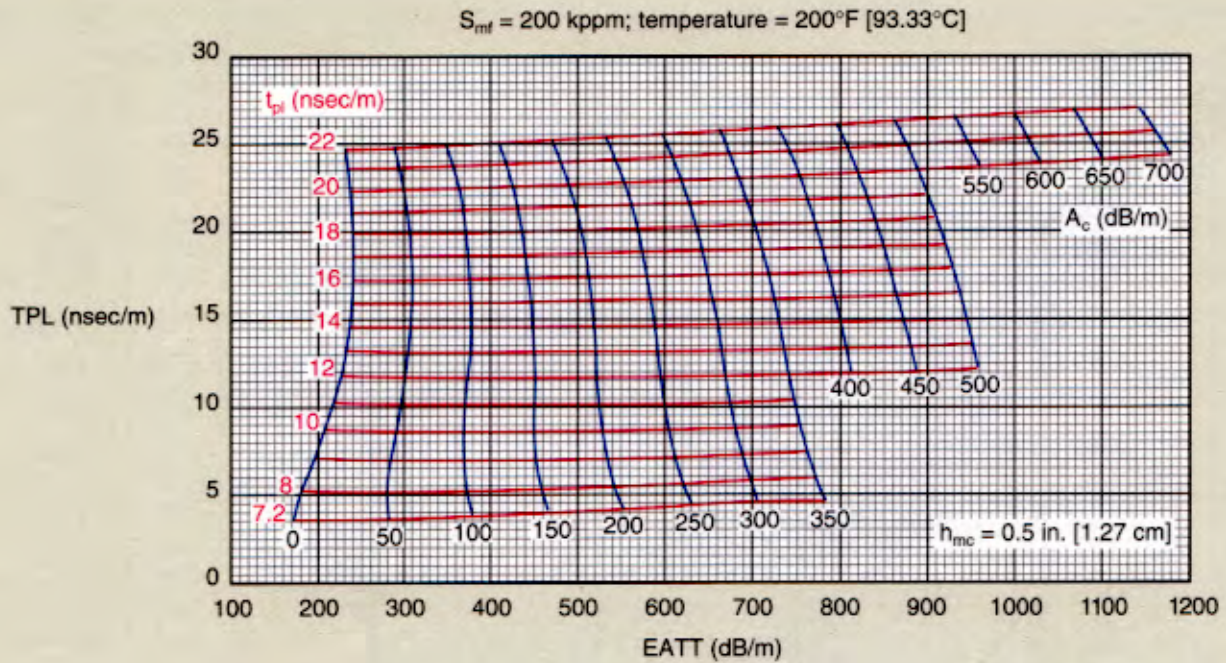
Reference 31.) The mudcake thicknesses are estimated from a caliper or a Microlog using Chart Rxo-1.

Continued on next page

EPT-G Mudcake Correction Charts for Water-Base Mud

BMD-S (broadside array)

EPTcor-4b



© Schlumberger

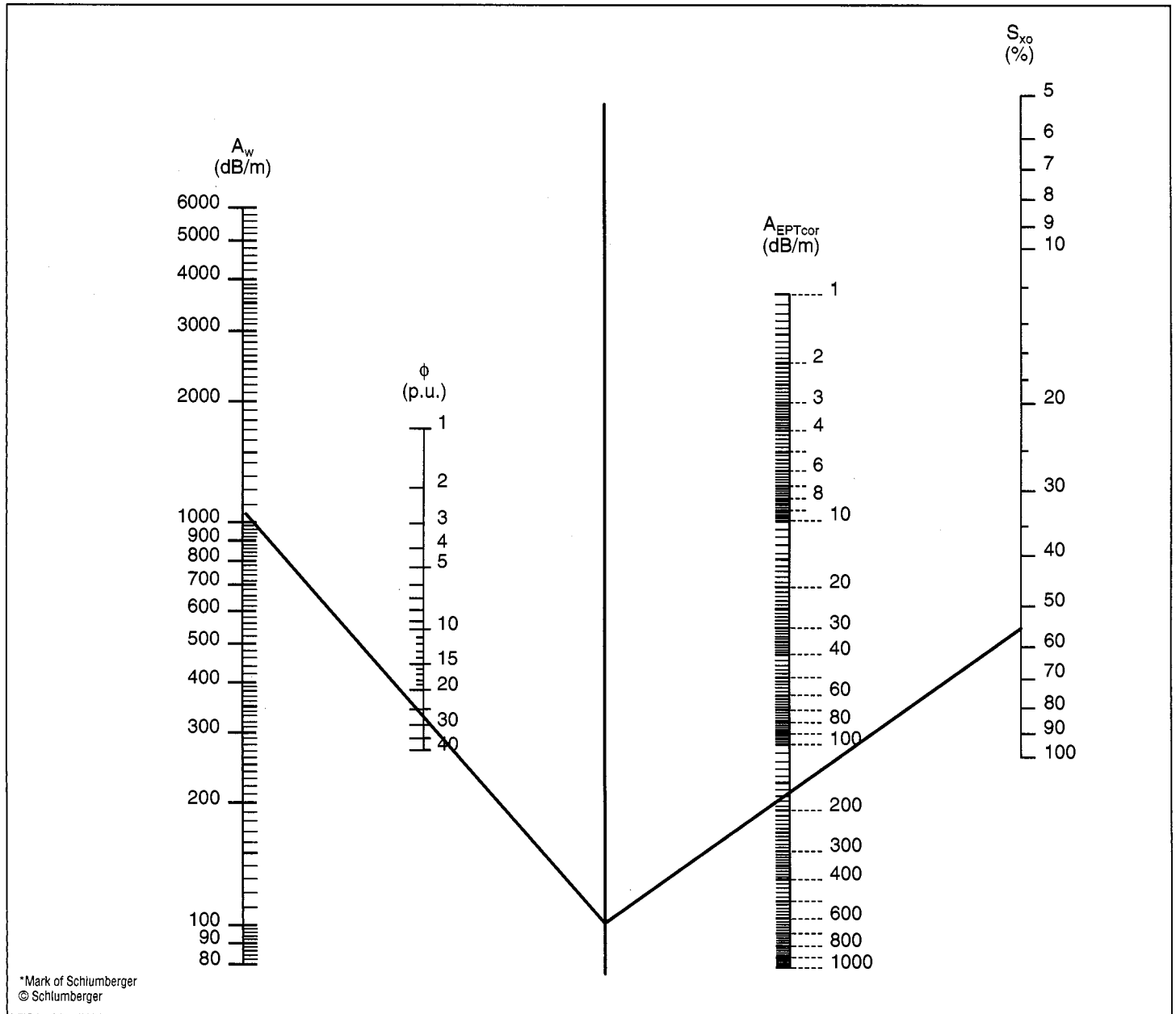
Example: EMD-L array

- $h_{mc} = 0.5 \text{ in.}$ (estimated from bit size and caliper)
- Borehole temperature = 125°F
- Mud filtrate salinity = 27,000 ppm NaCl
- Log TPL = 20 nsec/m
- Log EATT = 500 dB/m

Entering Chart EPTcor-3a with the above log values, one reads a true formation travel time, $t_{pl} = 19.7 \text{ nsec/m}$, and true formation attenuation, $A_c = 307 \text{ dB/m}$.

Flushed Zone Saturation from EPT* Attenuation

Sxo-2



*Mark of Schlumberger
© Schlumberger

The nomograph defines water saturation in the rock immediately adjacent to the borehole, S_{xo} , using the EPT attenuation measurement. It requires knowledge of saturating fluid (usually mud filtrate) attenuation (A_w), porosity and the EPT attenuation (A_{EPTcor}) corrected for spreading loss.

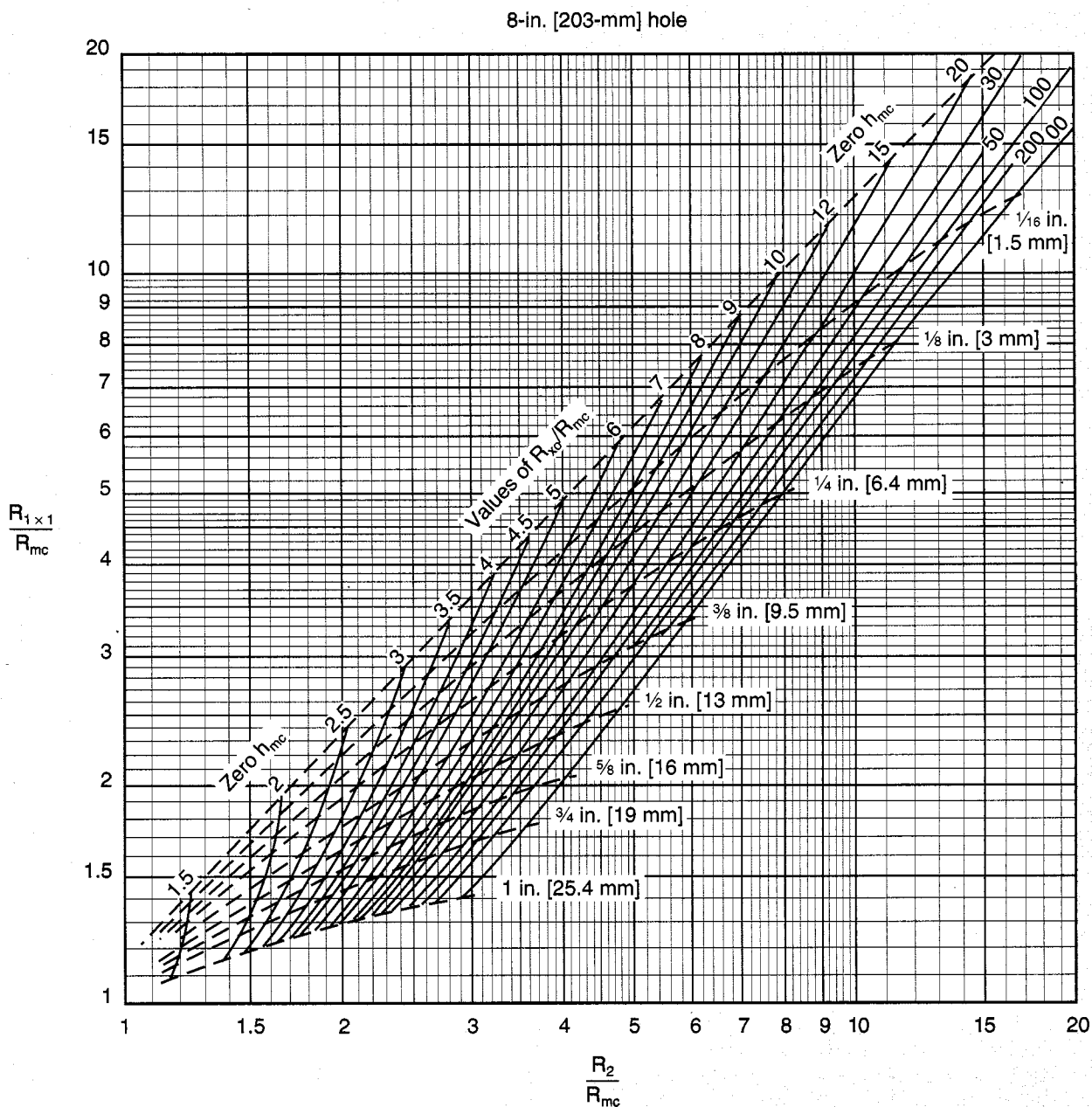
Fluid attenuation (A_w) can be estimated from Chart EPTcor-2 by knowing the equivalent water salinity and formation temperature. EPT-D spreading loss is also determined from Chart EPTcor-2 based on the uncorrected EPT t_{pl} measurement. The spreading loss correction algebraically added to the EPT-D attenuation measurement gives the corrected EPT attenuation, A_{EPTcor} .

These values, together with porosity, inserted into the nomograph lead to the flushed zone water saturation, S_{xo} .

Example: $A_{EPT} = 250$ dB/m
 $t_{pl} = 10.9$ nsec/m
 $\phi = 28\%$
 Water salinity = 20 kppm
 BHT = 150°F
 giving Spreading loss = -82 dB/m
 $A_{EPT} = 250 - 82 = 168$ dB/m
 $A_w = 1100$ dB/m
 and $S_{xo} = 56\%$

Microlog Interpretation Chart

Rxo-1



© Schlumberger

Enter the chart with the ratios R_{1x1}/R_{mc} and R_2/R_{mc} . The point of intersection defines the R_{xo}/R_{mc} ratio and the mudcake thickness, h_{mc} . Knowing R_{mc} , R_{xo} can be calculated.

For hole sizes other than 8 in. [203 mm], multiply R_{1x1}/R_{mc} by the following factors before entering the chart: 1.15 for 4³/₄-in. [120-mm] hole, 1.05 for 6-in. [152-mm] hole, and 0.93 for 10-in. [254-mm] hole.

Note: An incorrect R_{mc} will displace the points in the chart along a 45° line. In certain cases this can be recognized when

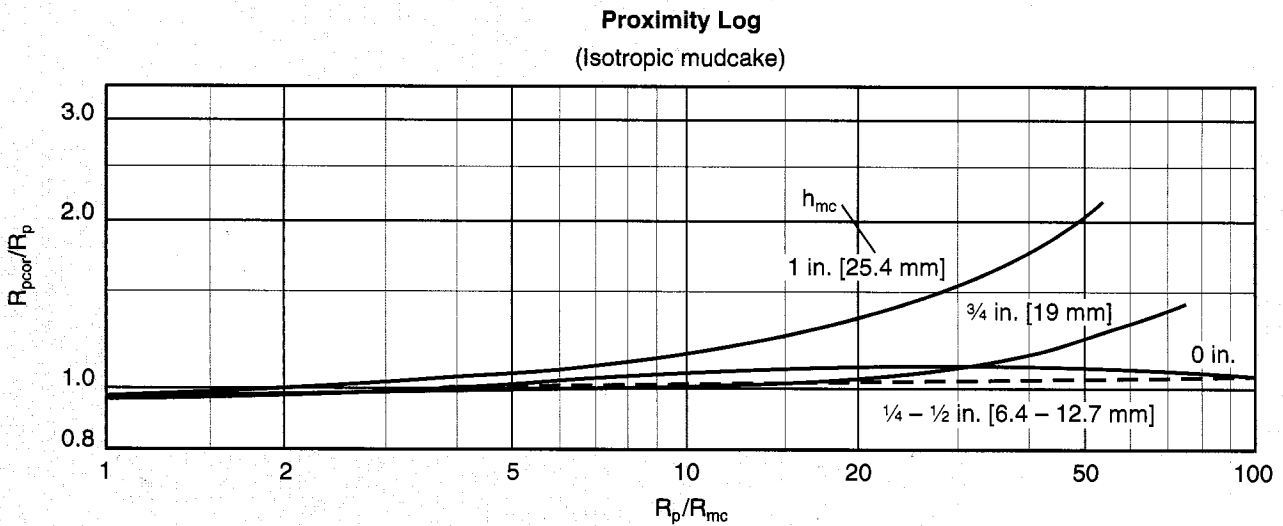
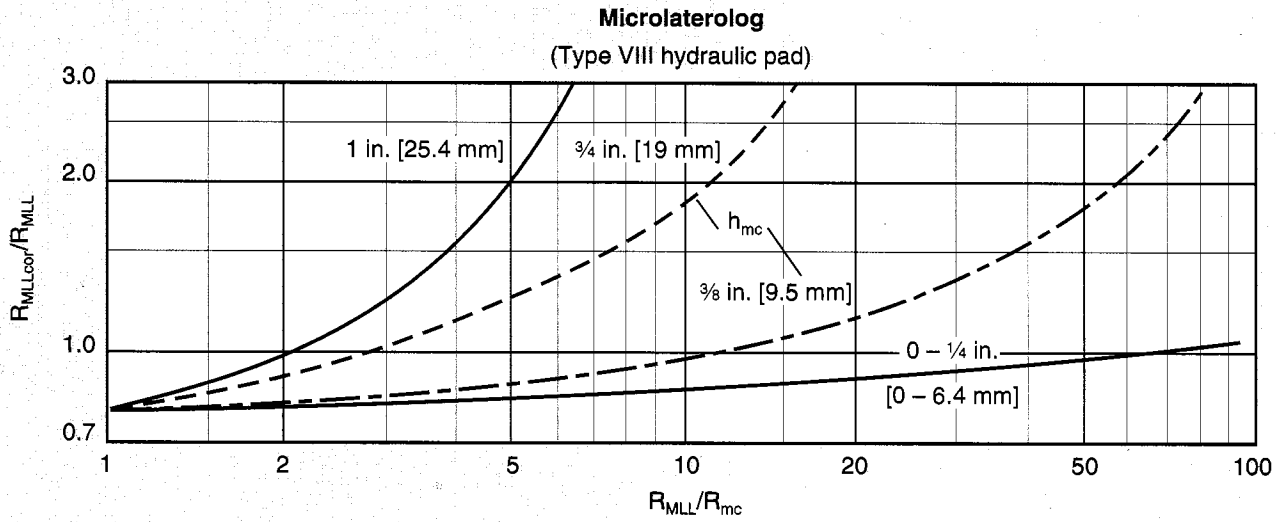
the mudcake thickness is different from direct measurement by the microcaliper. To correct, move the plotted point at 45° to intersect the known h_{mc} . For this new point, read R_{xo}/R_{mc} from the chart and R_2/R_{mc} from the bottom scale of the chart.

$$R_{xo} = R_2 \left(\frac{R_{xo}/R_{mc}}{R_2/R_{mc}} \right)$$

Rxo

Microlaterolog and Proximity Log
Mudcake Correction

Rxo-2



© Schlumberger

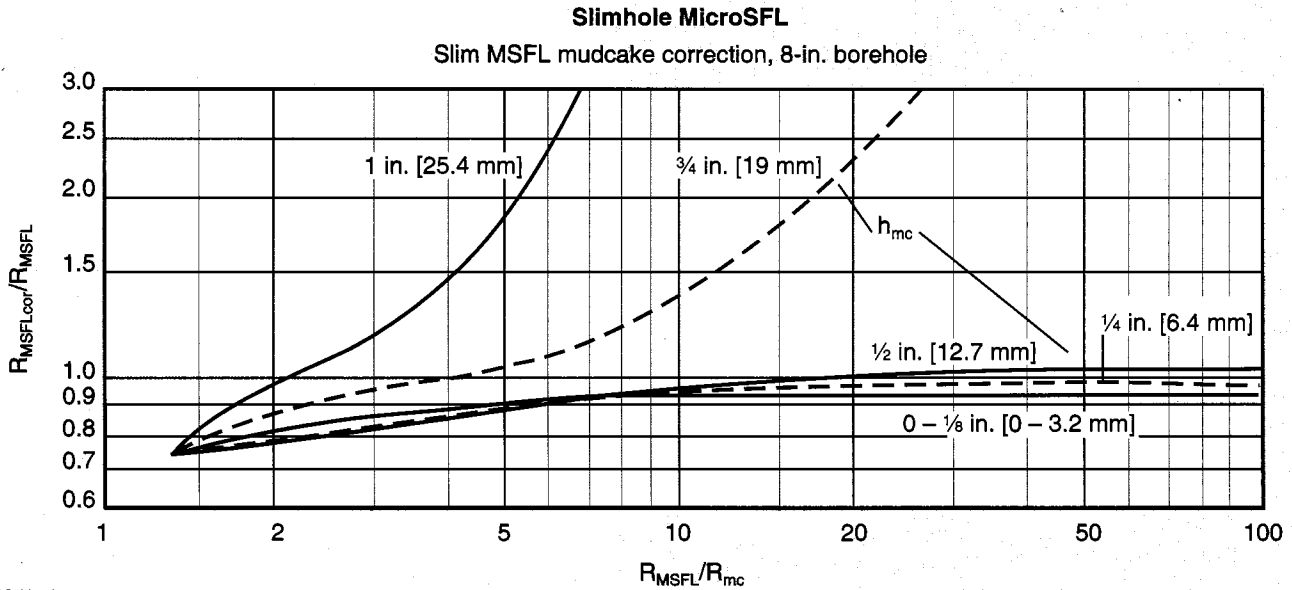
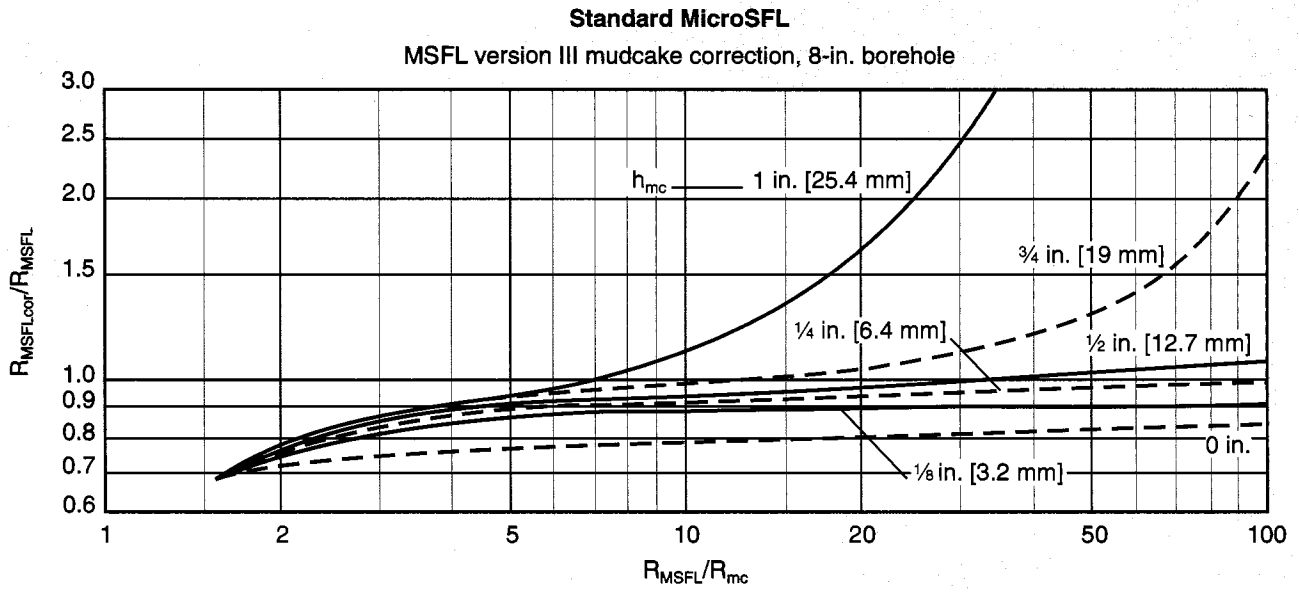
Charts Rxo-2 and Rxo-3 correct microresistivity measurements for mudcake effect. To use, enter the ratio of the microresistivity log reading divided by the mudcake resistivity into the abscissa of the appropriate chart. Go vertically to the mudcake thickness;

the ratio of the corrected microresistivity value to the microresistivity log reading is then given on the ordinate. Multiplication of this ratio by the microresistivity log reading yields the corrected microresistivity.

Continued on next page

MicroSFL* Mudcake Correction

Rxo-3



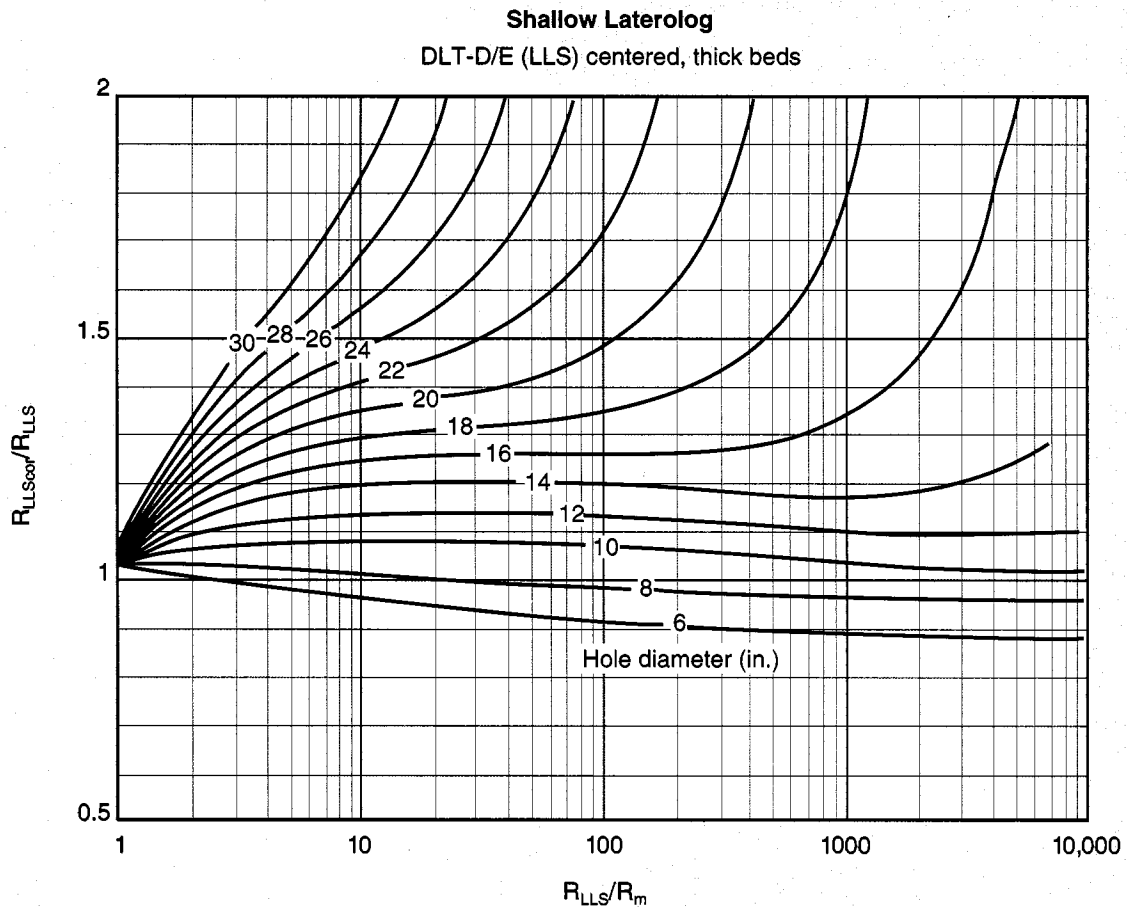
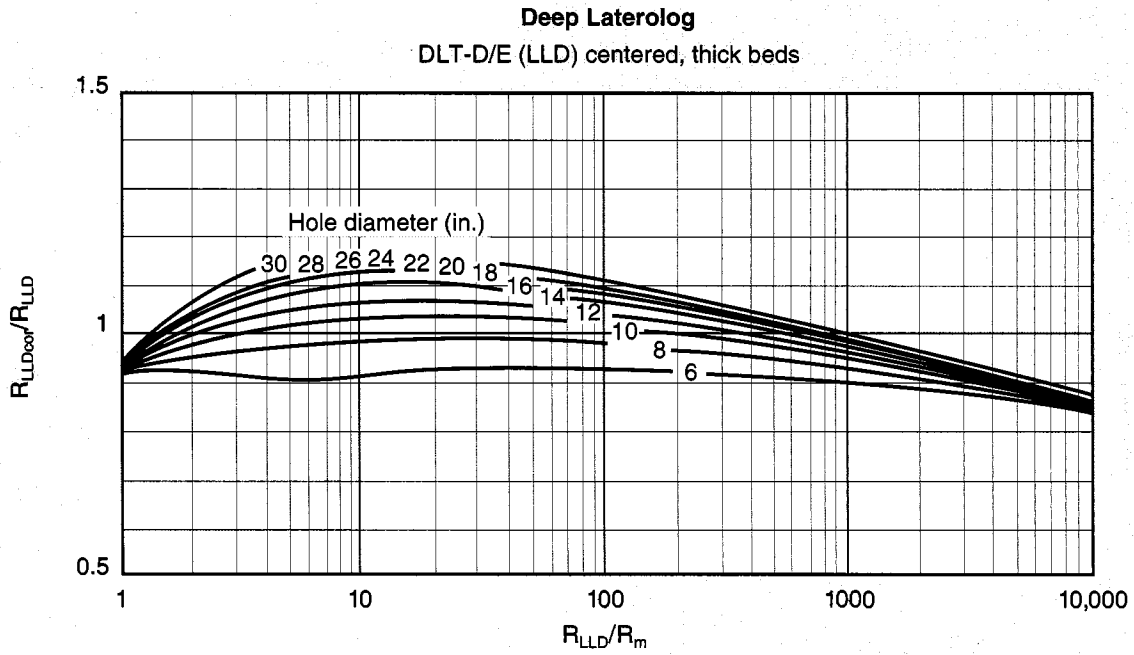
*Mark of Schlumberger
© Schlumberger

Example: $R_{MLL} = 9.0$ ohm-m
 $R_{mc} = 0.15$ ohm-m at formation temperature
 $h_{mc} = 9.5$ mm
 giving $R_{MLL}/R_{mc} = 9.0/0.15 = 60$
 Therefore, $R_{MLLcor}/R_{MLL} = 2$
 and $R_{MLLcor} = 2(9.0) = 18$ ohm-m

Rxo

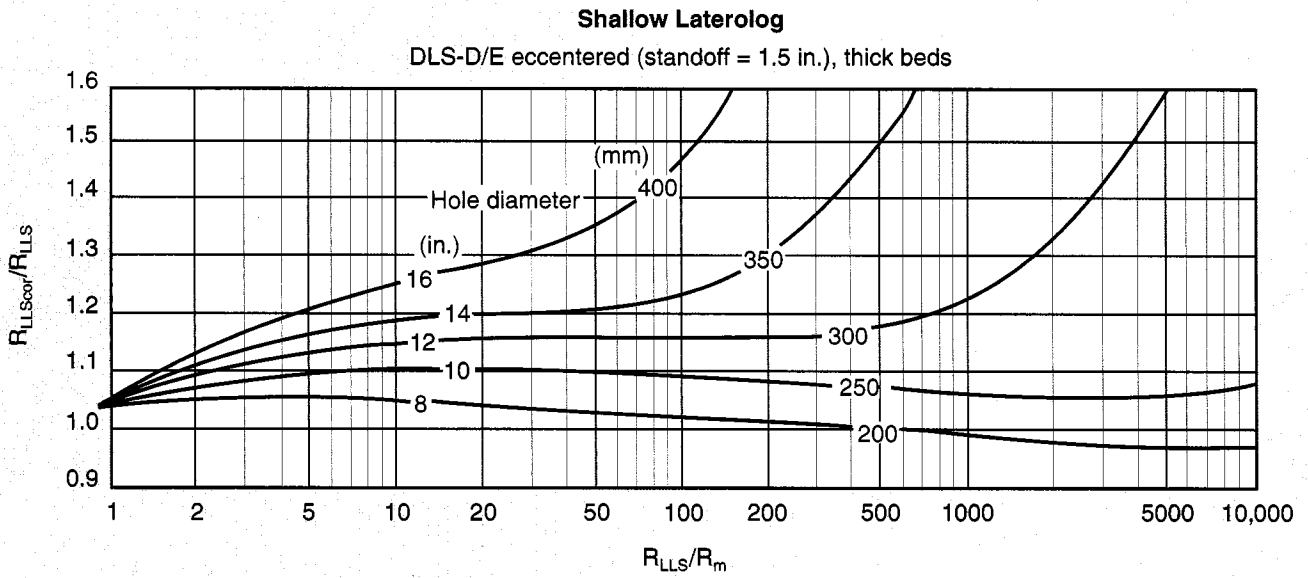
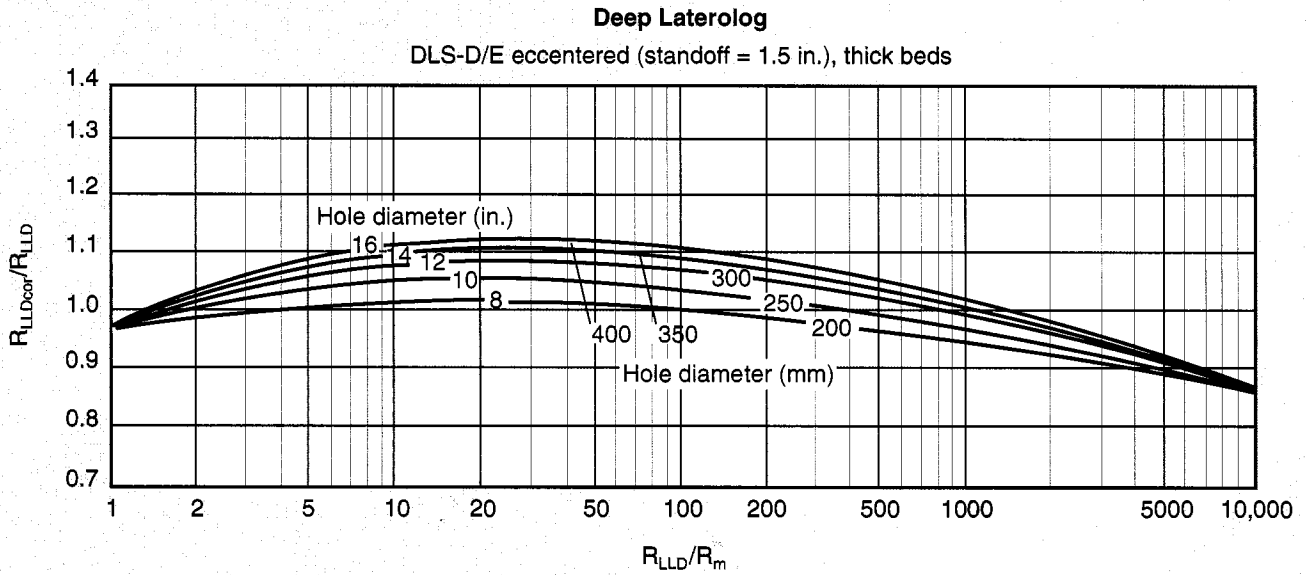
Dual Laterolog (D/E) Borehole Correction

Rcor-2b



Dual Laterolog (D/E) Borehole Correction

Rcor-2c

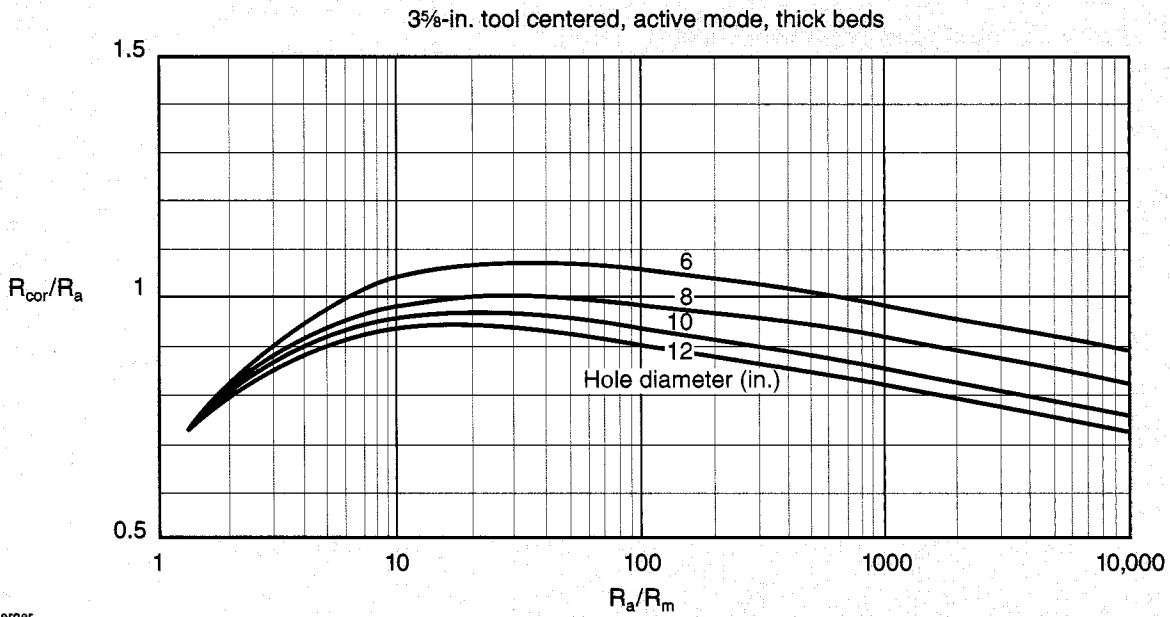


Rcor

ARI* Azimuthal Resistivity Imager Borehole Correction

For high-resolution LLhr curve

Rcor-14



*Mark of Schlumberger
© Schlumberger

The high-resolution deep resistivity curve available from the ARI Azimuthal Resistivity Imager log is subject to borehole effects like any other laterolog measurement. Borehole correction is performed using Chart Rcor-14 in the same way as the deep and shallow laterolog borehole corrections and the microlog and MicroSFL* mudcake corrections (see Charts Rxo-2 and Rxo-3 for an explanation and illustration).

LLD and LLS curves recorded with the ARI tool are identical to the curves recorded with a standard dual laterolog tool (type D or E) and may be corrected for borehole effects using Chart Rcor-2b or Rcor-2c.

Rcor

Dual Laterolog (D/E) Bed-Thickness Corrections

Chart Rcor-10 corrects the Dual Laterolog (LLD and LLS) for bed thickness.

To use, laterolog readings should first be corrected for borehole effects (see Charts Rcor-2b and -2c). Then, enter Chart Rcor-10 with the bed thickness and proceed upward to the proper R_{LL}/R_s ratio (apparent laterolog reading corrected for borehole/adjacent-bed resistivity) curve. Read the ratio of the corrected laterolog value (R_{LLcor}) to the apparent laterolog value (R_{LL}) in ordinate.

Example: $R_{LLD} = 4.2$ ohm-m
 $R_{LLS} = 3.0$ ohm-m
 $R_s \approx 30$ ohm-m
 Bed thickness = 6 ft

Given $\frac{R_{LLD}}{R_s} = \frac{4.2}{30} = 0.14$

$$\frac{R_{LLS}}{R_s} = \frac{3.0}{30} = 0.10$$

Therefore, $\frac{R_{LLDcor}}{R_{LLD}} = 0.88$

$$\frac{R_{LLScor}}{R_{LLS}} = 0.80$$

and $R_{LLDcor} = 3.7$ ohm-m
 $R_{LLScor} = 2.4$ ohm-m

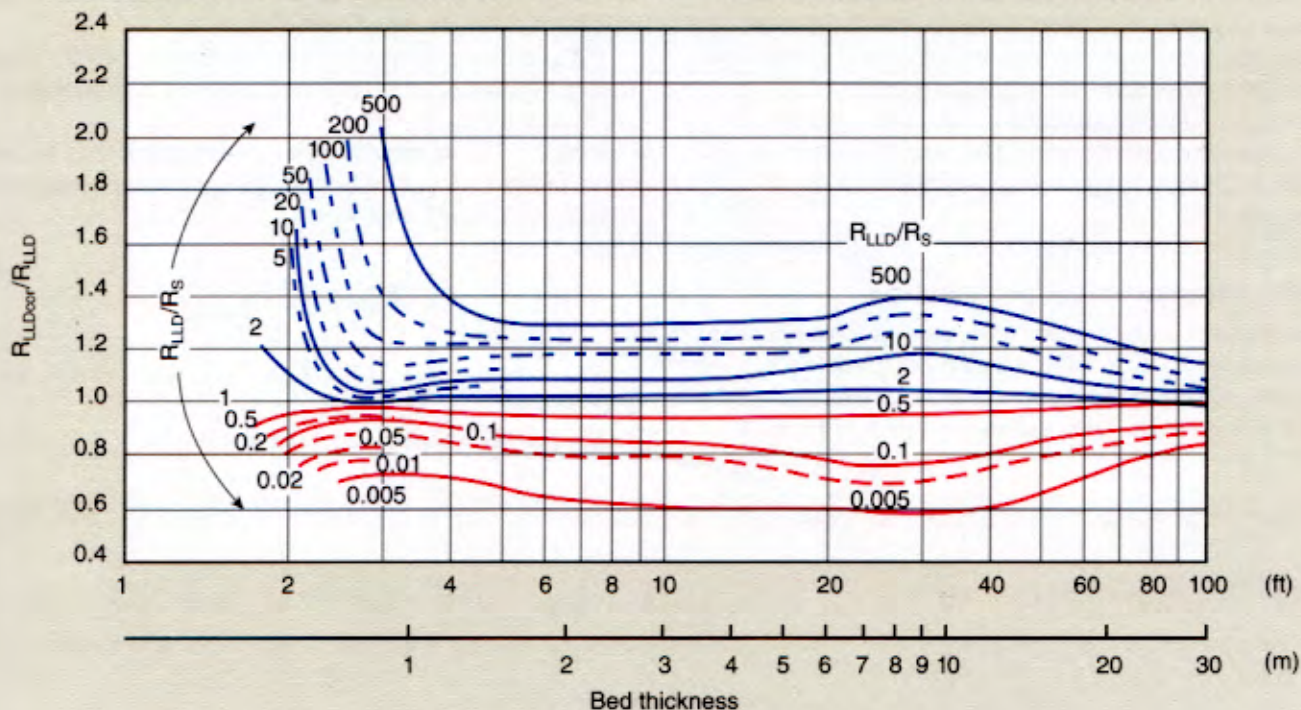
Dual Laterolog (D/E) Bed-Thickness Corrections

DLS-D/E

Rcor-10

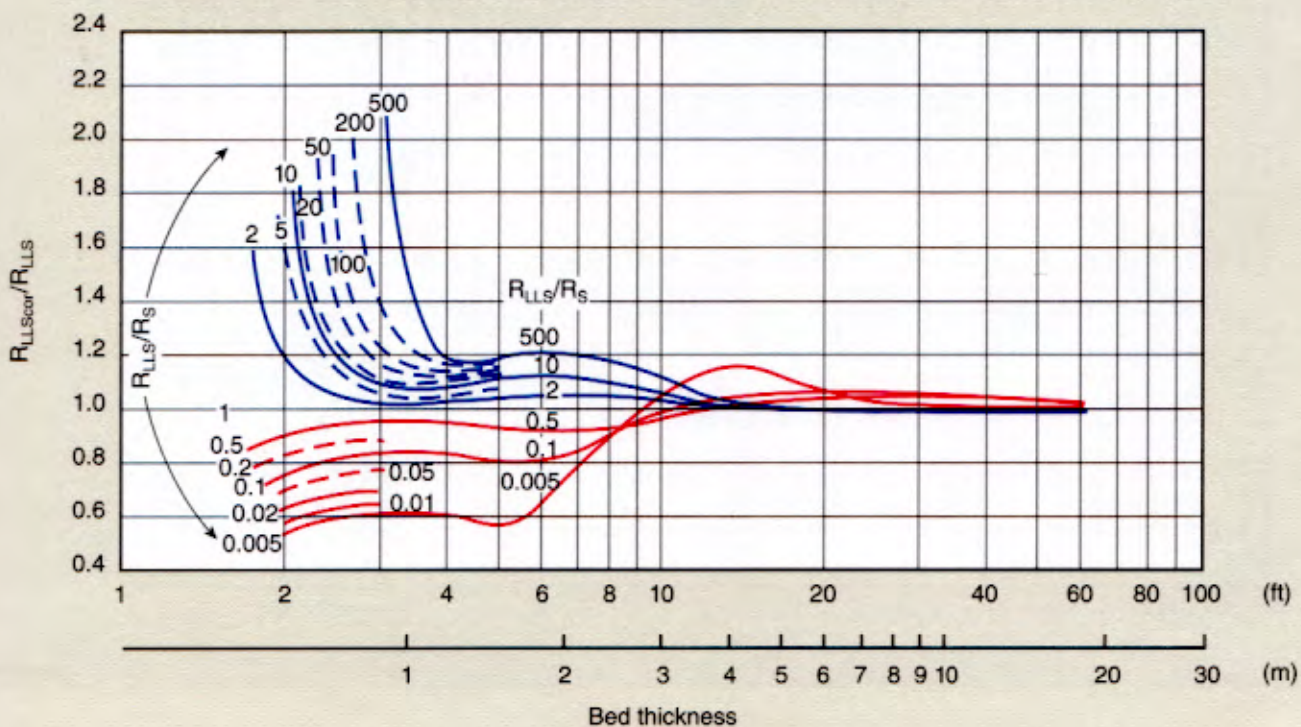
Deep Laterolog

No invasion, semi-infinite shoulder, 8-in. [203-mm] borehole, squeeze: $R_t/R_m \approx 30$, antisqueeze: $R_s/R_m \approx 30$



Shallow Laterolog

No invasion, semi-infinite shoulder, 8-in. [203-mm] borehole, squeeze: $R_t/R_m \approx 30$, antisqueeze: $R_s/R_m \approx 30$



Invasion Correction Charts

Rint-1

The invasion correction charts, sometimes referred to as “tornado” or “butterfly” charts, of the next several pages (labeled Rint-) are used to define the depth of invasion d_i , the R_{xo}/R_t ratio and the true resistivity R_t . All assume a step-contact profile of invasion and that all resistivity measurements have been corrected, where necessary, for borehole effect and bed thickness using the appropriate R_{cor} -chart, prior to entry.

To use any of these charts, enter the abscissa and ordinate with the required resistivity ratios. The point of intersection defines d_i , R_{xo}/R_t and R_t as a function of one resistivity measurement.

Saturation determination in clean formations

Either of the chart-derived values of R_t and R_{xo}/R_t can be used to find values for S_w . One value, which is designated as S_{wA} (S_w -Archie), is found using the Archie saturation formula (or Chart Sw-1) with the R_t value and known values of F_R and R_w .

An alternate S_w value, designated as S_{wR} (S_w -Ratio), is found using R_{xo}/R_t with R_{mf}/R_w as in Chart Sw-2.

If S_{wA} and S_{wR} are equal, the assumption of a step-contact invasion profile is indicated to be correct, and all values found (S_w , R_t , R_{xo} , d_i) are considered good.

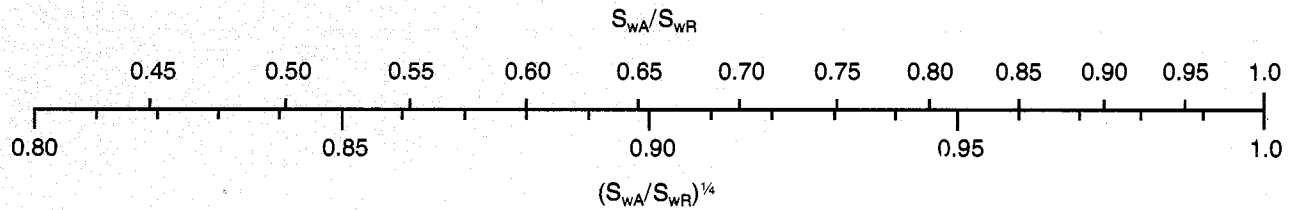
If $S_{wA} > S_{wR}$, either invasion is very shallow or a transition type of invasion profile is indicated, and S_{wA} is considered a good value for S_w .

If $S_{wA} < S_{wR}$, an annulus-type invasion profile may be indicated. In this case a more accurate value of water saturation may be estimated using the relation:

$$S_{wCOR} = S_{wA} \left(\frac{S_{wA}}{S_{wR}} \right)^{\frac{1}{4}}$$

The correction factor $(S_{wA}/S_{wR})^{1/4}$ can be found from the scale below.

For more information see Reference 9.



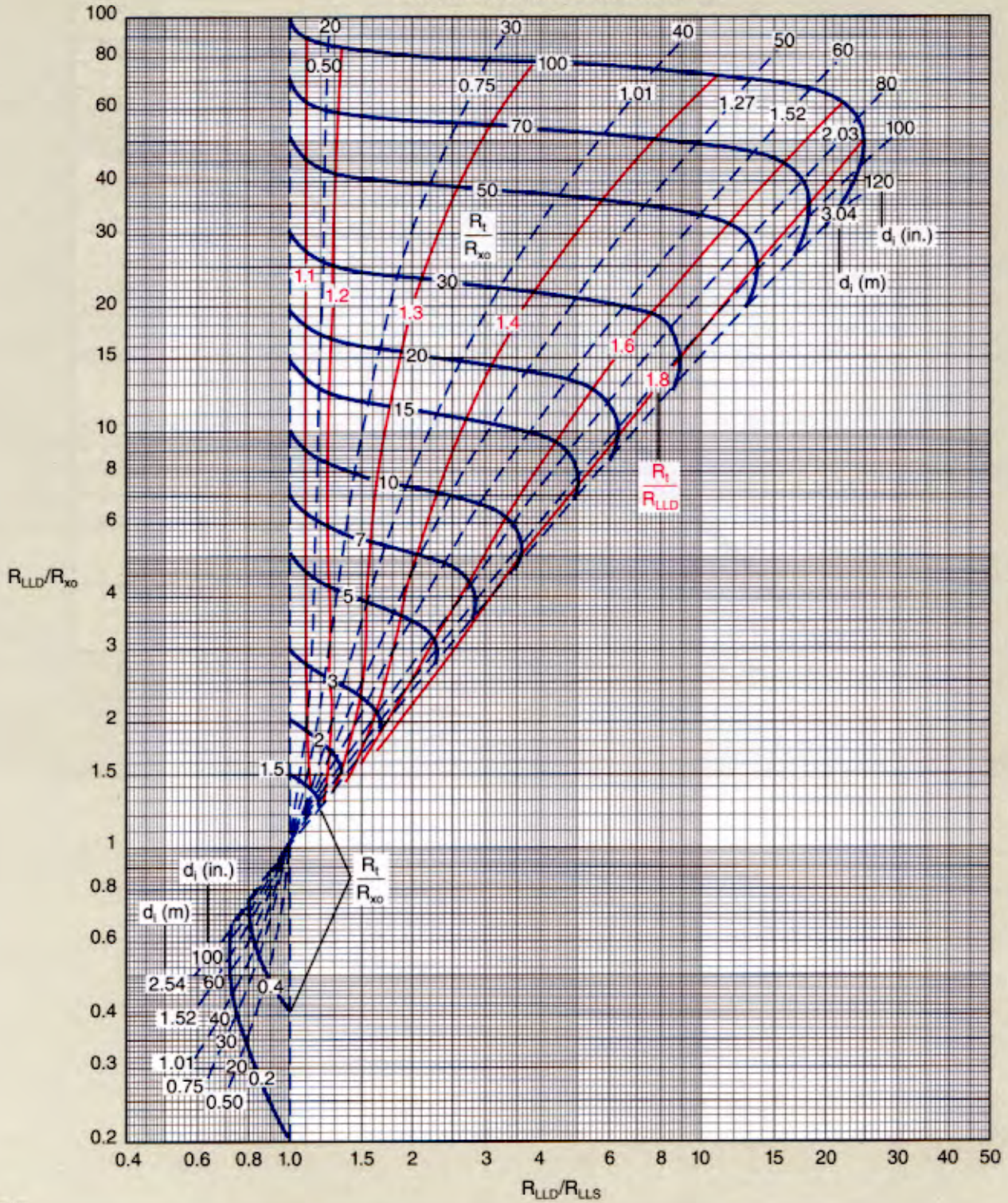
© Schlumberger

Dual Laterolog-R_{x0} Device

DLT-D/E LLD-LLS-R_{x0} device

Rint-9b

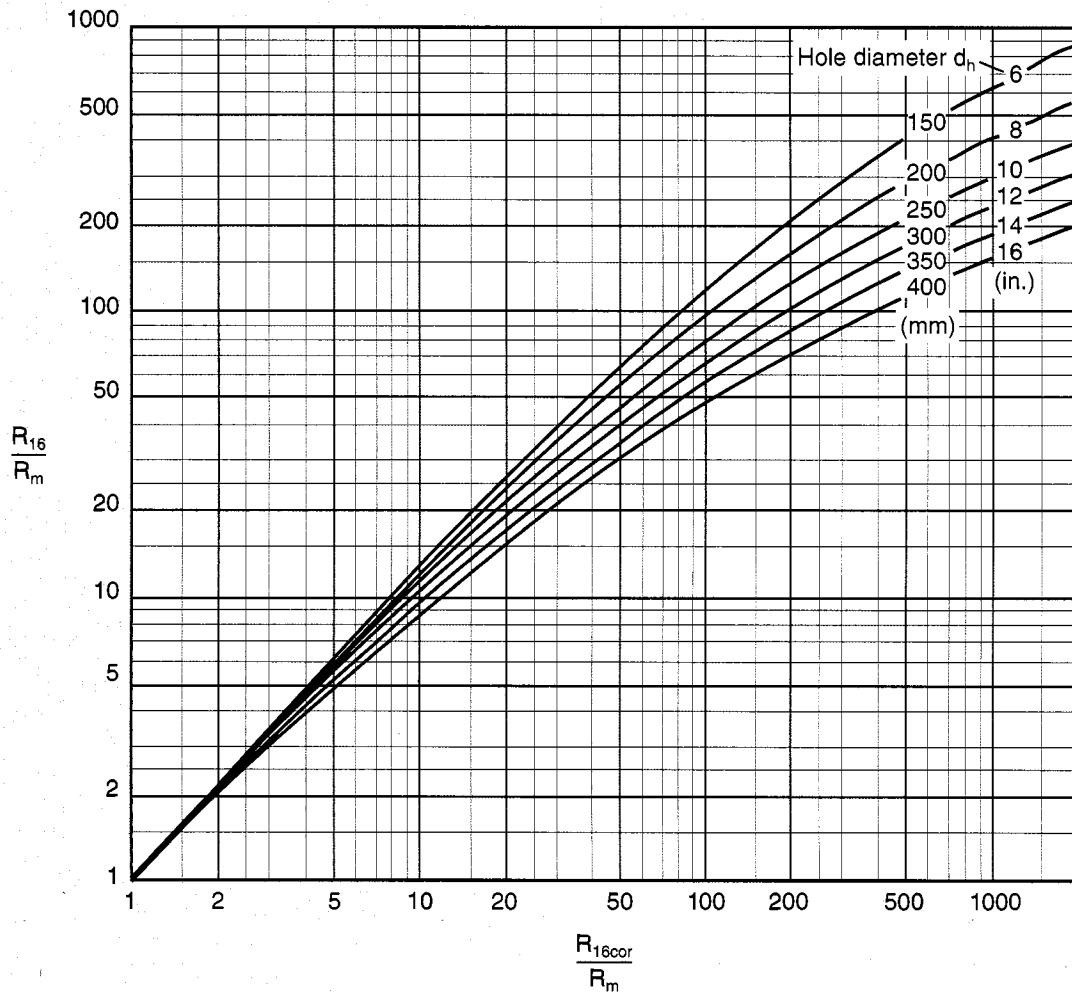
Thick beds, 8-in. [203-mm] hole,
no annulus, no transition zone, $R_{x0}/R_m = 50$,
use data corrected for borehole effect



Borehole Correction for 16-in. Normal

Recorded with induction-electrical log

Rcor-8



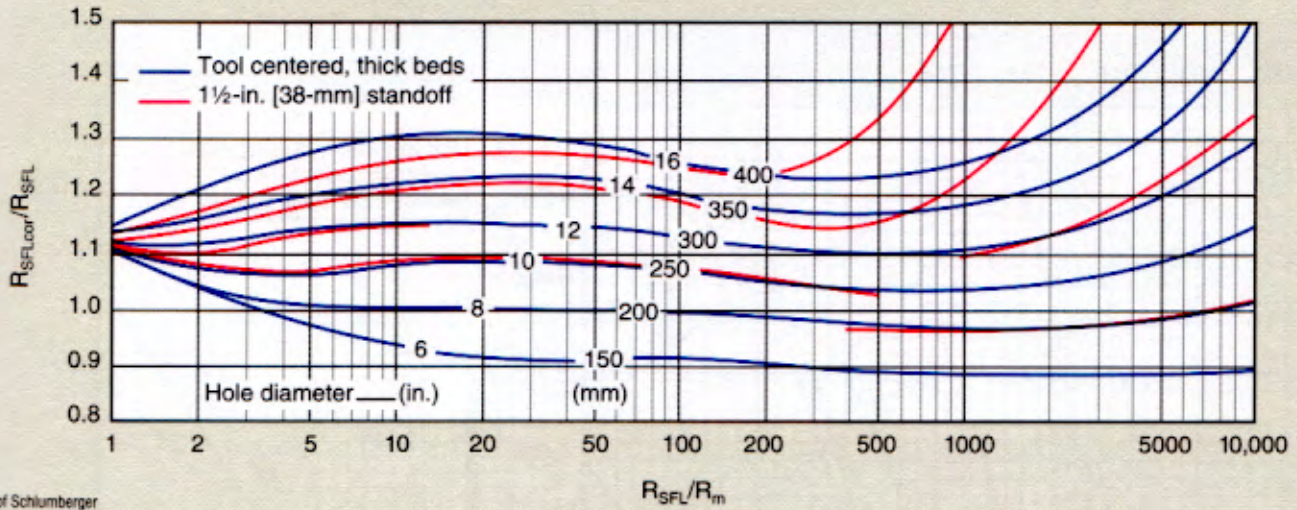
Rcor

© Schlumberger

SFL* Spherically Focused Resistivity Borehole Correction

Recorded with DIS-DB, EA or equivalent

Rcor-1



*Mark of Schlumberger
© Schlumberger

Most resistivity measurements should be corrected for borehole effect. Charts Rcor-1 and Rcor-8 provide the borehole correction for the 16-in. Normal and the SFL measurements.

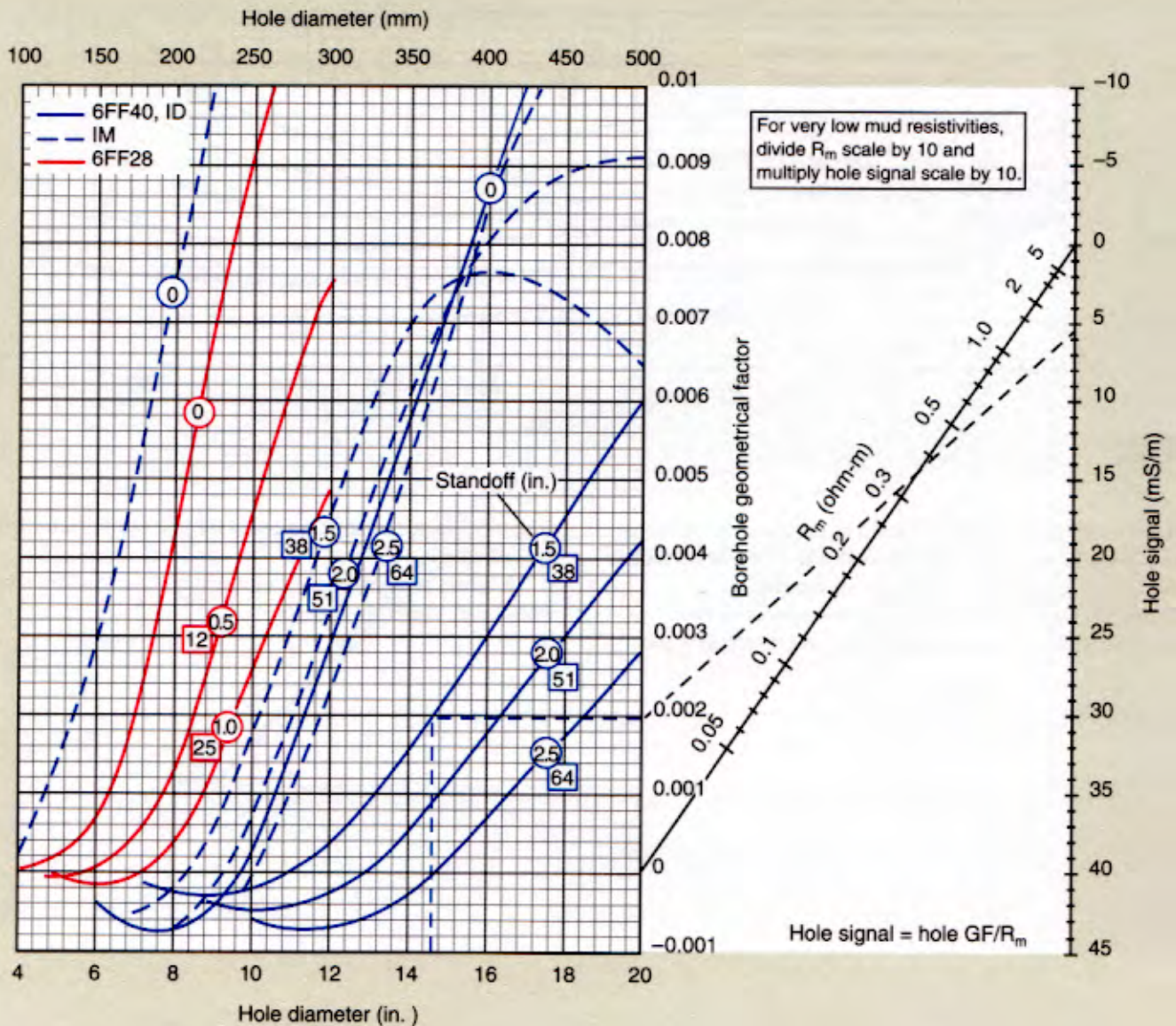
To use, the ratio of the resistivity measurement divided by the mud resistivity, R_m , is entered in abscissa. Proceed to the

proper borehole diameter, and read the correction factor from the ordinate.

The chart contains curves for a centered tool and for a tool with 1 1/2-in. standoff.

Induction Log Borehole Correction

Rcor-4a



© Schlumberger

The hole-conductivity signal is to be subtracted, where necessary, from the induction log conductivity reading before other corrections are made.[†] This correction applies to all zones (including shoulder beds) having the same hole size and mud resistivity.

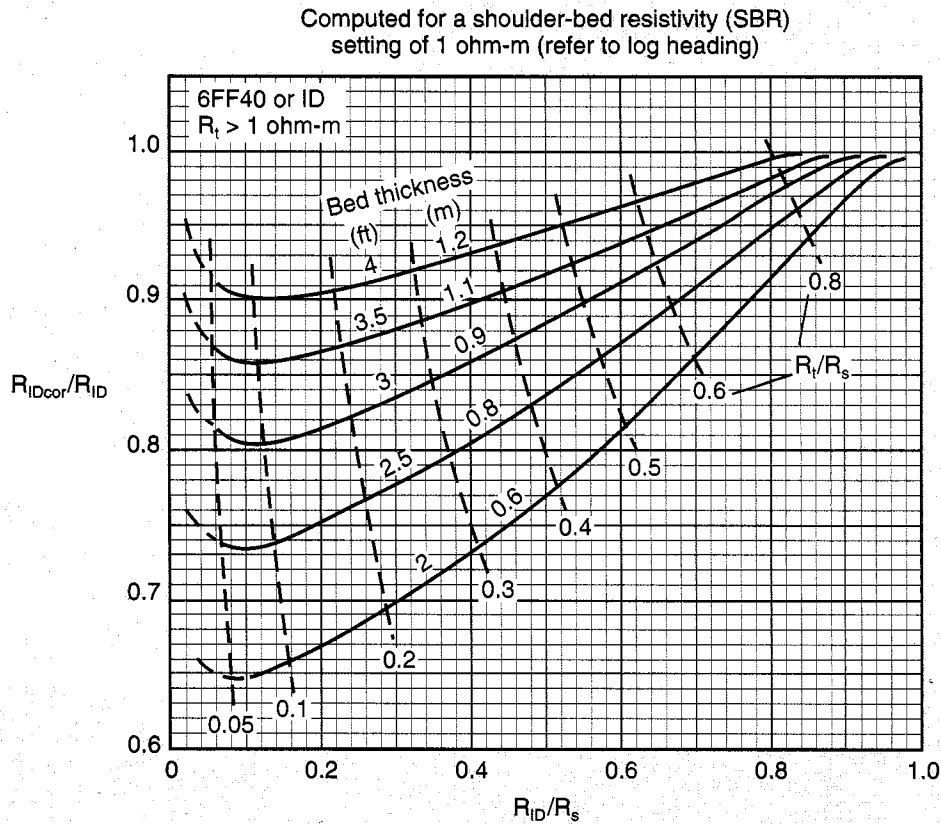
[†] Some induction logs, especially in salty muds, are adjusted so that the hole signal for the nominal hole size is already subtracted out of the recorded curve. Refer to the log heading.

Rcor-4 gives corrections for 6FF40 or ID, IM and 6FF28 for various wall standoffs. Dashed lines illustrate the use of the chart for a 6FF40 sonde with a 1.5-in. standoff in a 14.6-in. borehole, and $R_m = 0.35$ ohm-m. The hole signal is found to be 5.5 mS/m. If the log reads $R_1 = 20$ ohm-m, C_1 (conductivity) = 50 mS/m. The corrected C_1 is then $(50 - 5.5) = 44.5$ mS/m. $R_1 = 1000/44.5 = 22.4$ ohm-m.

Induction Log Correction for Thin Conductive Beds

6FF40, ID, 6FF28

Rcor-7



© Schlumberger

Charts Rcor-5, Rcor-6 and Rcor-7 correct the induction logs (6FF40, ID, 6FF28 and IM) for bed thickness. A skin-effect correction is included in these charts.

To use, select the chart appropriate for the tool type and for the adjacent bed resistivity (R_s). For Charts Rcor-5 and Rcor-6, enter the bed thickness and proceed upward to the proper R_a curve. Read the corrected resistivity value (R_t) in ordinate.

For Chart Rcor-7, enter the chart with the R_{ID}/R_s ratio (apparent ID reading/adjacent bed resistivity) and go upward to the bed thickness. Read the correction factor (R_{IDcor}/R_{ID}) in ordinate.

Example: $R_{ID} = 4.2$ ohm-m
 $R_{IM} = 6.0$ ohm-m
 $R_s = 2.0$ ohm-m
 Bed thickness = 3 m
 giving, from the $R_s = 2$ ohm-m charts,
 $R_{IDcor} = 4.5$ ohm-m
 $R_{IMcor} = 6.2$ ohm-m

For the small-diameter 6FF28, multiply the bed thickness by 1.43 before entering these correction charts. For example, in a 7-ft bed, the bed thickness used in correcting the 6FF28 reading is 10 ft ($7 \times 1.43 = 10$).

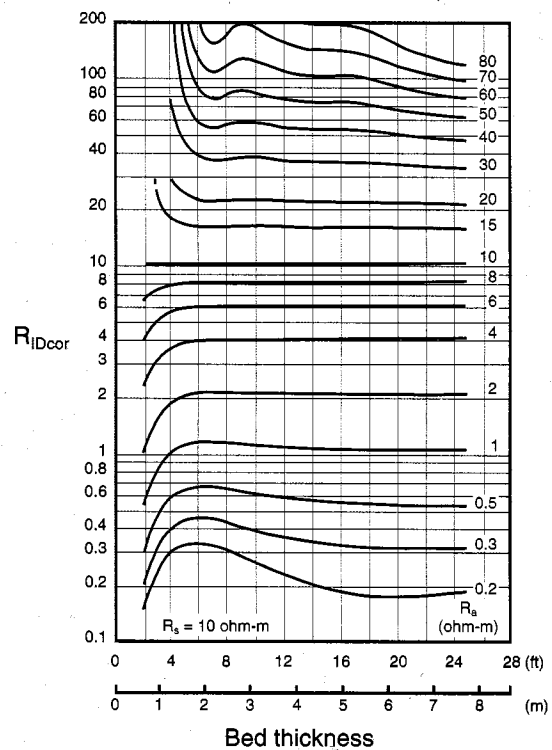
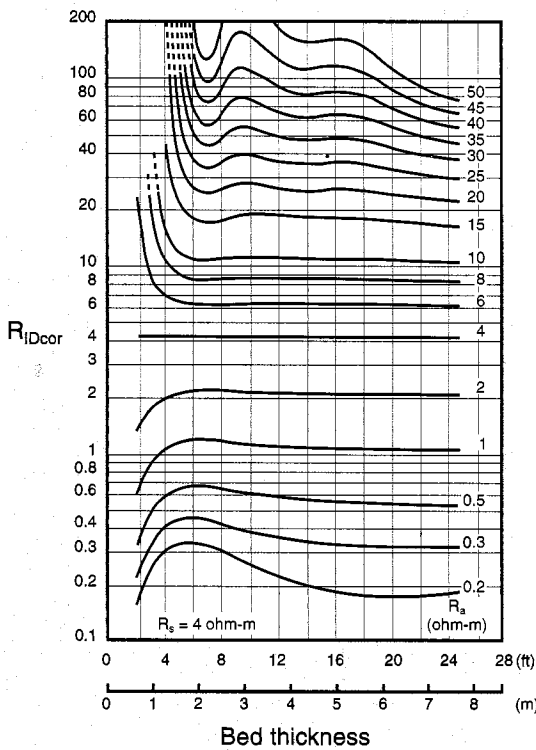
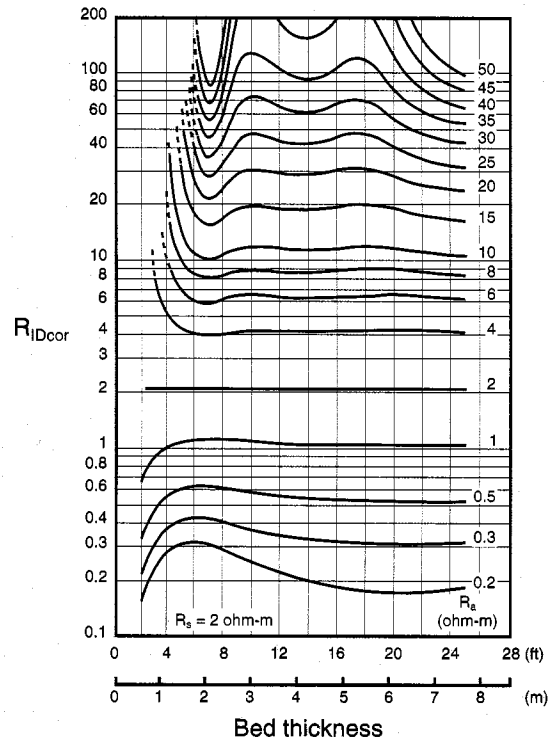
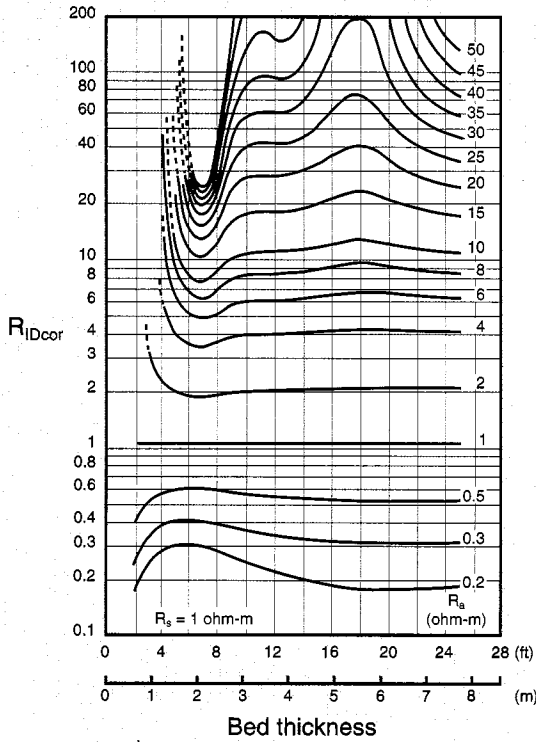
Rcor

Induction Log Bed-Thickness Correction

6FF40 (ID) and 6FF28

Rcor-5

Computed for a shoulder-bed resistivity (SBR) setting of 1 ohm-m (refer to log heading)



Rcor

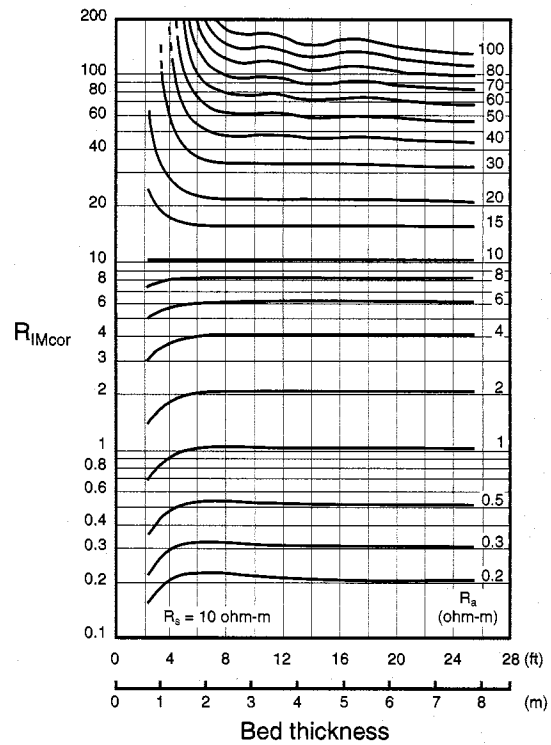
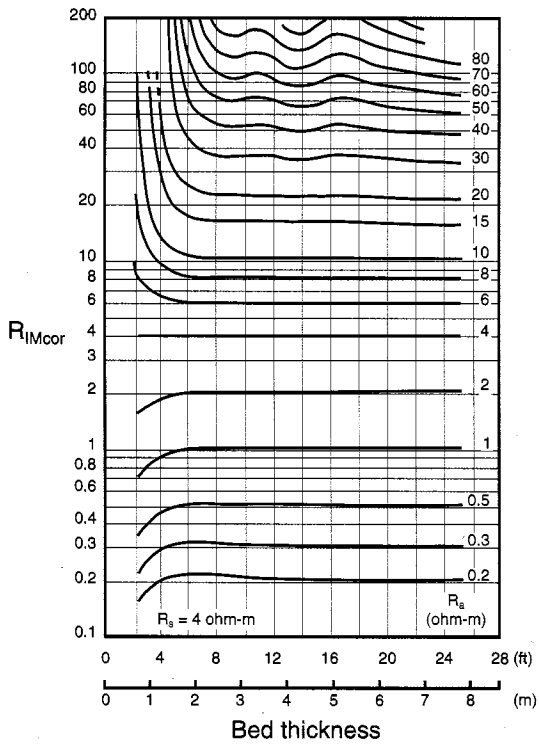
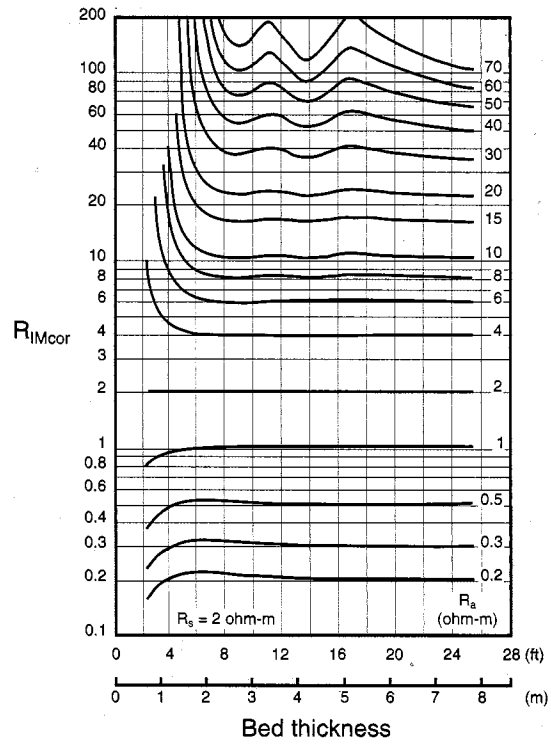
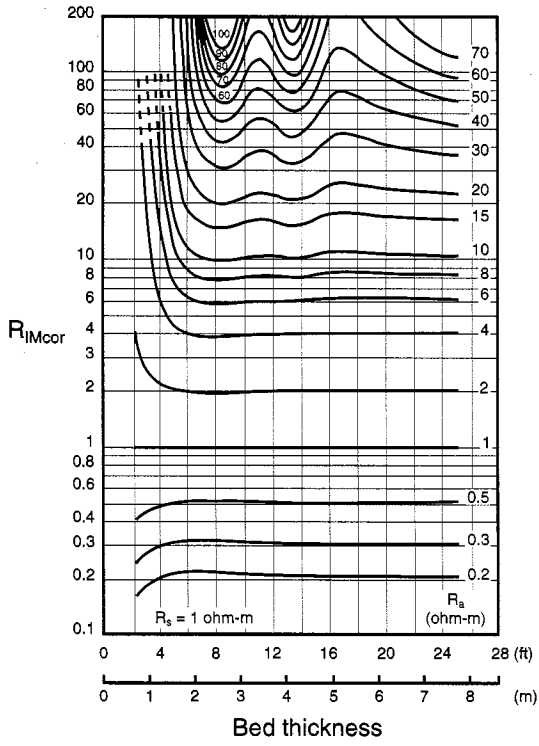
For the small-diameter 6FF28 sonde, multiply the bed thickness by 1.43 before entering these correction charts. For example, in

a 7-ft bed, the bed thickness used in correcting the 6FF28 reading is 10 ft ($7 \times 1.43 = 10$).

Induction Log Bed-Thickness Correction

IM medium induction

Rcor-6



Rcor

Invasion Correction Charts

Rint-1a

The invasion correction charts, sometimes referred to as "tornado" or "butterfly" charts, of the next several pages (labeled Rint-) are used to define the depth of invasion d_i , the R_{xo}/R_t ratio and the true resistivity R_t . All assume a step-contact profile of invasion and that all resistivity measurements have been corrected, where necessary, for borehole effect and bed thickness using the appropriate Rcor- chart, prior to entry.

To use any of these charts, enter the abscissa and ordinate with the required resistivity ratios. The point of intersection defines d_i , R_{xo}/R_t and R_t as a function of one resistivity measurement.

Example: $R_{SFL} = 25 \text{ ohm-m}$
 $R_{IM} = 5.9 \text{ ohm-m}$
 $R_{ID} = 4.8 \text{ ohm-m}$
 $R_m = 0.5 \text{ ohm-m}$

} After correction
for borehole effect
and bed thickness

Entering the $R_{xo}/R_m \approx 100$ chart (Chart Rint-2c) with

$$R_{SFL}/R_{ID} = 25/4.8 = 5.2$$

$$R_{IM}/R_{ID} = 5.9/4.8 = 1.2$$

yields $R_{xo}/R_t = 8$

$$d_i = 39 \text{ in. or } 1 \text{ m}$$

$$R_t/R_{ID} = 0.97$$

Therefore, $R_t = R_{ID} (R_t/R_{ID}) = 4.8 \times 0.97 = 4.7 \text{ ohm-m}$

$$R_{xo} = R_t (R_{xo}/R_t) = 4.7 \times 8 = 37.6 \text{ ohm-m}$$

Use of Chart Rint-2c is confirmed since $R_{xo}/R_m = 75$ (i.e., $R_{xo}/R_m \approx 100$).

Saturation determination in clean formations

Either of the chart-derived values of R_t and R_{xo}/R_t can be used to find values for S_w . One value, which is designated as S_{wA} (S_w -Archie), is found using the Archie saturation formula (or Chart Sw-1) with the R_t value and known values of F_R and R_w . An alternate S_w value, designated as S_{wR} (S_w -Ratio), is found using R_{xo}/R_t with R_{mf}/R_w , as in Chart Sw-2.

If S_{wA} and S_{wR} are equal, the assumption of a step-contact invasion profile is indicated as correct, and all values found (S_w , R_t , R_{xo} and d_i) are considered good.

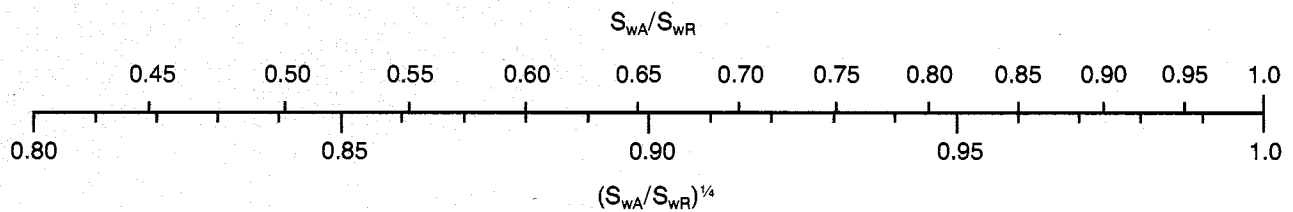
If $S_{wA} > S_{wR}$, either invasion is very shallow or a transition-type invasion profile is indicated, and S_{wA} is considered a good value for S_w .

If $S_{wA} < S_{wR}$, an annulus-type invasion profile may be indicated. In this case a more accurate value of water saturation may be estimated using the relation:

$$S_{wcor} = S_{wA} \left(\frac{S_{wA}}{S_{wR}} \right)^{\frac{1}{4}}$$

The correction factor $(S_{wA}/S_{wR})^{1/4}$ can be found from the scale below.

For more information see Reference 9.



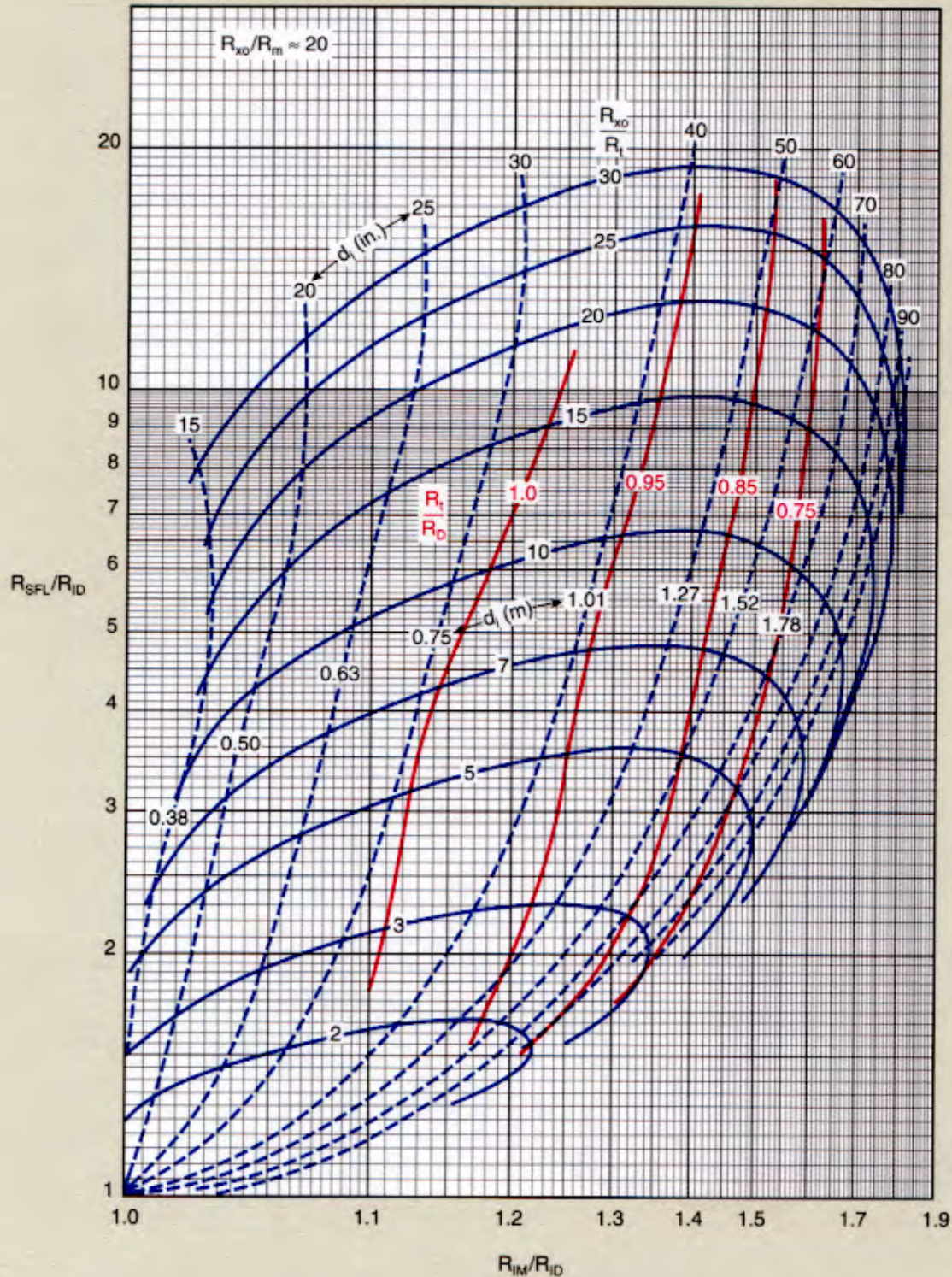
© Schlumberger

Rint

DIL* Dual Induction-SFL* Spherically Focused Resistivity Log
ID-IM-SFL

Rint-2b

Thick beds, 8-in. [203-mm] hole, skin-effect corrected,
DIS-EA or equivalent

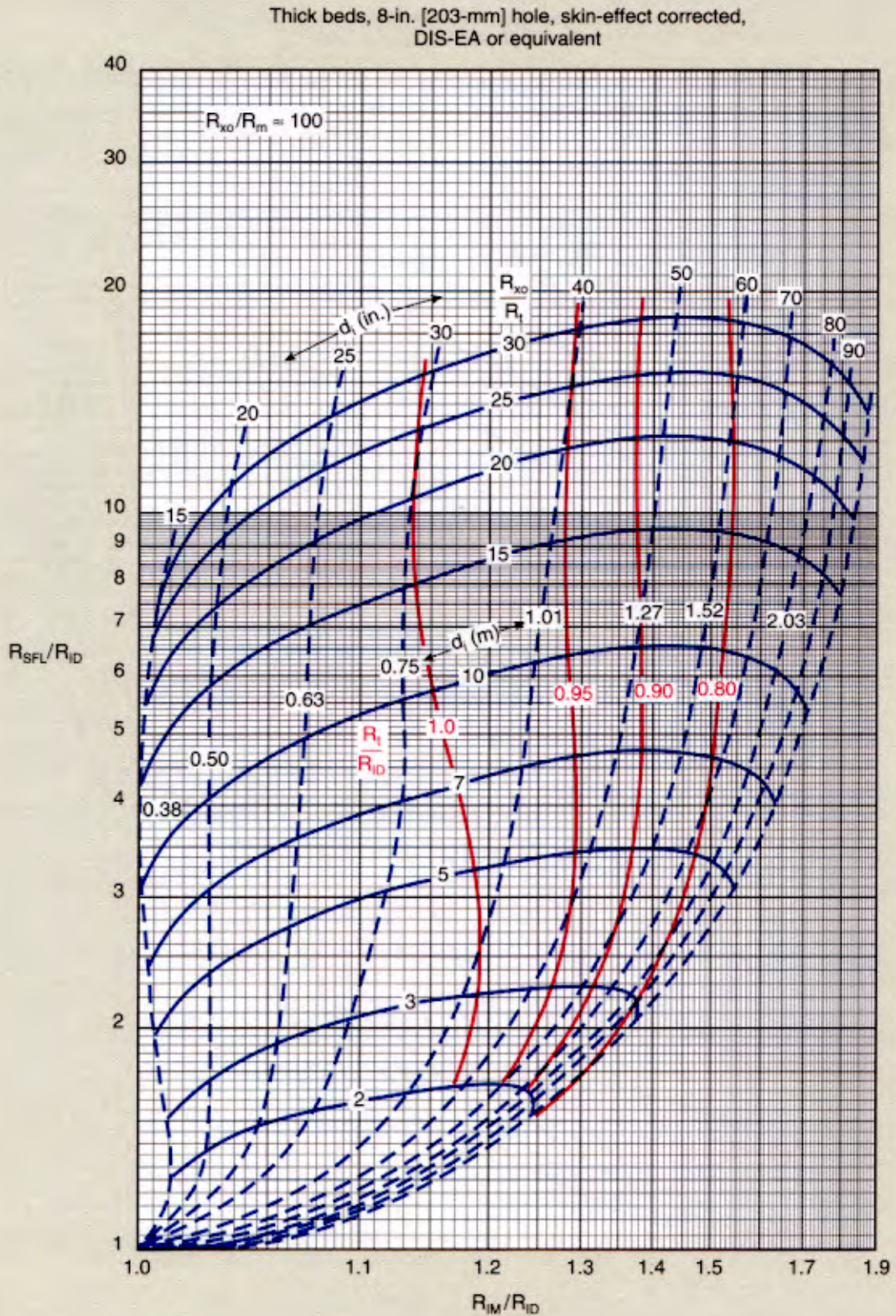


*Mark of Schlumberger
© Schlumberger

Rint

DIL* Dual Induction-SFL* Spherically Focused Resistivity Log
ID-IM-SFL

Rint-2c

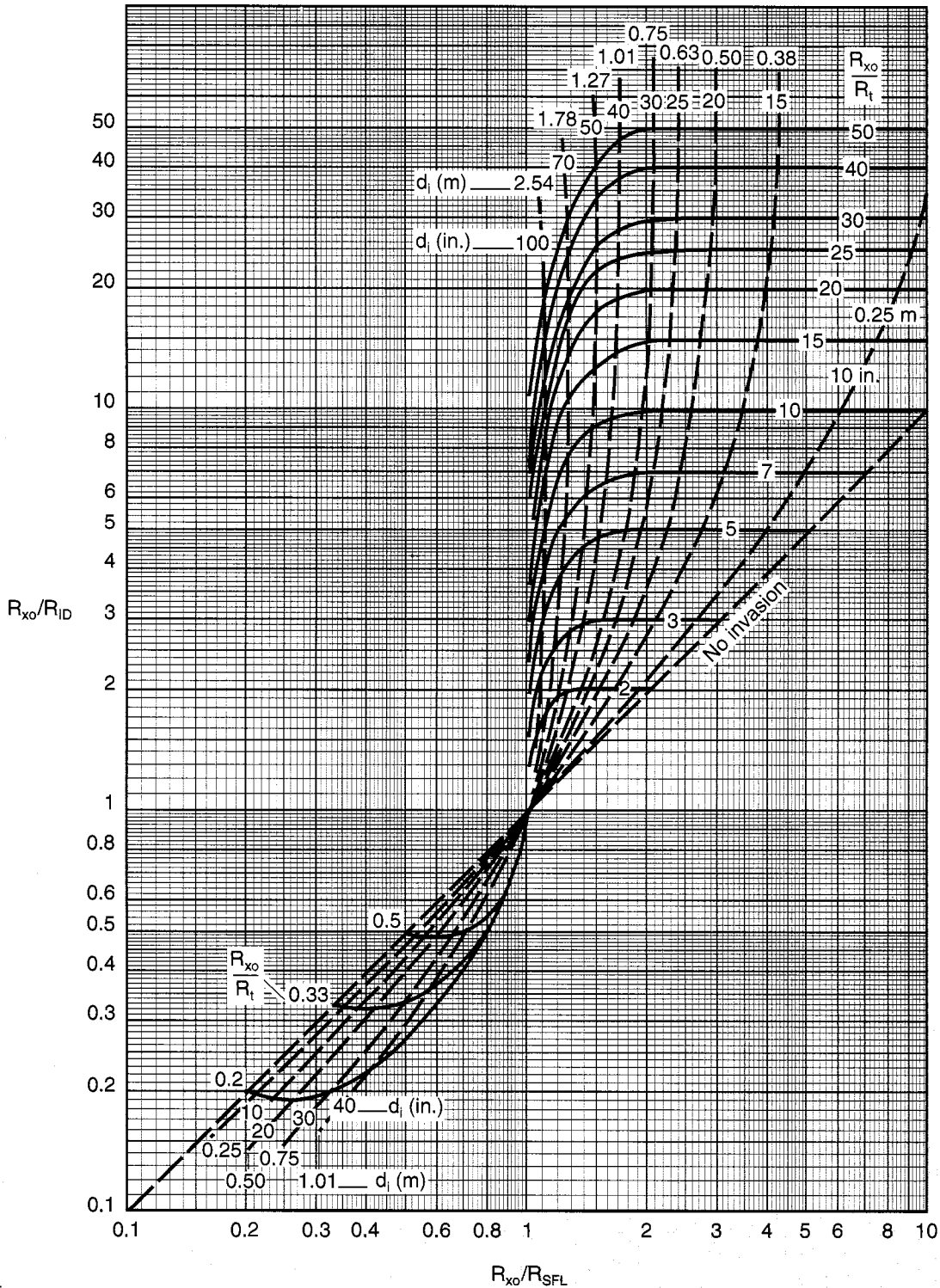


*Mark of Schlumberger
© Schlumberger

Deep Induction-SFL* Spherically Focused Resistivity Log-
 R_{x0} Device
 ID-SFL- R_{x0} device

Rint-5

Thick beds, 8-in. [203-mm] hole,
 no annulus, no transition zone,
 induction log is skin-effect corrected



Rint

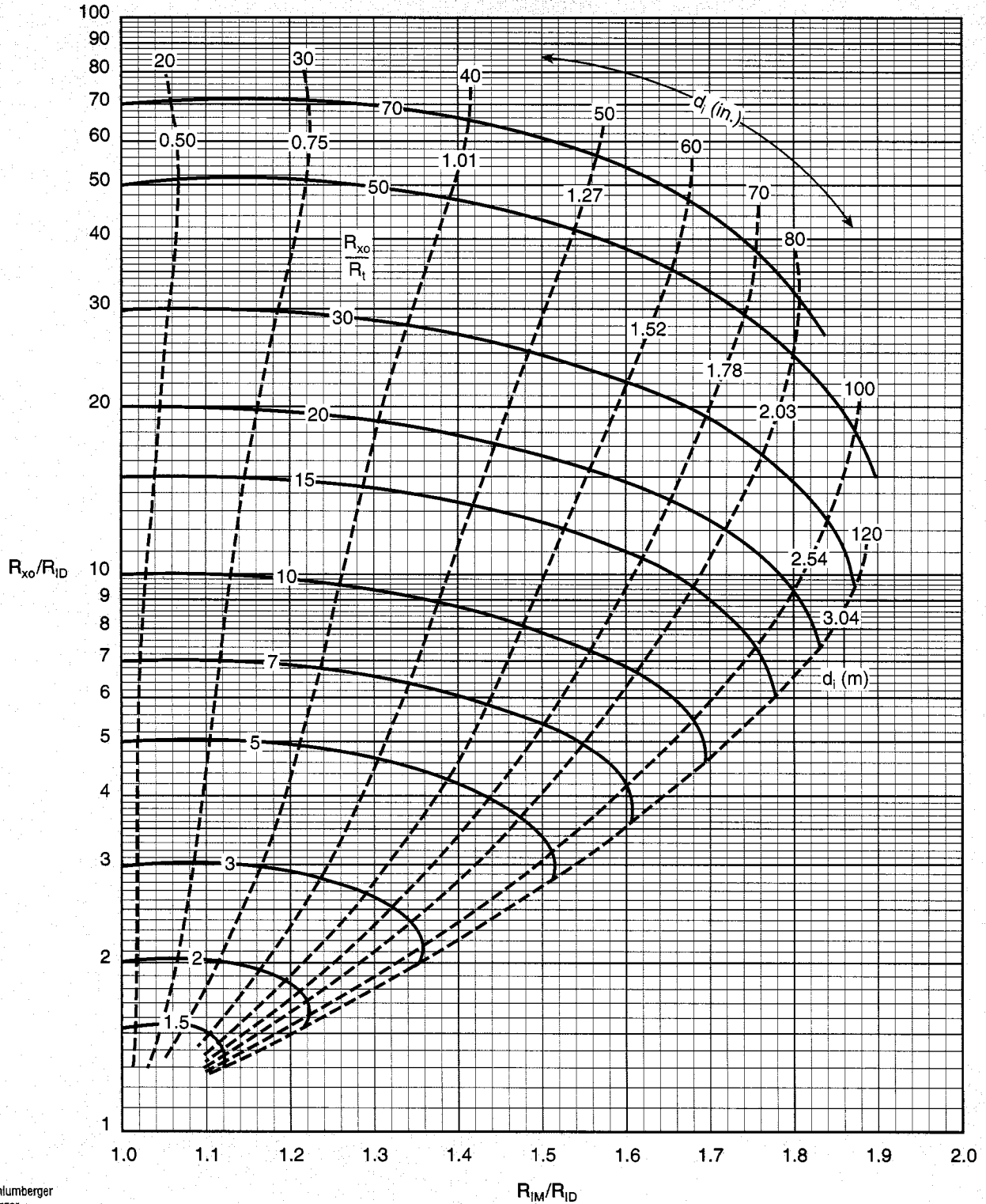
*Mark of Schlumberger
 © Schlumberger

DIL* Dual Induction- R_{x0} Device

ID-IM- R_{x0} device

Rint-10

Thick beds, 8-in. [203-mm] hole,
no annulus, no transition zone, $R_{x0} \approx 20$,
induction log is skin-effect corrected



*Mark of Schlumberger
© Schlumberger

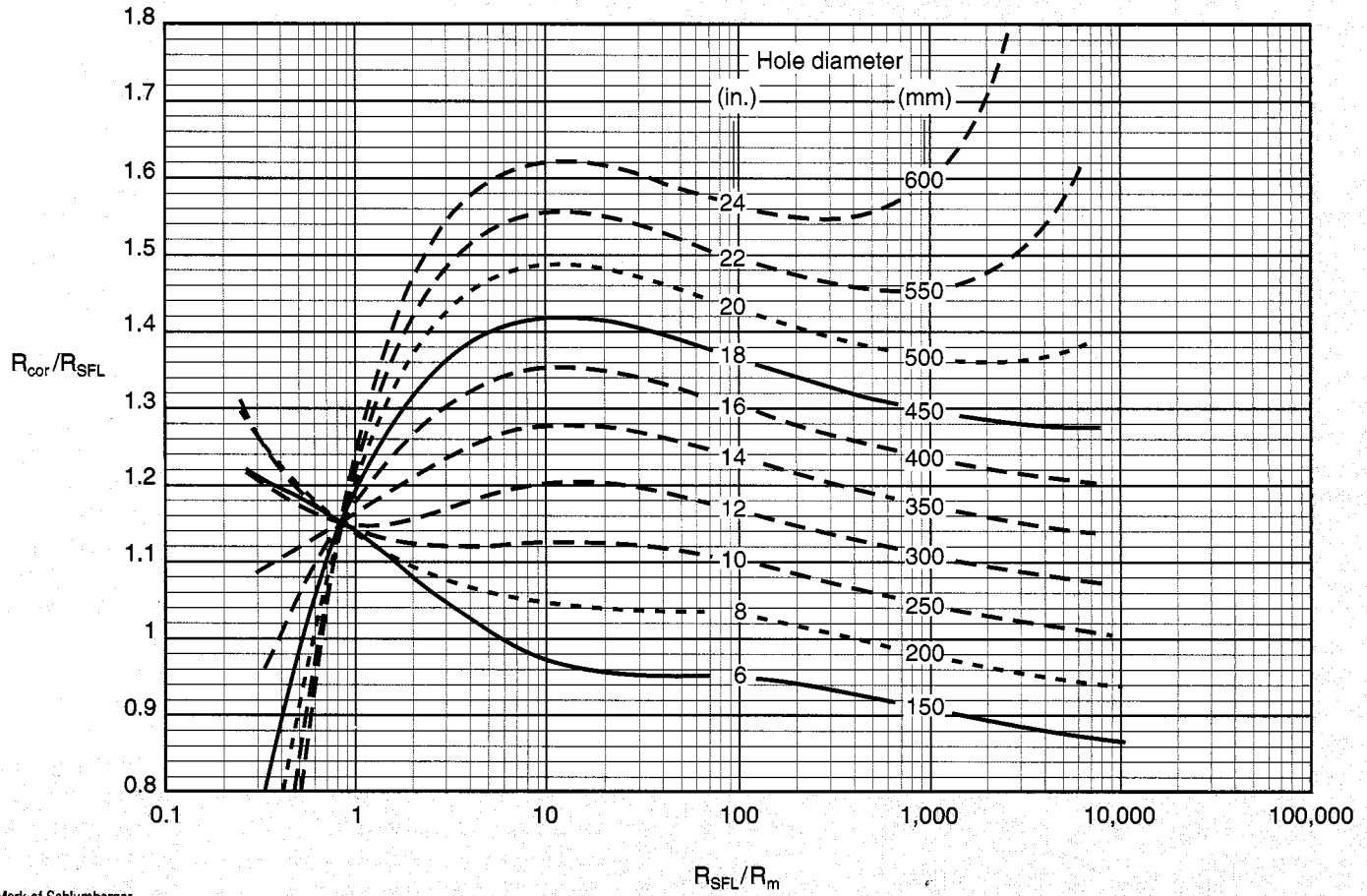
To use this chart in an oil-base mud environment, use synthetic R_{x0} calculated from EPT* or TDT* logs.

SFL* Borehole Correction

DIT-E Phasor* Induction tool

Rcor-3

Tool centered, thick beds



*Mark of Schlumberger
© Schlumberger

Rcor

Phasor* Induction Borehole Correction

Borehole corrections can now be based on exact modeling as well as on traditional experiments. Borehole correction requires four inputs: borehole conductivity (C_B), formation conductivity (C_f), borehole diameter (D) and standoff (S). For smooth round holes, correction of Phasor Induction logs may be based on Charts Rcor-4b and Rcor-4c. For cases when $R_t/R_m > 100$, Chart Rcor-4b is used alone. For cases when $R_t/R_m < 100$, both Charts Rcor-4b and Rcor-4c are needed. Each chart gives the borehole geometrical factor (G_B) as a function of borehole diameter and standoff. G_B is used to get from apparent conductivity (C_a) to corrected conductivity (C_{cor}) through the correction formula

$$C_{cor} = \frac{C_a - C_B G_B}{1 - G_B} \quad (1)$$

G_B is obtained from the charts for the appropriate borehole and standoff. All conductivities are expressed in mS/m and are calculated through the formula

$$C = \frac{1000}{R} \quad (2)$$

where R is the resistivity in ohm-m.

When the formation-to-borehole contrast is low and the boreholes are large enough to warrant correction, the following formula for interpolation between charts gives the approximate borehole geometrical factor:

$$G_{B_{DM}} = A_M G_{B_{M4c}} + (1 - A_M) G_{B_{M4b}} \quad (3)$$

$$G_{B_{ID}} = A_D G_{B_{D4c}} + (1 - A_D) G_{B_{D4b}} \quad (4)$$

where $G_{B_{D4b}}$ is the ID GF from Chart Rcor-4b and $G_{B_{D4c}}$ is from Chart Rcor-4c (D refers to ID and M refers to IM). The parameter A_M is derived from the formation and mud conductivities through the formula

$$A_M = -2.58414 + 3.59087F - 1.49684F^2 \quad (5)$$

and

$$A_D = 0.994584 - 1.59245F + 0.663813F^2 \quad (6)$$

where

$$F = \frac{C_B - C_f}{C_B + C_f} \quad (7)$$

Since C_f represents the formation conductivity just inside the borehole, SFL is the best estimator of this conductivity. The interpolated borehole geometrical factor is used in Eq. 1.

Note: All resistivity logs are limited near 2000 ohm-m. Borehole conditions can cause legitimate negative conductivity readings in conditions such as very resistive formations. The conductivity channels CIDP and CIMP are not limited and are better choices for borehole correction.

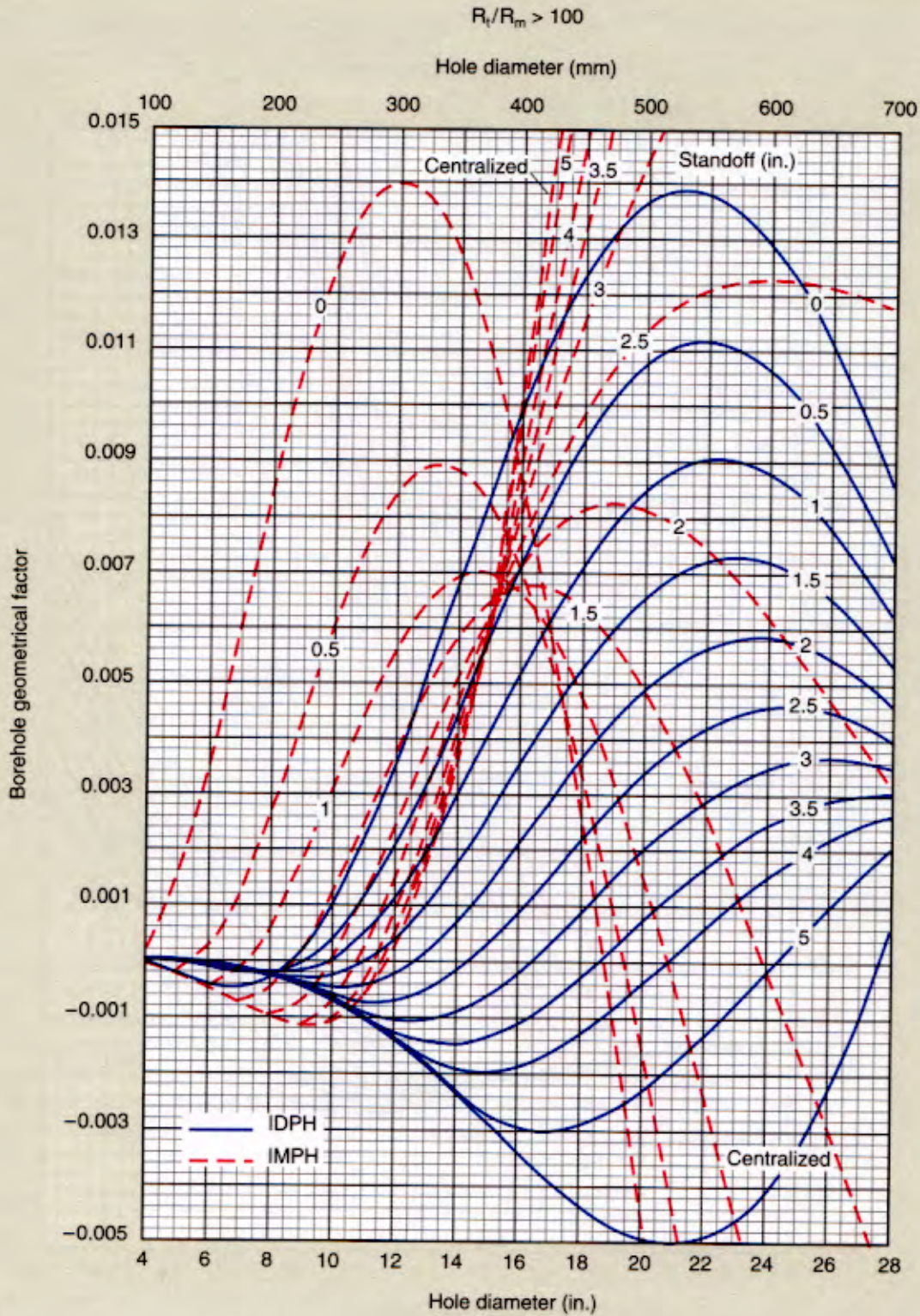
All Phasor Induction borehole corrections are applicable to ERL* Enhanced Resolution Logging and ERA* Enhanced Resolution Analysis presentations.

Borehole corrections for the Phasor Induction tool are usually made in real time. These charts provide only approximate corrections for specific cases of R_t/R_m and unique hole diameters. Any discrepancy between real-time (or Data Services Center) and manual chart-based corrections should normally be resolved in favor of the real-time corrections.

*Mark of Schlumberger

Phasor* Induction Borehole Correction

Rcor-4b

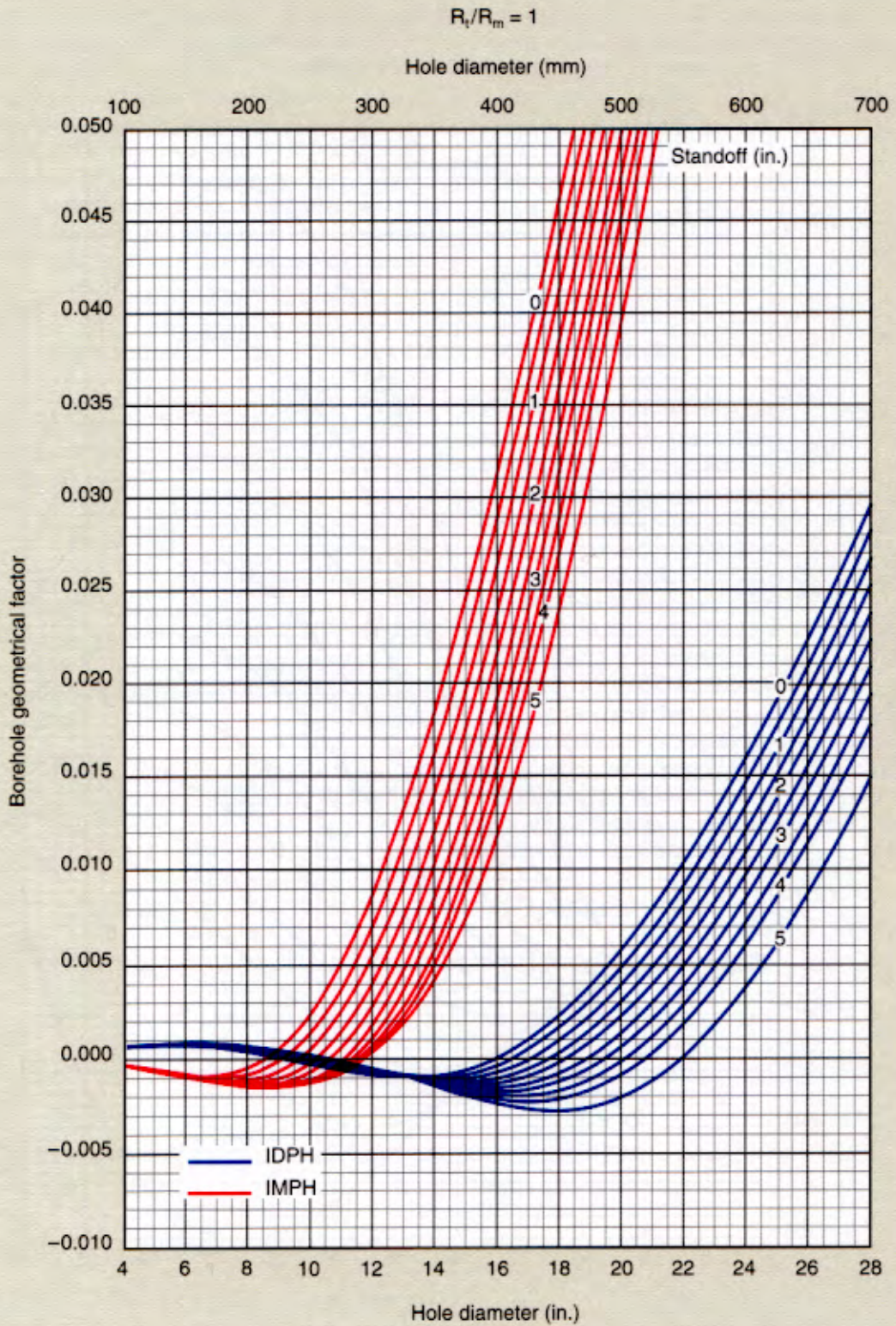


*Mark of Schlumberger
© Schlumberger

The borehole geometrical factor obtained from this chart or Chart Rcor-4c can be inserted into Nomograph Rcor-4a with the mud resistivity (R_m) to determine the hole signal (in mS/m).

Phasor* Induction Borehole Correction

Rcor-4c

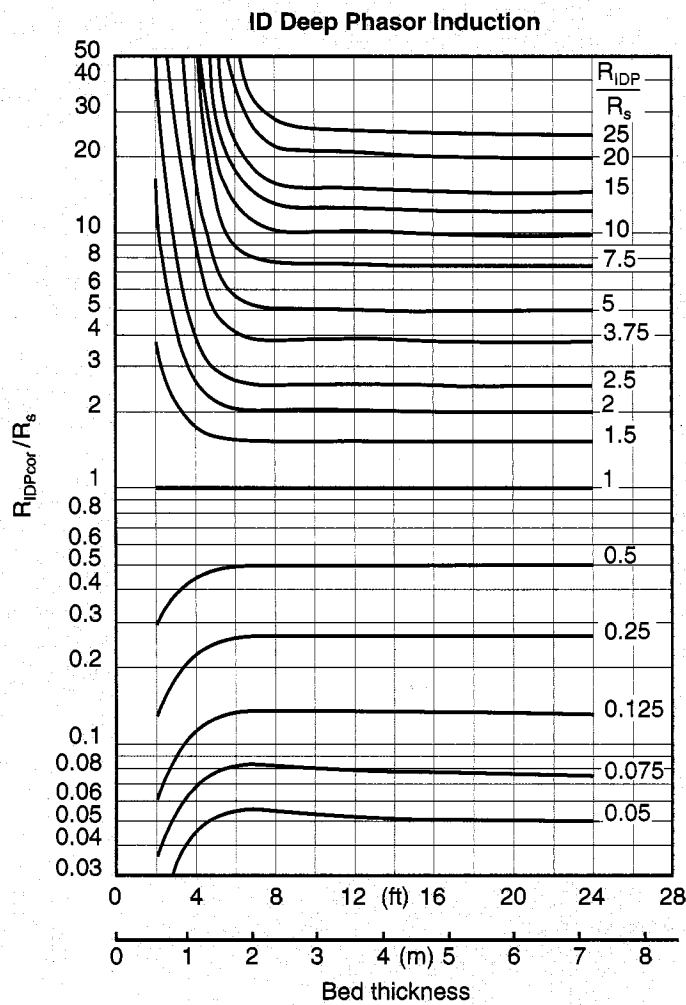
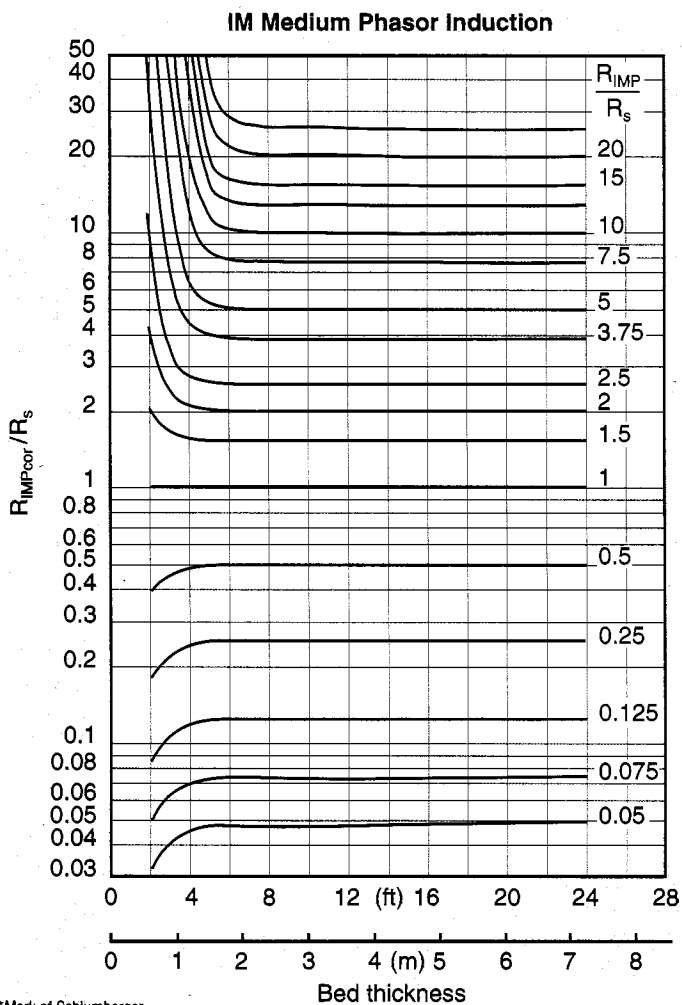


*Mark of Schlumberger
© Schlumberger

Phasor* Induction Bed-Thickness Correction

DIT-E Phasor Dual Induction-SFL

Rcor-9



*Mark of Schlumberger
© Schlumberger

Rcor

These charts (Rcor-9) correct the DIT-E Phasor Induction (IM and ID) measurements for bed thickness.

To use, enter the appropriate chart with the ratio of the apparent resistivity (R_{IMP} or R_{IDP}) divided by the adjacent bed resistivity (R_s) and the bed thickness. At this resulting intersection, the ratio of the corrected resistivity to the adjacent bed resistivity is read on the ordinate.

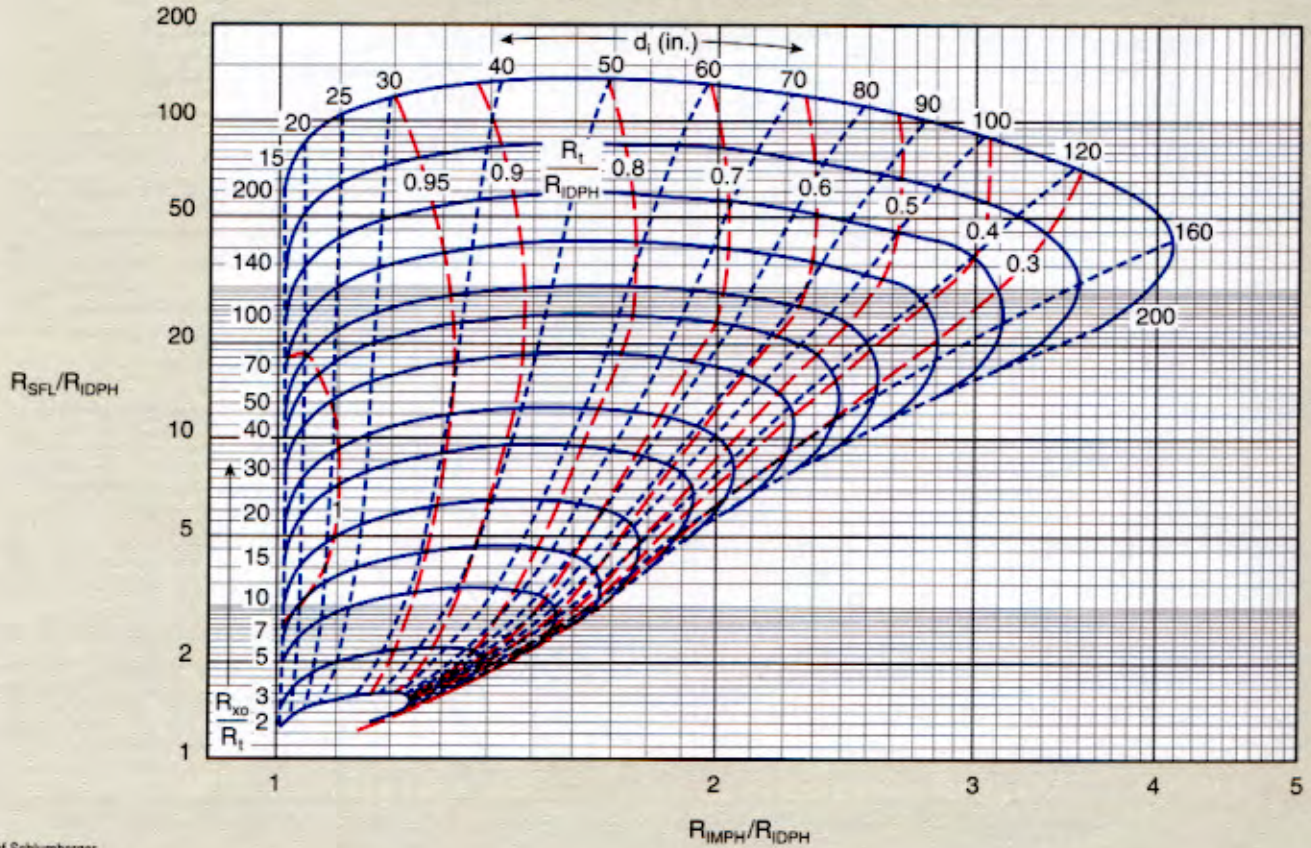
Example: $R_{IDP} = 7.5$ ohm-m
 $R_{IMP} = 6$ ohm-m
 $R_s = 2$ ohm-m
 Bed thickness = 6 ft
 giving $R_{IDP}/R_s = 7.5/2 = 3.75$
 $R_{IMP}/R_s = 6/2 = 3$
 Therefore, $R_{ID\ Pcor}/R_s = 4$
 $R_{IM\ Pcor}/R_s = 3.1$
 and $R_{ID\ Pcor} = 8$ ohm-m
 $R_{IM\ Pcor} = 6$ ohm-m

Phasor* Dual Induction-SFL* Spherically Focused Resistivity Log

ID Phasor-IM Phasor-SFL

Rint-11a

Thick beds, 8-in. [203-mm] hole, skin-effect and borehole corrected
 $R_{xo}/R_m = 100$, DIT-E or equivalent, frequency = 20 kHz



*Mark of Schlumberger
 © Schlumberger

Charts Rint-11, Rint-12, Rint-13 and Rint-15 apply to the Phasor Induction tool when operated at a frequency of 20 kHz. Similar charts (not presented here) are available for tool operation at 10 kHz and 40 kHz.

The 20-kHz charts provide reasonable approximations of

R_{xo}/R_t and R_t/R_{IDPH} for tool operation at 10 kHz and 40 kHz when only moderately deep invasion exists (less than 100 in.).

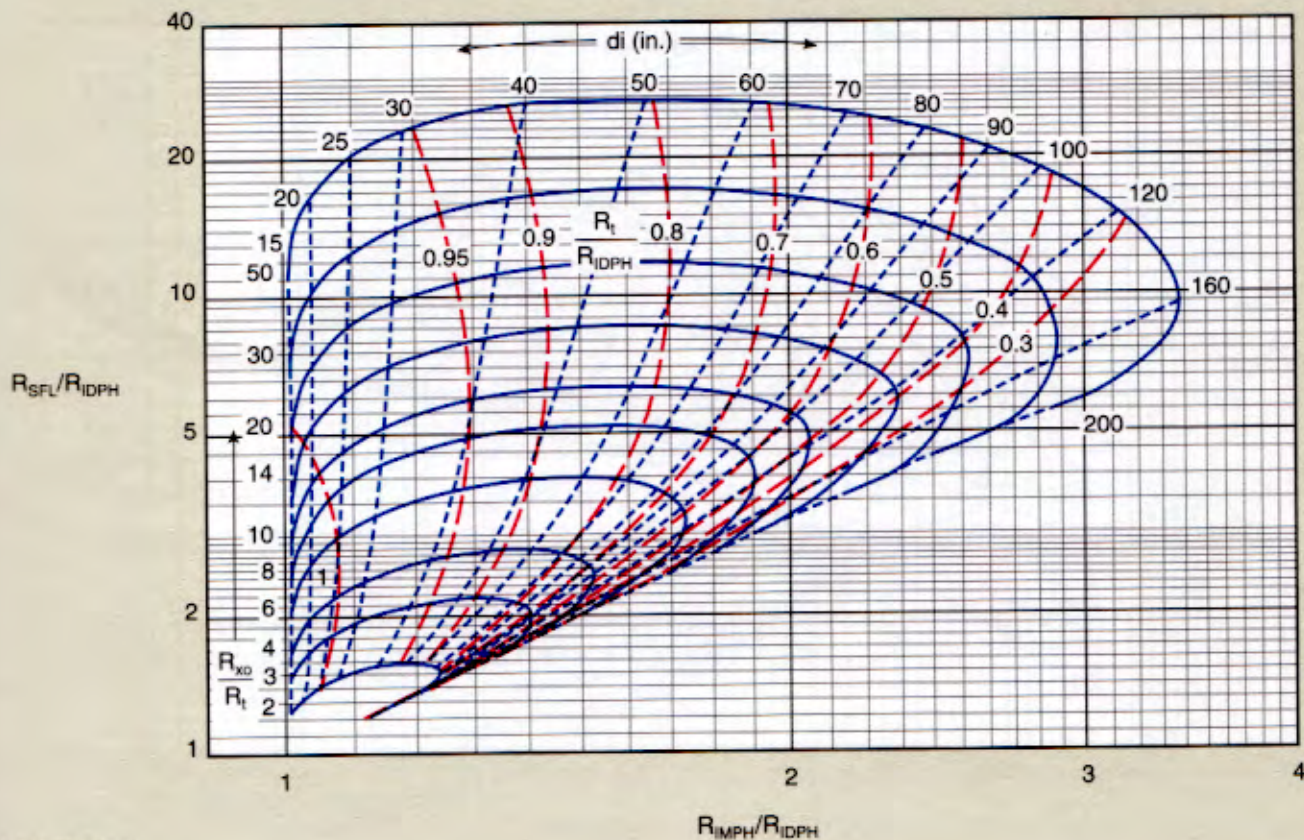
All Phasor Induction invasion correction charts are applicable to ERL* Enhanced Resolution Logging and ERA* Enhanced Resolution Analysis presentations.

Phasor* Dual Induction-SFL* Spherically Focused Resistivity Log

ID Phasor-IM Phasor-SFL

Rint-11b

Thick beds, 8-in. [203-mm] hole, skin-effect and borehole corrected
 $R_{xo}/R_m = 20$, DIT-E or equivalent, frequency = 20 kHz



*Mark of Schlumberger
 © Schlumberger

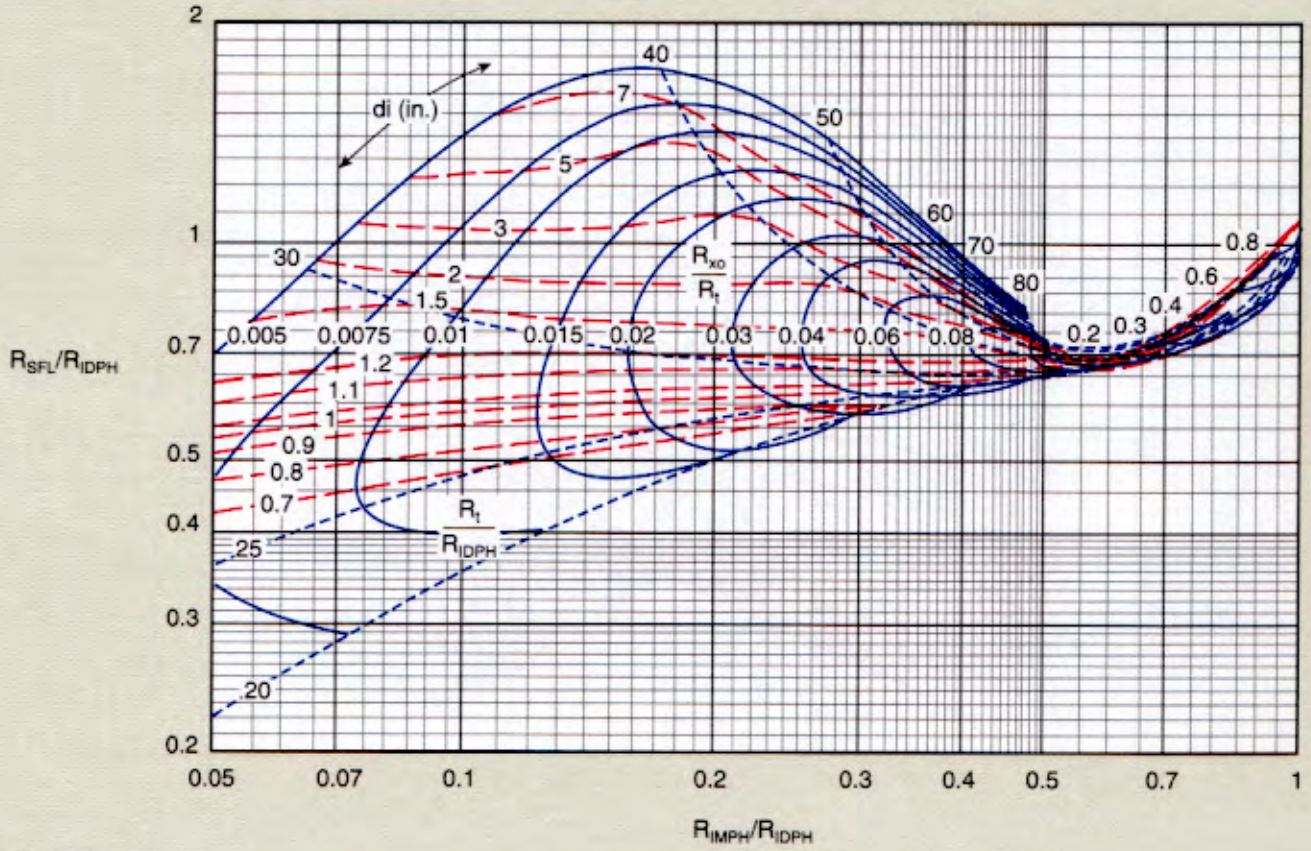
Rint

Phasor* Dual Induction-SFL* Spherically Focused Resistivity Log

ID Phasor-IM Phasor-SFL

Rint-11c

Thick beds, 8-in. [203-mm] hole, skin-effect and borehole corrected
 $R_{xo} < R_t$, $R_{xo} < 2$ ohm-m, frequency = 20 kHz



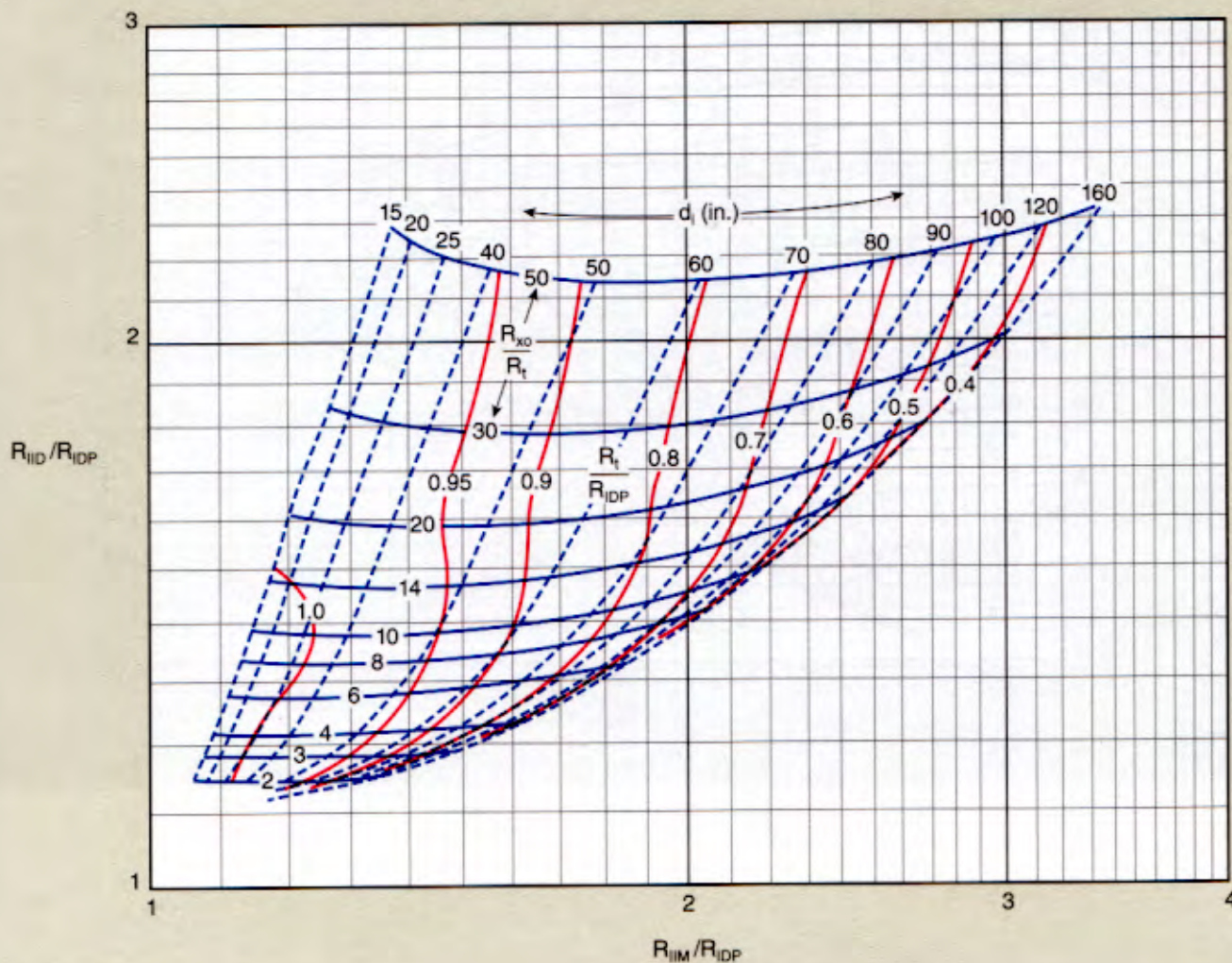
*Mark of Schlumberger
 © Schlumberger

Phasor* Dual Induction in Oil-Base Mud

ID Phasor-IM Phasor-Raw, unboosted I signals

Rint-12

Thick beds, 8-in. [203-mm] hole
 $R_{IDP} < 10$ ohm-m, DIT-E or equivalent, frequency = 20 kHz



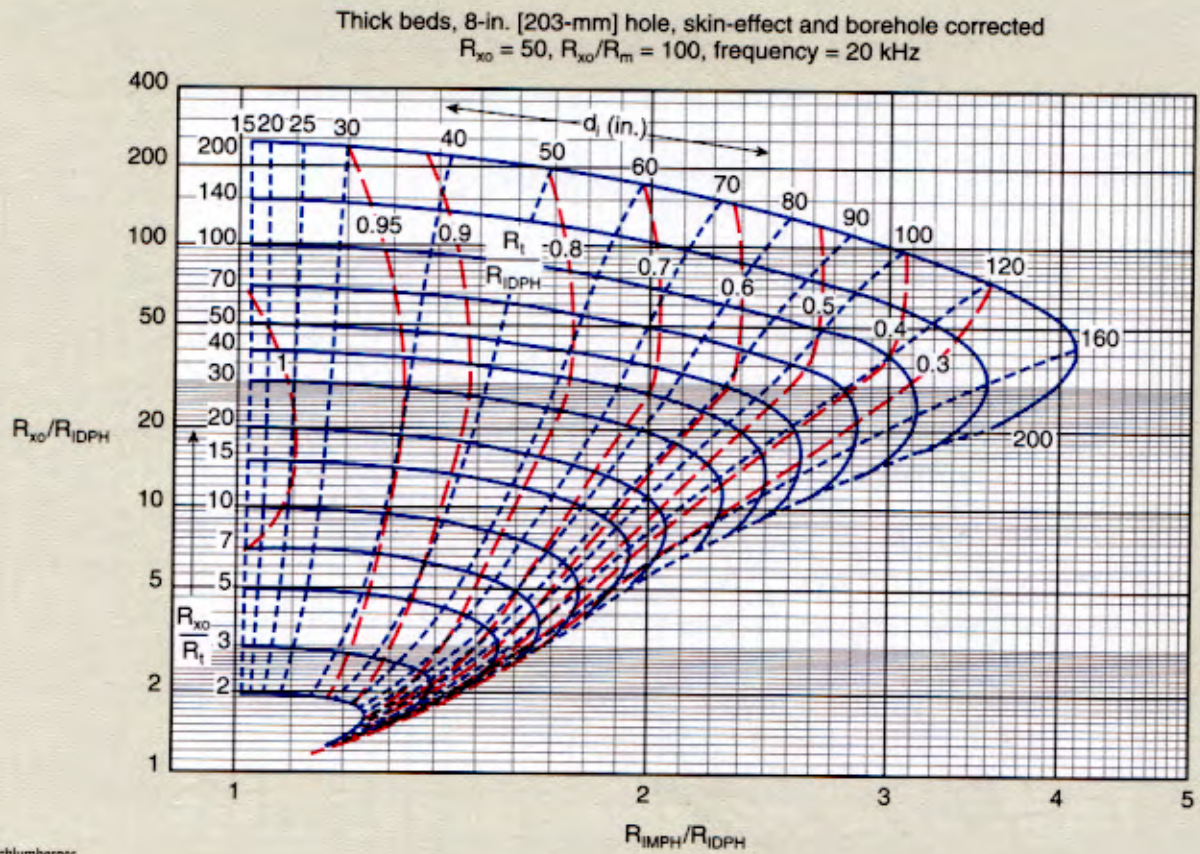
*Mark of Schlumberger
 © Schlumberger

This chart uses the raw, unboosted induction signals and the ID Phasor value to define the invasion profile in a rock drilled with oil-base mud. To use the chart, the ratio of the raw, unboosted medium induction signal (IIM) and the deep Phasor induction (IDP) is entered in abscissa. The ratio of the raw, unboosted deep induction signal (IID) and the deep Phasor induction (IDP) is entered in ordinate. Their intersection defines d_i , R_{xo}/R_t and R_t/R_{IDP} .

Example: $R_{IDP} = 1.6$ ohm-m
 $R_{IID} = 2.4$ ohm-m
 $R_{IIM} = 2.4$ ohm-m
 giving $R_{IID}/R_{IDP} = 2.4/1.6 = 1.5$
 $R_{IIM}/R_{IDP} = 2.4/1.6 = 1.5$
 Therefore, $d_i = 50$ in.
 $R_{xo}/R_t = 15$
 $R_t/R_{IDP} = 0.94$
 $R_t = 0.94 (1.6) = 1.5$ ohm-m

Phasor* Dual Induction- R_{x0} DeviceID Phasor-IM Phasor- R_{x0} device

Rint-13a

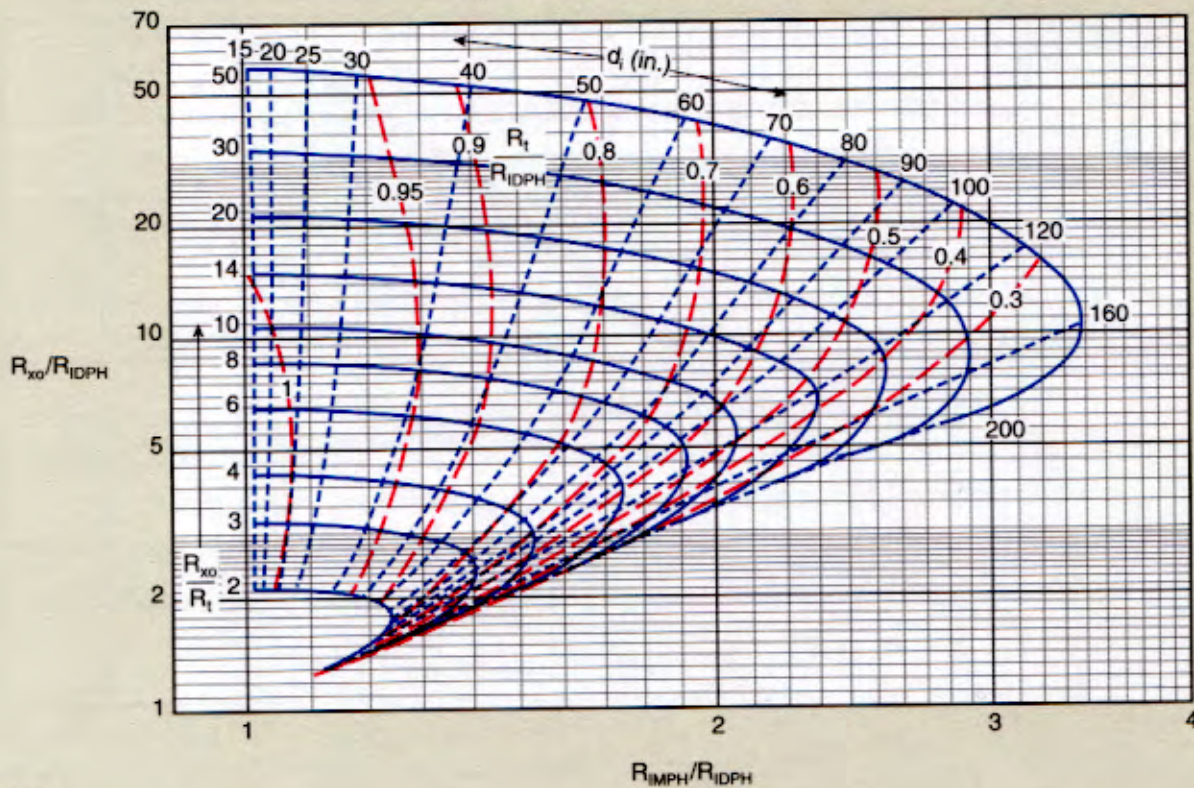


Phasor* Dual Induction- R_{xo} Device

ID Phasor-IM Phasor- R_{xo} device

Rint-13b

Thick beds, 8-in. [203-mm] hole, skin-effect and borehole corrected
 $R_{xo} = 10$, $R_{xo}/R_m = 20$, frequency = 20 kHz



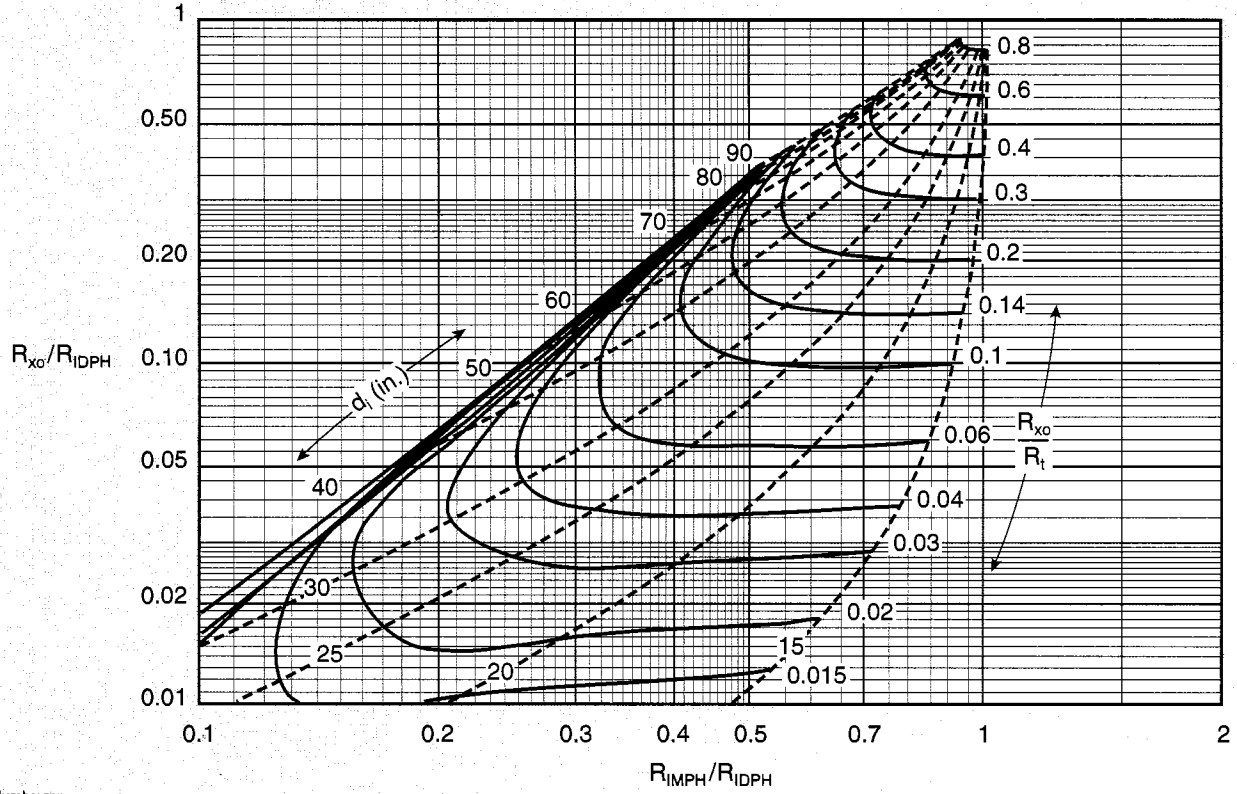
*Mark of Schlumberger
 © Schlumberger

Phasor* Dual Induction- R_{x0} Device

ID Phasor-IM Phasor- R_{x0} device

Rint-13c

Thick beds, 8-in. [203-mm] hole, skin-effect and borehole corrected
 $R_{x0} < R_t$, frequency = 20 kHz



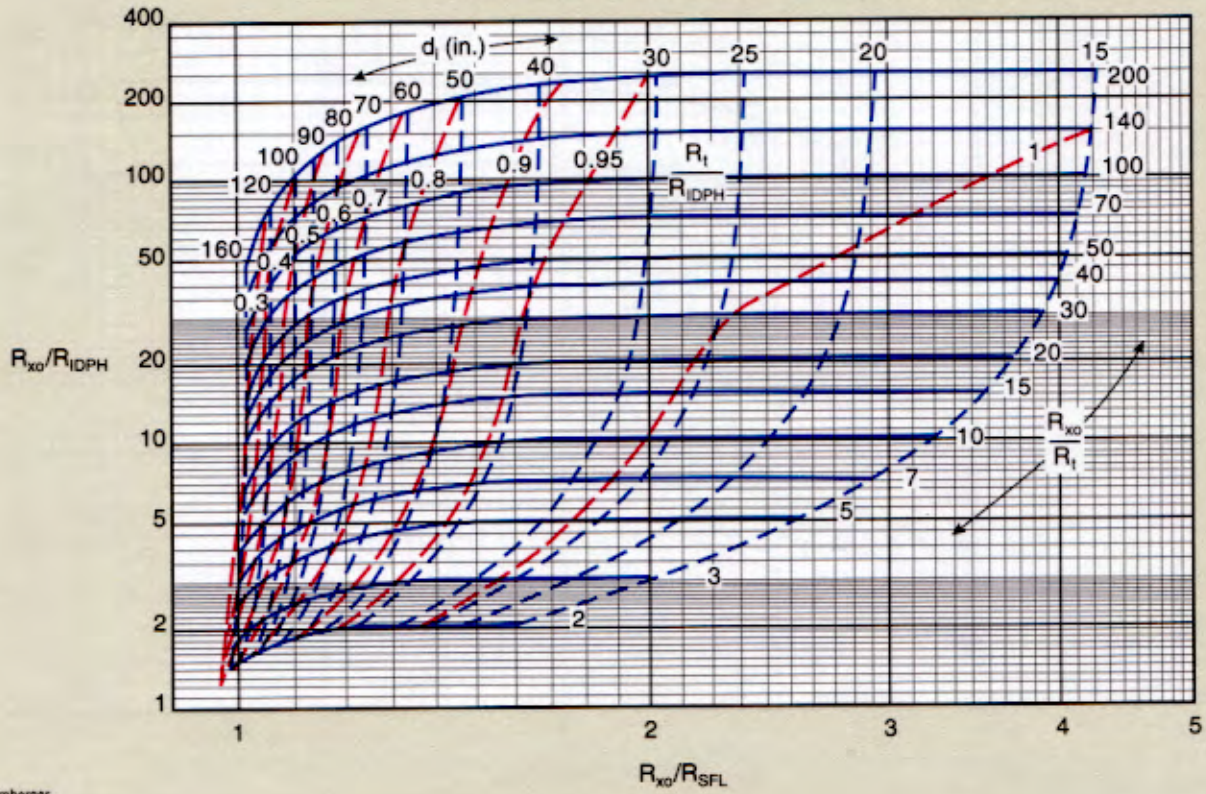
*Mark of Schlumberger
 © Schlumberger

Phasor* Dual Induction-SFL*- R_{x0} Device

ID Phasor-SFL- R_{x0} device

Rint-15a

$R_{x0} = 50$, $R_{x0}/R_m = 100$, frequency = 20 kHz



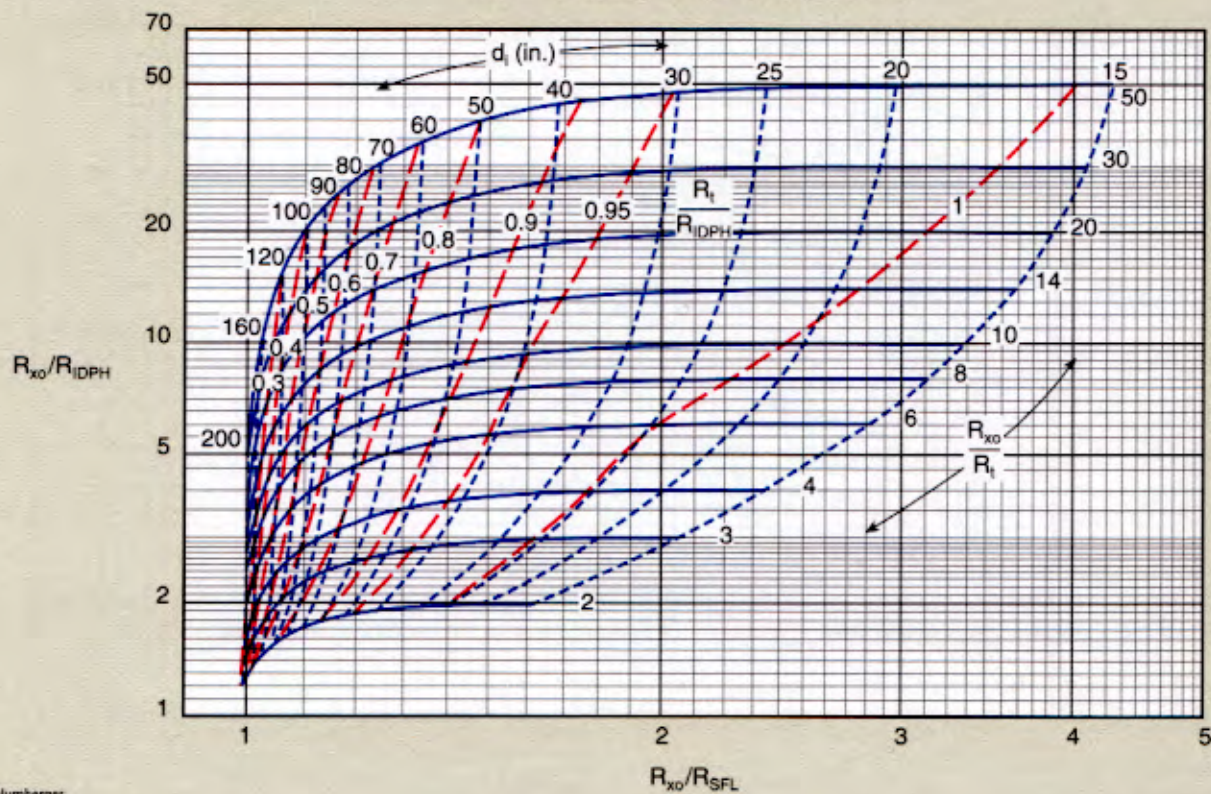
*Mark of Schlumberger
© Schlumberger

Phasor* Dual Induction-SFL*-R_{x0} Device

ID Phasor-SFL-R_{x0} device

Rint-15b

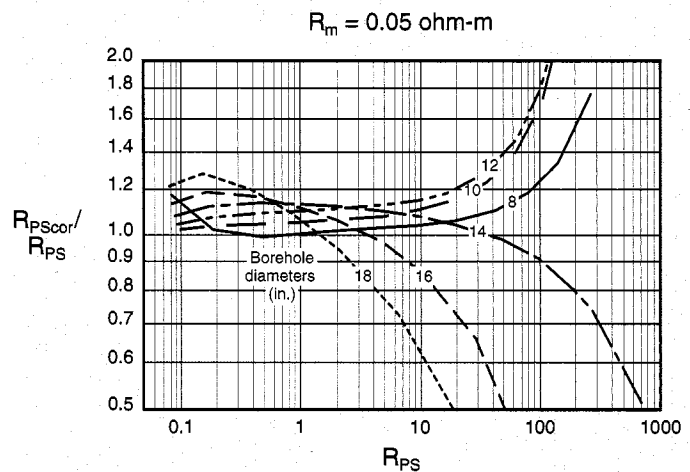
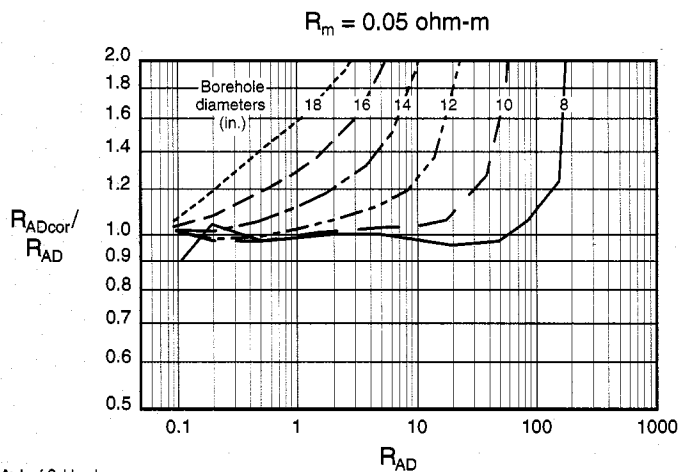
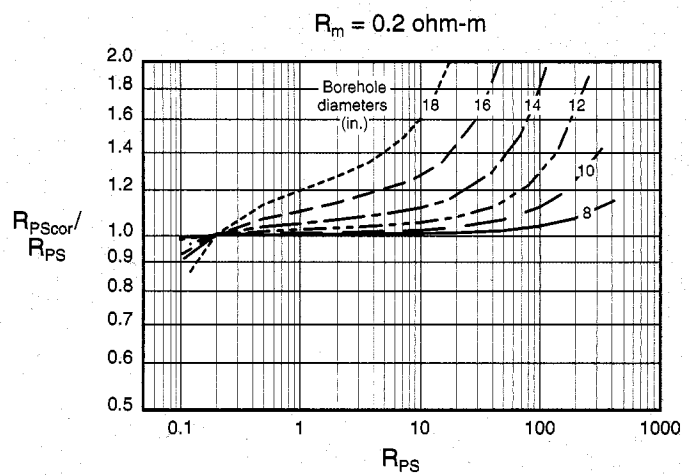
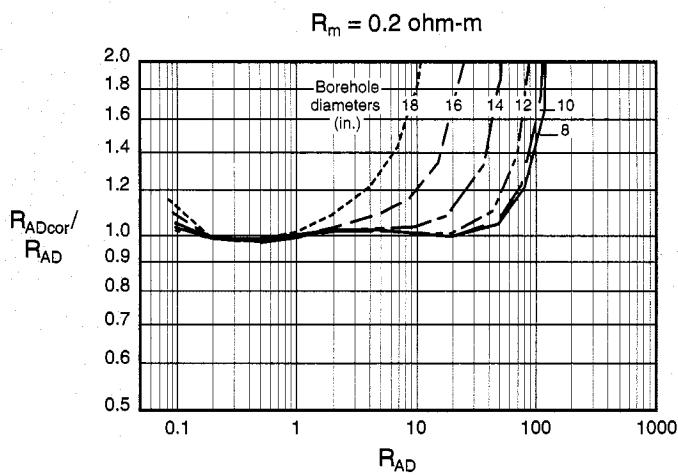
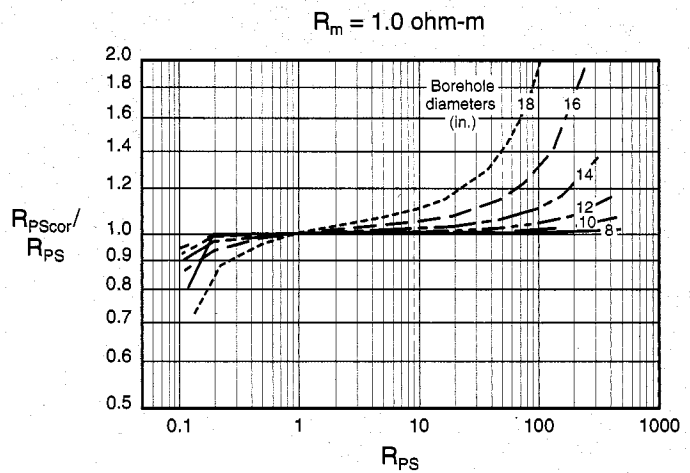
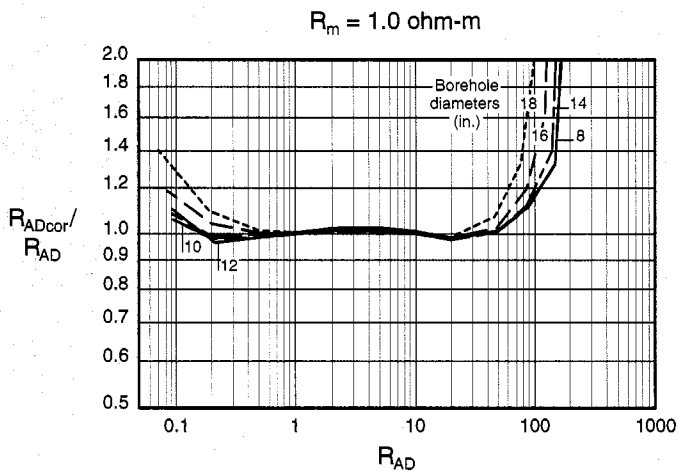
$R_{x0} = 10, R_{x0}/R_m = 20, \text{frequency} = 20 \text{ kHz}$



*Mark of Schlumberger
© Schlumberger

CDR* Compensated Dual Resistivity Borehole Correction for 6.5-in. Tool

Rcor-11a



*Mark of Schlumberger
© Schlumberger

Rcor

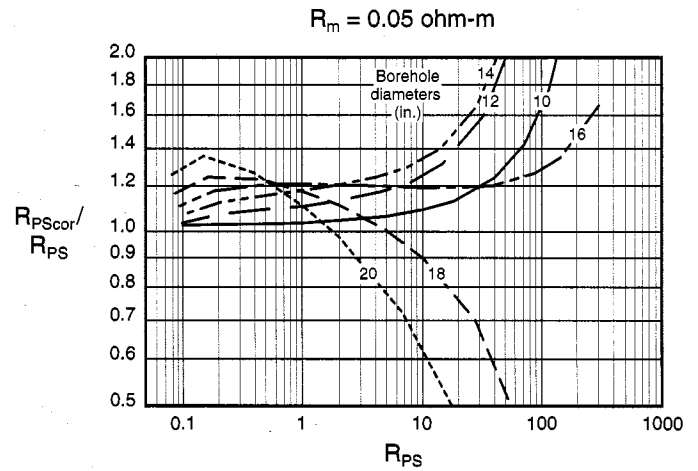
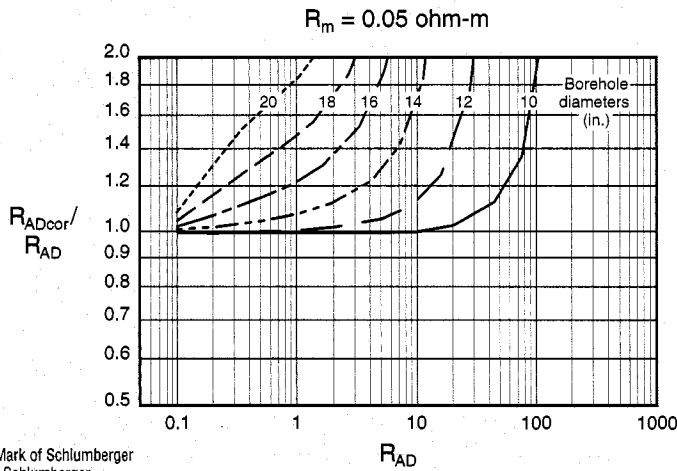
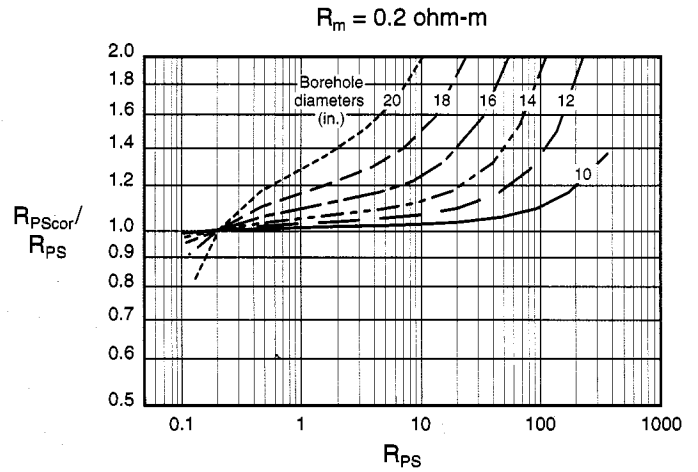
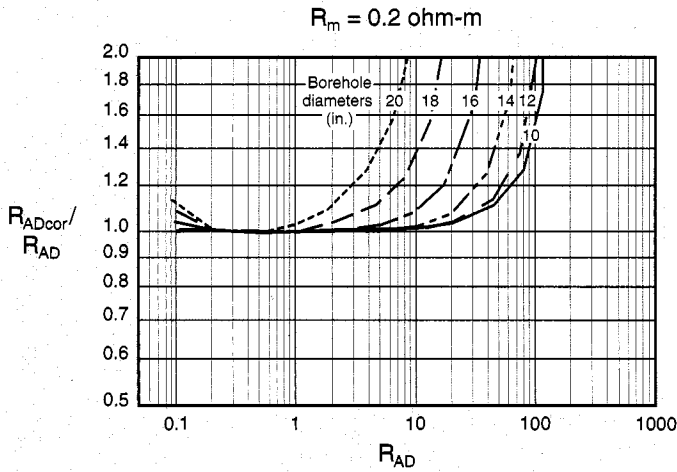
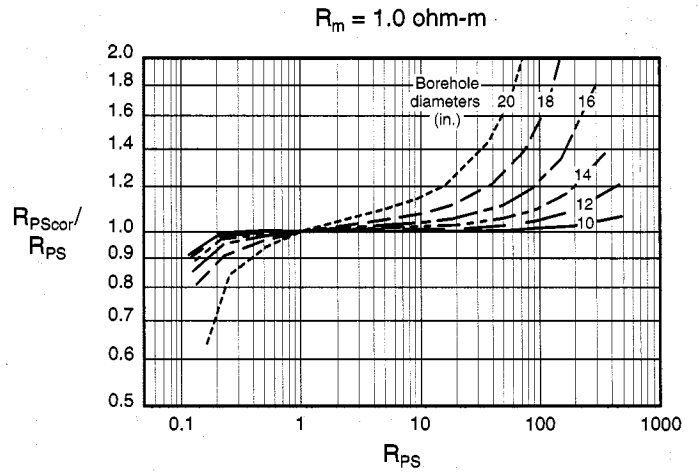
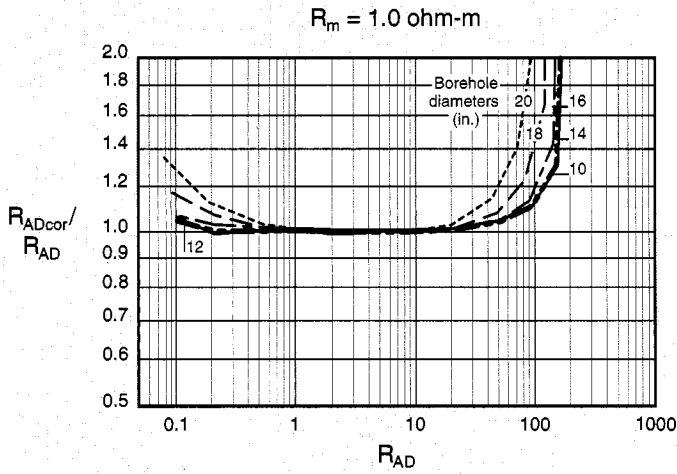
The CDR Compensated Dual Resistivity tool, a logging-while-drilling (LWD) electromagnetic propagation tool, provides measurements with similarities to the medium (IM) and deep (ID) wireline induction logs. The phase shift and attenuation of

2-MHz electromagnetic waves are independently transformed into two apparent resistivities—providing two depths of investigation.

Continued on next page

CDR* Compensated Dual Resistivity Borehole Correction for 8-in. Tool

Rcor-11b



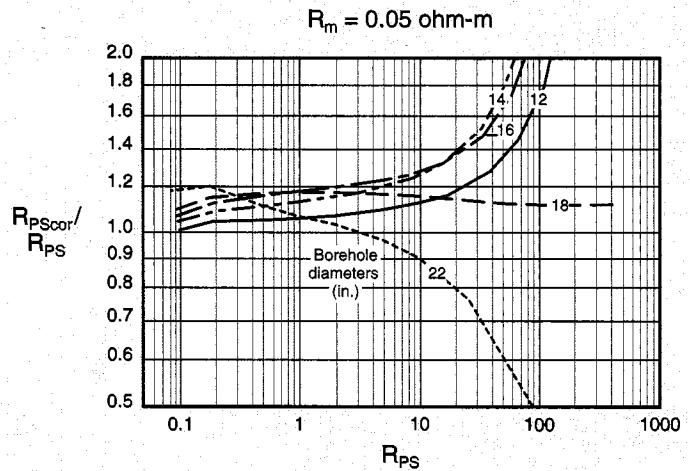
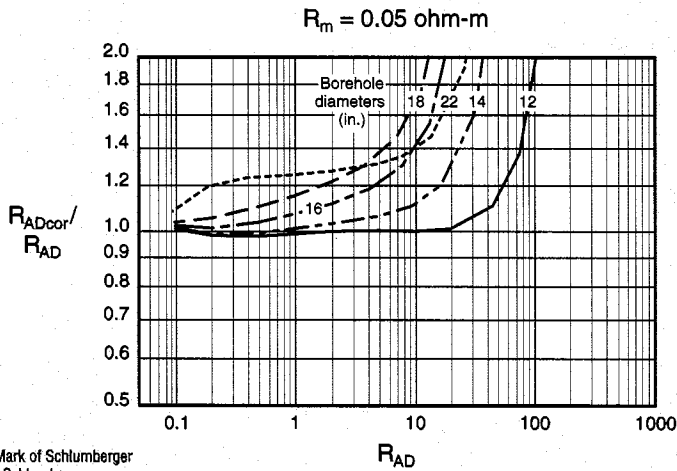
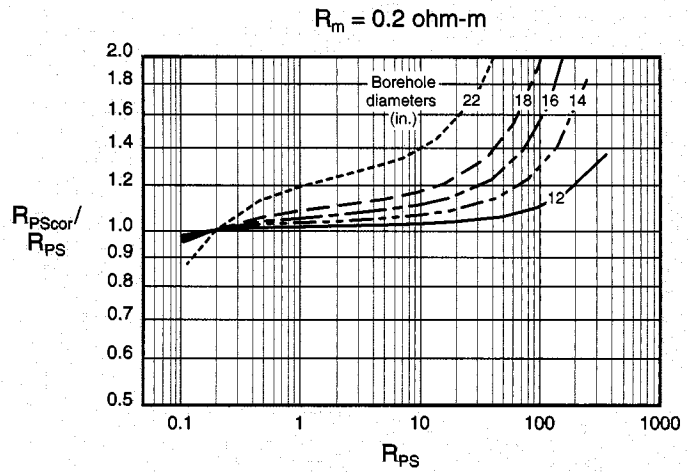
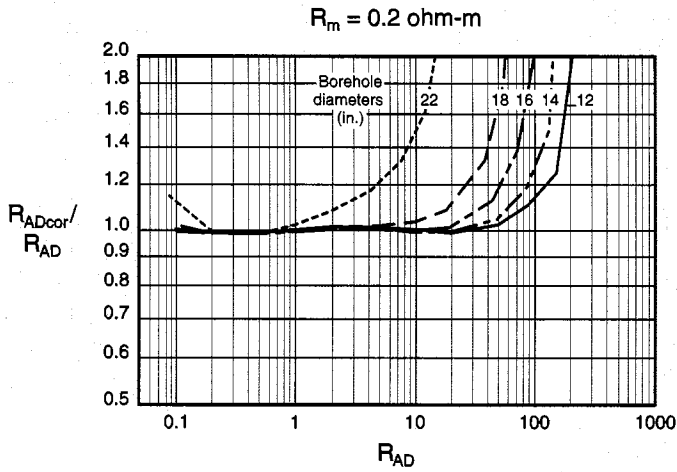
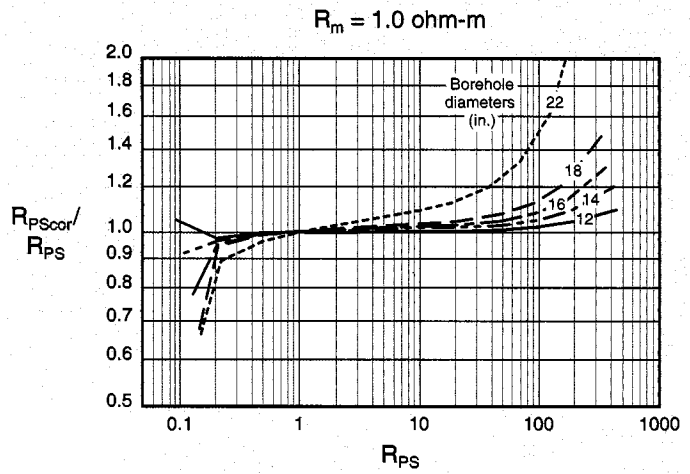
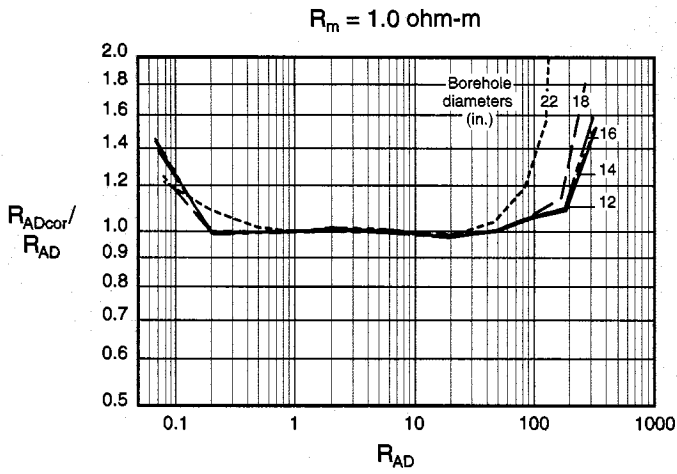
*Mark of Schlumberger
© Schlumberger

R_{PS} is the apparent resistivity from the phase shift-shallow, and R_{AD} is the apparent resistivity from the attenuation-deep. Charts Rcor-11a, -11b and -11c provide borehole corrections for the 6.5-, 8- and 9.5-in. CDR tools run in mud resistivities

of 0.05, 0.2 and 1 ohm-m. To use, select the chart appropriate for the tool size, the measurement (R_{PS} or R_{AD}) and the proper mud resistivity. Enter the chart in abscissa with the apparent resistivity. Proceed upward to the proper hole diameter curve and read the correct/apparent resistivity value on the ordinate.

CDR* Compensated Dual Resistivity Borehole Correction for 9.5-in. Tool

Rcor-11c

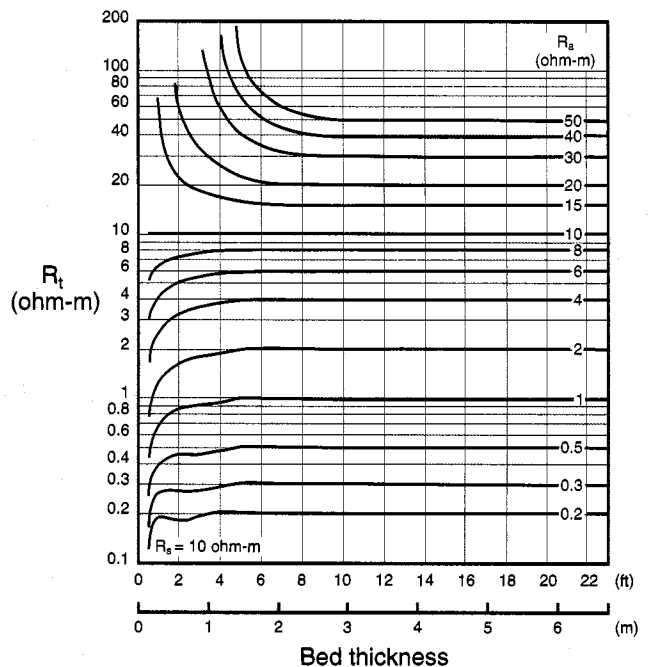
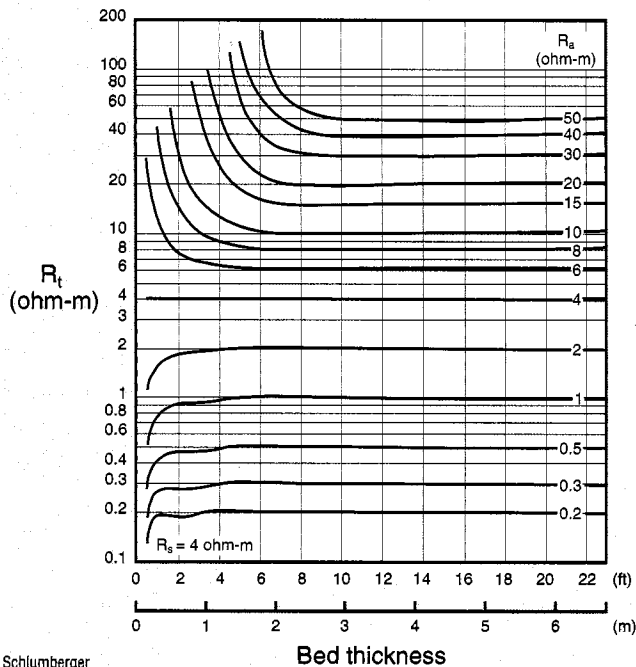
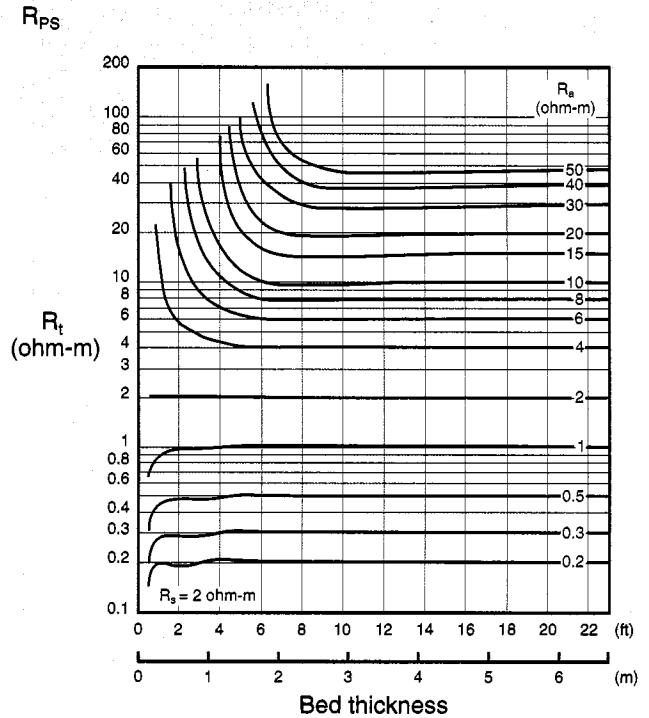
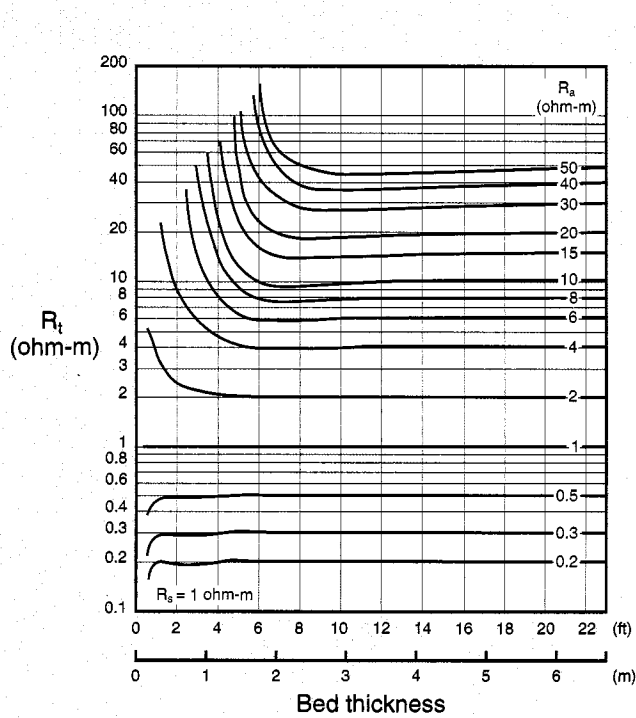


Rcor

*Mark of Schlumberger
© Schlumberger

CDR* Bed-Thickness Correction

Rcor-12



Rcor

*Mark of Schlumberger
© Schlumberger

Charts Rcor-12 and Rcor-13 correct the CDR tool resistivities for bed thickness. To use, select the chart appropriate for the measurement (R_{PS} or R_{AD}) and for the adjacent bed resistivity (R_s). Enter the chart with the bed thickness, which can be determined from the distance between the crossovers of R_{PS} and R_{AD} .

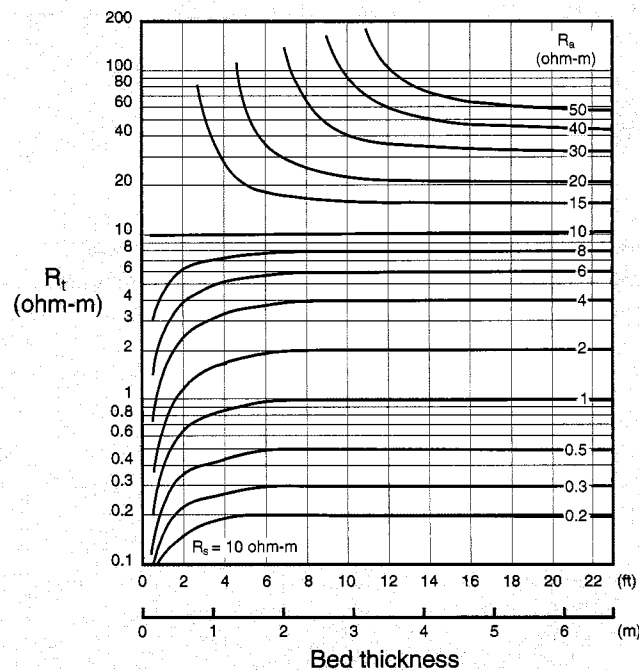
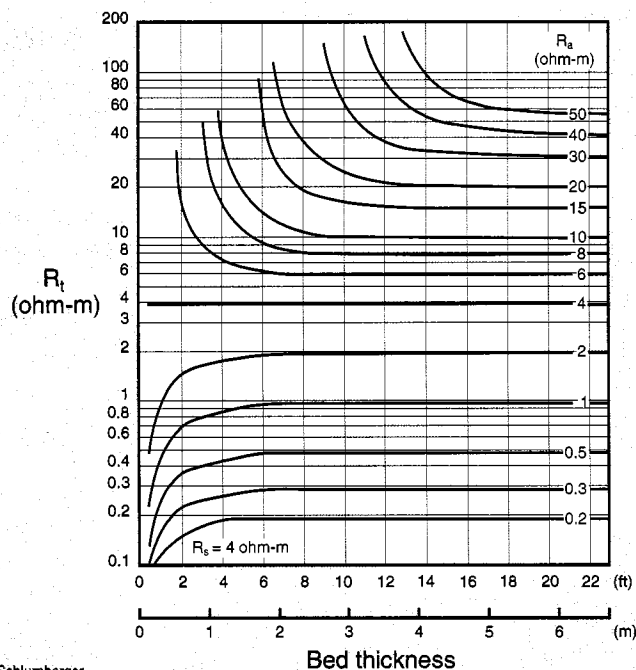
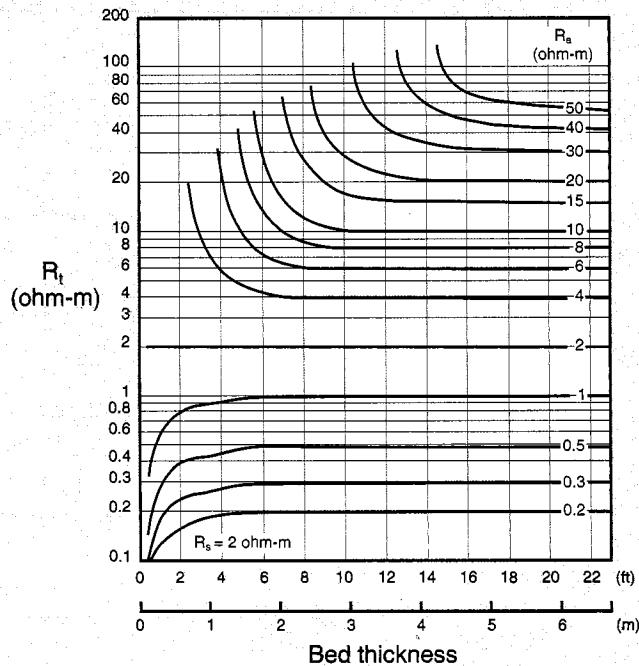
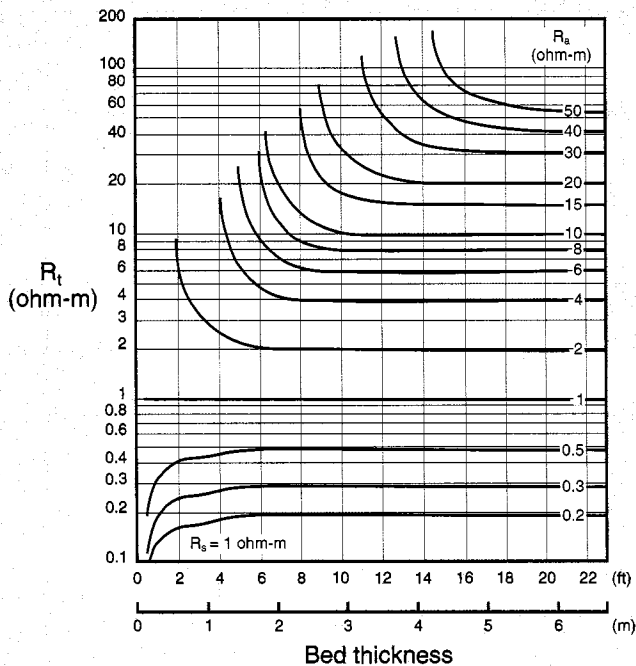
Proceed upward to the R_a curve corresponding to the center bed resistivity value. Read the corrected resistivity value (R_t) on the ordinate.

For more information see Reference 37.

CDR* Bed-Thickness Correction

Rcor-13

R_{AD}

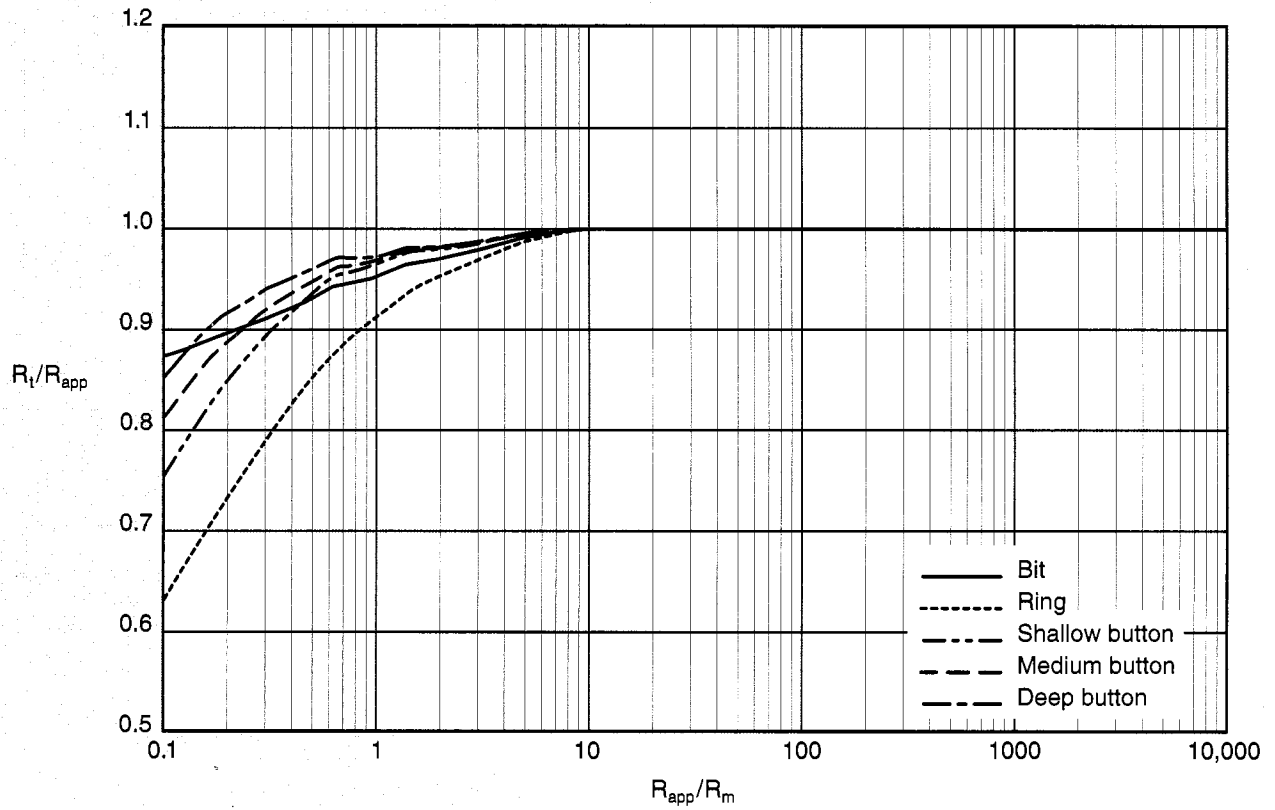


Rcor

*Mark of Schlumberger
© Schlumberger

RAB* Resistivity-at-the-Bit Borehole Correction
 for 6.75-in. Tool
 8.5-in. borehole

Rcor-15



*Mark of Schlumberger
 © Schlumberger

Rcor

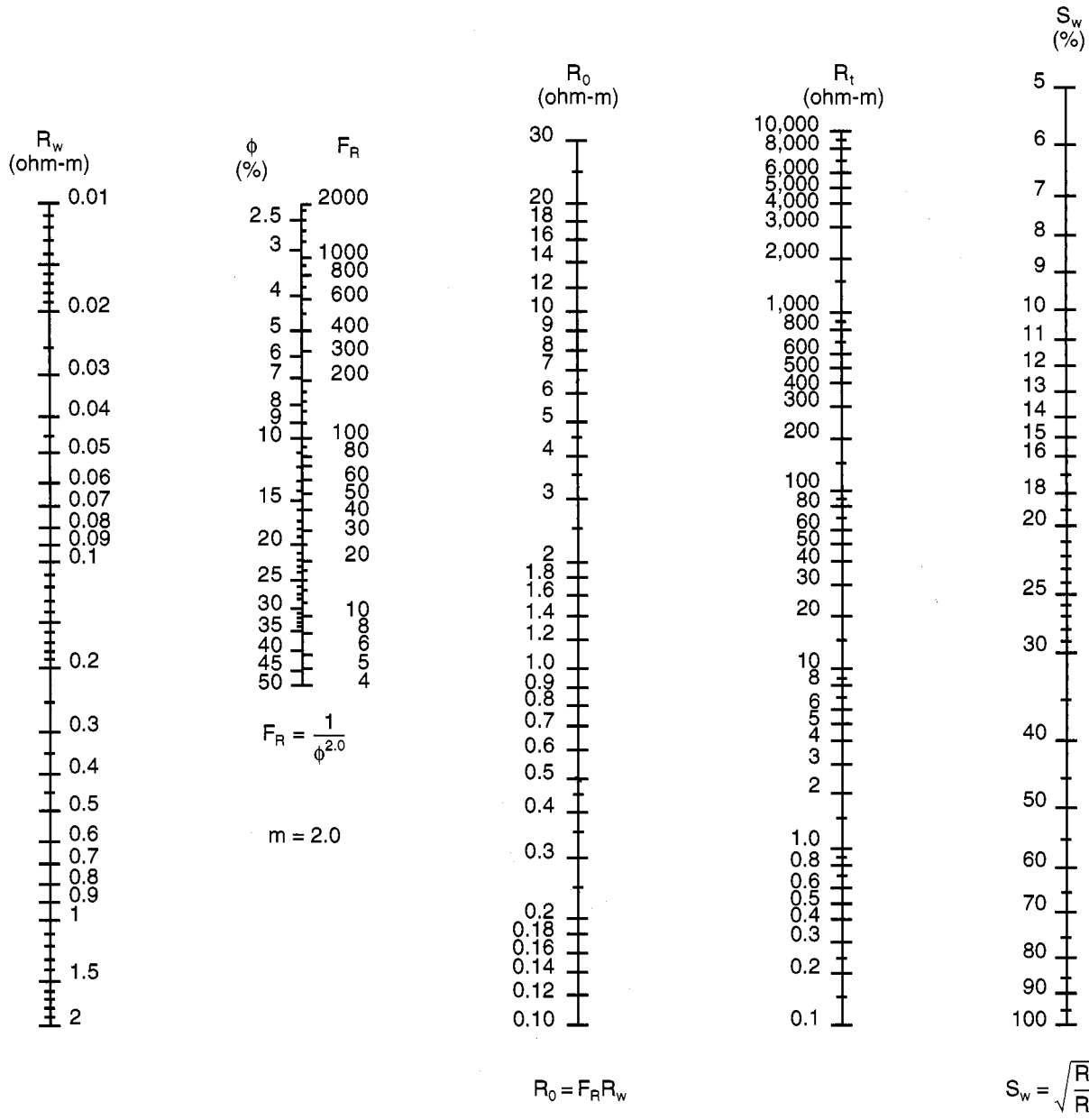
Chart Rcor-15 demonstrates the relative size of the borehole corrections for RAB measurements as a function of mud resistivity. This chart is for illustration purposes only. Borehole corrections

are dependant upon the bottomhole assembly and are normally applied in the software. This example was generated for a RAB tool running behind a 12-in. bit.

Saturation Determination

Sw-1

Clean formations, m = 2



Sw

© Schlumberger

This nomograph solves the Archie water saturation equation

$$S_w = \sqrt{\frac{R_0}{R_t}} = \sqrt{\frac{F_R R_w}{R_t}}$$

It should be used in clean (nonshaly) formations only. If R_0 (resistivity when 100% water saturated) is known, a straight line from the known R_0 value through the measured R_t value gives water saturation, S_w . If R_0 is unknown, it may be determined by

connecting the formation water resistivity, R_w , with the formation resistivity factor, F_R , or porosity, ϕ .

Example: $R_w = 0.05$ ohm-m at formation temperature
 $\phi = 20\%$ ($F_R = 25$)
 $R_t = 10$ ohm-m

Therefore, $S_w = 35\%$

For other ϕ/F relations, the porosity scale should be changed according to Chart Por-1.

Saturation Determination

Ratio method

Chart Sw-2 (next page) is used to determine water saturation in shaly or clean formations when knowledge of porosity is unavailable. It may also be used to verify the water saturation determination from another interpretation method. The main chart assumes

$$S_{xo} = \sqrt[5]{S_w}$$

however, the small chart to the right provides an S_{xo} correction when S_{xo} is known. Note, too, that the SP portion of the chart does not provide for any water activity (Chart SP-2) correction.

For clean sands, plot the ratio R_{xo}/R_t against R_{mf}/R_w to find water saturation at average residual oil saturation. If R_{mf}/R_w is unknown, the chart may be entered with the SP value and the formation temperature. If S_{xo} is known, proceed diagonally upward, parallel to the constant S_{wa} lines, to the edge of the chart. Then, go horizontally to the known S_{xo} (or S_{or}) value to obtain the corrected water saturation S_w .

Example: $R_{xo} = 12$ ohm-m

$$R_t = 2 \text{ ohm-m}$$

$$R_{mf}/R_w = 20$$

$$S_{or} = 20\%$$

Therefore, $S_w = 43\%$ (after ROS correction)

In shaly sands, plot R_{xo}/R_t against E_{pSP} (the SP in the shaly sand). This point gives an apparent water saturation. Draw a line from the chart's origin (the small circle located at $R_{xo}/R_t = R_{mf}/R_w = 1$) through this point. Extend this line to intersect with the value of E_{SSP} to obtain a value of R_{xo}/R_t corrected for shaliness. Plot this value of R_{xo}/R_t versus R_{mf}/R_w to find S_w . If R_{mf}/R_w is unknown, the point defined by R_{xo}/R_t and E_{SSP} is a reasonable approximation of S_w . Use the diagram at right to further refine S_w if S_{or} is known.

Example: $R_{xo}/R_t = 2.8$

$$R_{mf}/R_w = 25$$

$$E_{pSP} = -75 \text{ mV}$$

$$E_{SSP} = -120 \text{ mV}$$

$$K = 80 \text{ (formation temperature} = 150^\circ\text{F)}$$

Therefore, $S_w = 38\%$

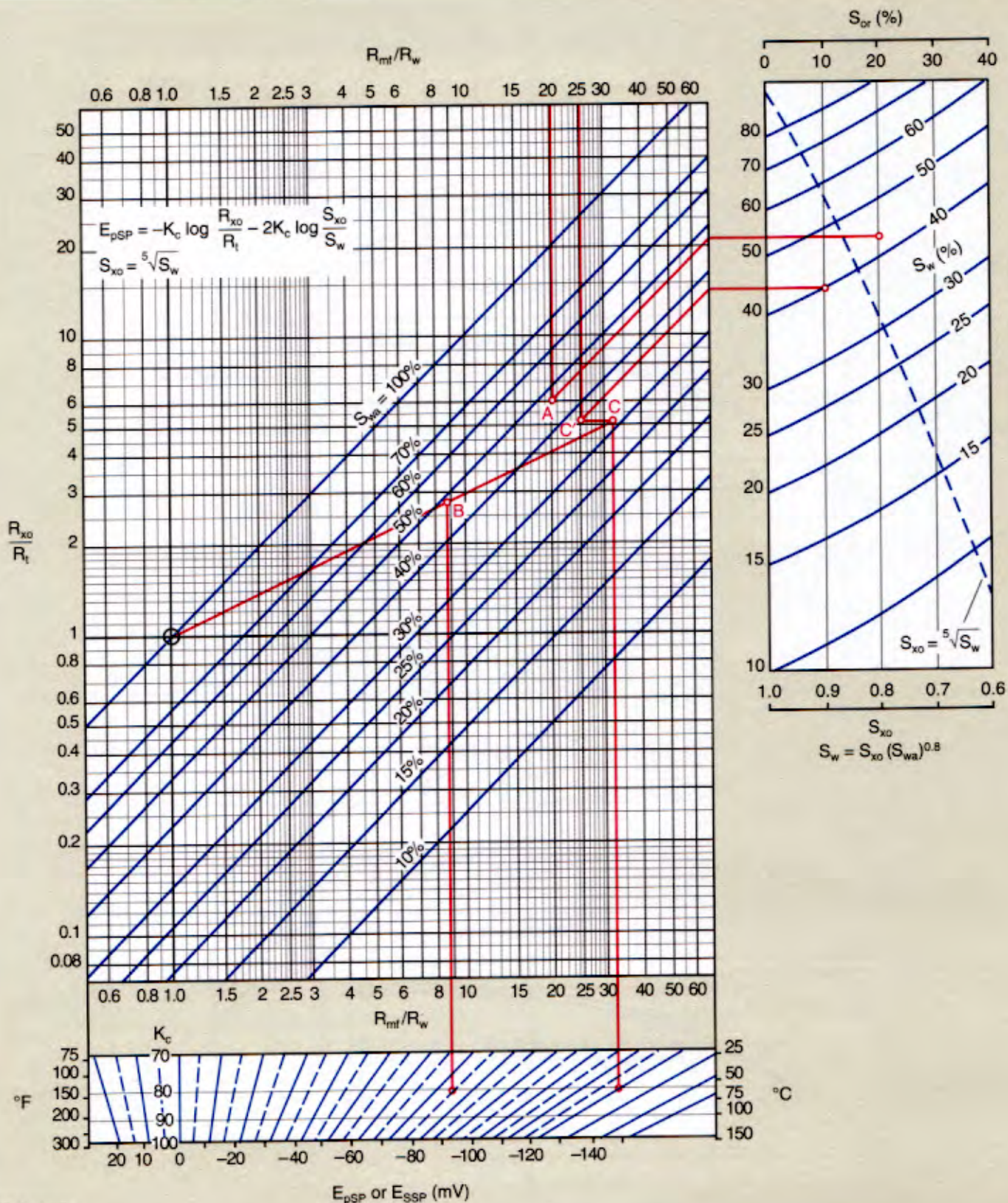
(If S_{or} were known to be 10%, $S_w = 40\%$)

For more information see Reference 12.

Saturation Determination

Ratio method

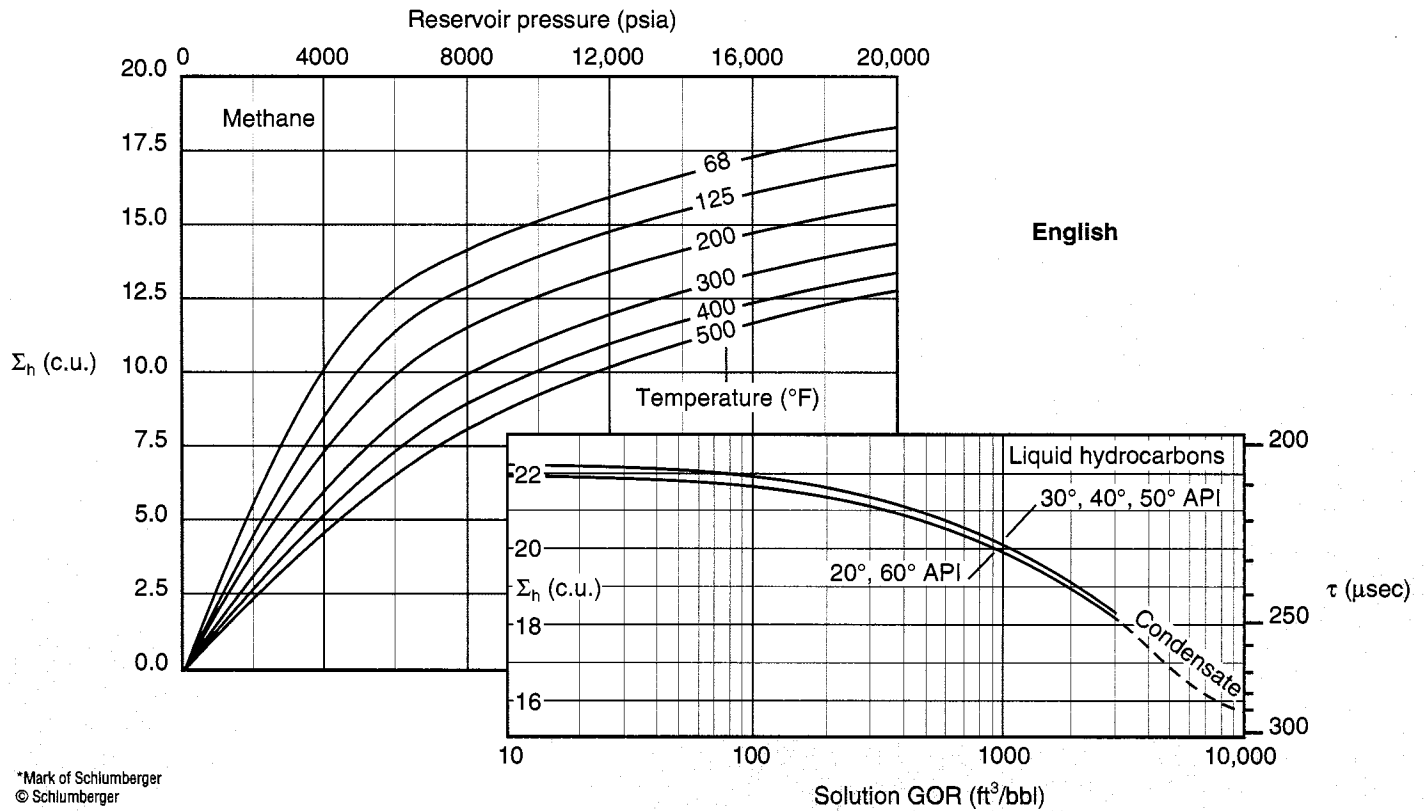
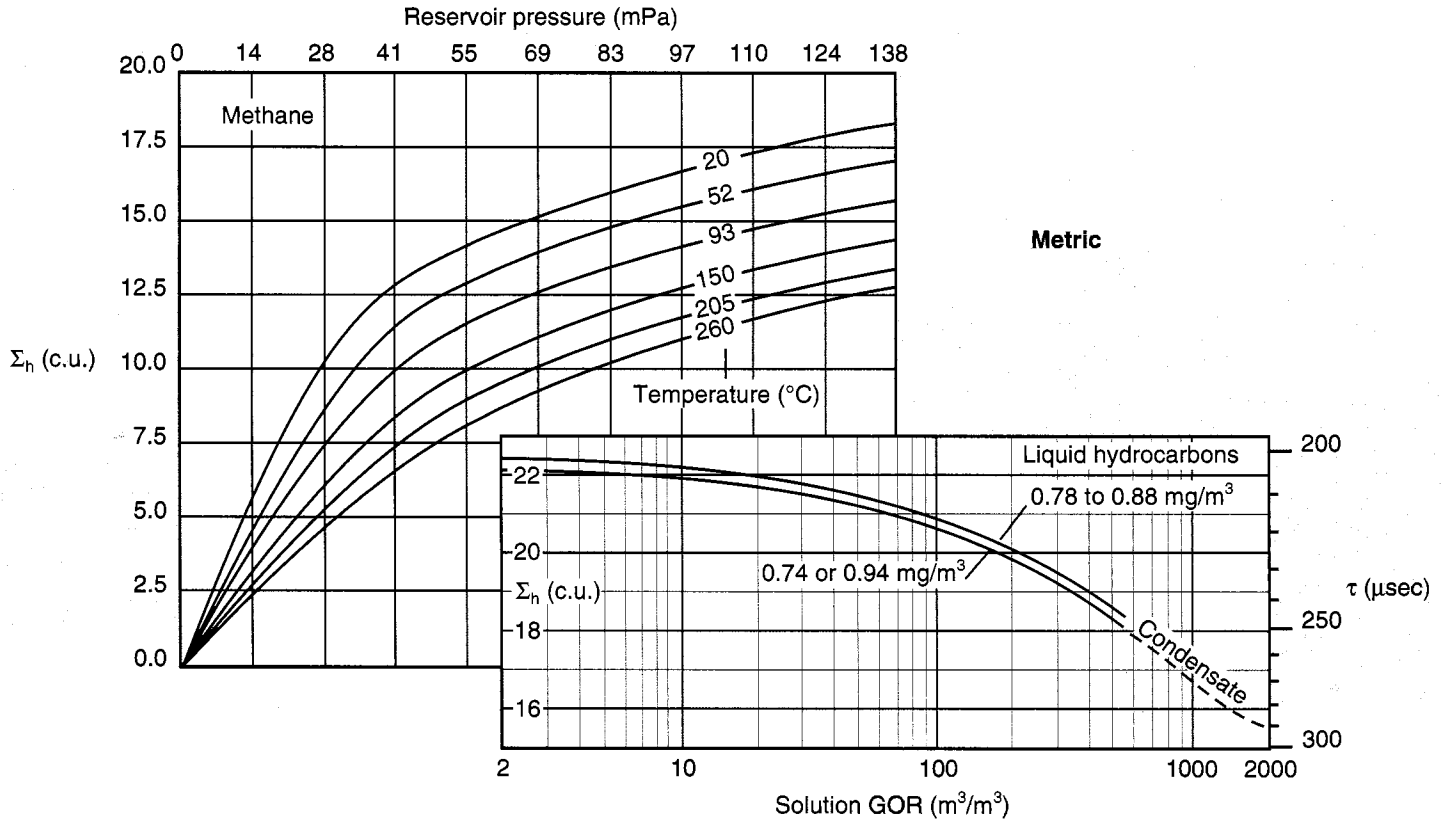
Sw-2



See instructions on previous page. For more information see Reference 12.

TDT* Thermal Decay Time Log
Hydrocarbon Corrections

Tcor-1



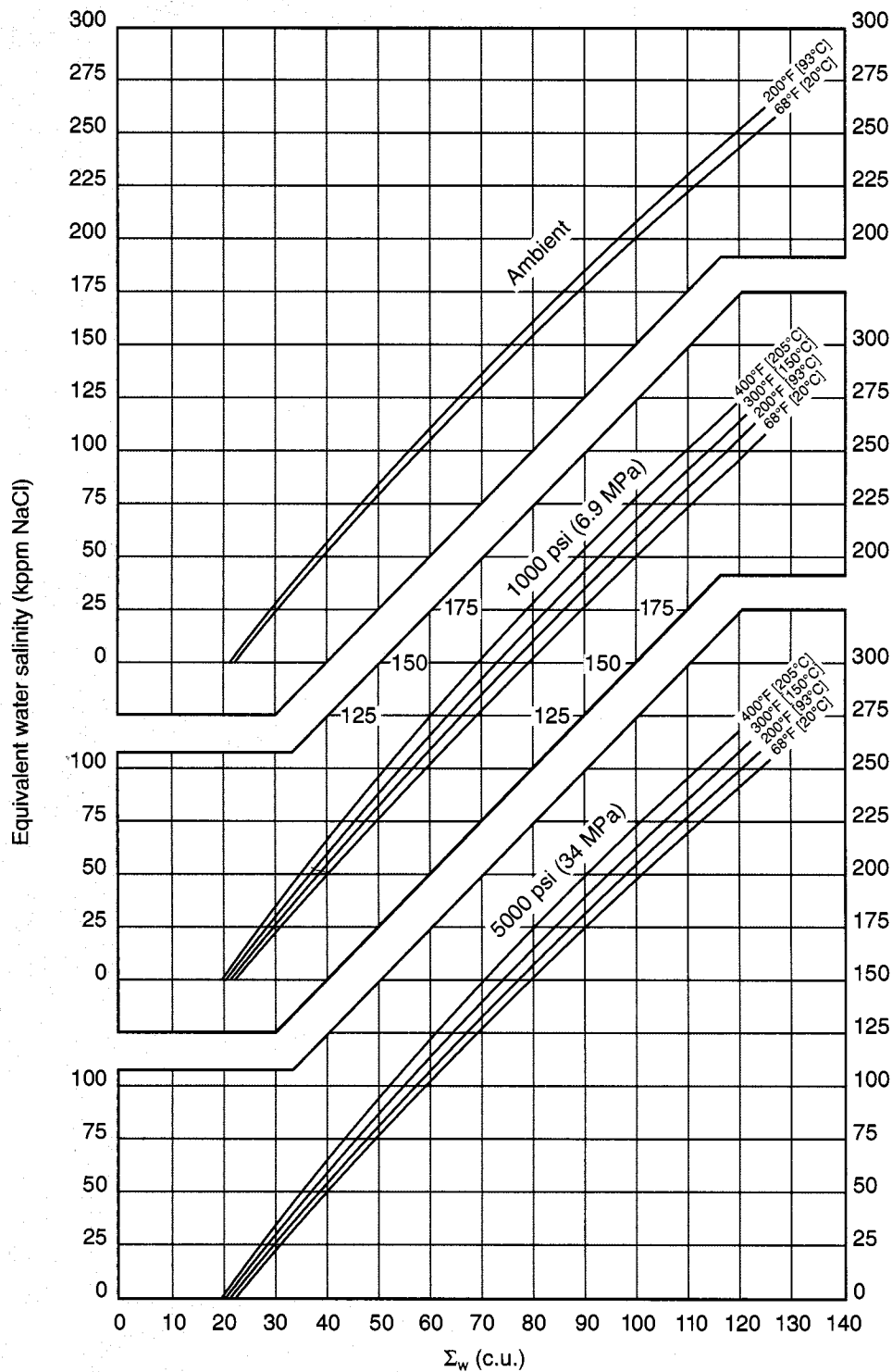
*Mark of Schlumberger
© Schlumberger

For more information see References 10 and 11.

TDT* Thermal Decay Time Log

Equivalent water salinity

Tcor-2a



Tcor

*Mark of Schlumberger
© Schlumberger

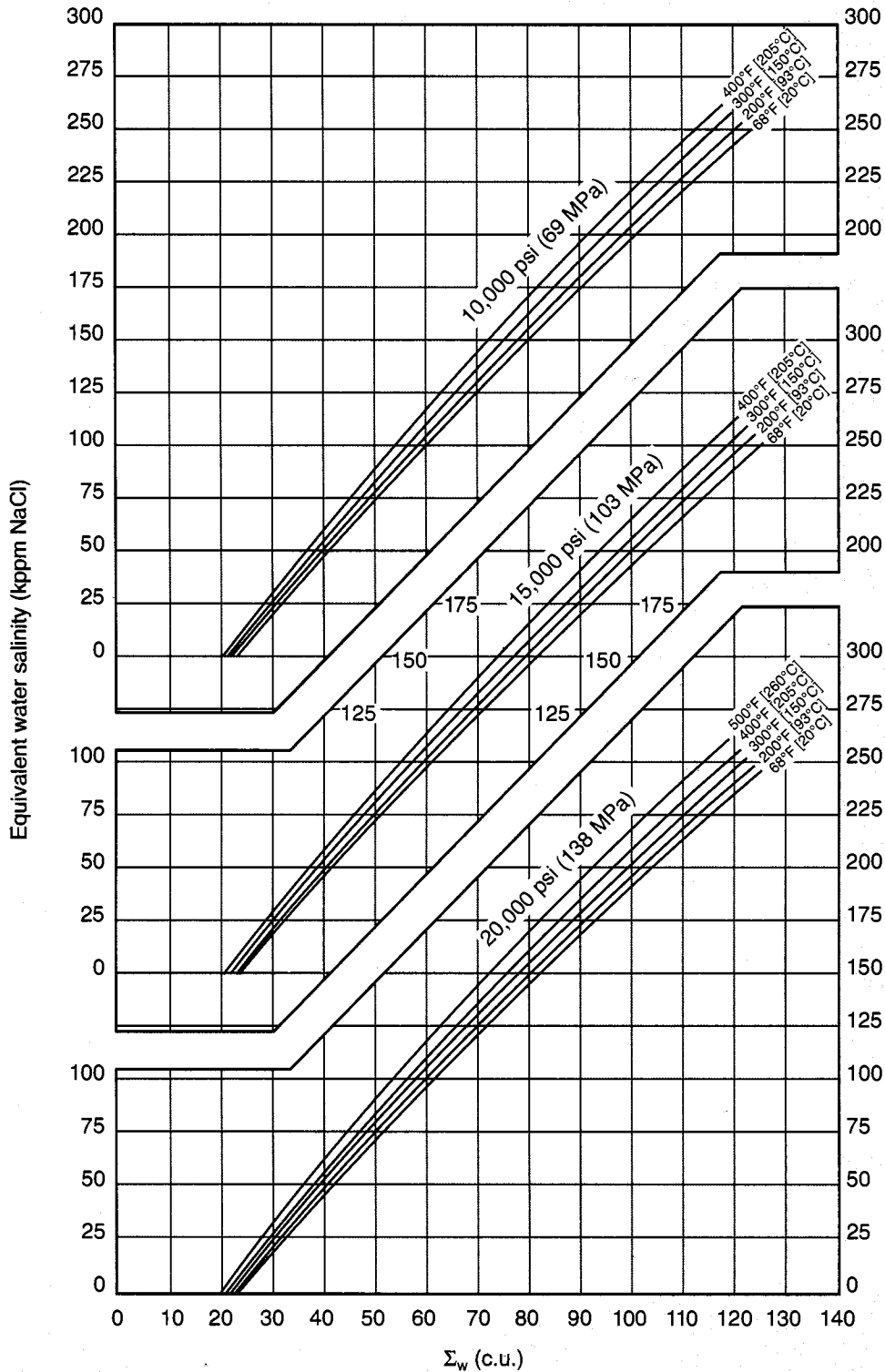
Chart Tcor-1 provides the capture cross section, Σ , for oil and methane, while Charts Tcor-2a and Tcor-2b give the Σ value for water salinity. These updated charts have an extended utility

range to 500°F and 20,000 psia. Knowledge of water salinity, reservoir pressure, GOR and reservoir temperature is required.

TDT* Thermal Decay Time Log

Equivalent water salinity

Tcor-2b



*Mark of Schlumberger
© Schlumberger

Example:

Given: A reservoir section at 90°C temperature and 25-MPa pressure contains water of 175,000-ppm (NaCl) salinity, 30° API oil with a gas/oil ratio of 2000 ft³/bbl and methane gas.

Results: $\Sigma_w = 87$ c.u.
 $\Sigma_o = 19$ c.u.
 $\Sigma_g = 6.9$ c.u.

Tcor

Saturation Determination from TDT* Thermal Decay Time Logs

Neutron capture cross section, Σ , is expressed in capture units (c.u.). Σ is related to thermal decay time, τ (in μsec), by the formula $\Sigma = 4550/\tau$. A capture unit is equivalent to one-thousandth of a reciprocal centimeter (cm^{-1}).

Matrix capture cross section, Σ_{ma} , varies over a small range for each lithology. Practical values, empirically determined, are somewhat larger than those calculated for the pure rock minerals. Average values commonly used are sandstone, 8 c.u.; dolomite, 9 c.u.; and limestone, 11 to 12 c.u.

Σ_{w} , the capture cross section of the formation water, depends on the type and abundance of the elements in solution. The value of Σ_{w} corresponding to the NaCl concentration can be considered a minimum value; traces of certain elements in the water can increase Σ_{w} beyond the value indicated by the chemically equivalent concentration of NaCl.

For more information see Reference 11.

Description and use of Chart Sw-12

If Σ_{ma} , Σ_{w} and porosity are known, Chart Sw-12 may be used to determine water saturation. It may be used in shaly formations if porosity, ϕ , and the fraction of shale in the formation, V_{sh} , are known.

Clean formations

Information required:

Σ_{ma}	Matrix capture cross section, based on lithology
ϕ	Porosity
Σ_{w}	From NaCl salinity; see Tcor-2a or Tcor-2b
Σ_{h}	See Tcor-1

Procedure:

Enter the value of Σ_{ma} on Bar **B**; draw Matrix Line **a** from Σ_{ma} to Pivot Point **B**. Enter Σ_{LOG} on Bar **B**; draw Line **b** through the intersection of Line **a** and the value of ϕ to Σ_{f} on Bar **C**. Draw Line **5** from Σ_{f} through the intersection of Σ_{h} and Σ_{w} to the value of S_{w} .

Example:

Given: $\Sigma_{\text{LOG}} = 20$ c.u.
 $\Sigma_{\text{ma}} = 8$ c.u. (sandstone)
 $\Sigma_{\text{h}} = 21$ c.u. (oil)
 $\Sigma_{\text{w}} = 80$ c.u. (150,000 ppm or mg/kg)
 $\phi = 30$ p.u.

Solution: $S_{\text{w}} = 43\%$

Shaly formations

Information required:

Σ_{ma}	Based on lithology
Σ_{sh}	Read from TDT log in adjacent shale
Σ_{w}	From NaCl salinity; see Tcor-2a or Tcor-2b
Σ_{h}	See Tcor-1
V_{sh}	From porosity-log crossplot or gamma ray
ϕ_{sh}	Read from porosity log in adjacent shale
ϕ	From porosity log, corrected for shaliness; for neutron and density logs in liquid-filled formations, $\phi = \phi_{\text{LOG}} - V_{\text{sh}} \phi_{\text{sh}}$.

Procedure:

Enter the value of Σ_{ma} on Bar **B**; connect with Pivot Point **A** (Line **1**). From the value of Σ_{sh} on Bar **A**, draw Line **2** through the intersection of Line **1** and V_{sh} to determine Σ_{cor} . Draw Line **3** from Σ_{cor} to the value of Σ_{ma} on the scale at left of Bar **C**. Enter Σ_{LOG} on Bar **B**; draw Line **4** through the intersection of Line **3** and ϕ to Σ_{f} . From Σ_{f} draw Line **5** through Σ_{h} and Σ_{w} to S_{w} .

Example:

Given: $\Sigma_{\text{LOG}} = 25$ c.u.
 $\Sigma_{\text{ma}} = 8$ c.u.
 $\Sigma_{\text{h}} = 21$ c.u.
 $\Sigma_{\text{w}} = 80$ c.u.
 $\Sigma_{\text{sh}} = 45$ c.u.
 $\text{LOG} = 33$ p.u.
 $\phi_{\text{sh}} = 45$ p.u.
 $V_{\text{sh}} = 20\%$
 $\phi = \phi_{\text{LOG}} - V_{\text{sh}} \phi_{\text{sh}}$
 $\phi = 24$ p.u.

Solution: $S_{\text{w}} = 43\%$

*Mark of Schlumberger

Graphical Determination of Total Water Saturation (S_{wt}) from TDT* Thermal Decay Time Data

Grid Sw-17 can be used for graphical interpretation of the TDT Thermal Decay Time log. In one technique, applicable in shaly as well as clean sands, apparent water capture cross section, Σ_{wa} , is plotted versus bound water saturation on a specially constructed grid.

To construct this grid, refer to the chart on this page. Three fluid points must be located: a free water point, a hydrocarbon point and a bound water point. The free (or connate/formation) water point is located on the left edge of the grid and can be obtained from measurement of a formation water sample, from Chart Tcor-2 if water salinity is known, or from the TDT log in a clean water-bearing sand using the following equation:

$$\Sigma_{wa} = \frac{\Sigma_{log} - \Sigma_{ma}}{\phi} + \Sigma_{ma} \quad (1)$$

The hydrocarbon point is also located on the left edge of the grid. It can be determined from Chart Tcor-1 based upon the known or expected hydrocarbon type.

The bound water point, Σ_{wb} , can be obtained from the TDT log in shale intervals using Eq. 1 above. It is located on the right edge of the grid.

The distance between the free water and hydrocarbon points is linearly divided into constant water saturation lines drawn parallel to a straight line connecting the free water and bound water points. The $S_{wt} = 0\%$ line originates from the hydrocarbon point, and the $S_{wt} = 100\%$ line originates from the free water point.

Apparent water capture cross section, Σ_{wa} , from Eq. 1, is then plotted versus bound water saturation, S_{wb} , to give the total water saturation. Bound water saturation can be estimated from the gamma ray or other bound water saturation estimator.

Knowing the total water saturation and the bound water saturation, the effective water saturation (water saturation of reservoir rock exclusive of shale) can be determined using Chart Sw-14.

Example (see chart on this page):

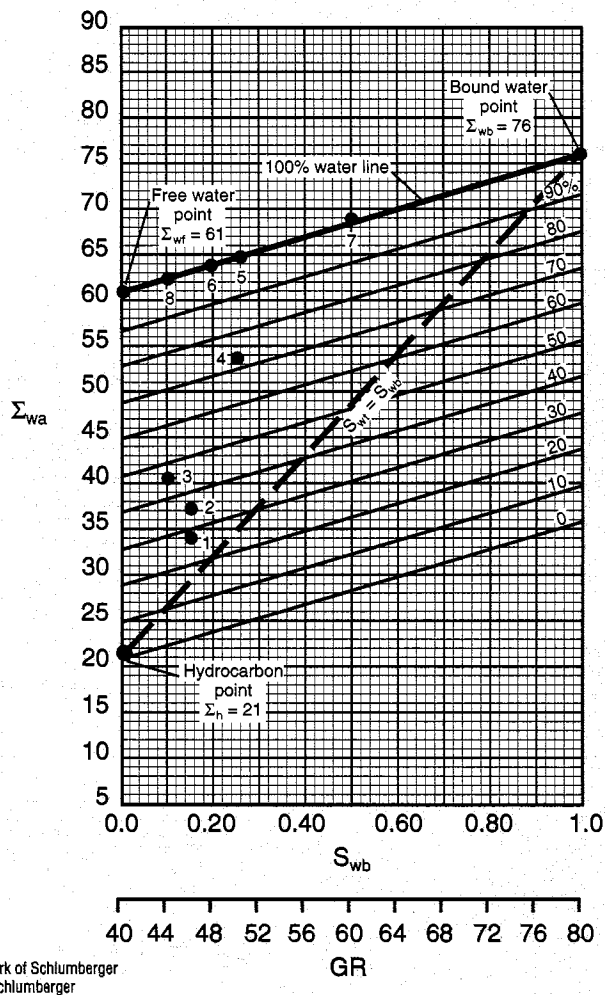
- Free water point = 61 c.u.
(from TDT log in a water-bearing clean sand—
Eq. 1, Chart Tcor-2 or measurement of a water
sample)
- Hydrocarbon point = 21 c.u.
(medium-gravity oil with modest gas/oil ratio—
Chart Tcor-1)
- Bound water point = 76 c.u.
(from TDT log in a shale interval—Eq. 1)

Analysis of Point 4:

- $\Sigma_{wa} = 54$ c.u. (from Eq. 1)
- $S_{wb} = 25\%$ (from gamma ray)

Therefore, $S_{wt} = 72\%$

and $S_w = 63\%$ (from Chart Sw-14)



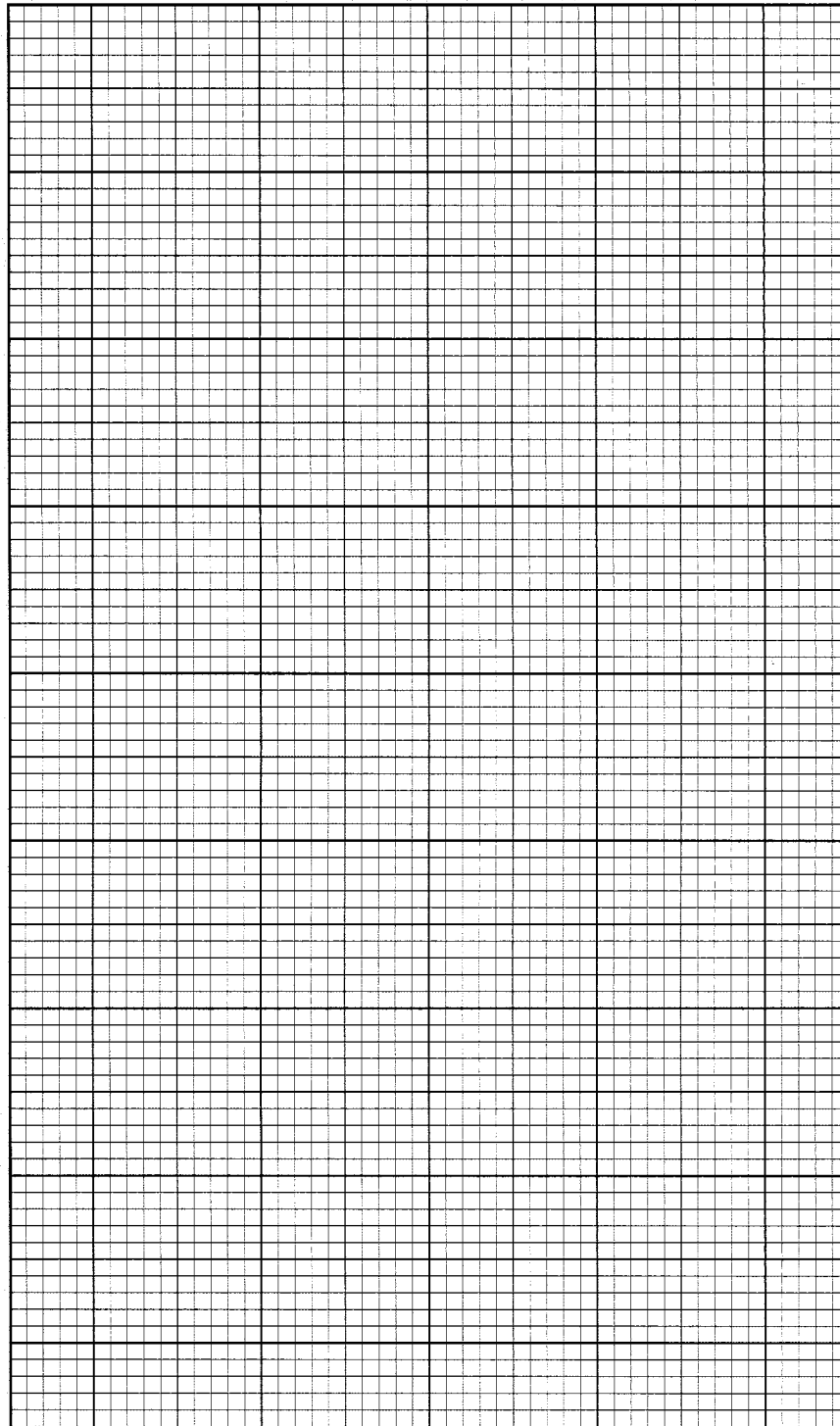
*Mark of Schlumberger
© Schlumberger

The grid can also be used to graphically determine water saturation, S_w , in clean formations by crossplotting Σ_{LOG} in ordinate versus porosity, ϕ , in abscissa. The matrix capture cross section, Σ_{ma} , and the formation water capture cross section, Σ_w , need not be known but must be constant over the interval studied. There must be some points from 100% water zones, and there must be a good variation in porosity. These water points define the $S_w = 100\%$ line; when extrapolated, this line intersects the zero-porosity axis at Σ_{ma} . The $S_w = 0\%$ line is drawn from Σ_{ma} at $\phi = 0$ p.u. to $\Sigma = \Sigma_h$ at $\phi = 100$ p.u. [or $\Sigma = \frac{1}{2}(\Sigma_{ma} + \Sigma_h)$ at $\phi = 50$ p.u.]. The vertical distance from $S_w = 0\%$ to $S_w = 100\%$ is divided linearly to define lines of constant water saturation. The water saturation of any plotted point can thereby be determined.

Graphical Determination of Water Saturation (S_w) or Total Water Saturation (S_{wt}) from TDT* Thermal Decay Time Log

Sw-17

Σ_{LOG}
OR
 Σ_{wa}



ϕ or S_{wb}

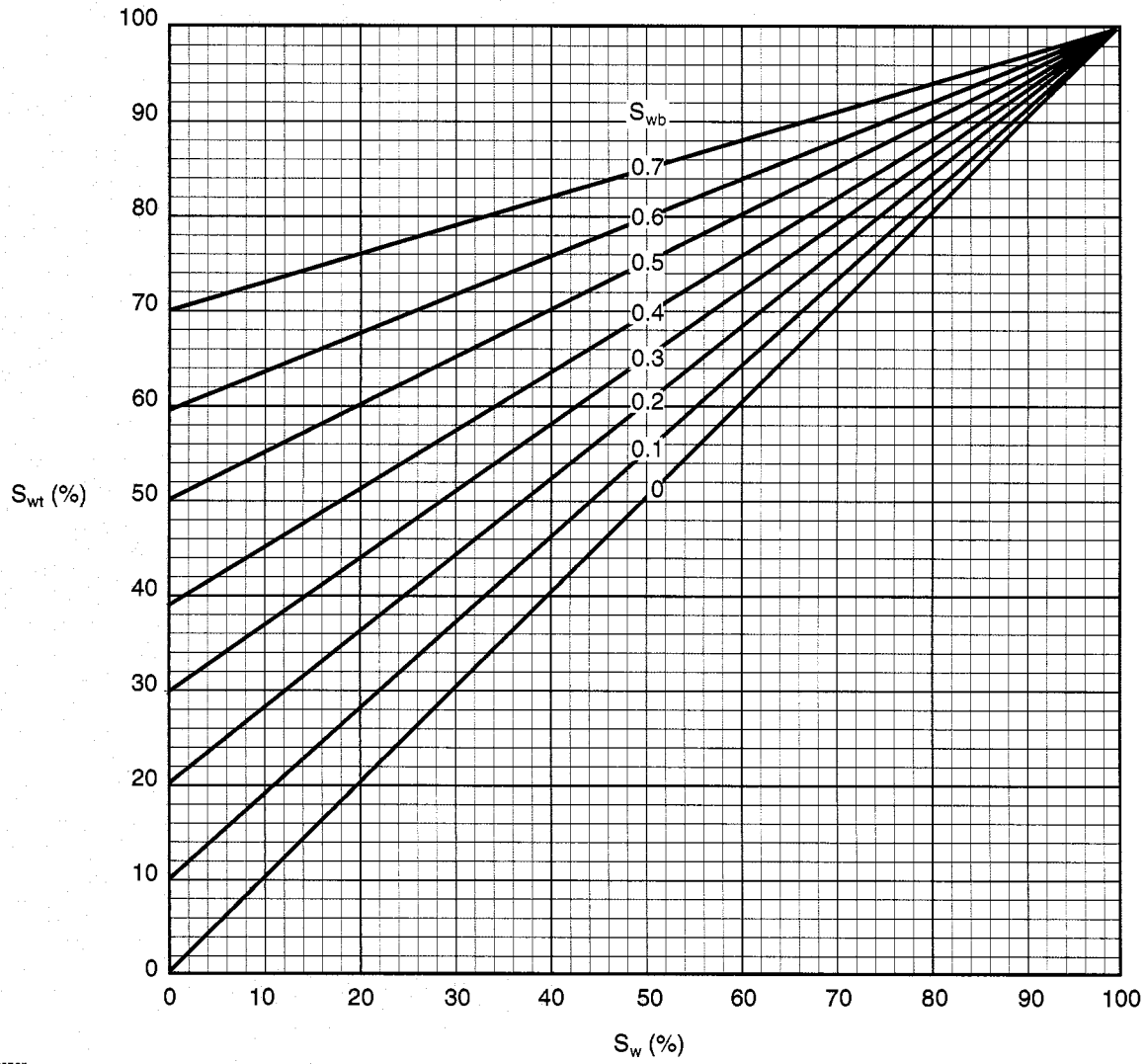
Sw

*Mark of Schlumberger
© Schlumberger

Graphical Determination of S_w from S_{wt} and S_{wb}

SW-14

$$S_w = \frac{S_{wt} - S_{wb}}{1 - S_{wb}}$$

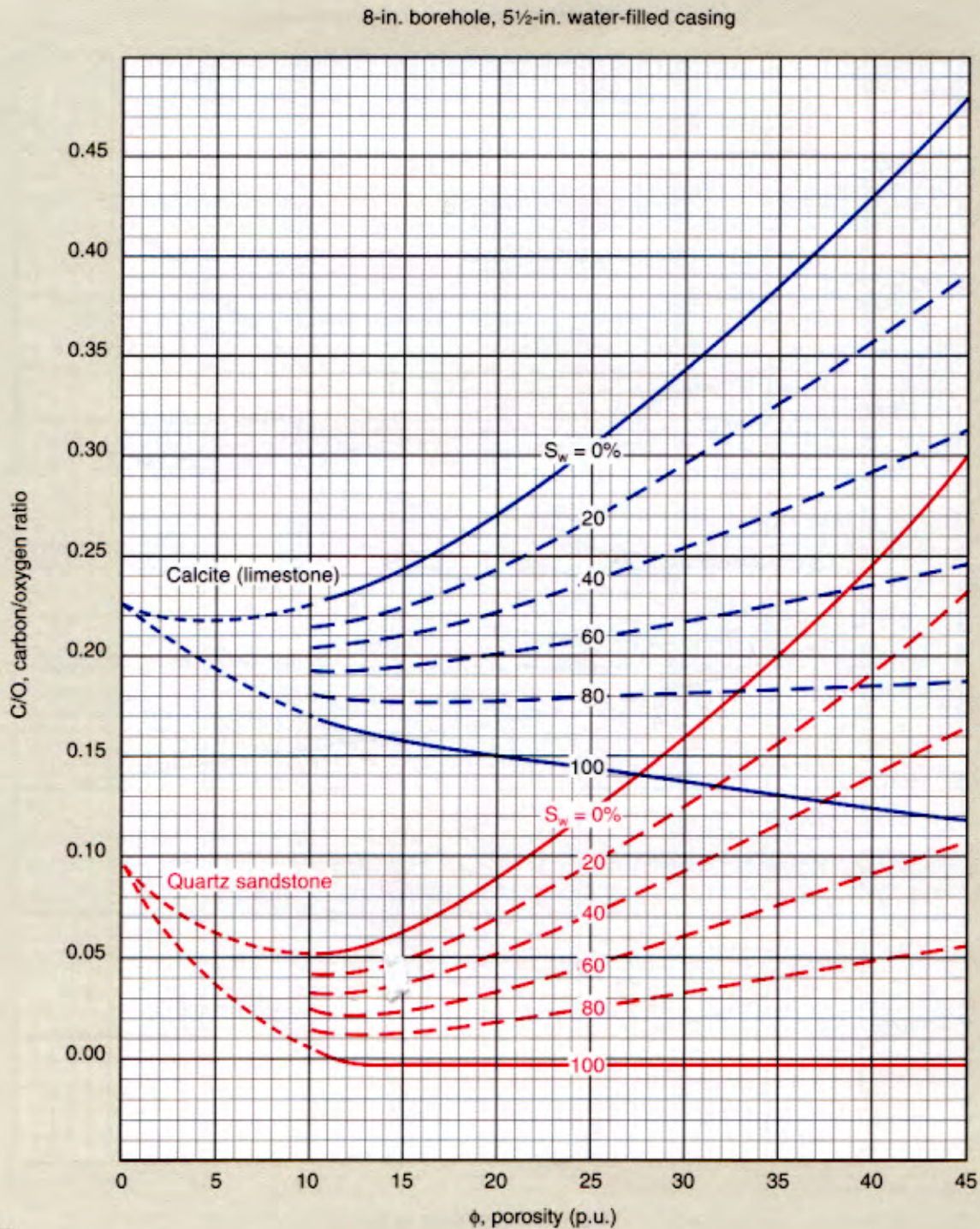


SW

*Mark of Schlumberger
© Schlumberger

Saturation Determination from GST* Induced Gamma Ray Spectrometry Log

GST-1



GST

These charts permit the determination of water saturation from carbon/oxygen (C/O) ratio measurements made with the GST Induced Gamma Ray Spectrometry Tool in inelastic mode operation.

To use, the C/O ratio and the porosity, ϕ , are entered in

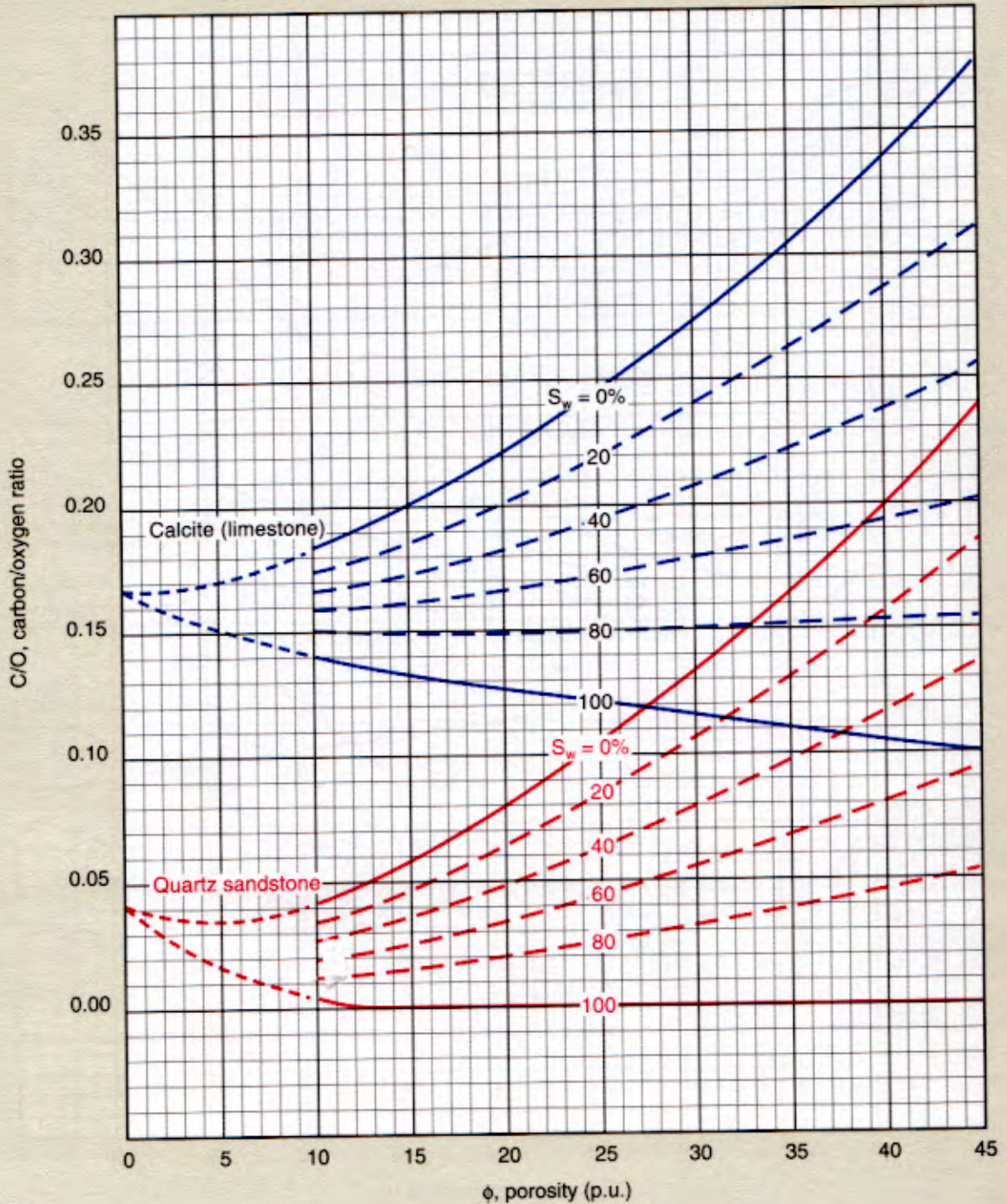
ordinate and abscissa, respectively, on the appropriate chart (dependent upon borehole and casing size). Water saturation is defined by the location of the plotted point within the appropriate matrix "fan chart."

Continued on next page

Saturation Determination from GST* Induced Gamma Ray Spectrometry Log

GST-2

10-in. borehole, 7 7/8-in. water-filled casing



*Mark of Schlumberger
© Schlumberger

Example: 5 1/2-in. water-filled casing cemented in 7 7/8-in. borehole (use Chart GST-1)

C/O ratio = 0.10

$\phi = 28$ p.u.

Lithology is quartz sandstone

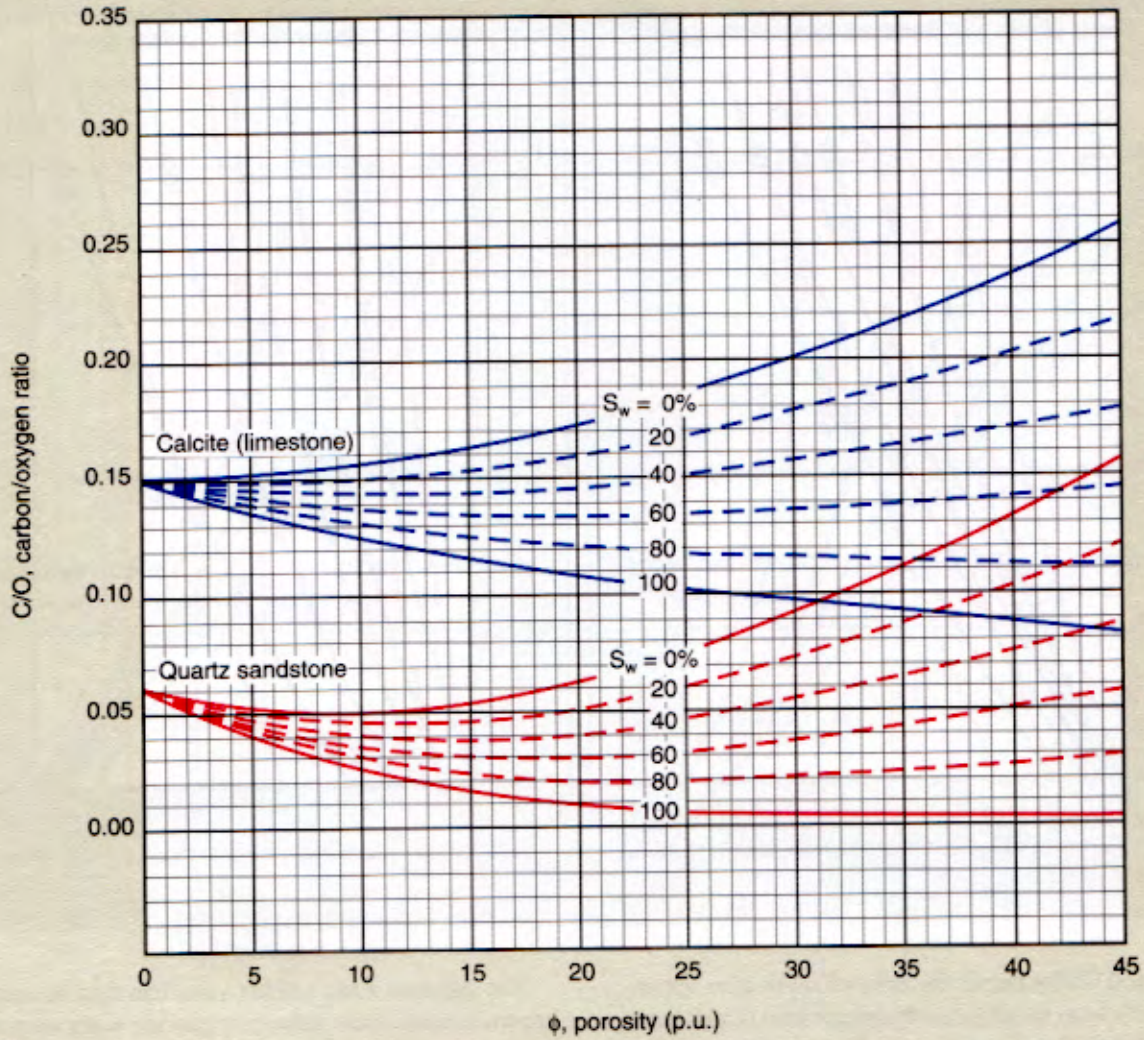
Therefore, $S_w = 30\%$

GST

Saturation Determination from GST* Induced Gamma Ray Spectrometry Log

GST-5

1 1/4-in. borehole; 9 5/8-in., 40-lbm/ft casing

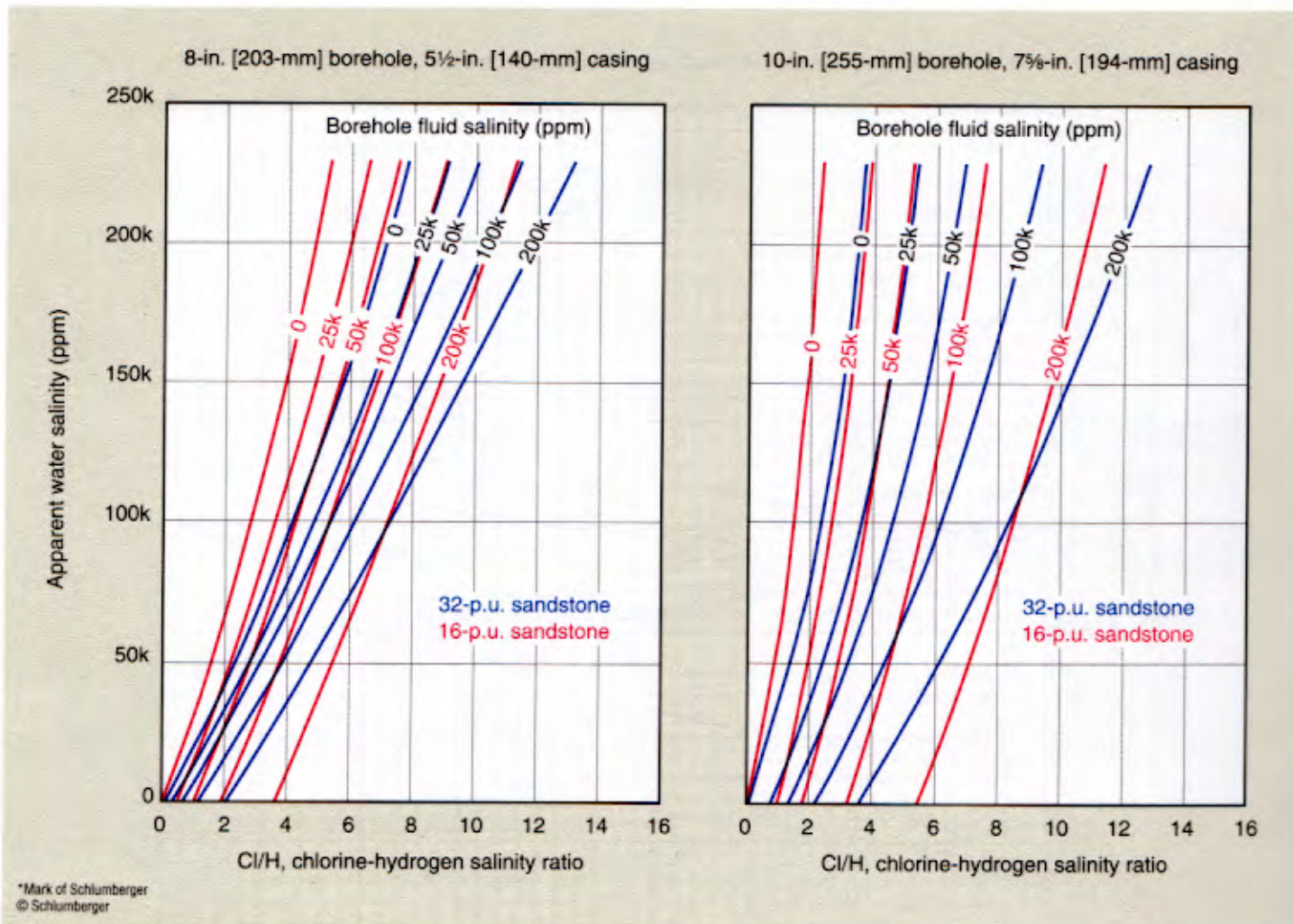


*Mark of Schlumberger
© Schlumberger

Apparent Water Salinity Determination from GST* Induced Gamma Ray Spectrometry Log

Inelastic mode

GST-3



Charts GST-3 and GST-4 permit the determination of an apparent water salinity from the chlorine-hydrogen ratio (Cl/H) as recorded with the GST Induced Gamma Ray Spectrometry Tool. Two sets of charts are presented. Chart GST-3 applies when the GST tool is operated in inelastic mode; Chart GST-4 applies when the tool is operated in capture-tau mode.

To use, enter the chlorine-hydrogen (Cl/H) ratio into the chart that most nearly matches the borehole and casing size conditions and matches the tool operating mode. Proceed upward to the appropriate combination of borehole fluid salinity and formation porosity conditions. Interpolation between curves may be necessary. The apparent water salinity is given in ordinate.

The apparent water salinity value can then be compared to the known connate water salinity to provide water saturation in clean formations.

Example: Cl/H ratio = 5

$\phi = 30\%$

Borehole fluid salinity = 25,000 ppm

5½-in. casing in a 7⅞-in. borehole

Tool operating in capture-tau mode

From Chart GST-4,

Apparent water salinity = 80,000 ppm

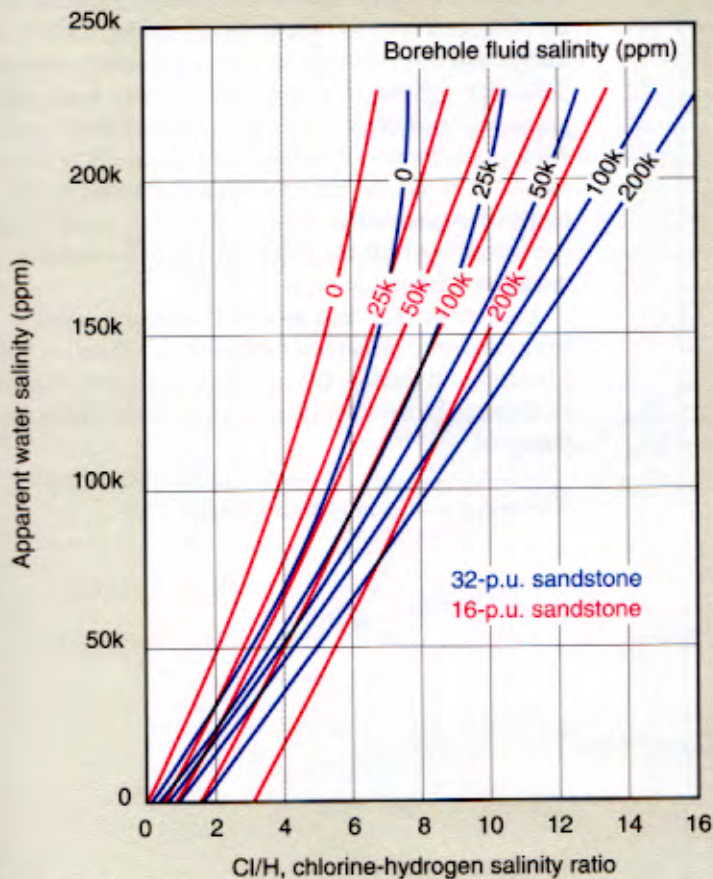
If the connate water salinity were 200,000 ppm, water saturation would be 40% ($S_w = 80,000/200,000$).

Apparent Water Salinity Determination from GST* Induced Gamma Ray Spectrometry Log

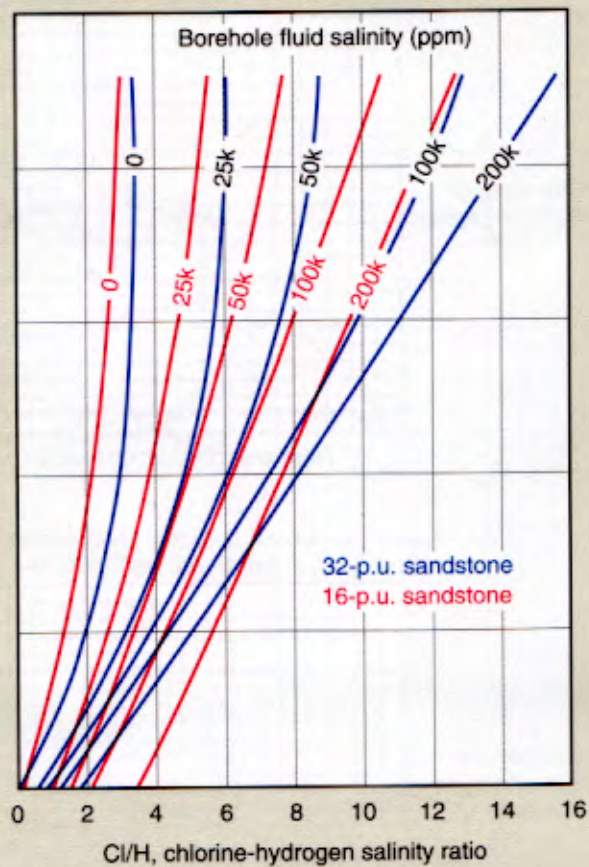
GST-4

Capture-Tau mode

8-in. [203-mm] borehole, 5½-in. [140-mm] casing



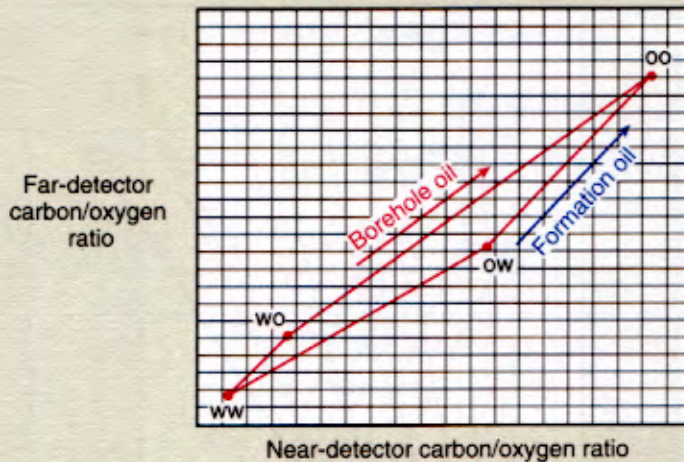
10-in. [255-mm] borehole, 7½-in. [194-mm] casing



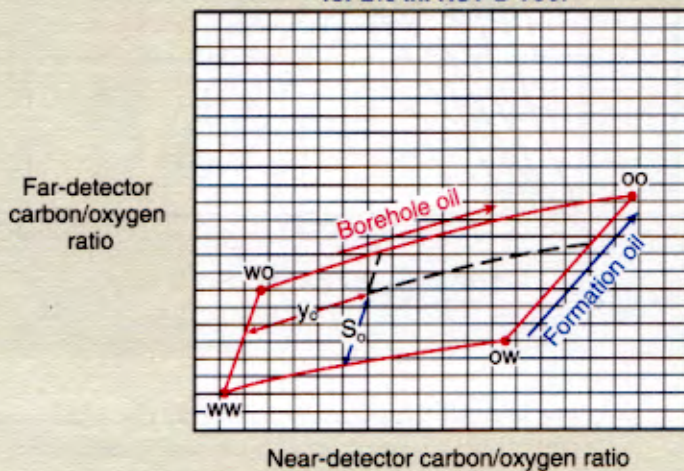
*Mark of Schlumberger
© Schlumberger

RST* Reservoir Saturation Tool Carbon/Oxygen Ratio Response

Dual-Detector COR Model
for 1 $\frac{1}{8}$ -in. RST-A Tool



Dual-Detector COR Model
for 2 $\frac{1}{2}$ -in. RST-B Tool



WW: water in borehole, water in formation
OW: oil in borehole, water in formation
OO: oil in borehole, oil in formation
WO: water in borehole, oil in formation

*Mark of Schlumberger
© Schlumberger

Charts RST-1, -2 and -3, drawn for specific cased hole and openhole cases, help to ensure that the measured near-detector and far-detector carbon/oxygen ratio data are consistent with the interpretation model. Known formation and borehole data define the expected values of carbon/oxygen ratio for each detector using water saturation and borehole holdup values ranging from 0 to 1. All log data for levels with porosity greater than 10 p.u. should lie within the trapezoidal area bounded by the limits on oil saturation, S_o , and oil holdup, y_o . If data fall consistently outside the trapezoid, the interpretation model may require revision.

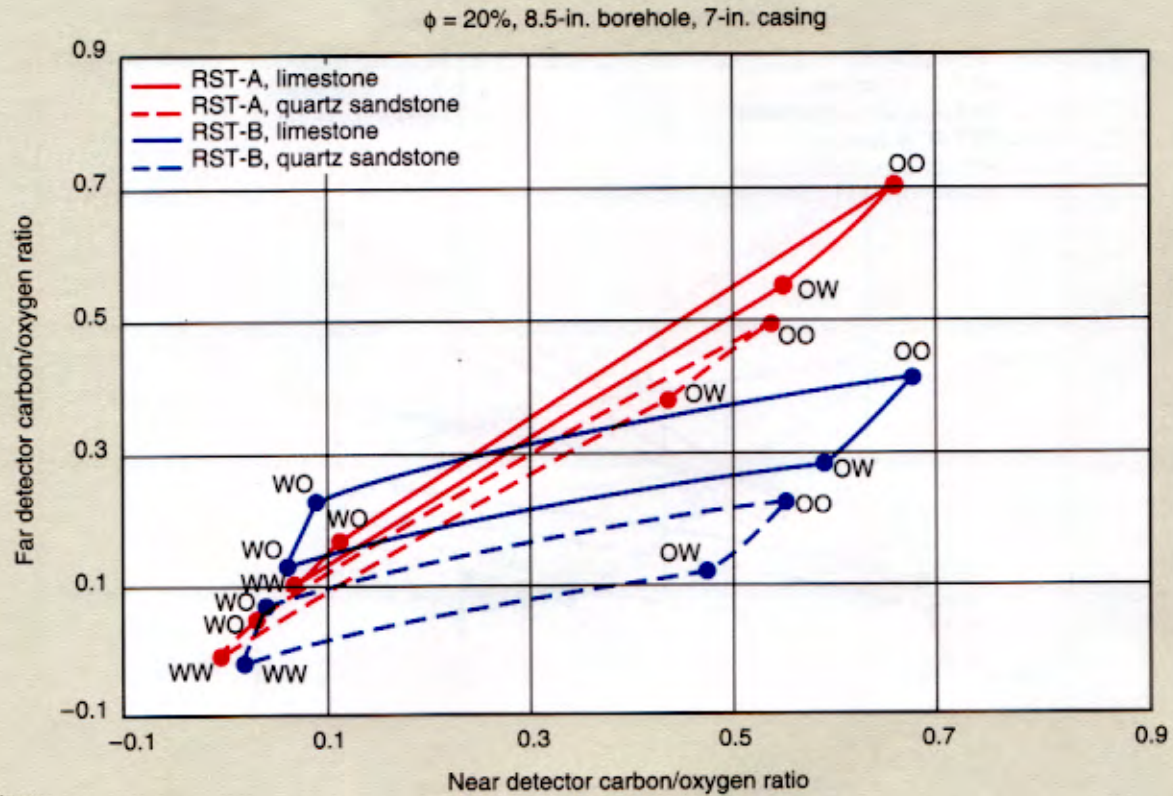
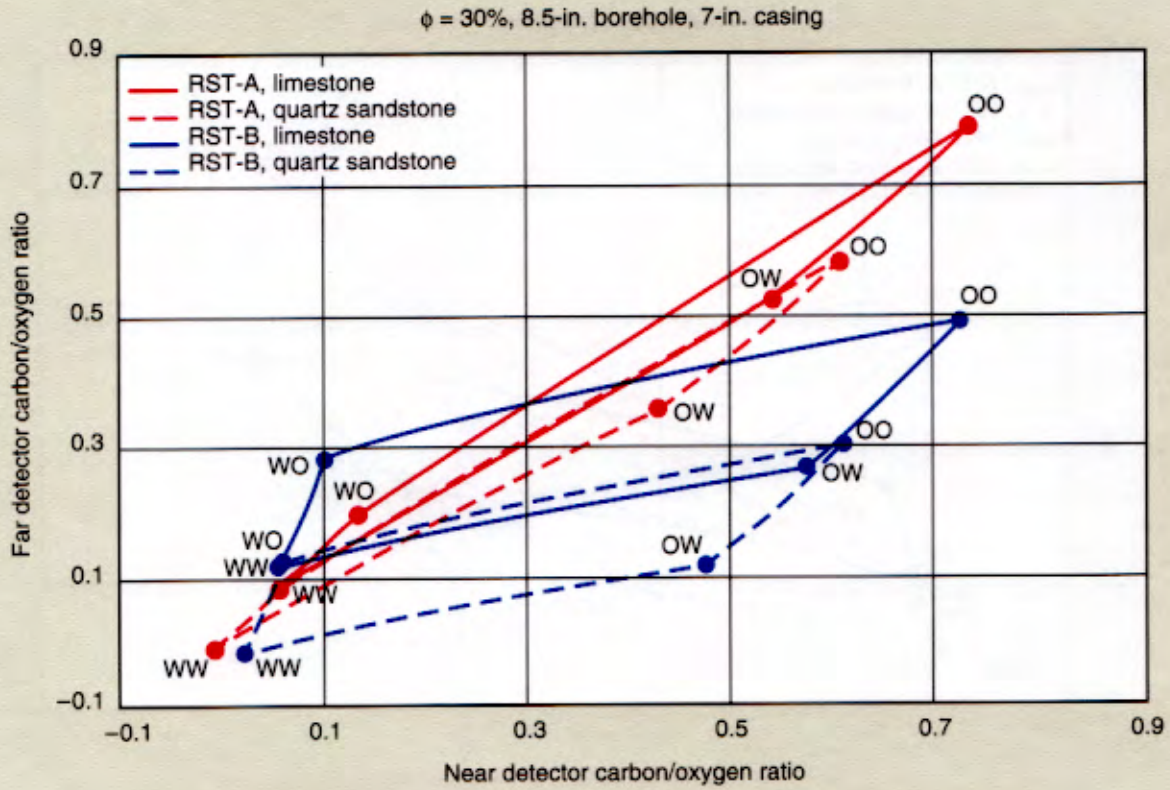
Each set of near-detector and far-detector carbon/oxygen ratios represents a formation oil saturation and a borehole oil holdup. Oil saturation and oil holdup can be estimated for each level by interpolation within the trapezoid.

Additional trapezoid charts can be constructed for alternative casing and borehole sizes.

RST* Reservoir Saturation Tool Carbon/Oxygen Ratio Response

RST-1

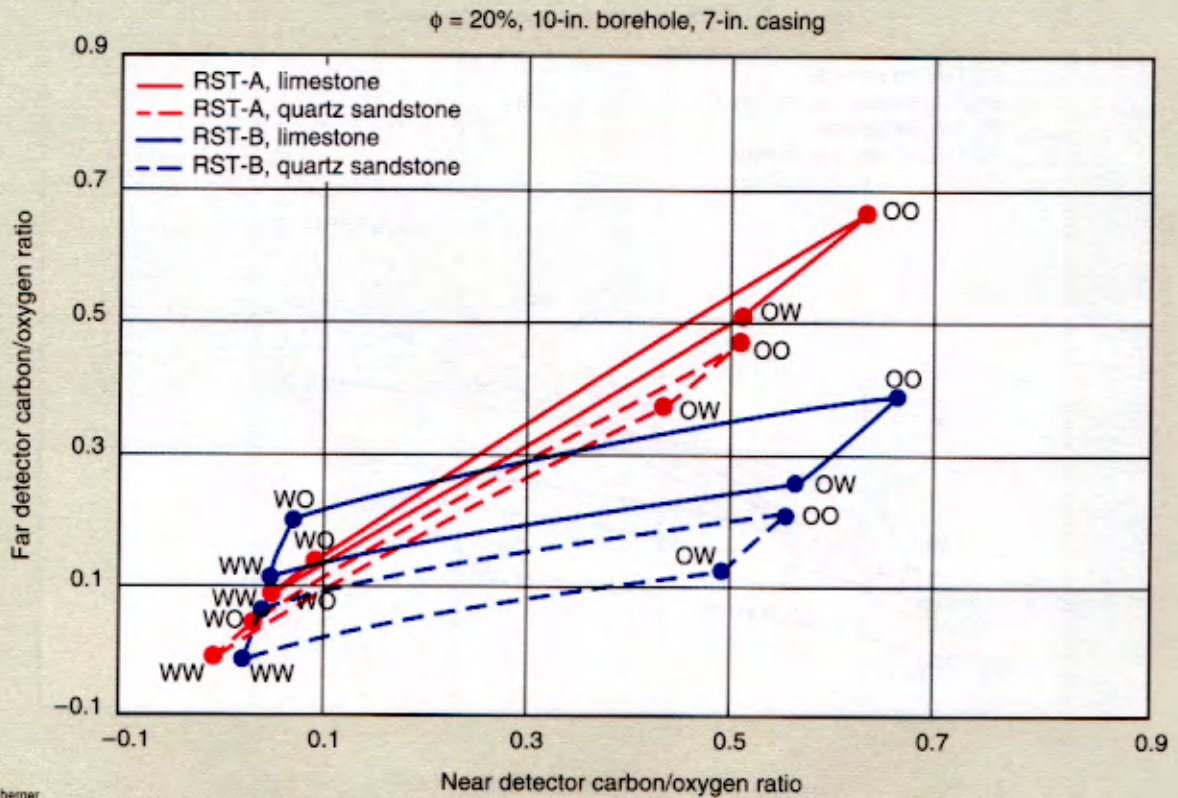
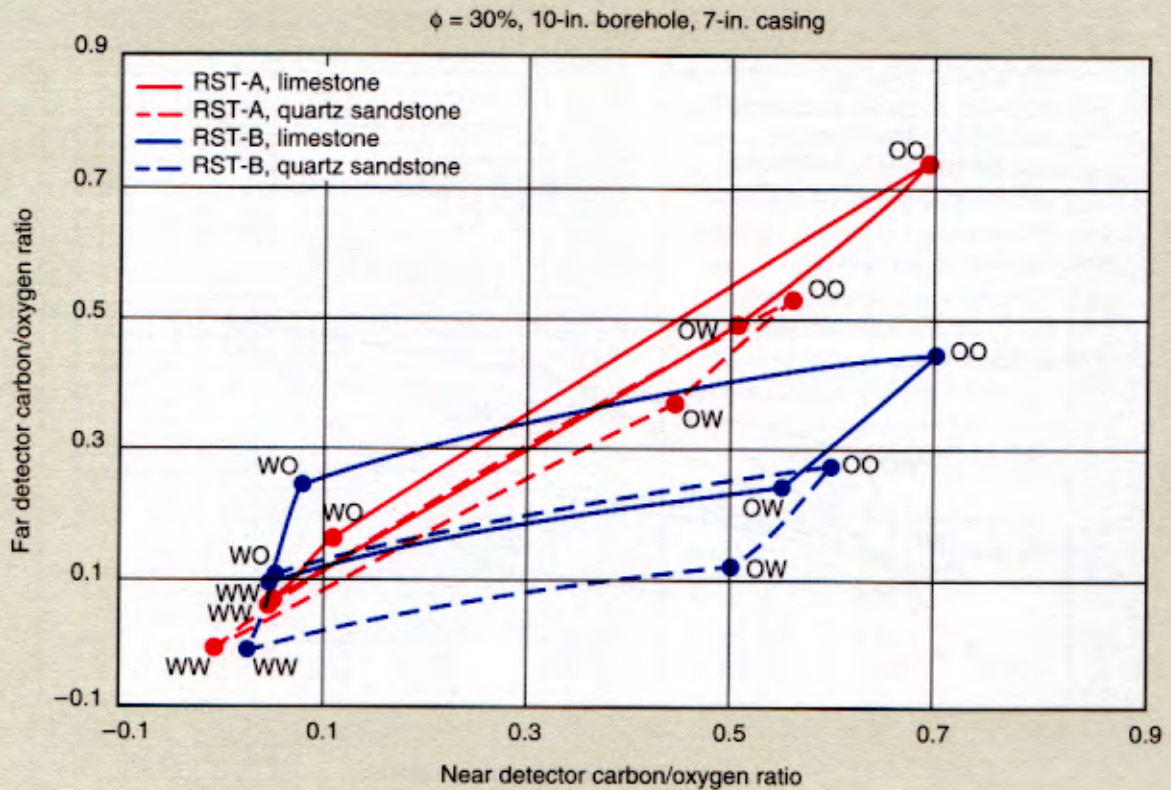
RST-A and RST-B in cased holes



RST* Reservoir Saturation Tool Carbon/Oxygen Ratio Response

RST-2

RST-A and RST-B in cased holes

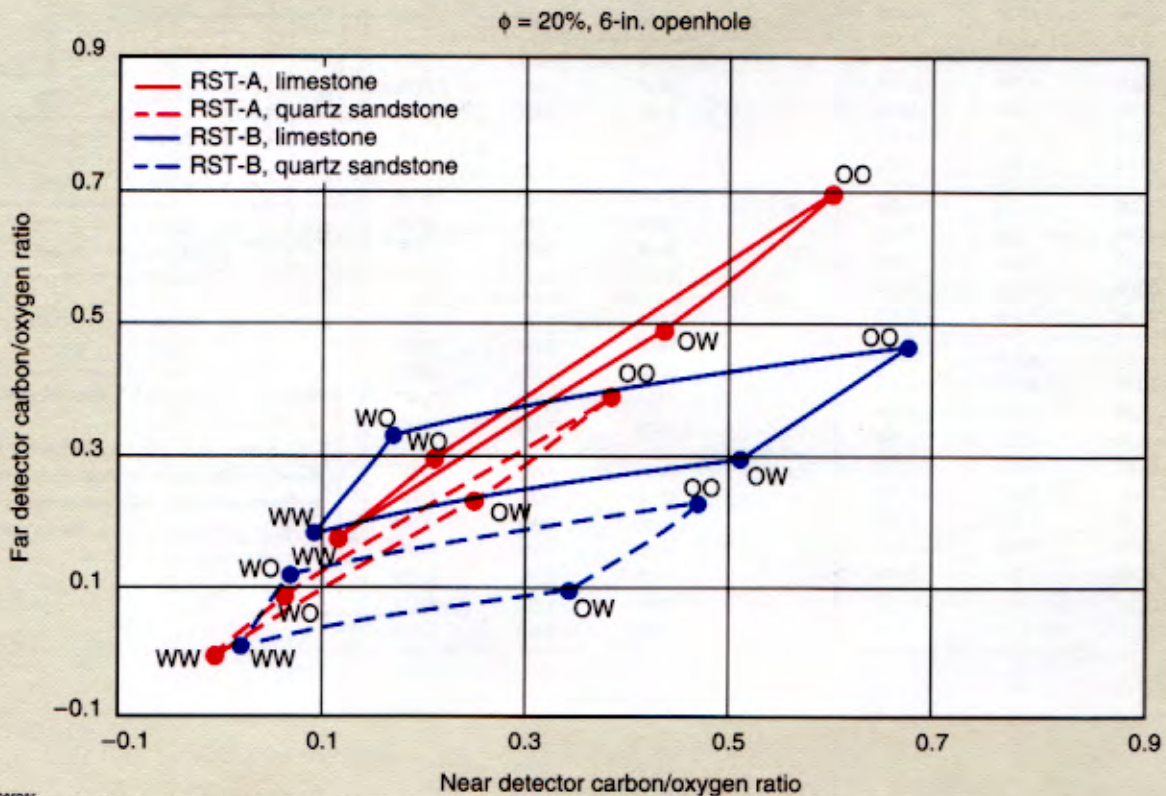
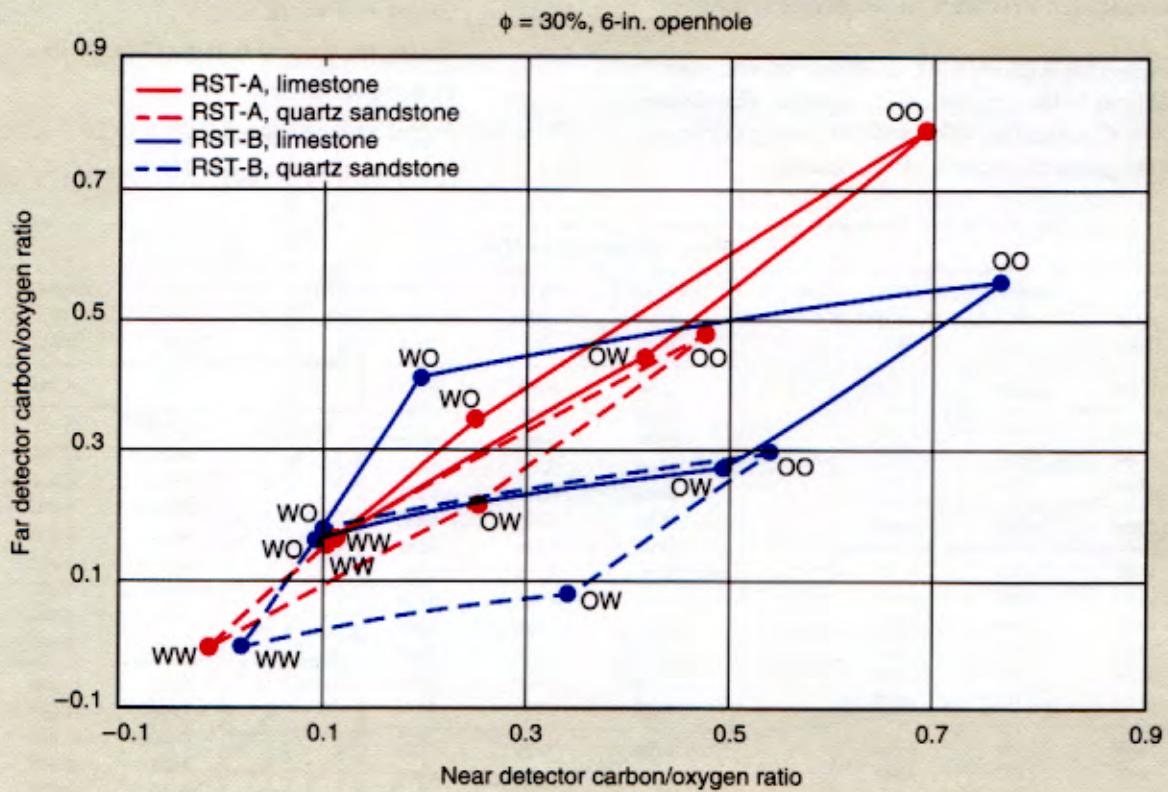


*Mark of Schlumberger
© Schlumberger

RST* Reservoir Saturation Tool Carbon/Oxygen Ratio Response

RST-3

RST-A and RST-B in openholes



*Mark of Schlumberger
© Schlumberger

RST

CBL Interpretation—Casing Data

The compressive strength of bonded cement (either standard or foamed) can be estimated from the CBL amplitude recording using Chart M-1.

Enter the nomograph with the CBL amplitude in mV; then follow diagonal lines to the appropriate casing size. This defines signal attenuation. Connect this value with the casing thickness to estimate the compressive strength of the cement.

Example: CBL amplitude = 3.5 mV

Casing size = 7 in.

Casing thickness = 0.41 in. (7 in. 29 lbm)

Cement is standard

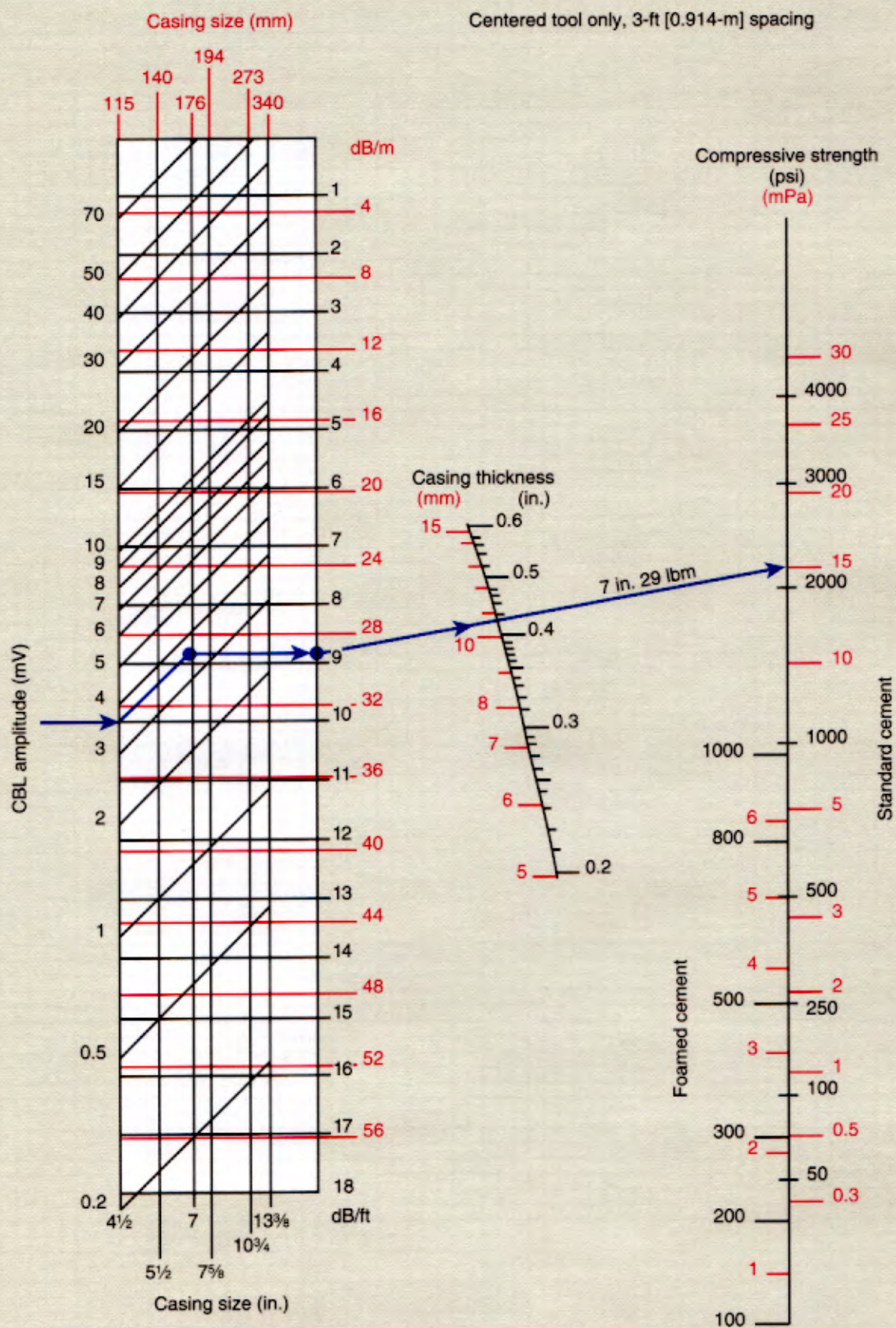
Therefore, Signal attenuation = 8.9 dB/ft or 29.2 dB/m

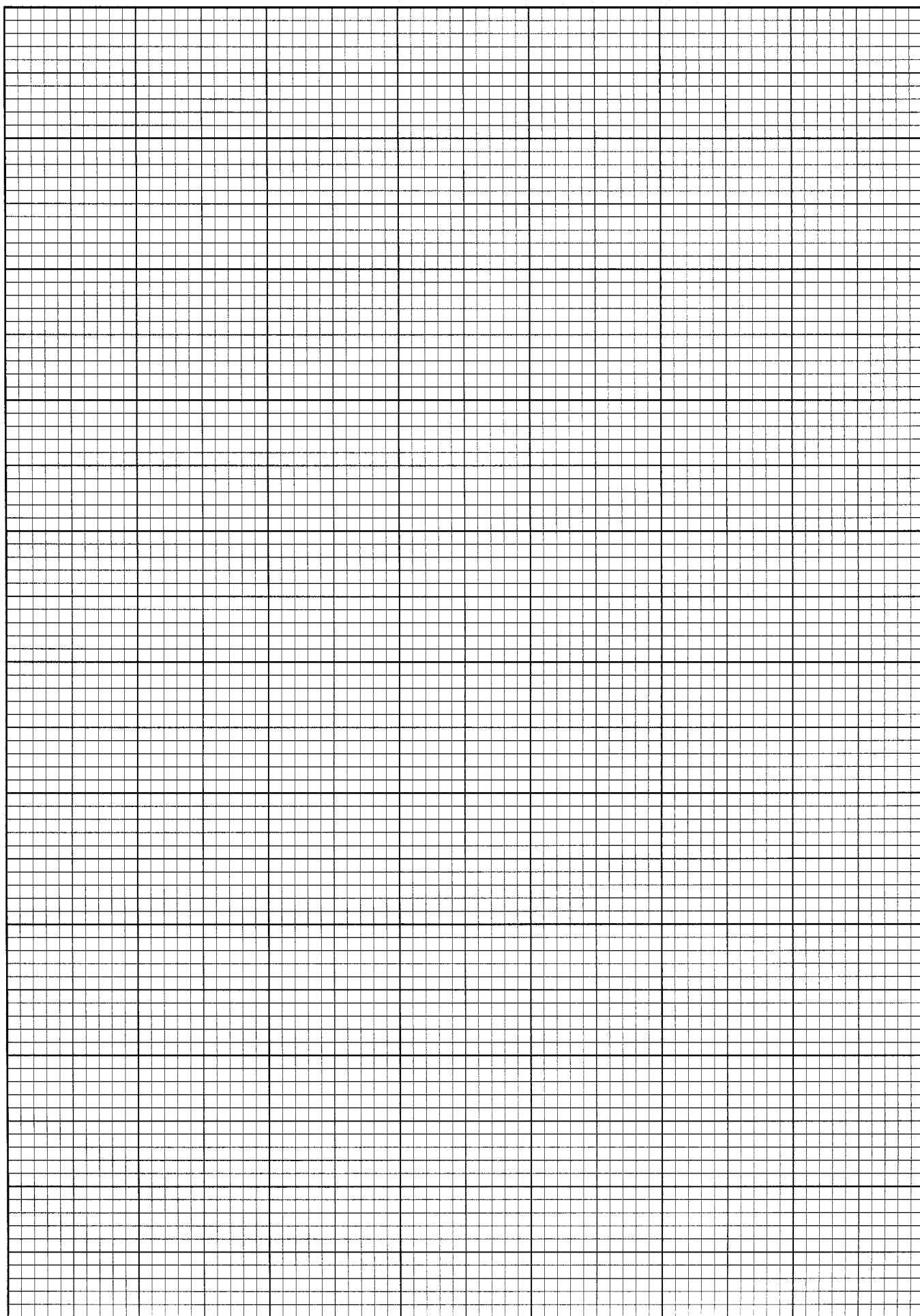
and Compressive strength = 2100 psi or 14.5 mPa

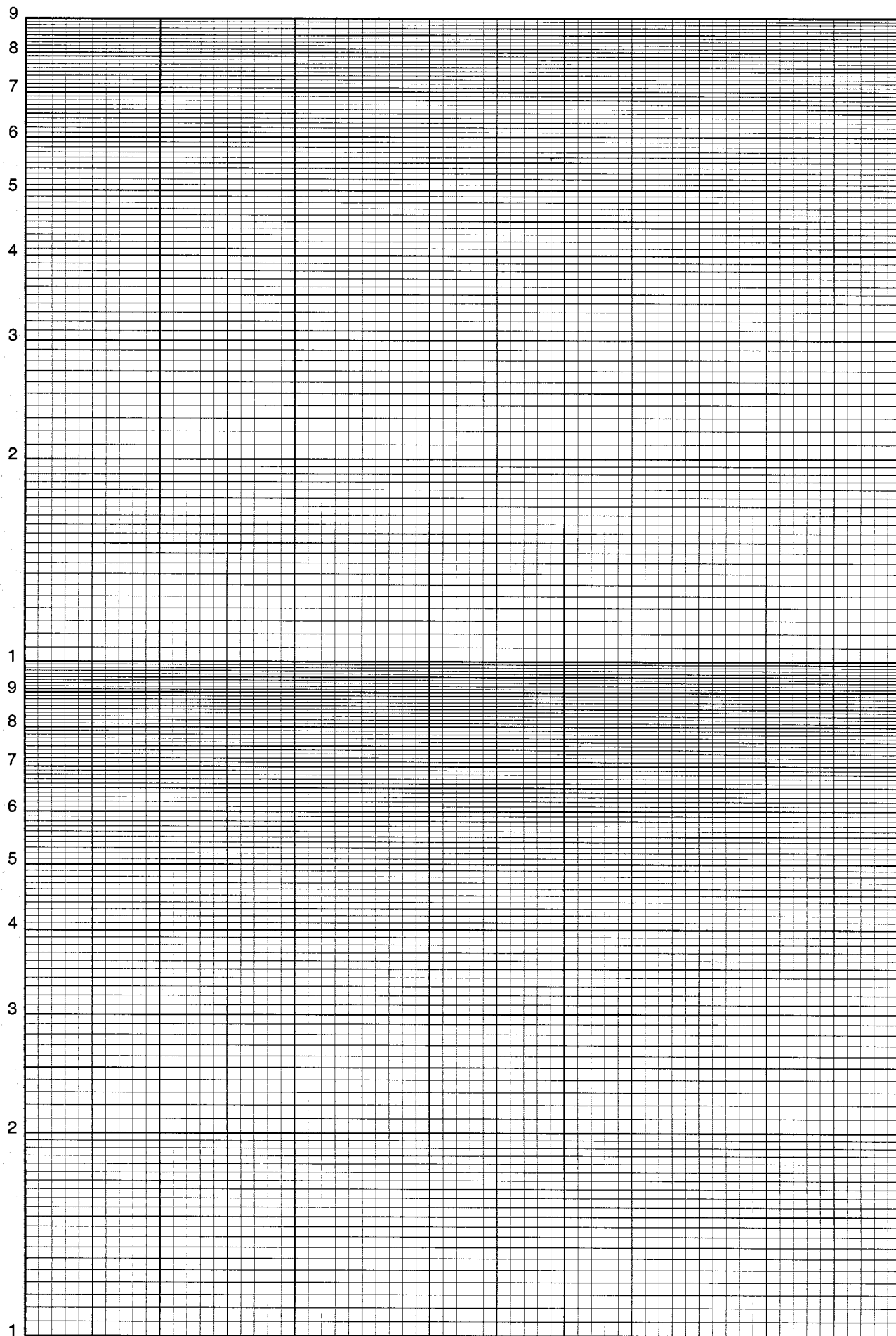
Data for Threaded Nonupset Casing																																
OD (in.)	Weight [†] per ft (lbm)	Nominal ID (in.)	Drift Diameter [‡] (in.)	OD (in.)	Weight [†] per ft (lbm)	Nominal ID (in.)	Drift Diameter [‡] (in.)	OD (in.)	Weight [†] per ft (lbm)	Nominal ID (in.)	Drift Diameter [‡] (in.)																					
4	11.60	3.428	3.303	7	17.00	6.538	6.413	10	33.00	9.384	9.228																					
4½	9.50	4.090	3.965		20.00	6.456	6.331		10¾	32.75	10.192	10.036																				
	11.60	4.000	3.875		22.00	6.398	6.273			40.00	10.054	9.898																				
	13.50	3.920	3.795		23.00	6.366	6.241			40.50	10.050	9.894																				
4¾	16.00	4.082	3.957		24.00	6.336	6.211			45.00	9.960	9.804																				
	5	11.50	4.560		4.435	26.00	6.276			6.151	45.50	9.950	9.794																			
		13.00	4.494		4.369	28.00	6.214			6.089	48.00	9.902	9.746																			
15.00		4.408	4.283		29.00	6.184	6.059			51.00	9.850	9.694																				
17.70		4.300	4.175		30.00	6.154	6.029			54.00	9.784	9.628																				
18.00		4.276	4.151		32.00	6.094	5.969			55.50	9.760	9.604																				
21.00		4.154	4.029	35.00	6.004	5.879	11¾	38.00		11.150	10.994																					
5½	13.00	5.044	4.919	38.00	5.920	5.795		42.00	11.084	10.928																						
	14.00	5.012	4.887	40.00	5.836	5.711		47.00	11.000	10.844																						
	15.00	4.974	4.849	7¾	20.00	7.125		7.000	54.00	10.880	10.724																					
	15.50	4.950	4.825		24.00	7.025		6.900	60.00	10.772	10.616																					
	17.00	4.892	4.767		26.40	6.969		6.844	12	40.00	11.384	11.228																				
	20.00	4.778	4.653		29.70	6.875		6.750		13	40.00	12.438	12.282																			
23.00	4.670	4.545	33.70		6.765	6.640		13¾			48.00	12.715	12.559																			
5¾	14.00	5.290	5.165		39.00	6.625					6.500	16	55.00	15.375	15.187																	
	17.00	5.190	5.065	8¾	24.00	8.097					7.972	18¾	78.00	17.855	17.667																	
	19.50	5.090	4.965		28.00	8.017	7.892				20	90.00	19.190	19.002																		
	22.50	4.990	4.865		32.00	7.921	7.796		21½			92.50	20.710	20.522																		
	6	15.00	5.524		5.399	36.00	7.825			7.700		24½	103.00	20.610	20.422																	
		16.00	5.500		5.375	38.00	7.775	7.650		† Weight per foot in pounds is given for plain pipe (no threads or coupling).			114.00	20.510	20.322																	
18.00		5.424	5.299		40.00	7.725	7.600	‡ Drift diameter is the guaranteed minimum internal diameter of any part of the casing. Use drift diameter to determine the largest-diameter equipment that can be safely run inside the casing. Use internal diameter for volume capacity calculations.					21½	92.50	20.710	20.522																
20.00		5.352	5.227	43.00	7.651	7.526	9							103.00	20.610	20.422																
23.00		5.240	5.115	44.00	7.625	7.500					9¾			114.00	20.510	20.322																
6¾		17.00	6.135	6.010	49.00	7.511			7.386					9¾	100.50	23.750	23.562															
	20.00	6.049	5.924	9	34.00	8.290			8.165			24½			113.00	23.650	23.462															
	22.00	5.989	5.864		38.00	8.196			8.071	† Weight per foot in pounds is given for plain pipe (no threads or coupling).					‡ Drift diameter is the guaranteed minimum internal diameter of any part of the casing. Use drift diameter to determine the largest-diameter equipment that can be safely run inside the casing. Use internal diameter for volume capacity calculations.	24½	100.50	23.750	23.562													
	24.00	5.921	5.796		40.00	8.150		8.025	9¾				24½				113.00	23.650	23.462													
	26.00	5.855	5.730		45.00	8.032	7.907	9¾												24½	113.00	23.650	23.462									
	26.80	5.837	5.712		55.00	7.812	7.687				9¾													24½	113.00	23.650	23.462					
28.00	5.791	5.666	9¾		29.30	9.063	8.907							9¾														24½	113.00	23.650	23.462	
29.00	5.761	5.636		32.30	9.001	8.845	9¾					24½																				113.00
32.00	5.675	5.550		36.00	8.921	8.765				9¾					24½	113.00																
6	15.00	5.524		5.399	40.00	8.835			8.679				9¾				24½	113.00	23.650													
	16.00	5.500		5.375	43.50	8.755		8.599	9¾											24½	113.00	23.650	23.462									
	18.00	5.424		5.299	47.00	8.681		8.525			9¾													24½	113.00	23.650	23.462					
	20.00	5.352	5.227	53.50	8.535	8.379		9¾						24½														113.00	23.650	23.462		
	23.00	5.240	5.115	9	34.00	8.290	8.165					9¾																			24½	113.00
	6	15.00	5.524		5.399	38.00	8.196			8.071					9¾	24½																
16.00		5.500	5.375		40.00	8.150	8.025			9¾			24½				113.00	23.650	23.462													
18.00		5.424	5.299		45.00	8.032	7.907		9¾											24½	113.00	23.650	23.462									
20.00		5.352	5.227		55.00	7.812	7.687				9¾													24½	113.00	23.650	23.462					
23.00		5.240	5.115		9	29.30	9.063	8.907						9¾														24½	113.00	23.650		
6		15.00	5.524	5.399		32.30	9.001	8.845				9¾																			24½	113.00
	16.00	5.500	5.375	36.00		8.921	8.765	9¾							24½	113.00																
	18.00	5.424	5.299	40.00		8.835	8.679			9¾			24½				113.00	23.650	23.462													
	20.00	5.352	5.227	43.50		8.755	8.599		9¾											24½	113.00	23.650	23.462									
	23.00	5.240	5.115	47.00		8.681	8.525				9¾													24½	113.00	23.650	23.462					
	6	15.00	5.524	5.399	53.50	8.535	8.379							9¾														24½	113.00	23.650		
16.00		5.500	5.375	9	34.00	8.290	8.165					9¾																			24½	113.00
18.00		5.424	5.299		38.00	8.196	8.071	9¾							24½	113.00																
20.00		5.352	5.227		40.00	8.150	8.025			9¾			24½				113.00	23.650	23.462													
23.00		5.240	5.115		45.00	8.032	7.907		9¾											24½	113.00	23.650	23.462									
6		15.00	5.524		5.399	55.00	7.812				7.687													9¾	24½	113.00	23.650					
	16.00	5.500	5.375		9	29.30	9.063				8.907			9¾														24½	113.00	23.650		
	18.00	5.424	5.299	32.30		9.001	8.845				9¾	24½																			113.00	23.650
	20.00	5.352	5.227	36.00		8.921	8.765	9¾							24½	113.00																
	23.00	5.240	5.115	40.00		8.835	8.679			9¾			24½				113.00	23.650	23.462													
	6	15.00	5.524	5.399		43.50	8.755		8.599											9¾	24½	113.00	23.650									
16.00		5.500	5.375	47.00		8.681	8.525		9¾															24½	113.00	23.650	23.462					
18.00		5.424	5.299	53.50	8.535	8.379	9¾							24½														113.00	23.650	23.462		
20.00		5.352	5.227	9	34.00	8.290					8.165	9¾																			24½	113.00
23.00		5.240	5.115		38.00	8.196		8.071			9¾				24½	113.00																
6		15.00	5.524		5.399	40.00		8.150		8.025			9¾				24½	113.00	23.650													
	16.00	5.500	5.375		45.00	8.032		7.907		9¾										24½	113.00	23.650	23.462									
	18.00	5.424	5.299		55.00	7.812		7.687	9¾															24½	113.00	23.650	23.462					
	20.00	5.352	5.227		9	29.30	9.063	8.907						9¾														24½	113.00	23.650		
	23.00	5.240	5.115	32.30		9.001	8.845	9¾				24½																			113.00	23.650
	6	15.00	5.524	5.399		36.00	8.921				8.765				9¾	24½																
16.00		5.500	5.375	40.00		8.835	8.679				9¾		24½				113.00	23.650	23.462													
18.00		5.424	5.299	43.50		8.755	8.599			9¾										24½	113.00	23.650	23.462									
20.00		5.352	5.227	47.00		8.681	8.525		9¾															24½	113.00	23.650	23.462					
23.00		5.240	5.115	53.50	8.535	8.379	9¾							24½														113.00	23.650	23.462		
6		15.00	5.524	5.399	9	34.00		8.290				8.165																			9¾	24½
	16.00	5.500	5.375	38.00		8.196		8.071				9¾			24½	113.00																
	18.00	5.424	5.299	40.00		8.150		8.025			9¾		24½				113.00	23.650	23.462													
	20.00	5.352	5.227	45.00		8.032		7.907		9¾										24½	113.00	23.650	23.462									
	23.00	5.240	5.115	55.00		7.812		7.687	9¾															24½	113.00	23.650	23.462					
	6	15.00	5.524	5.399		9	29.30	9.063						8.907														9¾	24½	113.00		
16.00		5.500	5.375	32.30	9.001		8.845	9¾						24½																	113.00	23.650
18.00		5.424	5.299	36.00	8.921		8.765					9¾			24½	113.00																
20.00		5.352	5.227	40																												

CBL Interpretation Chart

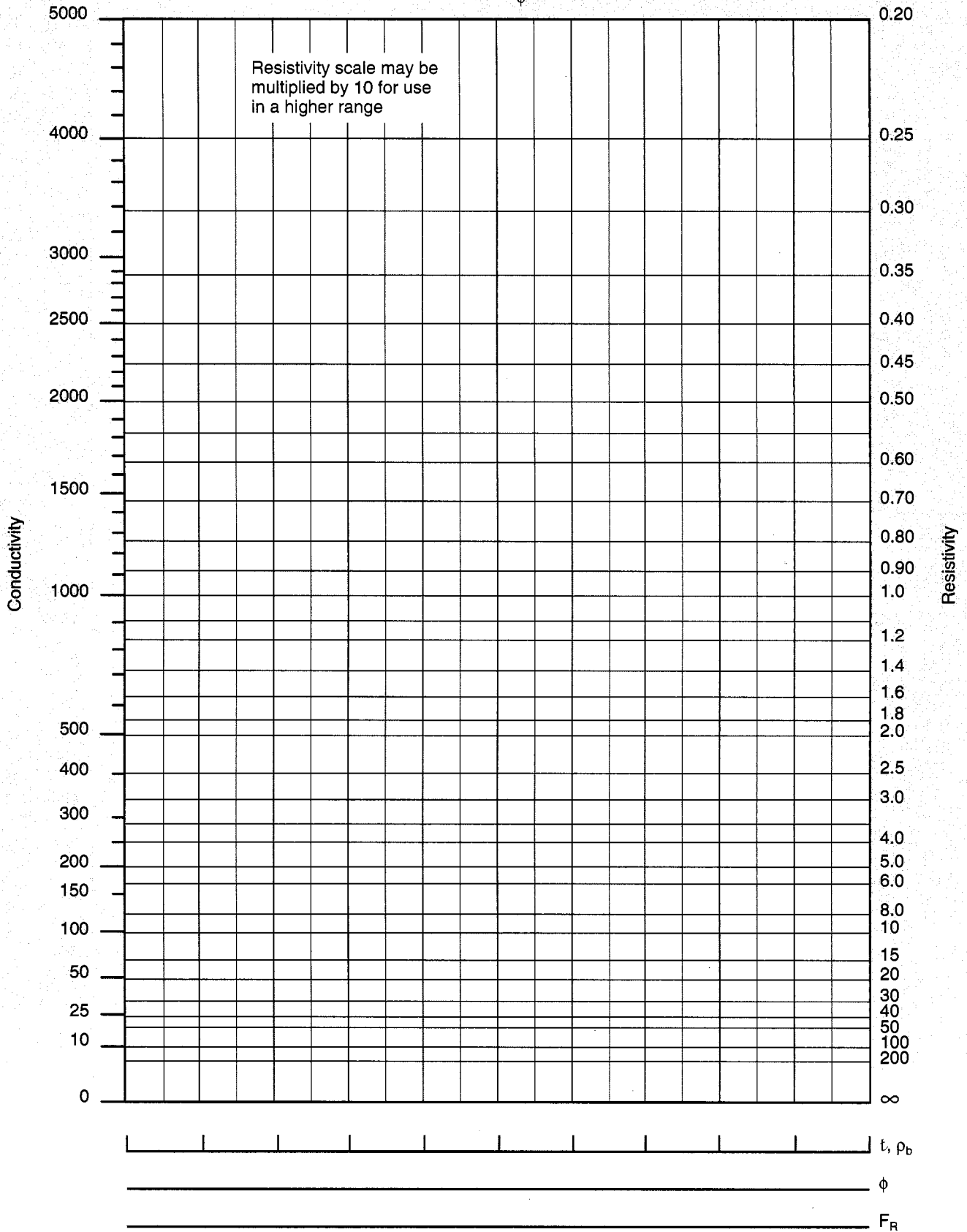
M-1



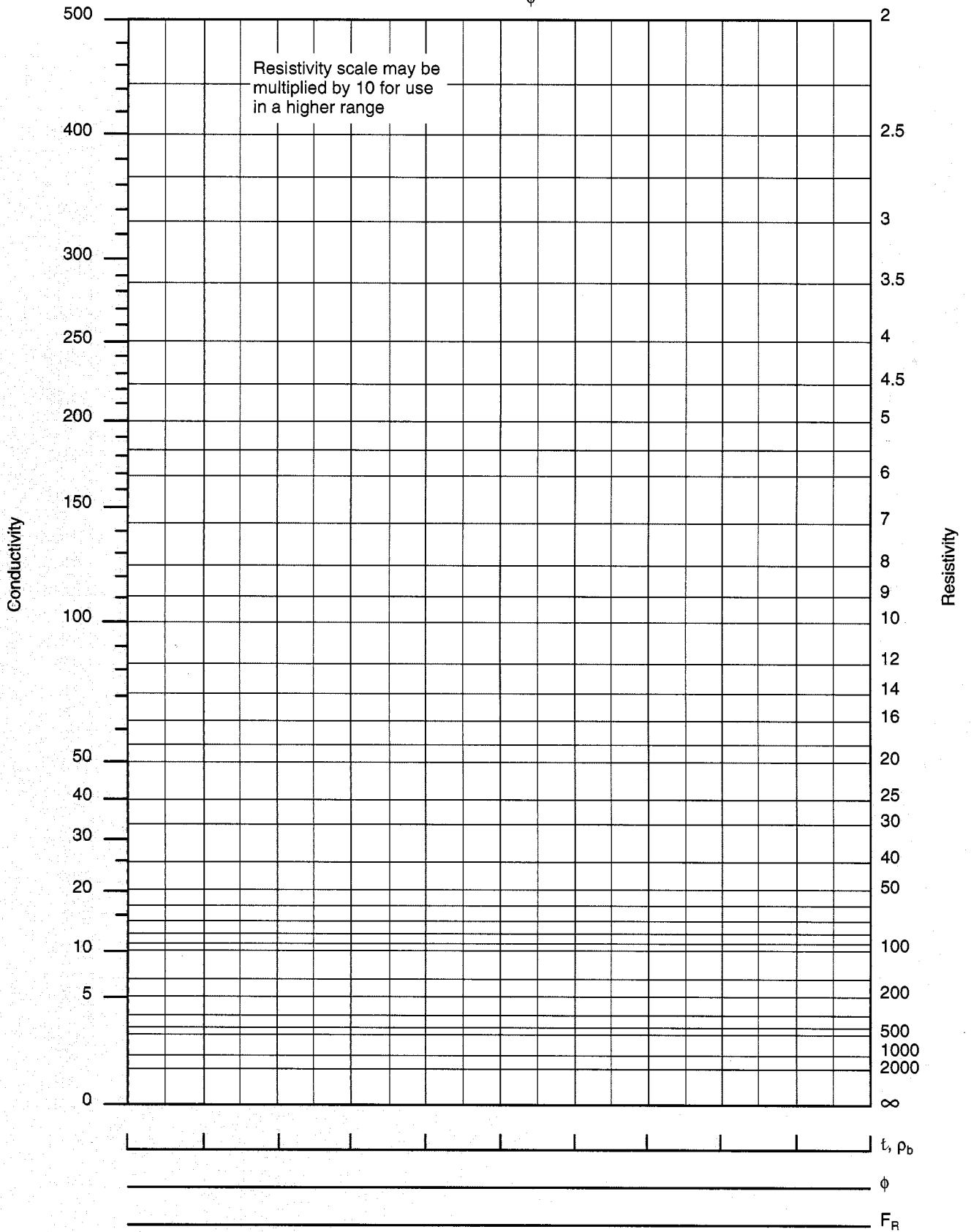




For $F_R = \frac{0.62}{\phi^{2.15}}$



For $F_R = \frac{1}{\phi^2}$



Name	Formula	ρ_{LOG} (g/cm ³)	ϕ_{SNP} (p.u.)	ϕ_{CNL} (p.u.)	$\phi_{\text{APS}}^{\dagger}$ (p.u.)	t_c ($\mu\text{sec}/\text{ft}$)	t_s ($\mu\text{sec}/\text{ft}$)	P_e	U	ϵ (farad/m)	t_p (nsec/m)	GR (API units)	Σ (c.u.)
Silicates													
Quartz	SiO ₂	2.64	-1	-2	-1	56.0	88.0	1.8	4.8	4.65	7.2		4.3
β -Cristobalite	SiO ₂	2.15	-2	-3				1.8	3.9				3.5
Opal (3.5% H ₂ O)	SiO ₂ (H ₂ O) _{0.1209}	2.13	4	2		58		1.8	3.7				5.0
Garnet [‡]	Fe ₃ Al ₂ (SiO ₄) ₃	4.31	3	7				11	48				45
Hornblende [‡]	Ca ₂ NaMg ₂ Fe ₂ AlSi ₈ O ₂₂ (O,OH) ₂	3.20	4	8		43.8	81.5	6.0	19				18
Tourmaline	NaMg ₃ Al ₆ B ₃ Si ₆ O ₂ (OH) ₄	3.02	16	22				2.1	6.5				7450
Zircon	ZrSiO ₄	4.50	-1	-3				69	311				6.9
Carbonates													
Calcite	CaCO ₃	2.71	0	0	0	49.0	88.4	5.1	13.8	7.5	9.1		7.1
Dolomite	CaCO ₃ MgCO ₃	2.85	2	1	1	44.0	72	3.1	9.0	6.8	8.7		4.7
Ankerite	Ca(Mg,Fe)(CO ₃) ₂	2.86	0	1				9.3	27				22
Siderite	FeCO ₃	3.89	5	12	3	47		15	57	6.8-7.5	8.8-9.1		52
Oxidates													
Hematite	Fe ₂ O ₃	5.18	4	11		42.9	79.3	21	111				101
Magnetite	Fe ₃ O ₄	5.08	3	9		73		22	113				103
Goethite	FeO(OH)	4.34	50+	60+				19	83				85
Limonite [‡]	FeO(OH)(H ₂ O) _{2.05}	3.59	50+	60+		56.9	102.6	13	47	9.9-10.9	10.5-11.0		71
Gibbsite	Al(OH) ₃	2.49	50+	60+				1.1					23
Phosphates													
Hydroxyapatite	Ca ₅ (PO ₄) ₃ OH	3.17	5	8		42		5.8	18				9.6
Chlorapatite	Ca ₅ (PO ₄) ₃ Cl	3.18	-1	-1		42		6.1	19				130
Fluorapatite	Ca ₅ (PO ₄) ₃ F	3.21	-1	-2		42		5.8	19				8.5
Carbonapatite	(Ca ₂ (PO ₄) ₃) ₂ CO ₃ H ₂ O	3.13	5	8				5.6	17				9.1
Feldspars—Alkali[‡]													
Orthoclase	KAISi ₃ O ₈	2.52	-2	-3		69		2.9	7.2	4.4-6.0	7.0-8.2	~220	16
Anorthoclase	KAISi ₃ O ₈	2.59	-2	-2				2.9	7.4	4.4-6.0	7.0-8.2	~220	16
Microcline	KAISi ₃ O ₈	2.53	-2	-3				2.9	7.2	4.4-6.0	7.0-8.2	~220	16
Feldspars—Plagioclase[‡]													
Albite	NaAlSi ₃ O ₈	2.59	-1	-2	-2	49	85	1.7	4.4	4.4-6.0	7.0-8.2		7.5
Anorthite	CaAl ₂ Si ₂ O ₈	2.74	-1	-2		45		3.1	8.6	4.4-6.0	7.0-8.2		7.2
Micas[‡]													
Muscovite	KAl ₂ (Si ₃ AlO ₁₀)(OH) ₂	2.82	12	~20	~13	49	149	2.4	6.7	6.2-7.9	8.3-9.4	~270	17
Glauconite	K _{0.7} (Mg,Fe ₂ ,Al) (Si ₄ ,Al ₁₀)O ₂ (OH)	2.86		~38	~15			4.8	14				21
Biotite	K(Mg,Fe) ₃ (AlSi ₃ O ₁₀)(OH) ₂	~2.99	~11	~21	~11	50.8	224	6.3	19	4.8-6.0	7.2-8.1	~275	30
Phlogopite	KMg ₃ (AlSi ₃ O ₁₀)(OH) ₂					50	207						33

[†]APS porosity derived from near-to-array ratio (APLC)

[‡]Mean value, which may vary for individual samples

For more information see Reference 41.

Name	Formula	ρ_{LOG} (g/cm ³)	ϕ_{SNP} (p.u.)	ϕ_{CNL} (p.u.)	ϕ_{APS}^\dagger (p.u.)	t_c (μ sec/ft)	t_s (μ sec/ft)	P_e	U	ϵ (farad/m)	t_p (nsec/m)	GR (API units)	Σ (c.u.)
Clays[‡]													
Kaolinite	Al ₂ Si ₄ O ₁₀ (OH) ₈	2.41	34	~37	~34			1.8	4.4	~5.8	~8.0	80-130	14
Chlorite	(Mg,Fe,Al) ₆ (Si,Al) ₄ O ₁₀ (OH) ₈	2.76	37	~52	~35			6.3	17	~5.8	~8.0	180-250	25
Illite	K _{1-1.5} Al ₄ (Si _{7-6.5} ,Al _{1-1.5})O ₂₀ (OH) ₄	2.52	20	~30	~17			3.5	8.7	~5.8	~8.0	250-300	18
Montmorillonite	(Ca,Na) ₇ (Al,Mg,Fe) ₄ (Si,Al) ₈ O ₂₀ (OH) ₄ (H ₂ O) _n	2.12		~60	~60			2.0	4.0	~5.8	~8.0	150-200	14
Evaporites													
Halite	NaCl	2.04	-2	-3	21	67.0	120	4.7	9.5	5.6-6.3	7.9-8.4		754
Anhydrite	CaSO ₄	2.98	-1	-2	2	50		5.1	15	6.3	8.4		12
Gypsum	CaSO ₄ (H ₂ O) ₂	2.35	50+	60+	60	52		4.0	9.4	4.1	6.8		19
Trona	Na ₂ CO ₃ NaHCO ₃ H ₂ O	2.08	24	35		65		0.71	1.5				16
Tachydrate	CaCl ₂ (MgCl ₂) ₂ (H ₂ O) ₁₂	1.66	50+	60+		92		3.8	6.4				406
Sylvite	KCl	1.86	-2	-3				8.5	16	4.6-4.8	7.2-7.3	500+	565
Camalite	KClMgCl ₂ (H ₂ O) ₆	1.57	41	60+				4.1	6.4			~220	369
Langbeinite	K ₂ SO ₄ (MgSO ₄) ₂	2.82	-1	-2				3.6	10			~290	24
Polyhalite	K ₂ SO ₄ MgSO ₄ (CaSO ₄) ₂ (H ₂ O) ₂	2.79	14	25				4.3	12			~200	24
Kainite	MgSO ₄ KCl(H ₂ O) ₃	2.12	40	60+				3.5	7.4			~245	195
Kieserite	MgSO ₄ H ₂	2.59	38	43				1.8	4.7				14
Epsomite	MgSO ₄ (H ₂ O) ₇	1.71	50+	60+				1.2	2.0				21
Bischofite	MgCl ₂ (H ₂ O) ₆	1.54	50+	60+		100		2.6	4.0				323
Barite	BaSO ₄	4.09	-1	-2				267	1090				6.8
Celestite	SrSO ₄	3.79	-1	-1				55	209				7.9
Sulfides													
Pyrite	FeS ₂	4.99	-2	-3		39.2	62.1	17	85				90
Marcasite	FeS ₂	4.87	-2	-3				17	83				88
Pyrrhotite	Fe ₇ S ₈	4.53	-2	-3				21	93				94
Sphalerite	ZnS	3.85	-3	-3				36	138	7.8-8.1	9.3-9.5		25
Chalcopyrite	CuFeS ₂	4.07	-2	-3				27	109				102
Galena	PbS	6.39	-3	-3				1630	10,400				13
Sulfur	S	2.02	-2	-3		122		5.4	11				20
Coals													
Anthracite	CH _{0.358} N _{0.009} O _{0.222}	1.47	37	38		105		0.16	0.23				8.7
Bituminous	CH _{0.793} N _{0.015} O _{0.078}	1.24	50+	60+		120		0.17	0.21				14
Lignite	CH _{0.849} N _{0.015} O _{0.211}	1.19	47	52		160		0.20	0.24				13
† APS porosity derived from near-to-array ratio (APLC)													
‡ Mean value, which may vary for individual samples													

For more information see Reference 41.

to Obtain \ Multiply Number of by	Centimeters	Feet	Inches	Kilometers	Nautical miles	Meters	Mils	Miles	Millimeters	Yards
Centimeters	1	30.48	2.540	10^5	1.853×10^5	100	2.540×10^{-3}	1.609×10^5	0.1	91.44
Feet	3.281×10^{-2}	1	8.333×10^{-2}	3281	6080.27	3.281	8.333×10^{-5}	5280	3.281×10^{-3}	3
Inches	0.3937	12	1	3.937×10^4	7.296×10^4	39.37	0.001	6.336×10^4	3.937×10^{-2}	36
Kilometers	10^{-5}	3.048×10^{-4}	2.540×10^{-5}	1	1.853	0.001	2.540×10^{-8}	1.609	10^{-6}	9.144×10^{-4}
Nautical miles		1.645×10^{-4}		0.5396	1	5.396×10^{-4}		0.8684		4.934×10^{-4}
Meters	0.01	0.3048	2.540×10^{-2}	1000	1853	1		1609	0.001	0.9144
Mils	393.7	1.2×10^4	1000	3.937×10^7		3.937×10^4	1		39.37	3.6×10^4
Miles	6.214×10^{-6}	1.894×10^{-4}	1.578×10^{-5}	0.6214	1.1516	6.214×10^{-4}		1	6.214×10^{-7}	5.682×10^{-4}
Millimeters	10	304.8	25.40	10^5		1000	2.540×10^{-2}		1	914.4
Yards	1.094×10^{-2}	0.3333	2.778×10^{-2}	1094	2027	1.094	2.778×10^{-5}	1760	1.094×10^{-3}	1

Area										
to Obtain \ Multiply Number of by	Acres	Circular mils	Square centimeters	Square feet	Square inches	Square kilometers	Square meters	Square miles	Square millimeters	Square yards
Acres	1			2.296×10^{-5}		247.1	2.471×10^{-4}	640		2.066×10^{-4}
Circular mils		1	1.973×10^5	1.833×10^8	1.273×10^6		1.973×10^9		1973	
Square centimeters		5.067×10^{-6}	1	929.0	6.452	10^{10}	10^4	2.590×10^{10}	0.01	8361
Square feet	4.356×10^4		1.076×10^{-3}	1	6.944×10^{-3}	1.076×10^7	10.76	2.788×10^7	1.076×10^{-5}	9
Square inches	6,272,640	7.854×10^{-7}	0.1550	144	1	1.550×10^9	1550	4.015×10^9	1.550×10^{-3}	1296
Square kilometers	4.047×10^{-3}		10^{-10}	9.290×10^{-8}	6.452×10^{-10}	1	10^{-6}	2.590	10^{-12}	8.361×10^{-7}
Square meters	4047		0.0001	9.290×10^{-2}	6.452×10^{-4}	10^6	1	2.590×10^6	10^{-6}	0.8361
Square miles	1.562×10^{-3}		3.861×10^{-11}	3.587×10^{-8}		0.3861	3.861×10^{-7}	1	3.861×10^{-13}	3.228×10^{-7}
Square millimeters		5.067×10^{-4}	100	9.290×10^4	645.2	10^{12}	10^6		1	8.361×10^5
Square yards	4840		1.196×10^{-4}	0.1111	7.716×10^{-4}	1.196×10^6	1.196	3.098×10^6	1.196×10^{-6}	1

Volume											
to Obtain	Multiply Number of by	Bushels (dry)	Cubic centimeters	Cubic feet	Cubic inches	Cubic meters	Cubic yards	Gallons (liquid)	Liters	Pints (liquid)	Quarts (liquid)
Bushels (dry)	1			0.8036	4.651×10^{-4}	28.38			2.838×10^{-2}		
Cubic centimeters	3.524×10^4	1		2.832×10^4	16.39	10^6	7.646×10^5	3785	1000	473.2	946.4
Cubic feet	1.2445	3.531×10^{-5}		1	5.787×10^{-4}	35.31	27	0.1337	3.531×10^{-2}	1.671×10^{-2}	3.342×10^{-2}
Cubic inches	2150.4	6.102×10^{-2}		1728	1	6.102×10^4	46,656	231	61.02	28.87	57.75
Cubic meters	3.524×10^{-2}	10^{-6}		2.832×10^{-2}	1.639×10^{-5}	1	0.7646	3.785×10^{-3}	0.001	4.732×10^{-4}	9.464×10^{-4}
Cubic yards		1.308×10^{-6}		3.704×10^{-2}	2.143×10^{-5}	1.308	1	4.951×10^{-3}	1.308×10^{-3}	6.189×10^{-4}	1.238×10^{-3}
Gallons (liquid)		2.642×10^{-4}		7.481	4.329×10^{-3}	264.2	202.0	1	0.2642	0.125	0.25
Liters	35.24	0.001		28.32	1.639×10^{-3}	1000	764.6	3.785	1	0.4732	0.9464
Pints (liquid)		2.113×10^{-3}		59.84	3.463×10^{-2}	2113	1616	8	2.113	1	2
Quarts (liquid)		1.057×10^{-3}		29.92	1.732×10^{-2}	1057	807.9	4	1.057	0.5	1

Mass and Weight										
to Obtain	Multiply Number of by	Grains	Grams	Kilograms	Milligrams	Ounces†	Pounds†	Tons (long)	Tons (metric)	Tons (short)
Grains	1		15.43	1.543×10^4	1.543×10^{-2}	437.5	7000			
Grams	6.481×10^{-2}		1	1000	0.001	28.35	453.6	1.016×10^6	10^6	9.072×10^5
Kilograms	6.481×10^{-5}		0.001	1	10^{-6}	2.835×10^{-2}	0.4536	1016	1000	907.2
Milligrams	64.81		1000	10^6	1	2.835×10^4	4.536×10^5	1.016×10^9	10^9	9.072×10^8
Ounces†	2.286×10^{-3}		3.527×10^{-2}	35.27	3.527×10^{-5}	1	16	3.584×10^4	3.527×10^4	3.2×10^4
Pounds†	1.429×10^{-4}		2.205×10^{-3}	2.205	2.205×10^{-6}	6.250×10^{-2}	1	2240	2205	2000
Tons (long)			9.842×10^{-7}	9.842×10^{-4}	9.842×10^{-10}	2.790×10^{-5}	4.464×10^{-4}	1	0.9842	0.8929
Tons (metric)			10^{-6}	0.001	10^{-9}	2.835×10^{-5}	4.536×10^{-4}	1.016	1	0.9072
Tons (short)			1.102×10^{-6}	1.102×10^{-3}	1.102×10^{-9}	3.125×10^{-5}	0.0005	1.120	1.102	1

†Avoirdupois pounds and ounces

Pressure or Force per Unit Area

Multiply Number of to Obtain by	Atmospheres [†]	Bayres or dynes per square centimeter [‡]	Centimeters of mercury at 0°C [§]	Inches of mercury at 0°C [§]	Inches of water at 4°C	Kilograms per square meter ^{††}	Pounds per square foot	Pounds per square inch ^{‡‡}	Tons (short) per square foot	Pascals
Atmospheres [†]	1	9.869×10^{-7}	1.316×10^{-2}	3.342×10^{-2}	2.458×10^{-3}	9.678×10^{-5}	4.725×10^{-4}	6.804×10^{-2}	0.9450	9.869×10^{-6}
Bayres or dynes per square centimeter [‡]	1.013×10^6	1	1.333×10^4	3.386×10^4	2.491×10^{-3}	98.07	478.8	6.895×10^4	9.576×10^5	10
Centimeters of mercury at 0°C [§]	76.00	7.501×10^{-5}	1	2.540	0.1868	7.356×10^{-3}	3.591×10^{-2}	5.171	71.83	7.501×10^{-4}
Inches of mercury at 0°C [§]	29.92	2.953×10^{-5}	0.3937	1	7.355×10^{-2}	2.896×10^{-3}	1.414×10^{-2}	2.036	28.28	2.953×10^{-4}
Inches of water at 4°C	406.8	4.015×10^{-4}	5.354	13.60	1	3.937×10^{-2}	0.1922	27.68	384.5	4.015×10^{-3}
Kilograms per square meter ^{††}	1.033×10^4	1.020×10^{-2}	136.0	345.3	25.40	1	4.882	703.1	9765	0.1020
Pounds per square foot	2117	2.089×10^{-3}	27.85	70.73	5.204	0.2048	1	144	2000	2.089×10^{-2}
Pounds per square inch ^{‡‡}	14.70	1.450×10^{-5}	0.1934	0.4912	3.613×10^{-2}	1.422×10^{-3}	6.944×10^{-3}	1	13.89	1.450×10^{-4}
Tons (short) per square foot	1.058	1.044×10^{-5}	1.392×10^{-2}	3.536×10^{-2}	2.601×10^{-3}	1.024×10^{-4}	0.0005	0.072	1	1.044×10^{-5}
Pascals	1.013×10^5	10^{-1}	1.333×10^3	3.386×10^3	2.491×10^{-4}	9.807	47.88	6.895×10^3	9.576×10^4	1

[†] One atmosphere (standard) = 76 cm of mercury at 0°C

[‡] Bar

[§] To convert height h of a column of mercury at t °C to the equivalent height h_0 at 0°C, use $h_0 = h \{1 - [(m - l)t / 1 + mt]\}$, where $m = 0.0001818$ and $l = 18.4 \times 10^{-6}$ if the scale is engraved on brass; $l = 8.5 \times 10^{-6}$ if on glass. This assumes the scale is correct at 0°C; for other cases (any liquid) see *International Critical Tables*, Vol. 1, 68.

^{††} 1 gram per square centimeter = 10 kilograms per square meter

^{‡‡} psi = MPa × 145.038

psi/ft = $0.433 \times \text{g/cm}^3 = \text{lb/ft}^3/144 = \text{lb/gal}/19.27$

Density or Mass per Unit Volume

Multiply Number of to Obtain by	Grams per cubic centimeter	Kilograms per cubic meter	Pounds per cubic foot	Pounds per cubic inch	Pounds per gallon
Grams per cubic centimeter	1	0.001	1.602×10^{-2}	27.68	0.1198
Kilograms per cubic meter	1000	1	16.02	2.768×10^4	119.8
Pounds per cubic foot	62.43	6.243×10^{-2}	1	1728	7.479
Pounds per cubic inch	3.613×10^{-2}	3.613×10^{-5}	5.787×10^{-4}	1	4.329×10^{-3}
Pounds per gallon	8.347	8.3×10^{-3}	13.37×10^{-2}	231.0	1

Temperature

°F	$1.8^\circ\text{C} + 32$
°C	$\frac{5}{9} (\text{°F} - 32)$
°R	$^\circ\text{F} + 459.69$
K	$^\circ\text{C} + 273.16$

Traditional symbol	Standard SPE and SPWLA ^a	Standard computer symbol ^a	Description	Customary unit or relation	Standard reserve symbol ^b
a	a	ACT	electrochemical activity	equivalents/liter, moles/liter	
a	K _R	COER	coefficient in F _R - φ relation	F _R = K _R /φ ^m	M _R , a, C
A	A	AWT	atomic weight	amu	
C	C	ECN	conductivity (electrical logging)	millimho per meter (mmho/m)	σ
C _p	B _{cp}	CORCP	sonic compaction correction factor	φ _{SVcor} = B _{cp} φ _{SV}	C _{cp}
D	D	DPH	depth	ft, m	y, H
d	d	DIA	diameter	in.	D
E	E	EMF	electromotive force	mV	V
F	F _R	FACHR	formation resistivity factor	F _R = K _R /φ ^m	
G	G	GMF	geometrical factor (multiplier)		f _G
H	I _H	HYX	hydrogen index		i _H
h	h	THK	bed thickness, individual	ft, m, in.	d, e
I	I	-X	index		i
FFI	I _{Ff}	FFX	free fluid index		i _{Ff}
SI	I _{sl}	SLX	silt index		I _{slt} , i _{sl} , i _{slt}
	I _φ	PRX	porosity index		i _φ
SPI	I _{φ2}	PRXSE	secondary porosity index		i _{φ2}
J	G _p	GMFP	pseudogeometrical factor		f _{Gp}
K	K _c	COEC	electrochemical SP coefficient	E _c = K _c log (a _w /a _{mf})	M _c , K _{ec}
k	k	PRM	permeability, absolute (fluid flow)	md	K
L	L	LTH	length, path length	ft, m, in.	s, ℓ
M	M	SAD	slope, sonic interval transit time versus density × 0.01, in M-N plot	M = [(t _f - t _{LOG})/(ρ _b - ρ _f)] × 0.01	m _{θD}
m	m	MXP	porosity (cementation) exponent	F _R = K _R /φ ^m	
N	N	SND	slope, neutron porosity versus density, in M-N Plot	N = (φ _{Nf} - φ _N)/(ρ _b - ρ _f)	m _{φND}
n	n	SXP	saturation exponent	S _w ⁿ = F _R R _w /R _t	
P	C	CNC	salinity	g/g, ppm	c, n
p	p	PRS	pressure	psi, kg/cm ² , atm	P
P _c	P _c	PRSCP	capillary pressure	psi, kg/cm ² , atm	P _c , p _c
P _e			photoelectric cross section		
<p>a References: "SPE Letter and Computer Symbols Standard," 1986.</p> <p>b Reserve symbols are to be used only if conflict arises between standard symbols used in the same paper.</p> <p>c The unit, kilograms per square centimeter, is to be replaced in use by the SI metric unit, the pascal.</p> <p>d "DEL" is in the operator field. "RAD" is in the main-quantity field.</p> <p>e Suggested computer symbol.</p>					

Traditional symbol	Standard SPE and SPWLA ^a	Standard computer symbol ^a	Description	Customary unit or relation	Standard reserve symbol ^b
Q_v			shaliness (CEC per ml water)	meq/ml	
q	$f_{\phi shd}$	FIMSHD	dispersed-shale volume fraction of intermatrix porosity		ϕ_{imfshd}, q
R	R	RES	resistivity (electrical)	ohm-m	ρ, r
r	r	RAD	radial distance from hole axis	in.	R
S	S	SAT	saturation	fraction or percent of pore volume	ρ, s
T	T	TEM	temperature	$^{\circ}F, ^{\circ}C, K$	θ
BHT, T_{bh}	T_{bh}	TEMBH	bottomhole temperature	$^{\circ}F, ^{\circ}C, K$	θ_{BH}
FT, T_{fm}	T_f	TEMF	formation temperature	$^{\circ}F, ^{\circ}C, K$	
t	t	TIM	time	$\mu\text{sec}, \text{sec}, \text{min}$	t
t	t	TAC	interval transit time		Δt
U			volumetric cross section	barns/cm ³	
v	v	VAC	velocity (acoustic)	ft/sec, m/sec	V, u
V	V	VOL	volume	cm ³ , ft ³ , etc.	v
V	V	VLF	volume fraction		f_v, F_v
Z	Z	ANM	atomic number		
α	α_{SP}	REDSP	SP reduction factor		
γ	γ	SPG	specific gravity (ρ/ρ_w or ρ_g/ρ_{air})		s, F_s
ϕ	ϕ	POR	porosity	fraction or percentage of bulk volume, p.u.	f, ϵ
	ϕ_1	PORPR	primary porosity	fraction or percentage of bulk volume, p.u.	f_1, e_1
	ϕ_2	PORSE	secondary porosity	fraction or percentage of bulk volume, p.u.	f_2, e_2
	ϕ_{ig}	PORIG	intergranular porosity	$\phi_{ig} = (V_b - V_{gr})/V_b$	f_{ig}, ϵ_{ig}
ϕ_z, ϕ_{im}	ϕ_{im}	PORIM	intermatrix porosity	$\phi_{im} = (V_b - V_{ma})/V_b$	f_{im}, ϵ_{im}
Δr	Δr	DELRAD ^d	radial distance (increment)	in.	ΔR
Δt	t	TAC	sonic interval transit time	$\mu\text{sec}/\text{ft}$	Δt
$\Delta\phi_{Nex}$		DELPORNX ^e	excavation effect	p.u.	
λ	K_{ani}	COEANI	coefficient of anisotropy		M_{ani}
ρ	ρ	DEN	density	g/cm ³	D
Σ	Σ	XST XSTMAC	neutron capture cross section macroscopic	c.u., cm ⁻¹	S
τ	τ_{dn}	TIMDN	thermal neutron decay time	μsec	t_{dn}

a References: "SPE Letter and Computer Symbols Standard," 1986.

b Reserve symbols are to be used only if conflict arises between standard symbols used in the same paper.

c The unit, kilograms per square centimeter, is to be replaced in use by the SI metric unit, the pascal.

d "DEL" is in the operator field. "RAD" is in the main-quantity field.

e Suggested computer symbol.

Traditional subscript	Standard SPE and SPWLA ^a	Standard computer subscript ^a	Explanation	Example	Standard reserve subscript ^b
a	LOG	L	apparent from log reading (or use tool description subscript)	R_{LOG}, R_{LL}	log
a	a	A	apparent (general)	R_a	ap
abs	cap	C	absorption, capture	Σ_{cap}	
anh	anh	AH	anhydrite		
b	b	B	bulk	ρ_b	B, t
bh	bh	BH	bottomhole	T_{bh}	w, BH
clay	cl	CL	clay	V_{cl}	cla
cor, c	cor	COR	corrected	t_{cor}	
c	c	C	electrochemical	E_c	ec
cp	cp	CP	compaction	B_{cp}	
D	D	D	density log		d
dis	shd	SHD	dispersed shale	V_{shd}	
dol	dol	DL	dolomite	t_{dol}	
e, eq	eq	EV	equivalent	R_{weq}, R_{mfeq}	EV
f, fluid	f	F	fluid	ρ_f	fl
fm	f	F	formation (rock)	T_f	fm
g, gas	g	G	gas	S_g	G
	gr	GR	grain	ρ_{gr}	
gx0	gx0	GXO	gas in flushed zone	S_{gx0}	GXO
gyp	gyp	GY	gypsum	ρ_{gyp}	
h	h	H	hole	d_h	H
h	h	H	hydrocarbon	ρ_h	H
hr	hr	HR	residual hydrocarbon	S_{hr}	
i	i	I	invaded zone (inner boundary)	d_i	I
ig	ig	IG	intergranular (incl. disp. and str. shale)	ϕ_{ig}	
im, z	im	IM	intermatrix (incl. disp. shale)	ϕ_{im}	
int	int	I	intrinsic (as opposed to log value)	Σ_{int}	
irr	i	IR	irreducible	S_{wi}	ir, i
J	j	J	liquid junction	E_j	i
k	k	K	electrokinetic	E_k	ek
l		L	log	t_{pl}	log
lam	ℓ	LAM	lamination, laminated	V_{sh}^{ℓ}	L
lim	lim	LM	limiting value	ϕ_{lim}	
liq	L	L	liquid	ρ_L	ℓ
a	References: "SPE Letter and Computer Symbols Standard," 1986.				
b	Reserve symbols are to be used only if conflict arises between standard symbols used in the same paper.				

Traditional subscript	Standard SPE and SPWLA ^a	Standard computer subscript ^a	Explanation	Example	Standard reserve subscript ^b
log	LOG	L	log values	t_{LOG}	log
ls	ls	LS	limestone	t_{ls}	1st
m	m	M	mud	R_m	
max	max	MX	maximum	ϕ_{max}	
ma	ma	MA	matrix	t_{ma}	
mc	mc	MC	mudcake	R_{mc}	
mf	mf	MF	mud filtrate	R_{mf}	
mfa	mfa	MFA	mud filtrate, apparent	R_{mfa}	
min	min	MN	minimum value		
ni			noninvaded zone	R_{ni}	
o	o	O	oil (except with resistivity)	S_o	N
or	or	OR	residual oil	S_{or}	
o, 0 (zero)	0 (zero)	ZR	100-percent water saturated	F_0	zr
p			propagation	t_{pw}	
PSP	pSP	PSP	pseudostatic SP	E_{pSP}	
pri	1 (one)	PR	primary	ϕ_1	p, pri
r	r	R	relative	k_{ro}, k_{rw}	R
r	r	R	residual	S_{or}, S_{hr}	R
s	s	S	adjacent (surrounding) formation	R_s	
sd	sd	SD	sand		sa
ss	ss	SS	sandstone		sst
sec	2	SE	secondary	ϕ_2	s, sec
sh	sh	SH	shale	V_{sh}	sha
silt	sl	SL	silt	I_{sl}	slt
SP	SP	SP	spontaneous potential	E_{SP}	sp
SSP	SSP	SSP	static spontaneous potential	E_{SSP}	
str	sh st	SH ST	structural shale	V_{shst}	s
t, ni	t	T	true (as opposed to apparent)	R_t	tr
T	t	T	total	C_t	T
w	w	W	water, formation water	S_w	W
wa	wa	WA	formation water, apparent	R_{wa}	W_{ap}
wf	wf	WF	well flowing conditions	p_{wf}	f
ws	ws	WS	well static conditions	p_{ws}	s
xo	xo	XO	flushed zone	R_{xo}	
z, im	im	IM	intermatrix	ϕ_{im}	

- a References: "SPE Letter and Computer Symbols Standard," 1986.
b Reserve symbols are to be used only if conflict arises between standard symbols used in the same paper.

Traditional subscript	Standard SPE and SPWLA ^a	Standard computer subscript ^a	Explanation	Example	Standard reserve subscript ^b
0 (zero)	0 (zero)	ZR	100 percent water saturated	R_0	zr
AD		RAD	from CDR* attenuation deep	R_{AD}	
D	D	D	from density log	ϕ_D	d
	GG	GG	from gamma-gamma log	ϕ_{GG}	gg
IL	I	I	from induction log	R_I	i
ILD	ID	ID	from deep induction log	R_{ID}	id
ILM	IM	IM	from medium induction log	R_{IM}	im
LL	LL (also LL3, LL8, etc.)	LL	from laterolog (also LL3, LL7, LL8, LLD, LLS)	R_{LL}	ll
N	N	N	from normal resistivity log	R_N	n
N	N	N	from neutron log	ϕ_N	n
PS		RPS	from CDR phase shift shallow	R_{PS}	
16", 16"N			from 16-in. normal Log	$R_{16''}$	
1" × 1"			from 1-in. by 1-in. microinverse (MI)	$R_{1'' \times 1''}$	
2"			from 2-in. micronormal (MN)	$R_{2''}$	
a	References: "SPE Letter and Computer Symbols Standard," 1986.				
b	Reserve symbols are to be used only if conflict arises between standard symbols used in the same paper.				

These unit abbreviations, which have been adopted by the Society for Petroleum Engineers (SPE), are appropriate for most publications. However, an accepted industry standard may be used instead. For instance, in the drilling field, *ppg* may be more common than *lbm/gal* when referring to pounds per gallon.

Unit abbreviations are followed by a period only when the abbreviation forms a word (for example, *in.* for *inch*).

acre	spell out
acre-foot	acre-ft
alternating-current (adj.)	AC
ampere	A
ampere-hour	amp-hr
angstrom unit (10^{-8} cm)	Å
atmosphere	atm
atomic mass unit	amu
average	avg
barrel	bbl
barrels of fluid per day	BFPD
barrels of liquid per day	BLPD
barrels of oil per day	BOPD
barrels of water per day	BWPD
barrels per day	B/D
barrels per minute	bbbl/min
billion cubic feet (billion = 10^9)	Bcf
billion cubic feet per day	Bcf/D
billion standard cubic feet per day	Bscf/D
bits per inch	bpi
bits per second	bps
bottomhole pressure	BHP
bottomhole temperature	BHT
British thermal unit	Btu
capture unit	c.u.
centimeter	cm
centipoise	cp
centistoke	cstk
coulomb	C
counts per second	cps
cubic centimeter	cm ³
cubic foot	ft ³
cubic feet per barrel	ft ³ /bbl
cubic feet per day	ft ³ /D
cubic feet per minute	ft ³ /min
cubic feet per pound	ft ³ /lbm
cubic feet per second	ft ³ /sec
cubic inch	in. ³

cubic meter	m ³
cubic millimeter	mm ³
cubic yard	yd ³
Curie	Ci
darcy, darcies	spell out
day	spell out
dead-weight ton	DWT
decibel	dB
degree (American Petroleum Institute)	°API
degree Celsius	°C
degree Fahrenheit	°F
degree Kelvin	(see "kelvin")
degree Rankine	°R
direct-current (as adjective)	DC
dots per inch	dpi
electromotive force	emf
electron volt	eV
farad	F
feet per minute	ft/min
feet per second	ft/sec
foot	ft
foot-pound	ft-lbf
gallon	gal
gallons per minute	gal/min
gallons per day	gal/D
gigabyte	Gbyte
gigahertz	GHz
gigaPascal	GPa
gigawatt	GW
gram	g
hertz	Hz
horsepower	hp
horsepower-hour	hp-hr
hour	hr
hyperbolic sine, cosine, etc.	sinh, cosh, etc.
inch	in.
inches per second	in./sec
kelvin	K
kilobyte	kbyte
kilogram	kg
kilogram-meter	kg-m
kilohertz	kHz
kilometer	km
kilopond (1000 lbf)	lbf

kilovolt	kV	pore volume	PV
kilowatt	kW	porosity unit	p.u.
kilowatt-hour	kW-hr	pound (force)	lbf
kip per square inch	ksi	pound (mass)	lbm
lines per inch	lpi	pound per cubic foot	lbm/ft ³
lines per minute	lpm	pound per gallon	lbm/gal
lines per second	lps	pounds per square inch	psi
liter	spell out	pounds per square inch absolute	psia
megabyte	Mbyte	pounds per square inch gauge	psig
megahertz	MHz	quart	qt
meter	m	reservoir barrel	res bbl
mho per meter	Ω/m	reservoir barrel per day	RB/D
microsecond	μsec	revolutions per minute	rpm
mile	spell out	saturation unit	s.u.
miles per hour	mph	second	sec
milliamperes	milliamp	self-potential	SP
milliCurie	mCi	shots per foot	spf
millidarcy, millidarcies	md	specific productivity index	SPI
milliequivalent	meq	square	sq
milligram	mg	square centimeter	cm ²
milliliter	mL	square foot	ft ²
millimeter	mm	square inch	in. ²
millimho	mmho	square meter	m ²
million cubic feet (million = 10 ⁶)	MMcf	square millimeter	mm ²
million cubic feet per day	MMcf/D	standard	std
million electron volts	MeV	standard cubic feet per day	scf/D
million Pascals	MPa	standard cubic foot	scf
million standard cubic feet per day	MMscf/D	stock-tank barrel	STB
millisecond	msec	stock-tank barrels per day	STB/D
millisiemen	mS	stoke	St
millivolt	mV	teragram	Tg
mils per year	mil/yr	thousand cubic feet	Mcf
minute	min	thousand cubic feet per day	Mcf/D
mole	mol	thousand pounds per square inch	kpsi
nanosecond	nsec	thousand standard cubic feet per day	Mscf/D
newton	N	tonne (metric ton)	t
ohm	ohm	trillion cubic feet (trillion = 10 ⁻¹²)	Tcf
ohm-centimeter	ohm-cm	trillion cubic feet per day	Tcf/D
ohm-meter	ohm-m	volt	V
ounce	oz	volume per volume	vol/vol
parts per million	ppm	watt	W
picofarad	pF	yard	yd
pint	pt	year	yr

1. Overton HL and Lipson LB: "A Correlation of the Electrical Properties of Drilling Fluids with Solids Content," *Transactions, AIME* (1958) **213**.
2. Desai KP and Moore EJ: "Equivalent NaCl Concentrations from Ionic Concentrations," *The Log Analyst* (May-June 1969).
3. Gondouin M, Tixier MP and Simard GL: "An Experimental Study on the Influence of the Chemical Composition of Electrolytes on the SP Curve," *JPT* (February 1957).
4. Segesman FF: "New SP Correction Charts," *Geophysics* (December 1962) **27**, No. 6, PI.
5. Alger RP, Locke S, Nagel WA and Sherman H: "The Dual Spacing Neutron Log-CNL," paper SPE 3565, presented at the 46th SPE Annual Meeting, New Orleans, Louisiana, USA (1971).
6. Segesman FF and Liu OYH: "The Excavation Effect," *Transactions of the SPWLA 12th Annual Logging Symposium* (1971).
7. Burke JA, Campbell RL Jr and Schmidt AW: "The Litho-Porosity Crossplot," *Transactions of the SPWLA 10th Annual Logging Symposium* (1969), paper Y.
8. Clavier C and Rust DH: "MID-PLOT: A New Lithology Technique," *The Log Analyst* (November-December 1976).
9. Tixier MP, Alger RP, Biggs WP and Carpenter BN: "Dual Induction-Laterolog: A New Tool for Resistivity Analysis," paper 713, presented at the 38th SPE Annual Meeting, New Orleans, Louisiana, USA (1963).
10. Wahl JS, Nelligan WB, Frentrop AH, Johnstone CW and Schwartz RJ: "The Thermal Neutron Decay Time Log," *SPEJ* (December 1970).
11. Clavier C, Hoyle WR and Meunier D: "Quantitative Interpretation of Thermal Neutron Decay Time Logs, Part I and II," *JPT* (June 1971).
12. Poupon A, Loy ME and Tixier MP: "A Contribution to Electrical Log Interpretation in Shaly Sands," *JPT* (June 1954).
13. Tixier MP, Alger RP and Tanguy DR: "New Developments in Induction and Sonic Logging," paper 1300G, presented at the 34th SPE Annual Meeting, Dallas, Texas, USA (1959).
14. Rodermund CG, Alger RP and Tittman J: "Logging Empty Holes," *OGJ* (June 1961).
15. Tixier MP: "Evaluation of Permeability from Electric Log Resistivity Gradients," *OGJ* (June 1949).
16. Morris RL and Biggs WP: "Using Log-Derived Values of Water Saturation and Porosity," *Transactions of the SPWLA 8th Annual Logging Symposium* (1967).
17. Timur A: "An Investigation of Permeability, Porosity, and Residual Water Saturation Relationships for Sandstone Reservoirs," *The Log Analyst* (July-August 1968).
18. Wyllie MRJ, Gregory AR and Gardner GHF: "Elastic Wave Velocities in Heterogeneous and Porous Media," *Geophysics* (January 1956) **21**, No. 1.
19. Tixier MP, Alger RP and Doh CA: "Sonic Logging," *JPT* (May 1959) **11**, No. 5.
20. Raymer LL, Hunt ER and Gardner JS: "An Improved Sonic Transit Time-to-Porosity Transform," *Transactions of the SPWLA 21st Annual Logging Symposium* (1980).
21. Coates GR and Dumanoir JR: "A New Approach to Improved Log-Derived Permeability," *The Log Analyst* (January-February 1974).
22. Raymer LL: "Elevation and Hydrocarbon Density Correction for Log-Derived Permeability Relationships," *The Log Analyst* (May-June 1981).
23. Westaway P, Hertzog R and Plasic RE: "The Gamma Spectrometer Tool, Inelastic and Capture Gamma Ray Spectroscopy for Reservoir Analysis," paper SPE 9461, presented at the 55th SPE Annual Technical Conference and Exhibition, Dallas, Texas, USA (1980).
24. Quirein JA, Gardner JS and Watson JT: "Combined Natural Gamma Ray Spectral/Litho-Density Measurements Applied to Complex Lithologies," paper SPE 11143, presented at the 57th SPE Annual Technical Conference and Exhibition, New Orleans, Louisiana, USA (1982).
25. Harton RP, Hazen GA, Rau RN and Best DL: "Electromagnetic Propagation Logging: Advances in Technique and Interpretation," paper SPE 9267, presented at the 55th SPE Annual Technical Conference and Exhibition, Dallas, Texas, USA (1980).
26. Serra O, Baldwin JL and Quirein JA: "Theory and Practical Application of Natural Gamma Ray Spectrometry," *Transactions of the SPWLA 21st Annual Logging Symposium* (1980).
27. Gardner JS and Dumanoir JL: "Litho-Density Log Interpretation," *Transactions of the SPWLA 21st Annual Logging Symposium* (1980).
28. Edmondson H and Raymer LL: "Radioactivity Logging Parameters for Common Minerals," *Transactions of the SPWLA 20th Annual Logging Symposium* (1979).
29. Barber TD: "Real-Time Environmental Corrections for the Phasor Dual Induction Tool," *Transactions of the SPWLA 26th Annual Logging Symposium* (1985).
30. Roscoe BA and Grau J: "Response of the Carbon-Oxygen Measurement for an Inelastic Gamma Ray Spectroscopy Tool," paper SPE 14460, presented at the 60th SPE Annual Technical Conference and Exhibition, Las Vegas, Nevada, USA (1985).

31. Freedman R and Grove G: "Interpretation of EPT-G Logs in the Presence of Mudcakes," paper presented at the 63rd SPE Annual Technical Conference and Exhibition, Houston, Texas, USA (1988).
32. Gilchrist WA Jr, Galford JE, Flaum C, Soran PD and Gardner JS: "Improved Environmental Corrections for Compensated Neutron Logs," paper SPE 15540, presented at the 61st SPE Annual Technical Conference and Exhibition, New Orleans, Louisiana, USA (1986).
33. Tabanou JR, Glowinski R and Rouault GF: "SP Deconvolution and Quantitative Interpretation in Shaly Sands," *Transactions of the SPWLA 28th Annual Logging Symposium* (1987).
34. Kienitz C, Flaum C, Olesen J-R and Barber T: "Accurate Logging in Large Boreholes," *Transactions of the SPWLA 27th Annual Logging Symposium* (1986).
35. Galford JE, Flaum C, Gilchrist WA Jr and Duckett SW: "Enhanced Resolution Processing of Compensated Neutron Logs, paper SPE 15541, presented at the 61st SPE Annual Technical Conference and Exhibition, New Orleans, Louisiana, USA (1986).
36. Lowe TA and Dunlap HF: "Estimation of Mud Filtrate Resistivity in Fresh Water Drilling Muds," *The Log Analyst* (March-April 1986).
37. Clark B, Luling MG, Jundt J, Ross M and Best D: "A Dual Depth Resistivity for FEWD," *Transactions of the SPWLA 29th Annual Logging Symposium* (1988).
38. Ellis DV, Flaum C, Galford JE and Scott HD: "The Effect of Formation Absorption on the Thermal Neutron Porosity Measurement," paper presented at the 62nd SPE Annual Technical Conference and Exhibition, Dallas, Texas, USA (1987).
39. Wafra M and Nurmi R: "Calculation of Saturation, Secondary Porosity and Producibility in Complex Middle East Carbonate Reservoirs," *Transactions of the SPWLA 28th Annual Logging Symposium* (1987).
40. Brie A, Johnson DL and Nurmi RD: "Effect of Spherical Pores on Sonic and Resistivity Measurements," *Transactions of the SPWLA 26th Annual Logging Symposium* (1985).
41. Serra O: *Element Mineral Rock Catalog*, Schlumberger (1990).